THE UNIVERSITY *of* EDINBURGH

THE UNIVERSITY *of* EDINBURGH

Analysis of axon tract formation in *Gli3* conditional mutant mice

Eleni-Maria M Amaniti

Thesis submitted for the degree of

Doctor of Philosophy

The University of Edinburgh

2013

"ὁ δὲ ἀνεξέταστος βίος οὐ βιωτὸς ἀνθρώπῳ"

Απολογία Σωκράτους

"The unexamined life is not worth living for a human being"

The Apology of Socrates

Doctor of Philosophy – The University of Edinburgh – 2013

Disclaimer

I (Eleni Maria Amaniti) composed this thesis and pTTerformed all of the experiments presented herein unless otherwise indicated in the text. In particular, Ziwen Li, Chaoying Fu and Marina Saisana performed the experiments described in p105 and p146;148;150-152 and p179, respectively. No part of this work has been, or is being submitted for any other degree or professional qualification.

Signed…….

Date……

Contents in brief:

List of Figures:

List of Tables:

Acknowledgements:

I am indebted to my supervisor Thomas Theil for the guidance, insight, mentorship and never-ending support and patience he has shown throughout the duration of this project. I am also deeply grateful to John Mason for useful discussions and advice during the course of this work.

I could not have completed the work presented in this thesis without the assistance of numerous people. I am indebted to Kerstin Hasenpusch-Theil for the help in all aspects of lab working. Also, I am particularly grateful to Dario Magnani for the expert training in various metholodogies, all the assistance in the lab, the in depth discussions and for the amazing/chatty three years of having a desk next to him. Particular thanks are owed to Lasani Wijetunge for her expert training in perfusion techniques and to Gosia Borkowska for assistance with *in utero* electroporation techniques.

I thank Ziwen Li, Chaoying Fu and Marina Saisana whose work is briefly described and referenced in this thesis. I also thank Trudi Gillespie from IMPACT Imaging facility for expert assistance with confocal microscopy and image analysis. Thanks are also owed to the BRR members and particularly Adrian White for his assistance with animal care.

Thank you to Jim Clegg, Dario Magnani, Rosalie Brown, Kerstin Hasenpusch-Theil and Gosia Borkowska for taking on the boring task of proofreading my thesis.

A big thank you goes to David Price, Peter Kind, Tom Pratt and the rest of DBUG for many helpful acts and the inspirational conversations.

To my family, thank you for your strength and endless support, for always being there and for inspiring me to move forward.

Abstract

The cerebral cortex is the largest subdivision of the human brain and is associated with higher cognitive functions. These functions are based on the interconnections between the neurons that form pre- and postnatally in the different telencephalic regions. The processes of neurons with similar functions and connectivity follow the same course and form axon tracts. There are three main axons tracts analysed in this thesis the corpus callosum, the corticothalamic/thalamocortical tracts and the lateral olfactory tract that transfers olfactory information to the telencephalon. In the mouse, these tracts are generated during embryogenesis as axons project to their target area. The mechanisms by which axons navigate still need to be elucidated.

Studies of a number of mutant mice have shown that axon pathfinding is under the control of genes. *Gli3* is a zinc finger transcription factor with known roles in axon pathfinding. *Gli3* is widely expressed in progenitor cells of the dorsal and ventral telencephalon complicating the elucidation of the molecular mechanisms by which *Gli3* controls axon tract formation. My aim here is to investigate the spatial and temporal requirements for Gli3 in axon pathfinding in the forebrain using *Gli3* conditional mutants as a tool.

Regarding the corpus callosum, my findings demonstrated a crucial role for *Gli3* in the dorsal telencephalon, but not in the septum or medial ganglionic eminence, to control corpus callosum formation and indicated that defects in the formation of the corticoseptal boundary affect the positioning of callosal guidepost cells. Moreover, conditional inactivation of *Gli3* in dorsal telencephalic progenitors led to few corticothalamic axons leaving the cortex in a restricted lateral neocortical domain. This restricted entry is at least partially caused by an expansion of the piriform cortex, which forms from an enlarged progenitor domain of the ventral pallium. Transplantation experiments showed that the expanded piriform cortex repels corticofugal axons. Moreover, expression of *Sema5B*, a chemorepellent for corticofugal axons produced by the piriform cortex, is similarly expanded. Hence, control of lateral cortical development by *Gli3* at the progenitor level is crucial for

corticothalamic pathfinding. Finally, by using *Emx1Cre;Gli3*$^{fl/fl}$ mutants I analysed the consequences of the expansion of the piriform cortex on the formation of the lateral olfactory tract (LOT). This analysis showed that LOT axons also appear to be medially shifted with LOT collaterals aberrantly colonising the expanded piriform cortex. Time course analysis confirmed an expansion of the paleocortical primordium from E13.5 onwards, coinciding with the arrival of the LOT axons. Hence, it is possible that the expanded piriform cortex contributed to the medial shift of the LOT.

In conclusion, these findings support a strong link between *Gli3* controlled early patterning defects and axon pathfinding defects and form the basis for future analysis of the molecular mechanisms by which Gli3 controls axon pathfinding in the forebrain. My findings also reveal how alterations in *GLI3* function may contribute to connectivity defects in human patients with mutations in *GLI3*.

Abbreviations

AC	anterior commissure
CB	calbindin
CC	corpus callosum
Cgc	cingulate cortex
CGE	caudal ganglionic eminence
CH	choroid plexus
CR	calretinin
CR	cajal retzius
CTAs	corticothalamic axons
CSB	corticoseptal boundary
Ctx	neocortex
DP	dorsal pallium
DPd	deep pyramidal
EN	endopiriform nuclueus
GW	glial wedge
HC	hippocampal commissure
Hip	hippocampus
IG	indusium griseum
Lcx	lateral neocortex
LGE	lateral ganglionic eminence
LOT	lateral olfactory tract
LP	lateral pallium
MGE	medial ganglionic eminence

MP	medial pallium
MZG	midline zipper glia
OB	olfactory bulb
OT	olfactory tubercle
PC	piriform cortex
PSPB	pallial subpallial boundary
Rf	rhinal fissure
SCS	subcallosal sling
Sep	septum
SL	semilunar
SPd	superficial pyramidal
Str	striatum
TCAs	thalamocortical axons
Th	thalamus
VZ	ventricular zone
VP	ventral pallium

Preface

Part of the central nervous system is the brain, a unique organ that keeps the body's physiology stable, generates behaviour, allows interaction with the environment and enables reproduction (Squire *et al.*, 2008). Historically, the function of the brain troubled scientists since ancient times. The earliest reference to the brain in human records is in an Egyptian papyrus written in the 17th century BC (Kandel *et al.*, 2000). In 5th century BC Hippocrates wrote "*Men ought to know that from the brain, and from the brain only, arise our pleasures, joys… pains, grieves and tears… These things that we suffer all come from the brain, when it is not healthy… But when the brain is still, a man can think properly*". In recent times, the goal of neuroscience is to understand the brain; how it develops, functions and changes to form a mature nervous system that allow us to perceive, think, learn, behave etc.

The human brain is by far the most complex and versatile system. Neurons are the core component of the brain which consists of more than 100 billion neurons and 100 trillion synapses (Sheperd, 2003). The cerebral cortex is the largest subdivision of the human brain and is associated with higher brain functions. It consists of the left and right hemispheres which are formed of grey matter enriched with neurons and the white matter enriched with neuronal processes usually ensheathed in myelin. The processes of neurons with similar functions and connectivity follow the same course and form axon tracts. Some of the major axon tracts of the forebrain are the commissures i.e. corpus callosum or anterior commissure, the corticothalamic / thalamocortical tract, the lateral olfactory tract and the optic tract. It is generally perceived that these pathways convey information to and from the cortex or decussate information between the hemispheres.

All the higher functions of the brain are based on the interconnections between these neurons that form pre- and postnatally. The development of these interconnections is based on gradual and continuous molecular and cellular mechanisms. These mechanisms depend on the correct spatial and temporal expression pattern of

guidance cues. These can act either extrinsic or intrinsic and will work in a very time- and space-specific manner. Moreover, the combinatorial effect of genes, transcription factors and signalling molecules is critical for the induction and patterning of the embryonic neural tissue.

Advances in molecular techniques and the use of evolutionarily simpler organisms including rodents, zebrafish and frogs as animal models has enabled the further examination of the developmental connection between the above mentioned mechanisms and axon tract formation. Thus, in the following chapters by using *Gli3* mutant mice as an animal model I will elucidate the formation of axon projections in the telencephalon.

1 Introduction

1.1 Early brain development

1.1.1 Early patterning of the nervous system

The embryonic development of the nervous system begins with the establishment of the primordial nervous system. An initial complex step in this process is gastrulation in which the invagination of a group of embryonic cells forms three distinct germ layers: the ectoderm, the mesoderm and the endoderm (Purves *et al.*, 2007). The ectoderm, the outer primitive germ layer, receives signals from the node/Spemann's organiser which induce cells in the ectoderm to undergo distinct cellular changes and ultimately cause differentiation into neural precursor cells (Purves *et al.*, 2007, Squire *et al.*, 2008). The neuroepithelium of the neuroectoderm undergoes further morphological and cellular changes, which results in the formation of the neural plate (Figure 1-1). During neurulation, the lateral margins of the neural plate fold to form the neural tube, which invaginates into the embryo (Figure 1-1) (Purves *et al.*, 2007, Squire *et al.*, 2008, Crossman and Neary, 2010). The neural tube receives induction signals from the notochord, the floorplate at the ventral midline of the neural tube and the roofplate positioned at the dorsal midline of the neural tube. The floorplate, roofplate and the notochord orchestrate the expression of different signals that define the anteriorposterior and dorsoventral axis of the neural tube and enables the neural precursor cells to proliferate, differentiate and acquire regional identity (Wilson and Rubenstein, 2000, Rallu *et al.*, 2002a, Purves *et al.*, 2007). Neural tube defects are quite common human birth defects due to the complexity of the process (Wallingford *et al.*, 2013).

Simultaneously with these events, the basic anatomical structures of the developing brain are formed. The neural tube gives rise to the brain and spinal cord and is initially subdivided into pros-, mes-, rhombencephalon and spinal cord with further subdivisions into many functionally specialised areas occurring later (see Table 1-1) (Crossman and Neary, 2010). For the purposes of this thesis, the subsequent rounds

of subdivision of the prosencephalon will be further explained. The lateral prosencephalon forms the telencephalon that is further divided into dorsal and ventral regions. From medial to lateral the dorsal telencephalon will give rise to the medial pallium; containing the *archicortex* (Briata *et al.*, 1996); the dorsal pallium containing the *neocortex* (ctx); the lateral pallium which is thought to give rise to the *paleocortex* or *olfactory cortex* (Puelles *et al.*, 2000, Hirata *et al.*, 2002) and the ventral pallium which contributes to specific components of the claustroamygdaloid complex and the piriform cortex (Puelles *et al.*, 2000, Hirata *et al.*, 2002, Medina *et al.*, 2004). The ventral telencephalon will give rise to the basal ganglia from which the medial (MGE) and lateral (LGE) ganglionic eminences and the basal forebrain nuclei and olfactory bulbs (OB) will arise (Figure 1-2). The pallial and subpallial regions of the telencephalon are separated by a boundary (PSPB), which represents a border for the differential expression of genes. The more caudal part of the prosencephalon will form the diencephalon (Purves *et al.*, 2007, Squire *et al.*, 2008, Crossman and Neary, 2010). How these telencephalic regions are established is outlined below.

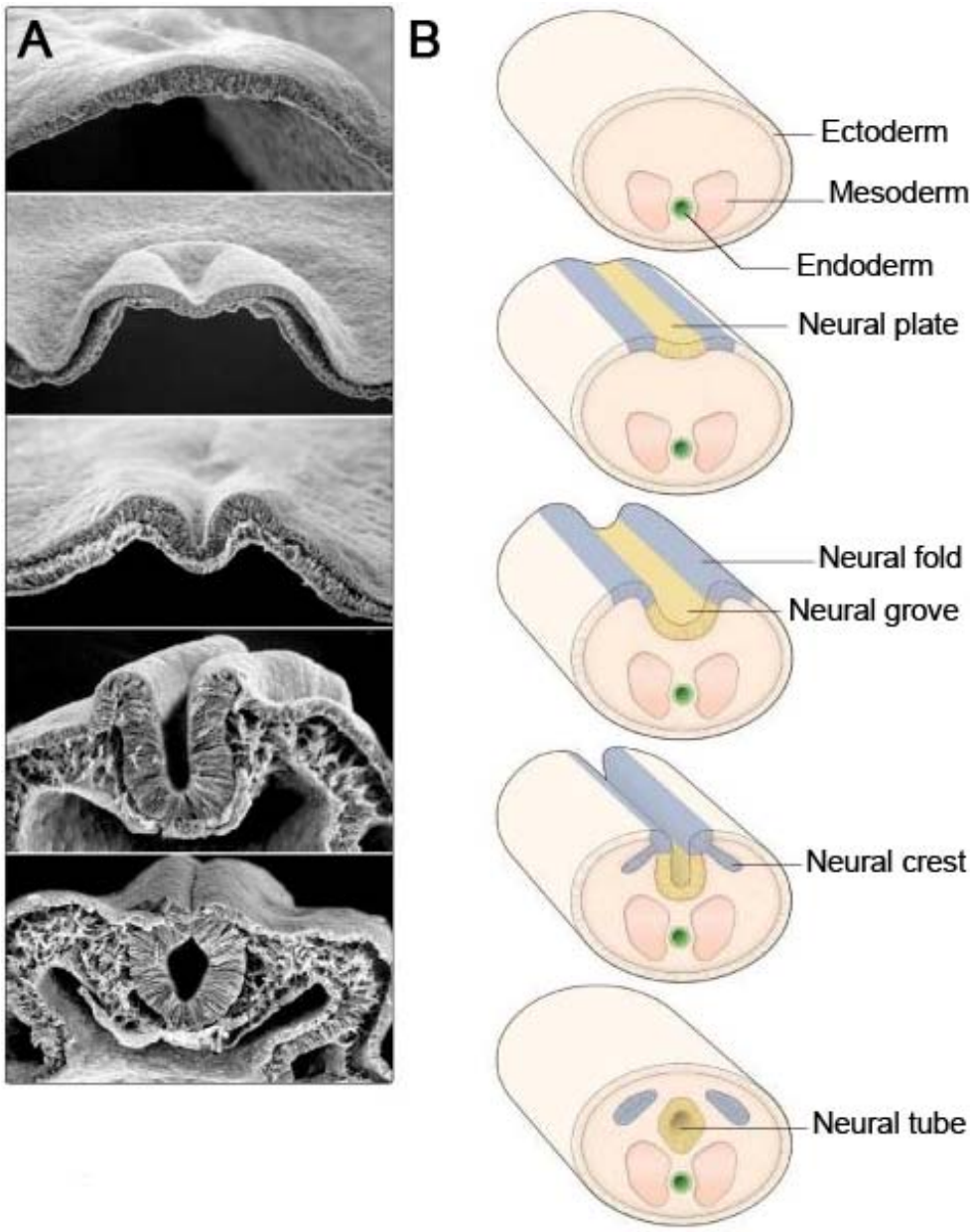

Figure 1-1: Neurulation: formation of the neural tube.

(A) Scanning electron micrographs of sections through the ectoderm of a chick embryo showing the gradual formation of the neural tube (top to bottom) (B) Schematic representation of the formation of the neural tube (top to bottom) (Crossman and Neary, 2010).

Primary brain vesicles	Secondary brain vesicles	Derivatives in mature brain
Prosencephalon (forebrain)	Telencephalon	Cerebral hemisphere
	Diencephalon	Thalamus
Mesencephalon (midbrain)	Mesencephalon	Midbrain
Rhombencephalon (hindbrain)	Metencephalon	Pons, cerebellum
	Myelencephalon	Medulla oblongata

Table 1-1: Embryonic development of the brain.

Parts of the embryonic subdivisions of the brain and the derivatives into which they develop (Crossman and Neary 2010).

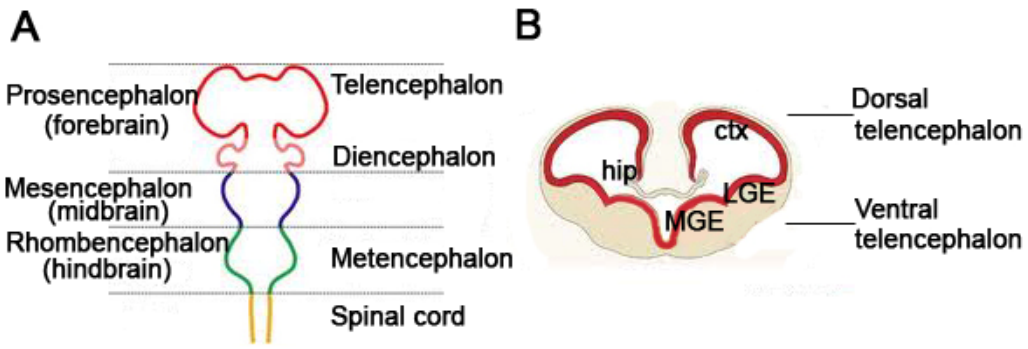

Figure 1-2: Regional specification of the brain.

(A) The neural tube is subdivided into primary brain vesicles from which will arise anatomically and functionally distinct cortical regions. (B) The telencephalon is further specified into dorsal and ventral regions. Abbreviations: ctx, neocortex; hip, hippocampus; LGE, lateral ganglionic eminence; MGE, medial ganglionic eminence (Rallu *et al.*, 2002a, Purves *et al.*, 2007).

1.1.2 **Patterning of the telencephalon**

1.1.2.1 Key signalling centres regulate telencephalic regionalisation

How the different regions of the telencephalon and the individual cell types of each anatomical subdivision gain their identity during early development remains a great puzzle. It has been shown that signals are involved in the early induction of the telencephalon and regulate the anteriorposterior and dorsoventral patterning of the cortex (Wilson and Rubenstein, 2000). These molecules are released from signalling centres that lie along key areas of the cortex and set up the expression of combinations of specific transcription factors. These transcription factors in turn, regulate other genes or the signalling molecules themselves (feedback-loops) and control further regional specification and growth (Ragsdale and Grove, 2001, Rallu *et al.*, 2002a).

Specific signalling molecules identified at key locations include: in the anterior neural ridge called the rostral patterning centre the fibroblast growth factors (FGFs) (Shimamura and Rubenstein, 1997, Crossley *et al.*, 2001, Fukuchi-Shimogori and Grove, 2001, Garel *et al.*, 2003); along the caudo-dorsal midline called the cortical hem, bone morphogenetic proteins (BMPs) and WNTs (Furuta *et al.*, 1997, Grove *et al.*, 1998, Crossley *et al.*, 2001, Monuki and Walsh, 2001, Hebert *et al.*, 2002); along the ventral telencephalon, Sonic hedgehog (Shh) (Crossley *et al.*, 2001, Rash and Grove, 2007, Hayhurst *et al.*, 2008); and at the boundary between pallium and subpallium called the antihem, *Fgf7*, *Fgf15*, transforming growth factor-α (*Tgfα*) and the Wnt antagonist secreted frizzled related protein-2 (*Sfrp2*) (Assimacopoulos *et al.*, 2003, Borello *et al.*, 2008, O'Leary and Sahara, 2008). The location of those signalling centres is schematically summarized below (Figure 1-3).

a) **FGFs**

FGFs are a family of 22 polypeptides that vary in size from 150 to 300 amino acids and can be subdivided into seven subfamilies including the FGF8 subfamily (Ornitz and Itoh, 2001, Itoh and Ornitz, 2004). FGF signals are

mainly mediated by four high-affinity receptor tyrosine kinases, the FGF receptors, but only three, *Fgfr*1-3, mediate the signal in the mammalian cortex (Mason, 2007).

The FGF8 subfamily including *Fgf8, Fgf17* and *Fgf18* (Ornitz and Itoh, 2001) has been implicated in the patterning and arealisation of the telencephalon (Fukuchi-Shimogori and Grove, 2001, Garel *et al.*, 2003, Paek *et al.*, 2009). *Fgf8, Fgf17* and *Fgf18* are expressed at the anterior neural ridge (ANR) (Shimamura and Rubenstein, 1997, Crossley *et al.*, 2001) at E8.5 and their expression persists at the commissural plate of the rostro-caudal telencephalon at later stages (Crossley *et al.*, 2001, Fukuchi-Shimogori and Grove, 2003, Cholfin and Rubenstein, 2007). *Fgf17* also has a wider expression domain which includes the septum (Cholfin and Rubenstein, 2007).

In particular, *Fgf8* acts as a diffusible morphogen (Toyoda *et al.*, 2010) and its function in forebrain was first demonstrated in mice by ectopically overexpressing *Fgf8* or *Fgfr*3, which is known to sequester *Fgf8*, by *in utero* electroporation (Fukuchi-Shimogori and Grove, 2001). Expansion of the *Fgf8* source shifts cortical area boundaries posteriorly while reducing the signal shifts the boundaries anteriorly (Fukuchi-Shimogori and Grove, 2001). Moreover, *Fgf8* suppresses the expression of the homeodomain transcription factor *Emx2*, important for caudal telencephalic development (Bishop *et al.*, 2000, Fukuchi-Shimogori and Grove, 2001, Fukuchi-Shimogori and Grove, 2003). Recently, *in vitro* assays showed that the *Sp8* transcription factor is a direct activator of *Fgf8* at the commissural plate and *Emx2* in return suppresses *Sp8* induction in the rest of the cortical primordium (Sahara *et al.*, 2007). This suggests that *Fgf8* regulates and in turn is regulated by transcription factors.

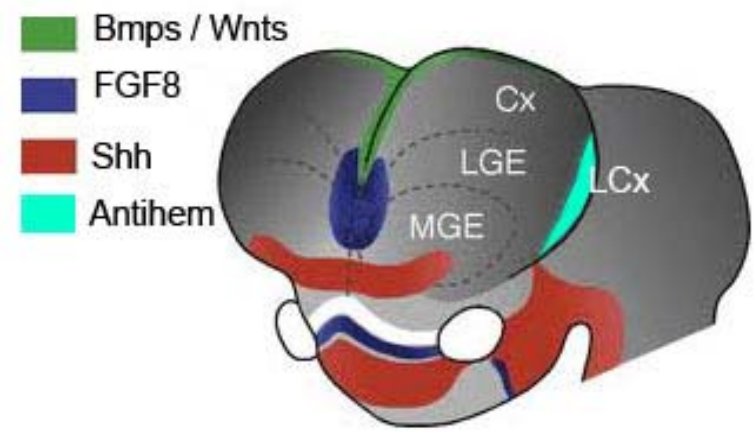

Figure 1-3:Distinct telencephalic signalling centres instruct regionalisation.

A rostral patterning centre (blue) which secretes Fgfs; a caudo-dorsal centre (green) called the cortical hem which secretes Bmps / Wnts; a ventral centre that secrets Shh (dark red) and the antihem (light blue) that secretes Fgf7, Fgf15, Tgfα and Sfrp2. Abbreviations: cx, neocortex; Lcx, lateral neocortex; lateral ganglionic eminence; MGE, medial ganglionic eminence [adapted from (Hoch, Rubenstein, & Pleasure, 2009).

Hypomorphic mouse mutants have been used to demonstrate the function of *Fgf8* in neocortical regionalisation since homozygous *Fgf8* null mutants show defective gastrulation (Meyers *et al.*, 1998). In hypomorphic *Fgf8* mutants, there was an expansion of caudal gene expression including *Emx2* and *CoupTf1* that correlated with the reduction in the size of rostral areas (Garel *et al.*, 2003). In contrast, *Fgf17*$^{-/-}$ mutants show more restricted effects by demonstrating reduction of the cortical surface of the frontal cortex with specific loss of dorsal frontal regions (Cholfin and Rubenstein, 2007). Moreover, *Fgf15* promotes neurogenesis and opposes *Fgf8* function during neocortical development (Borello *et al.*, 2008). Further information comes from a study in which the use of a triple mutant for *Fgfrs*1-3 show that these mutants lack the telencephalon completely except the dorso-caudal midline (Paek *et al.*, 2009). Overall, these studies suggest a complicated role of Fgfs in neocortical regionalisation. In fact, orchestration of different Fgf ligands and receptors expressed at the ANR appear to specify the rostral telencephalon.

b) **BMPs/WNTs**

The cortical hem lies along the dorso-medial cortex and is the source of multiple *Wnt* and *Bmp* proteins (Grove *et al.*, 1998). The WNTs are a family of secreted glycoproteins grouped into two classes, the canonical and noncanonical. Canonical *Wnt*s stabilise β-catenin and activate transcription of Tcf/LEF target genes. Noncanonical *Wnt*s activate other pathways such as the planar-cell-polarity pathway and the Wnt/Ca^{2+} pathway and can antagonise the canonical pathway (Kawano and Kypta, 2003). In fact, Wnts act as morphogens that specify hippocampal fate (Tole *et al.*, 1997). An interesting study showed that mice deficient in *Wnt3a*, one of the Wnts expressed at the hem, show a nearly complete deletion of the hippocampus with only few cells remaining (Lee *et al.*, 2000). Also, mice with a *Lef1* mutation, which is a transcriptional mediator of Wnt/ β-catenin signalling, show a similar

phenotype (Galceran *et al.*, 2000). Finally, the roofplate of the dorso-medial telencephalon does not form if *Wnt2b* is not expressed (Monuki *et al.*, 2001).

Bone morphogenetic proteins (BMPs), a subfamily of the TGFβ superfamily, are also expressed at a distinct region of the dorso-medial telencephalon, the roofplate. BMPs signal through heteromeric receptor complexes composed of type I and II BMP receptors (Weis-Garcia and Massague, 1996). *Bmp* signalling can induce the formation of dorsal structures and *Bmp2* and *Bmp4* exogenous application on lateral telencephalic explants induced dorsal telencephalic fates suggesting that BMPs regulate regionalisation, cell proliferation and cell death at the cortical hem (Furuta *et al.*, 1997). Furthermore, in the absence of *Bmp2* and *Bmp4* receptors the roofplate in the dorso-medial telencephalon disappears together with *Wnt2b* expression (Monuki *et al.*, 2001). This implies that Wnts and Bmps collaborate to induce the dorsal telencephalon in a precise manner.

c) **SHH**

Sonic hedgehog is one of the three members of the mammalian hedgehog family that also includes Desert hedgehog (Dhh) and Indian hedgehog (Ihh). The earliest *Shh* expression appears around E7.5 in the midline mesoderm of the head process, the prechordal plate (Echelard *et al.*, 1993). Before the onset of neurogenesis *Shh* expression occurs in ventral telencephalic structures and around E9.0 *Shh* is expressed primarily in the MGE, preoptic area and presumptive amygdala (Shimamura *et al.*, 1995, Sussel *et al.*, 1999, Nery *et al.*, 2001).

In *Shh* null mutants the telencephalon is severely hypoplastic and it is impossible to morphologically identify distinct ventral telencephalic structures and most of ventral telencephalic markers are absent (Chiang *et al.*, 1996, Corbin *et al.*, 2000, Muenke and Beachy, 2000, Rallu *et al.*, 2002b). Ectopic expression of *Shh* in mice and fish induce the expression of ventral telencephalic markers in the pallium (Shimamura and Rubenstein, 1997,

Corbin *et al.*, 2000, Rallu *et al.*, 2002b). Moreover, null mutants for the *Nkx2.*1 and *Foxg1* transcription factors, whose expression precedes that of *Shh* (Shimamura *et al.*, 1995), show loss of *Shh* expression but with a less severe phenotype to *Shh* null mutants (Huh *et al.*, 1999, Sussel *et al.*, 1999, Martynoga *et al.*, 2005). This less severe phenotype could imply that the specification of the ventral telencephalon relies on an extra source of *Shh*. Nevertheless, these findings suggest that *Shh* is required for the maintenance of ventral identity.

Shh effects are also dependent on length of exposure to Shh rather than just Shh concentration (Kohtz *et al.*, 1998, Gunhaga *et al.*, 2000). Interestingly, MGE-like fate is acquired in response to *Shh* expression at gastrula stages whereas *Shh* expression at later stages signals ventro-lateral fate (Kohtz *et al.*, 1998, Gunhaga *et al.*, 2000). Finally, when *Shh* signal from the ventral telencephalon from E9.5 was inactivated by knocking out *Smo*, necessary for the activation of the intracellular *Shh* signalling, the embryos demonstrated reduction of the ventral telencephalon and expansion of the pallium (Fuccillo *et al.*, 2004). This work revealed the temporal competence of cells to respond to *Shh*.

The role of *Shh* in patterning of the dorsal telencephalon has been questioned. Hayhurst *et al*. 2008, suggested that *Shh* induces the dorsal midline through the regulation of *Fgf8* and *Bmp4* expression by performing an *in vitro* study that revealed that the use of HhAntag, a *Shh* signalling pathway inhibitor, caused loss of *Fgf8* and *Bmp4* expression (Hayhurst *et al.*, 2008). This work shows that *Shh* expression controls at least in part dorsal telencephalic patterning through *Fgf8* and *Bmp4*. These results where contradicted with *in vivo* experiments on *Shh* mutant mice that develop a dorsal telencephalic midline and two expanded cortical hemispheres (Rash and Grove, 2007). Although these studies contradict each other they provide valuable insight into the complicated mechanism of telencephalic development.

Shh has been shown to demonstrate accelerated molecular evolution (Dorus *et al.*, 2006). In fact, this acceleration was reported particularly in the lineage leading to humans posing *Shh* as a potential contributor to the evolution of primate and human-specific neural traits (Dorus *et al.*, 2006).

d) **Antihem**

The ventricular zone of the ventral pallium is defined as the antihem positioned at the pallial-subpallial boundary forming a narrow stripe along the entire anterior-posterior axis of the telencephalon and secretes *Fgf7*, *Fgf15, Tgfα* and *Sfrp2* (Assimacopoulos *et al.*, 2003, Borello *et al.*, 2008). The functions of the antihem have not yet been elucidated and further research is required for these to be established.

Phenotypic analysis of different mutant mice allowed the better understanding of the antihem functions. In *Fgf15*$^{-/-}$ mutant mice dorso-lateral patterning is disrupted and specifically *COUP-TF1*, a caudo-ventral cortical fate and differentiation promoter, expression levels are reduced (Borello *et al.*, 2008). Also, *Pax6* mutant mice lack antihem signals and the boundary between dorsal and subpallial regions is disrupted (Assimacopoulos *et al.*, 2003). These studies provide valuable insights into the antihem functions yet the analysis should be cautious as for example in the *Fgf15*$^{-/-}$ mutant mice the patterning defects could be at least partially caused by the loss of *Fgf15* in the septum.

Finally, *Sfrp2* is one of the five members of the Sfrp gene family that directly inhibits Wnt signalling (Kawano and Kypta, 2003). Wnts transduce their signal through the Frizzled family of Wnt receptors and Sfrps possess a cysteine-rich domain of Frizzled that directly interacts with the Wnt ligand (Bhanot *et al.*, 1996, Kawano and Kypta, 2003). Analysis of *Pax6*$^{-/-}$ mutant mice showed loss of *Sfrp2* and *Wnt7b* expression in the PSPB and greatly reduced expression in the spinal cord (Kim *et al.*, 2001). Moreover, it was suggested that the expression of the Wnt antagonist *Sfrp2* at the antihem may

provide positional information in the region (Subramanian *et al.*, 2009). Although these suggestions are intriguing no concrete evidence has yet been provided for the antihem's role in patterning.

Overall, patterning centres have been identified in the cortical primordium, and existing evidence indicates that these regulate development of the telencephalon along both the anterioposterior and dorsoventral axes. Some of the studies mentioned above together with studies of embryonic signalling centres in the limb bud or in non-mammalian vertebrates suggest that the above mentioned signalling centres may also interact to regulate one another. For example, an interesting study showed that the maintenance of hem Wnt signaling and hippocampal development require a constraint on the *Fgf*8 (Shimogori *et al.*, 2004) suggesting a cross-regulation between Wnt and Fgf signalling. In conclusion, it appears that embryonic signalling centres and their interactions are crucial for normal cortical patterning.

1.1.2.2 Several transcription factors are implicated in regionalisation

Cues in the vicinity of these signalling centres respond to the reception of these signals by activating specific transcription factors. These in turn activate intrinsic cellular programmes that cause progenitors to acquire specific fates. For the purpose of this thesis I focused on the analysis of two major transcription factors expressed in the telencephalon: the *Foxg*1 and *Pax6*.

Forkhead transcription repressor (Foxg1 or BF1) is a crucial regulator of telencephalic development and FOXG1-truncating mutations have recently been identified in two patients affected by the congenital variant of Rett syndrome (Ariani *et al.*, 2008, Florian *et al.*, 2012). *Foxg1* is one of the earliest transcription factors expressed and it remains expressed throughout the telencephalon during embryonic development. *Foxg1* expression starts early at the neural plate stages in telencephalic anlage and mice lacking *Foxg1* have smaller cerebral hemispheres with loss of ventral telencephalic structures (Xuan *et al.*, 1995, Martynoga *et al.*, 2005). In these mutants, *Wnt* and *Bmp* expression is expanded (Dou *et al.*, 1999, Muzio and

Mallamaci, 2005) and *Shh* signalling is lost in the subpallium (Huh *et al.*, 1999, Martynoga *et al.*, 2005). Moreover, Martynoga *et al*., 2005 showed that markers of ventral telencephalic cell fate are never expressed in the *Foxg1*$^{-/-}$ telencephalon, suggesting that this transcription factor is required for the induction of ventral fates in the telencephalon. A recent study identified that *Foxg1* is a key downstream effector of the Shh pathway and that it inhibits Wnt/β-catenin signalling through direct transcriptional repression of *Wnt8b* expression (Danesin *et al.*, 2009). Overall, the above studies emphasize the position of *Foxg1* as a key regulator of several aspects of the telencephalic development while it appears to have a key role in patterning by integrating two opposing signalling centres.

Pax6 is an evolutionary conserved paired box domain transcription factor expressed by cortical progenitors in a low caudomedial to high rostrolateral gradient that opposes the expression of *Emx2* (Bopp *et al.*, 1986, Bishop *et al.*, 2000). *Pax6* is the earliest expressed gene of the *Pax* family and is almost exclusively confined to the developing nervous system (Walther and Gruss, 1991). *Pax6* mutant lack eyes and nasal placodes, have severe brain deformations, and die peri-partum (Hogan *et al.*, 1986, Hill *et al.*, 1991, Schmahl *et al.*, 1993, Manuel and Price, 2005). *Pax6* heterozygous mutants are viable, but show eye defects (Hogan *et al.*, 1986). Although the *Pax6* phenotype has been known since 1967 (Hogan *et al.*, 1986), it was only confirmed to be due to *Pax6* mutation in 1991 (Hill *et al.*, 1991). Loss of *Pax6* expression leads to the failure of the establishment of several expression boundaries and dorsal expansion of *Dlx1* and *Vax1* ventral telencephalic markers (Stoykova *et al.*, 2000). Moreover, *Pax6* is thought to specify dorsal regions, acting as a negative regulator of ventrally expressed genes including *Shh* (Grindley *et al.*, 1997) while there is also evidence to suggest *Pax6* is negatively regulated by *Shh* (Macdonald *et al.*, 1995), implying a two-way regulation system of dorsal-ventral patterning. Hence, these studies reveal a complex network in which *Pax6* has a leading role.

Overall these examples revealed that patterning requires unique expression and combinations of expression of these transcription factors in time and space to establish the various telencephalic territories. During and after patterning, telencephalic progenitors will proliferate and eventually differentiate into neurons

that will extend axons that will form tracts. How neurogenesis and neuronal specification occurs will be briefly outlined below.

1.2 Cortical lamination

1.2.1 A brief description of neurogenesis

Neurogenesis, neuronal migration and projectional identity are tightly controlled and occur simultaneously to patterning of the telencephalon. The neuroepithelium is initially a single sheet of cells that during neurogenesis will divide and give rise to six horizontal cell layers and numerous cell types including neocortical excitatory projection neurons, GABA (γ-aminobutyric acid) containing interneurons, astrocytes and oligodendrocytes (Doetsch *et al.*, 1999, Anderson *et al.*, 2002, Gorski *et al.*, 2002, Bedard and Parent, 2004). The division of neuroepithelial cells can be either symmetric by which two daughter cells with the same fate will be generated or asymmetric by which the two daughter cells have differing fates (McConnell, 1995, Rakic, 1995, Gotz and Huttner, 2005). From the division of the neuroepithelial cells, two more fate-restricted progenitor cell types can be generated; radial glial cells and basal progenitors (Kriegstein and Gotz, 2003, Miyata *et al.*, 2004, Noctor *et al.*, 2004, Gotz and Huttner, 2005). Radial glial cells serve both as progenitors (Malatesta *et al.*, 2003) and as a scaffold for the migration of neurons by extending a long basal process to the pia surface and a shorter process to the ventricle (Rakic, 1972, Rakic, 2003). Recently, it was also established that non-ventricular radial glia-like cells are present in the outer subventricular zone which is prominent in primate corticogenesis (Hansen *et al.*, 2010). Finally, basal progenitors originate from neuroepithelial and/or radial glial cells mitosis and are believed to function to increase the number of neurons by adding an additional round of division (Haubensak *et al.*, 2004). In this manner, multiple progenitors contribute to the rich variety of neuronal subtypes found in the neocortex.

1.2.2 **Neuronal specification in the neocortex**

The neocortex is composed of six layers (I-VI) that form in an "inside-out" manner and are cytoarchitectonically and functionally distinct. From inside to outside, cortical lamination comprises: the **ventricular zone** (VZ), the primary germinal zone adjacent to the ventricle which together with the later formed subventricular zone (SVZ) contain progenitor cells; the **intermediate zone** (IZ) through which projection neurons migrate and also contains axons that will form the white matter at postnatal stages; **layer VI** that contains projection neurons of the corticothalamic tract and to a lesser extend callosal neurons; **layer V** which mainly contains subcerebral projections and callosal neurons; **layer IV** that contains pyramidal cells and is the main recipient of thalamocortical projections; **layers II/III** that contain projection neurons that project intracortically and contribute significantly to the corpus callosum; layer I or **marginal zone** which contains Cajal-Retzius cells, the main source of reelin (Molyneaux *et al.*, 2007, Defelipe, 2011, Fame *et al.*, 2011, Kwan *et al.*, 2012). The earliest born neurons appear at E10.5 and form the preplate that will eventually split into the marginal zone and the subplate layer. The cortical plate, that will give rise to the layers II-VI, will form between the marginal zone and the subplate layer (Kandel *et al.*, 2000) (Figure 1-4). It is also important to mention that progenitors produce the projection neurons of the different neocortical layers in a tightly controlled temporal order from embryonic day (E) 11.5 to E17.5 in the mouse (Angevine and Sidman, 1961).

Focused analysis of specific projection neurons is a complex task since neurons in different layers have different electrophysiological properties and responses to neurotransmitters and form different axon tracts. Only from an anatomical point of view I will focus on distinct axon paths: the corpus callosum, the corticothalamic/thalamocortical tract and the lateral olfactory tract.

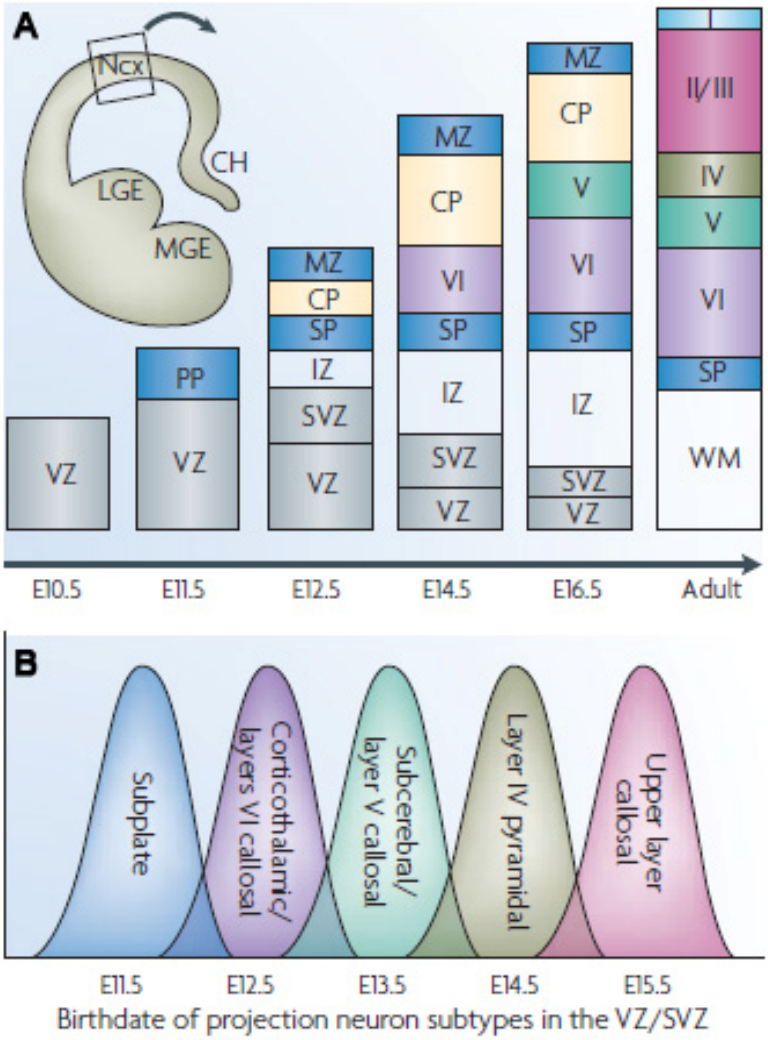

Figure 1-4:Schematic of the cortical layers and of the production of cortical projection neurons.

The preplate splits into the marginal zone and the subplate with the cortical plate residing between the latter. The six-layered cortex will form in an "inside-out" manner as late born neurons will surpass early born neurons and be positioned above them. (B) Projection neurons form in temporal overlapping waves from E11.5 onwards. Abbreviations: ncx, neocortex; ch, choroid plexus; LGE, lateral ganglionic eminence; MGE, medial ganglionic eminence (Molyneaux *et al.*, 2007).

1.3 Neocortical projections: corpus callosum and corticothalamic tract

1.3.1 Corpus callosum: anatomy and anatomical defects

The corpus callosum (CC) was first described in 1836 by Owen in the brain of placental mammals [reviewed in (Aboitiz and Montiel, 2003)]. The CC is the largest white matter tract in the brain residing in the depths of the great longitudinal fissure and connecting left and right hemispheres (Figure 1-5). Mid-sagittal sections of the CC from rostral to caudal allow the segmentation of the CC into the rostrum, genu, truncus, isthmus and splenium (Figure 1-5) (Ariens-Kapers *et al.*, 1936). In a healthy brain, the number of callosal fibres is already fixed around birth but structural changes occur during postnatal development, including myelination, redirection and pruning (Luders *et al.*, 2010).

It is suggested that the role of the CC is to mediate the interhemispheric transfer of sensory, motor and cognitive information between the cerebral hemispheres (Paul *et al.*, 2007). However, this suggestion is highly debatable. The classical experiments on "split-brain patients", whose callosum is severed to treat epilepsy, showed surprisingly subtle defects in everyday life when information is presented to each hemisphere independently (reviewed in (Paul *et al.*, 2007)). Yet, it is known that the CC is not the only tract connecting the hemispheres and for example the anterior commissure, which is not severed in "split-brain" patients, is also believed to mediate information. Although the above experiments have not provided a clear role of the CC, another disorder has also provided valuable information regarding the corpus callosum function and the role of altered connectivity in developmental disorders: the agenesis of the corpus callosum.

Agenesis of the CC is a developmental disorder i.e. present from birth that can manifest as partial agenesis e.g. in only the rostral or caudal region, hypoplasia of the entire structure or complete agenesis. Malformations of the CC are amongst the most

common brain anomalies found at birth and are thought to occur in up to 7/1000 of the total new born population (Bedeschi *et al.*, 2006). Agenesis of the CC is associated with more than 50 congenital syndromes (Richards *et al.*, 2004, Paul *et al.*, 2007). Recently, many disorders have been linked with the underconnectivity theory i.e. the underfunctioning of integrative circuitry and emergent cognitive, perceptual, and motor abilities with any facet of psychological or neurological function that is dependent on the **coordination** or **integration** of brain regions being susceptible to disruption, (Just *et al.*, 2004) for example autism (Hughes, 2007, Minshew and Williams, 2007, Anderson *et al.*, 2011), neuropsychiatric disorders including patients with deletion of the *disrupted-in-schizophrenia 1* (*DISC1*) gene (Parraga *et al.*, 2003), sleep disorders (Nielsen *et al.*, 1992) or even "phantom limb" sensations (Simoes *et al.*, 2012) causing a variety of behavioural and neurological consequences. For example patients with agenesis of the CC have shown normal intelligence quotients (IQ) but have trouble with meta-linguistics, or the secondary meanings of language e.g. struggling to understand things like jokes, sarcasm and figures of speech (Paul *et al.*, 2003). Overall, research in the field of agenesis of the CC and under-connectivity of the brain is promising for multiple scientific fields including developmental neuroscience. The pathogenesis of CC agenesis is complex since there are many developmental processes involved in the formation of the fully formed CC and the developmental mechanisms determining CC formation are not fully understood.

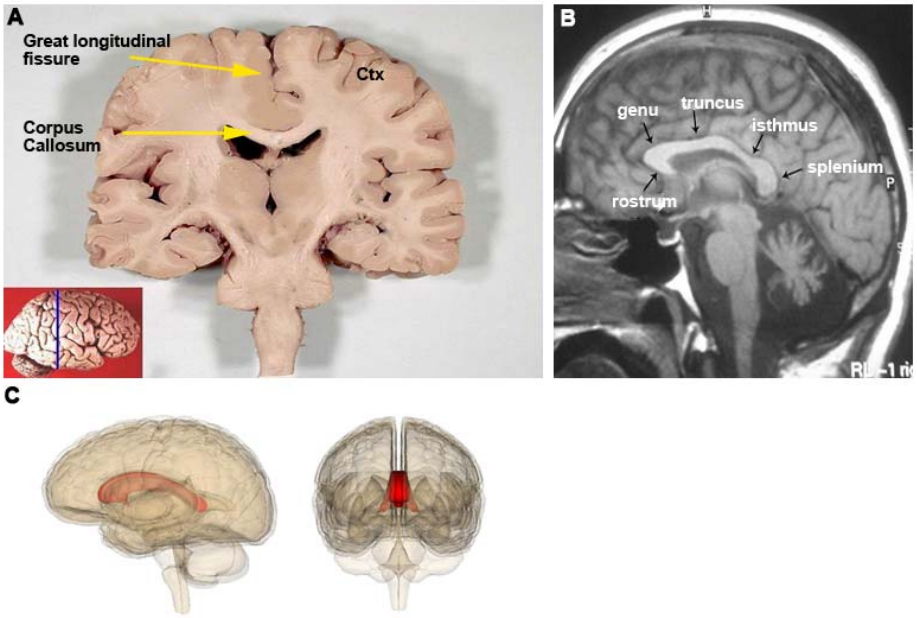

Figure 1-5:Anatomy of the corpus callosum.

(A) Coronal section of a human brain showing that the CC forms in the depth of the great longitudinal fissure (arrow) (University of Utah, Health Science Library). (B) MRI scanning of a human brain. Different anatomical regions of CC are illustrated (Aribandi, 2011). (C) Sagittal and dorsal view of a schematic representation of the CC position into the brain (Anatomography, Life Science Databases LSDB). Abbreviations: ctx, neocortex.

1.3.2 Corpus callosum development: cellular and molecular interactions

The study of mouse mutants in which CC development is disrupted has provided useful insight into the cellular and molecular mechanisms involved in this process.

Extensive studies of mouse mutants revealed that callosal projection neurons reside in cortical layer VI (few), born at approximately embryonic day E12.5; layer V (20%), born at around E13.5; and upper layers II/III (80%), born late in development around E15.5 (Angevine and Sidman, 1961, Aboitiz and Montiel, 2003). Callosal neurons send their axons ventrally towards the intermediate zone where they project towards the midline, cross it at the corticoseptal boundary (CSB) and innervate the contralateral hemisphere (Richards *et al.*, 2004). The CSB separates cortex and septum and represents a border for the differential expression of genes.

In the developing brain, axons use a number of cues to find their correct path i.e. intermediate targets and cell-cell interactions. Intermediate targets express either attractant or repellent guidance cues, which guide callosal axons to cover long distances (Lindwall *et al.*, 2007). At the CSB, callosal axons are guided through a number of cues including the pre-existing pioneer axons originating from the cingulate cortex (Rash and Richards, 2001), the midline glial populations (Shu and Richards, 2001, Shu *et al.*, 2003) and the callosal sling (Silver *et al.*, 1982, Niquille *et al.*, 2009):

a) **pioneer axons**: pioneer neurons at the cingulate cortex project axons that cross the midline and provide a path for the later arriving CC axons. These axons cross the midline at around E16 in mice (Rash and Richards, 2001). Cingulate pioneers express Neuropilin1 (Nrp1) and *Nrp1* knockin mice, in which Nrp1 is unable to bind to its high affinity receptor class 3 semaphorins (Sema) (He and Tessier-Lavigne, 1997), show malformation of the corpus callosum (Piper *et al.*, 2009). A recent study revealed that the axon guidance molecule Netrin1 is attractant to callosal pioneer axons derived from the

cingulate cortex but not for later arriving neocortical callosal axons (Fothergill *et al.*, 2013).

b) **midline glial populations** (Figure 1-6): these populations involve three main structures: the indusium griseum (IG), the glial wedge (GW) and the midline zipper glia (MZG) (Shu and Richards, 2001, Shu *et al.*, 2003). The indusium griseum is located dorsally to the CC, the glial wedge is a bilaterally symmetrical structure composed of glia and located ventrally to the CC and finally the MZG is extended in the septal midline. Around E16.5 radial glial cells translocate from the glial wedge at the ventricular zone to the indusium griseum at the pia surface and *Fgf* signalling is necessary and sufficient to control this translocation (Smith *et al.*, 2006). Glial cells of the glial wedge and the indusium griseum are located adjacent to callosal axons (Shu and Richards, 2001) and prevent them from migrating into the septum by producing the repellent axon guidance molecule *Slit1/2* (Bagri *et al.*, 2002, Shu *et al.*, 2003). Robo proteins are expressed at the growth cones of the callosal axons and are acting as Slit receptors.

c) **callosal sling (**Figure 1-6**)**: the sling consists of several neuronal populations i.e. Calbindin+ and GABAergic neurons and Calretinin+ glutamatergic neurons that are located within the CC and at the subcallosal sling. GABAergic neurons derive from the medial and caudal ganglionic eminence, migrate into the corpus callosum and channel axons across the midline (Niquille *et al.*, 2009, Niquille *et al.*, 2013). Moreover, Calretinin+ and Calbindin+ neurons located in the indusium griseum and in the cingulate cortex express the *Sema3C* attractant guidance factor which is required for callosal development (Niquille *et al.*, 2009, Piper *et al.*, 2009). Calretinin+ neurons are also detected within the corpus callosum where they delineate its dorsal and ventral components.

Another key region for CC development is the commissural plate where the corpus callosum, the hippocampal and the anterior commissures normally cross the midline. This region is delineated by several transcription factors including nuclear factor I

family (Nf1a) (Shu T, 2003), empty spiracles homologs (Emx1) (Qiu *et al.*, 1996) and sine oculis-related homeobox 3 (Six3) (Oliver *et al.*, 1995). Six3 is an important regulator of early forebrain development and mice mutant for *Emx1* or *Nf1a* lack the corpus callosum (Qiu *et al.*, 1996, Shu T, 2003). It was suggested that the correct formation of the commissural plate during patterning stages is essential for proper forebrain commissures development (Moldrich *et al.*, 2010). However, this result is debatable since the formation of the commissural plate during patterning stages was not extensively analysed.

Overall, CC development can be affected by defects in neurogenesis, axon growth and guidance, glial development and patterning of the midline. Several studies have already described that defects in each of these factors cause agenesis of the CC. Although understanding each factor independently is crucial and highly informative, it is plausible that each of the above mentioned factors work in combination with each other. Thus, understanding this connection will possibly lead to comprehending how the fully formed CC is produced. For the purpose of this thesis, I focused on elucidating the molecular mechanisms that control the positioning of the guidance cues at the midline during patterning stages.

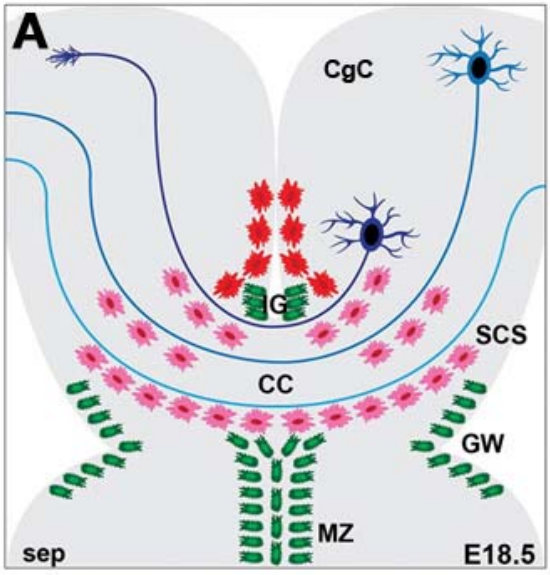

Figure 1-6:Schematic illustration of corpus callosum intermediate targets in E18.5 brains.

(A) Callosal axons (blue and light blue) cross the corticoseptal boundary at the midline region. Midline glial structures including indusium griseum (IG), glial wedge (GW) and midline zipper glia (MZG) (green cells). Calretinin+ glutamatergic neurons are positioned within the callosal tract (pink cells) and Calbindin+ neurons are positioned above the callosal axons (red cells). Abbreviations: CC, corpus callosum; Cgc, cingulate cortex; GW, glial wedge; IG, indusium griseum; MZ, midline zipper glia; SCS, subcallosal sling (Magnani *et al.*, 2012a).

1.3.3 **Corticothalamic tract: function and topography**

The neocortex and thalamus connect with each other through reciprocal connections: the corticothalamic (CTA) and thalamocortical tracts (TCA). The thalamus is not merely a relay station that relays periphery derived sensory information to the cortex (except olfactory input). Instead the cortex and thalamus represent an integrated unit through which thalamic transmission of input reaches the cortex for cortical processing (Sherman and Guillery, 2002). In return, the corticothalamic tract conveys processed sensory information to thalamic neurons to influence activity patterns and sensory responses in the thalamus. Thus, this axonal network is crucial for the synchronisation of cortex and thalamus.

During embryonic development, corticothalamic projection neurons send out their axons in a coordinated manner. Corticofugal axons initially grow laterally through the cortical intermediate zone to reach the pallial/subpallial boundary (PSPB) and after a waiting period, CTAs start crossing the PSPB in a widespread manner and extend deeply into the ventral telencephalon (Molnar and Cordery, 1999, Jacobs *et al.*, 2007). At the front of the internal capsule, CTAs pause until more dorsally derived axons have grown the extra distance (De Carlos and O'Leary, 1992). The axons project through the internal capsule at 15.5 and eventually cross the diencephalic-telencephalic boundary and pause once again around E17.5 (Jacobs *et al.*, 2007). Here, the corticothalamic axons enter the prethalamus and accumulate at the reticular thalamic nucleus and perireticular thalamic nucleus before innervating the appropriate nuclei (Molnar and Cordery, 1999, Jacobs *et al.*, 2007) (Figure 1-7). Overall, the CTAs need to cover large distances, change direction several times and pass through a variety of brain territories.

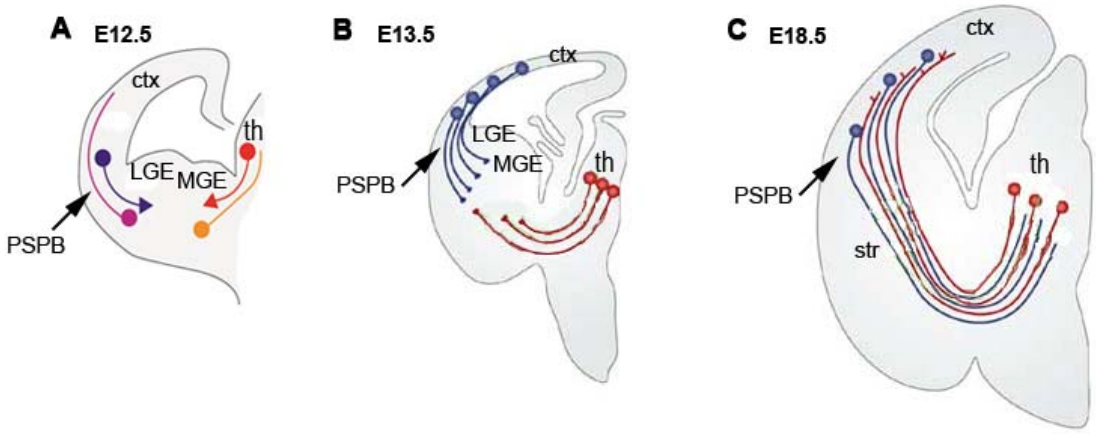

Figure 1-7:Schematic representation of corticothalamic tract development.

(A) Pioneer neurons within the ventral telencephalon provide scaffolds for CTAs (blue) and TCAs (red). Two populations of pioneer neurons are present, one in the LGE (purple) and one in the MGE (yellow). (B) Corticofugal axons (blue) project towards the ventral telencephalon and pause at the PSPB. Thalamic axons (red) have reached the ventral telencephalon. (C) Neocortex and thalamus are connected at E18.5 brains. Abbreviations: ctx, neocortex; LGE, lateral ganglionic eminence; MGE, medial ganglionic eminence; PSPB, pallial subpallial boundary; str, striatum; th, thalamus (Lopez-Bendito and Molnar, 2003).

1.3.4 **Corticothalamic tract**

Corticothalamic neurons as part of corticofugal projection neurons extend axonal projections 'away' from the cortex. These include subcerebral projection neurons and corticothalamic neurons. Corticofugal projections derive from subplate, and layer V and VI glutamatergic neurons while corticothalamic neurons are located in cortical layer VI, with a smaller population in layer V. Subplate neurons act as **pioneers** for the layer V/VI corticothalamic projections (McConnell *et al.*, 1989, Ghosh *et al.*, 1990, Ghosh and Shatz, 1993, Allendoerfer and Shatz, 1994). In particular a recent study showed that subplate axons are the first to reach the internal capsule (Jacobs *et al.*, 2007) and ablation of the subplate layer in cats leads CTAs to fail to innervate appropriate thalamic nuclei (McConnell *et al.*, 1994). Axons from layer VI neurons project to different thalamic nuclei i.e. visual projections terminate to the lateral geniculate nucleus, primary somatosensory cortical projections to the ventrobasal complex and auditory projections to the medial geniculate nucleus (Guillery, 1967, Jones and Powell, 1968, Diamond *et al.*, 1969). The temporal order in which these axons innervate the thalamus remains to be elucidated. For example, experiments in hamsters (Miller *et al.*, 1993) and ferrets (Clasca *et al.*, 1995) showed primarily axons of layer V in the thalamus of hamsters from P3-P5 while in ferrets layer V axons arrive at the thalamus much earlier.

Corticothalamic tract formation is a multifactorial process. The **PSPB** is a key decision point, as in this region CTAs experience a waiting period, change direction by sharply turning medially and change territory by radiating into the subpallium. Surprisingly, CTAs are defasciculated at the PSPB and striatum and radiate into the ventral telencephalon over a widespread domain in contrast to their normal fasciculated path in the cortex, MGE and thalamus. The PSPB is primarily a gene expression boundary characterised by the opposing domains of *Pax*6 and *Gsh*2 expression (Stoykova and Gruss, 1994, Yun *et al.*, 2001). *Pax*6 is expressed in cortical progenitors while *Gsh*2 is expressed in subpallial progenitors (Bishop *et al.*, 2000, Yun *et al.*, 2001). Many mutants including *Pax*6 knock-out mice, *Tbr*1 or

*Gbx*2 mutant mice show axon guidance defects at this boundary (Hevner *et al.*, 2002). As mentioned before, the CTA trajectory changes as they cross the PSPB and they begin to associate with the thalamocortical tract as they proceed to their target areas (Molnar *et al.*, 1998). The CTA/TCAs trajectory has been extensively studied by using different methods. An *in vitro* study, performed in poly-L-lysine, showed that CTAs and thalamic axons collapse each other (Bagnard *et al.*, 2001) while a more recent *in vivo* study provided the clearest evidence today that CTAs are necessary and sufficient to navigate thalamic axons through the PSPB (Chen *et al.*, 2012).

There are also many **guidance cues** along the corticofugal axon path that guide CTAs to their final targets. These guidance molecules act either as attractants or repellents. In particular, several members of the Semaphorin class have been implicated as corticothalamic axon guidance molecules e.g. *Sema3E* is attractive for CTAs (Bagnard *et al.*, 1998). In addition a recent study showed that *PlexinD1* and its ligand *Sema3E* are mediating the "waiting period" of CTAs at the front of the internal capsule (Deck *et al.*, 2013). Interestingly, *Sema5B* is specifically repulsive to corticofugal axons but not to dorsal thalamic axons (Lett *et al.*, 2009) while *Sema3A* is repulsive to cortical axons but not to dendrites originating from the same cortical cell (Polleux *et al.*, 1998, Polleux *et al.*, 2000). The chemorepulsive activity of Sema5B or Sema3A (Polleux *et al.*, 1998, Lett *et al.*, 2009) may guide corticofugal axons towards the ventral telencephalon and away from the cortex. In addition, chemoattractant activity might also turn the CTAs towards the ventral telencephalon as shown by *in vitro* experiments for example with the axonal attractant Netrin-1 expressed at the internal capsule and in the ventral telencephalon (Metin *et al.*, 1997). Interestingly, a recent study revealed that Unc5c, a Netrin-1 receptor that mediates repulsion, is up-regulated in subplate cells compared to layer V/VI cells (Oeschger *et al.*, 2012). According to this study, this finding could indicate that Unc5c/Netrin-1 has a repulsive role in regulating CTA projections into the ventral telencephalon since this activity coincides with the first "pause" of the corticofugal axons at the PSPB (Oeschger *et al.*, 2012).

In the ventral telencephalon, three main axon guidance mechanisms are proposed for CTAs and TCAs guidance: (i) pioneer neurons in the lateral and medial ganglionic eminences constitute a scaffold for growing CTAs and TCAs that orientates their direction of growth by extending axons across the PSPS and the diencephalic-telencephalic boundary, respectively (Metin and Godement, 1996, Molnar *et al.*, 1998, Magnani *et al.*, 2010) (Figure 1-7); (ii) a permissive corridor formed by *Isl1*+ and *Ebf1*+ cells that guides TCAs through the ventral telencephalon (Lopez-Bendito *et al.*, 2006); and (iii) that CTAs and TCAs meet in the ventral telencephalon and guide each other to their target areas as suggested by the "handshake hypothesis" (Molnar and Blakemore, 1995b).

Overall, the corticothalamic and thalamocortical tracts play essential roles in the communication between the cortex and thalamus. During development, axons forming these tracts have to follow a complex path to reach their target areas. While much attention has been paid to the mechanisms regulating their passage through the ventral telencephalon, very little is known about how the developing cortex contributes to corticothalamic/thalamocortical tract formation.

1.4 Development of the paleocortex

1.4.1 Anatomical subdivisions and function of the paleocortex

The encoding of odors in the olfactory system essentially involves combined activation of olfactory sensory neurons that are positioned at the nasal placode and results in complex firing patterns from the olfactory epithelium to the olfactory bulb (Mombaerts, 2006, Gottfried, 2010). These firing patterns need to be precisely recognized by downstream structural targets in the brain. How olfactory cues map onto the brain and how the brain is optimized to recognize, categorize and discriminate them is a fundamental question. The complexity of olfactory cues and the need for correct odor perception is reflected in the anatomical organization of higher-order brain regions collectively known as the olfactory cortex or paleocortex.

From anterior to posterior the paleocortex consists of: the anterior olfactory nucleus, the olfactory tubercle, the piriform cortex (pc), amygdaloid nuclei and the entorhinal cortex (Devor, 1976, Derer *et al.*, 1977). Downstream relays from the olfactory cortex link odor inputs to systems associated with learning and memory i.e. hippocampus, amygdala or orbitofrontal cortex (humans) (Gottfried, 2010). These connections are of vital importance to enable smell to cause physiological and behavioral responses (Stevenson, 2010). Thus, it is crucial to understand the molecular and cellular mechanisms behind paleocortical development and hence identify potential links between its development and odor coding.

1.4.2 **Lateral olfactory tract**

Three major cell types reside within the olfactory bulb: projection neurons (mitral and tufted cells), local inhibitory interneurons (periglomerular and granule cells) and glia (Shipley and Ennis, 1996). Mitral and tufted cells are present in the bulb primordium at around E13.5. Mitral cells reside within a distinct lamina and each mitral cell sends one apical dendrite to a single glomerulus and an axon towards the piriform cortex (Bulfone *et al.*, 1998). The axons of the mitral cells fasciculate as they leave the bulb to form the lateral olfactory tract. During lateral olfactory tract (LOT) development, mitral cell axons exhibit a protracted waiting period in the lateral olfactory tract before emitting collateral branches and innervating the target olfactory cortex (Devor, 1976, Derer *et al.*, 1977, Hirata and Fujisawa, 1999). In the mouse the first LOT collaterals colonise the amygdala (E15.5) and one day later they colonise the piriform cortex (Hirata and Fujisawa, 1999). Only a few studies have addressed the mechanisms that govern LOT branching and many open questions remain regarding guidance cues implicated in the collateralization of LOT axons or how synaptic connections between the different structures of the olfactory system are relevant to the formation of the LOT.

Many cellular and molecular mechanisms guide the axons of the LOT to innervate the piriform cortex. Cues from the telencephalon are likely to govern LOT formation

(Jimenez *et al.*, 2000). For example, in *Pax*6 mutants which form an OB-like structure mitral cell axons project towards the piriform cortex and form a LOT (Jimenez *et al.*, 2000). In *Lhx*2 mutants, an OB-like structure forms but the LOT axons grow only a few microns (Saha *et al.*, 2007). Yet, *Lhx*2 conditional inactivation in the dorsal telencephalon results in mitral cell axons projection to an ectopic piriform cortex (Chou *et al.*, 2009).

Moreover, the fact that cues from the telencephalon guide LOT axons is reinforced by a contact mediated mechanism that has been proposed to guide LOT axons. Early generated cells (lot cells) are believed to form in the dorsal pallium at E10.5 (Tomioka *et al.*, 2000) and to migrate from their original position to the piriform cortex where they are juxtaposed to the LOT axons (Sato *et al.*, 1998, Hirata *et al.*, 2001). The lot cells are thought to restrict LOT axon growth either through an attractant or repellent mechanism (Hirata *et al.*, 2001). The molecular mechanisms underlying lot cell migration have been extensively analyzed. *Sema3F* restricts lot cells migration to the pia (Ito *et al.*, 2008) while *ephrinA5* prevents their migration to the subpallium (Nomura *et al.*, 2006) and *Netrin-1* attracts lot cells to surround the piriform cortex (Kawasaki *et al.*, 2006).

A few secreted cues expressed by the telencephalon have also been implicated in the formation of the LOT. In brief, *Slit1/2* are major chemorepellents of LOT and single or double mutants for *Slit1* or *2* demonstrate major disturbances of the LOT formation including axons crossing to the contralateral hemisphere (Nguyen-Ba-Charvet *et al.*, 2002, Fouquet *et al.*, 2007). Although the secreted semaphorins of the Sema3 class are expressed by OB axons, they do not seem to influence LOT axon guidance (de Castro *et al.*, 1999, Kawasaki *et al.*, 2006). The extracellular matrix component Anosmin1 promotes the outgrowth of OB axons and this molecule is produced by LOT axon targets i.e. the olfactory cortex (Soussi-Yanicostas *et al.*, 2002). Finally, Sema*6A* mutant mice show aberrant axonal connectivity including LOT extending far further caudally than normal (Runker *et al.*, 2011). Thus, it could be proposed that external cues present in the telencephalic environment must orient this outgrowth towards the different target cells in the olfactory cortex.

1.4.3 **Piriform cortex morphology and development**

The piriform cortex (from Latin *pirum*, pear) is the largest subdivision of the olfactory cortex and the first cortical destination of olfactory information (Suzuki and Bekkers, 2007). In mice, the piriform cortex is located bilaterally in the ventrolateral forebrain and it is subdivided into anterior and posterior regions (Ekstrand *et al.*, 2001). The piriform cortex is a phylogenetically ancient, laminated structure with only 3 layers (Figure 1-8) that receives monosynaptic input from the olfactory bulb through the lateral olfactory tract (LOT) (Schwob and Price, 1984a). Although the piriform cortex mainly derives from the dorsal telencephalon its development and maturation is different from the adjacent neocortex. Rat experiments demonstrated that the piriform cortex lacks a cortical plate, yet it develops in an "inside-out" fashion (Schwob and Price, 1984a, Bayer *et al.*, 1991).

The organization of the piriform cortex from outside to inside contains (Figure 1-8): **layer I**, with afferent projections from the mitral cells and tufted cells of the olfactory bulb which collectively form the LOT (superficial part Ia), associational fibers from within the piriform cortex (deeper part Ib) (Sarma *et al.*, 2011) and a few neuronal somata; **layer II**, with glutamatergic superficial pyramidal cells which establish synaptic connections with the LOT and semilunar excitatory cells; **layer III**, with glutamatergic deep pyramidal cells (Haberly and Behan, 1983, Suzuki and Bekkers, 2007). Inhibitory interneurons are located in all layers and modulate the activity of pyramidal neurons (Suzuki and Bekkers, 2007).

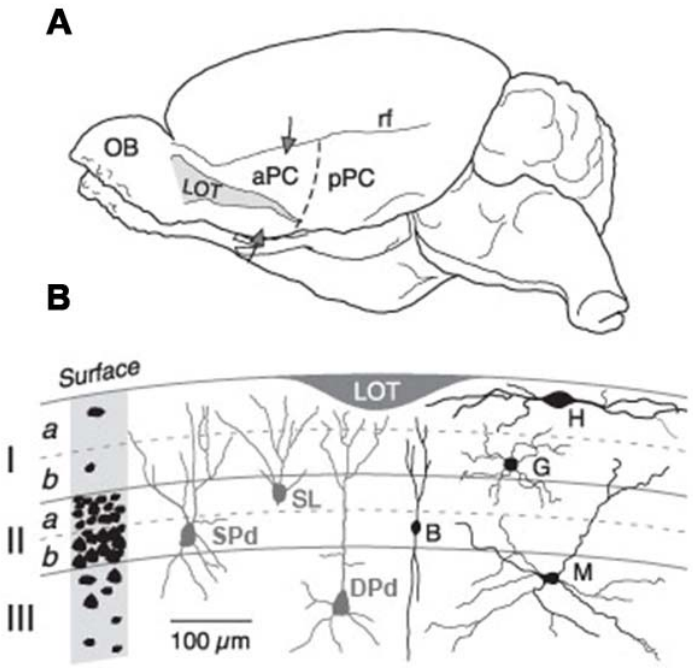

Figure 1-8: Schematic representation of the piriform cortex morphology.

(A) Anatomic illustration of the mouse brain. The piriform cortex is positioned at the ventrolateral end of the forebrain beneath the rhinal fissure. The LOT projects to the anterior piriform cortex (arrow). The end of the LOT is the boundary between anterior and posterior pc (dashed line). (B) Illustration of the 3 layered piriform cortex. Layer I contains the LOT and association fibers. Layer II contains excitatory semilunar cells (Sl) and superficial pyramidal neurons (SPd). Layer III contains deep pyramidal neurons (DPd). Inhibitory interneurons reside in all 3 layers of the piriform cortex (B: bitufted; G: neurogliaform; H: horizontal; M: multipolar). Abbreviations: aPC, anterior piriform cortex; LOT, lateral olfactory tract; OB, olfactory bulb; pPC, posterior piriform cortex; rf, rhinal fissure. (Suzuki and Bekkers, 2007).

Neuroepithelial progenitors from various dorsal and ventral telencephalic regions contribute to the piriform cortex (Figure 1-9). The majority of glutamatergic neurons derive from a progenitor lineage defined by the expression of the Emx1 transcription factor (Bishop *et al.*, 2000, Gorski *et al.*, 2002). In particular, the lateral pallium is thought to contribute to the mature olfactory cortex (Puelles *et al.*, 2000) while the ventral pallium contributes a population of cells in the deep layers of the piriform cortex (Hirata *et al.*, 2002). The dorsal pallium gives rise to the lot+ cells which migrate tangentially and ventrally down towards the LOT of the piriform cortex (Tomioka *et al.*, 2000). The dorsal most part of the LGE contributes *Dlx*2-lineage cells to the olfactory cortex and the olfactory tubercle through the lateral cortical stream (Hirata *et al.*, 2002, Carney *et al.*, 2006). In contrast, the majority of inhibitory neurons originate from the subpallium located mainly in the MGE and caudal ganglionic eminence (Suzuki and Bekkers, 2007). A recent fate mapping study, has also demonstrated *de novo* formation of glutamatergic pyramidal neurons from oligodendroglia progenitors within the adult murine piriform cortex (Guo *et al.*, 2010). These studies demonstrate the complex development of the piriform cortex and emphasize its mosaic nature.

Piriform cortex development is controlled by various transcription factors. Conditional deletion of *Lhx*2, a LIM homeodomain transcription factor gene in the dorsal telencephalon, results in the formation of an ectopic piriform cortex suggesting a *Lhx*2 dependent regulation of the regional fate of lateral neocortex/piriform cortex (Chou *et al.*, 2009). However, this *Lhx2* dependent mechanism is not elucidated yet.

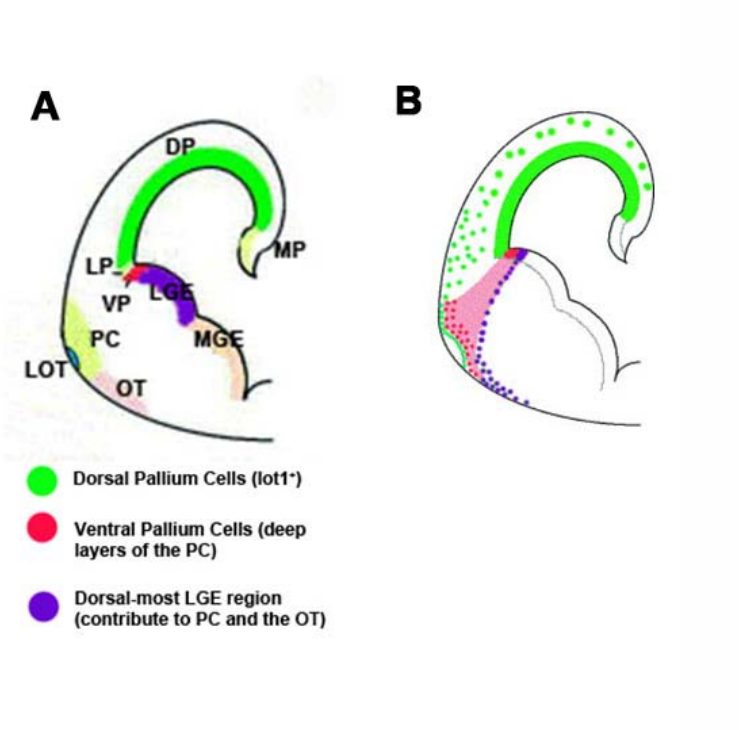

Figure 1-9: Schematic representation of the different telencephalic regions and how they contribute to the mosaic development of the piriform cortex.

(A) Schematic illustration of the different telencephalic regions including DP: green; LP: yellow; VP: red; LGE: purple; MGE: light brown. (B) Schematic illustration of colour coded cell contribution to the piriform cortex. Lot1+ cells derive from the DP. The VP contributes deeper layer cells of the piriform cortex and from the dorsal most part of the LGE originates *Dlx*2-lineage cells to the olfactory cortex and the olfactory tubercle. (Hirata *et al.*, 2002)]. Abbreviations: DP, dorsal pallium; LGE, lateral ganglionic eminence; LP, lateral pallium; LOT, lateral olfactory tract; MGE, medial ganglionic eminence; MP, medial pallium; OT, olfactory tubercle; PC, piriform cortex; VP, ventral pallium.

Moreover, mutants for *Dmrt5* a doublesex and mab-3-related transcription factor show an expansion of the piriform cortex (Saulnier *et al.*, 2012). In contrast in BF1 mutants when the ventral telencephalon is almost completely deleted the paleocortex is undetectable (Vyas *et al.*, 2003). Interestingly, these studies have only analysed the piriform cortex phenotype in these mutants without addressing the molecular mechanisms behind it.

Finally, the piriform cortex is the first cortical destination of olfactory information responsible for odor processing. Thus, understanding how it develops and how it connects with the other olfactory cortex structures and the OB is a fundamental question. Many studies have separately addressed the embryonic development of the piriform cortex and the formation of the LOT tract. Yet many questions remain regarding the role of the piriform cortex in LOT formation, LOT axon navigation and LOT axon colonisation. For the purpose of this thesis, I aim to elucidate a potential link between piriform cortex development and LOT formation.

1.5 The *Gli3* transcription factor

In mammals, *GLI3* is a member of the GLI-Krüppel family (Ruppert *et al.*, 1988) that also includes *GLI1* and *GLI2*. The GLI family encodes zinc finger transcription factors, which are closely related to each other and contain seven regions of similarity including the zinc finger domain (Ruppert *et al.*, 1990). *GLI3* is located on chromosome 7p13 in humans and its murine homologue is located on chromosome 13 (Vortkamp *et al.*, 1991). GLIs are homologues to *Drosophila cubitus interruptus* (*ci*) (Orenic *et al.*, 1990). In mammals and invertebrates, GLI and *ci* transcription factors act as transcriptional mediators of Shh and *hh* signalling, respectively (Ruppert *et al.*, 1990, Ingham and McMahon, 2001).

1.5.1 Human syndromes with various *Gli3* mutations

Mutations in the *GLI3* gene result in five syndromes including Greig cephalopolysyndactyly syndrome (GCPS) (Vortkamp *et al.*, 1991), Acrocallosal syndrome (Elson *et al.*, 2002), Pallister-Hall syndrome (Kang *et al.*, 1997), Postaxial polydactyly type-A (PAP-A) (Radhakrishna *et al.*, 1997) and preaxial polydactyly type-IV (PPD-IV) (Radhakrishna *et al.*, 1999). All are associated with limb defects and two coincide with brain abnormalities and mental retardation.

Acrocallosal syndrome was first described in 1979 (Schinzel, 1979). Features include postaxial polydactyly, hallux duplication, macrocephaly, absence of the CC and usually mental retardation. Acrocallosal syndrome is an autosomal recessive disorder (Schinzel and Kaufmann, 1986) with many clinical similarities to GCPS (Elson *et al.*, 2002). In fact, both type of patients display pre- and postaxial polydactyly and craniofacial abnormalities (Elson *et al.*, 2002, Johnston *et al.*, 2003, Johnston *et al.*, 2005). However, in GCPS patients the corpus callosum is usually present and these patients prevalently display a normal intellectual development (Bonatz *et al.*, 1997). Both syndromes can be caused by mutations in *GLI3* and the mutations vary from single point to large deletions or deletion of genes that flank *GLI3* (Elson *et al.*,

2002, Johnston *et al.*, 2003, Speksnijder *et al.*, 2013). The point mutation is a G to C substitution affecting a conserved amino acid which changes Gli3 protein function (Elson *et al.*, 2002). A recent study described a missense mutation in the same Gli3 domain (Speksnijder *et al.*, 2013) as previously reported by Elson *et al*., 2002 and therefore confirming that some cases of Acrocallosal syndrome are due to mutations in *GLI3*. Finally, the deletions can include large regions of up to 2Mb or more (Johnston *et al.*, 2003), however, one of the break points is always located with *GLI3*.

For the purpose of this thesis, I was particularly interested to analyze corpus callosum development. *Gli3* mouse mutants represent an excellent way to do so and will also provide insights into the pathogenesis of these syndromes.

1.5.2 *Gli3* mouse mutants

Understanding the pathogenesis of *GLI3* mutations was facilitated by the analyses of mouse mutants and comparing this data with human data. As mentioned above, the *GLI3* gene was mapped on chromosome 7p13 (Vortkamp *et al.*, 1991). Deletion of *Gli3* was identified in the $Gli3^{XtH/XtH}$ and $Gli3^{XtJ/XtJ}$ mouse (Schimmang *et al.*, 1992, Maynard *et al.*, 2002). $Gli3^{XtJ/XtJ}$ mutants have a deletion of 51.5Kb including most of the zinc finger coding domain and the complete 3' region (Maynard *et al.*, 2002). $Gli3^{XtH/XtH}$ mutants have a loss of the promoter and the 5' region (Vortkamp *et al.*, 1991, Schimmang *et al.*, 1992). $Gli3^{Xt/Xt}$ and $Gli3^{XtJ/XtJ}$ mutants represent null mutants and are considered to be the mouse homolog of GCPS (Winter and Huson, 1988).

Another *Gli3* mouse mutant is the hypomorph *Polydactyly Nagoya* ($Gli3^{Pdn/Pdn}$) (Hayasaka *et al.*, 1980) that arose through a spontaneous mutation. Suppression of *Gli3* gene expression is observed in these mice due to integration of a 5542bp retrotransponson into the third intron of the *Gli3* gene and results in the formation of two transcript classes (Thien and Ruther, 1999, Ueta *et al.*, 2002). Class I transcripts contain out of frame insertion, which lead to 3 truncated proteins while class II

transcripts contain an in-frame insertion that lead to 2 longer proteins (Thien and Ruther, 1999). *Gli3*$^{Pdn/Pdn}$ mutant mice show qualitatively similar but quantitatively weaker phenotypes compared to *Gli3*$^{Xt/Xt}$ mutants (Thien and Ruther, 1999).

Finally, an intermediate compound mutant can be generated between the *Gli3*$^{XtJ/XtJ}$ and the *Gli3*$^{Pdn/Pdn}$ mutant mice i.e *Gli3*$^{Xt/Pdn}$ with *Gli3*$^{XtJ/XtJ}$ having the strongest and *Gli3*$^{Pdn/Pdn}$ mutants the weakest phenotype (Kuschel *et al.*, 2003, Magnani *et al.*, 2012b).

1.5.3 *Gli3* in forebrain development

Roles of *Gli3* in telencephalic development have been clarified by the use of *Gli3*$^{XtJ/XtJ}$, *Gli3*$^{Pdn/Pdn}$ and *Gli3*$^{Xt/Pdn}$ mutant mice. These studies are restricted to embryonic and perinatal stages as homozygous mutants die a few hours after birth.

1.5.3.1 Anatomical defects

Gli3$^{XtJ/XtJ}$ mice display exencephaly, a failure of neural tube closure at the prosencephalon (Johnson, 1967). Those that do not display exencephaly show absence of medial cortical tissues i.e. the hippocampus, choroid plexus and the cortical hem (Johnson, 1967, Theil *et al.*, 1999). Moreover, *Gli3*$^{XtJ/XtJ}$ mice lack protruding olfactory bulbs which are dorsally misplaced and primary olfactory axons terminate in a small fibrocellular mass which lacks laminar organization (Theil *et al.*, 1999, St John *et al.*, 2003, Besse *et al.*, 2011). Finally, the paleocortex is specified but extended in the lateral telencephalon (Vyas *et al.*, 2003).

1.5.3.2 *Gli3* regulates forebrain development

Loss of medial cortical tissues at *Gli3*$^{XtJ/XtJ}$ mice correlates with a loss of Bmp and Wnt signaling in the rostrocaudal midline (Grove *et al.*, 1998, Theil *et al.*, 1999, Tole *et al.*, 2000). The cortical hem expresses *Wnt2b*, *3*a, *5*a, *7*a, *7*b and *8*b (Grove *et al.*, 1998). Specifically, *Gli3*$^{XtJ/XtJ}$ mice lack *Wnt3*a, *2*b and *5*a expression and show reduced *Wnt8*b expression (Tole *et al.*, 2000). Moreover, these mice lack *Bmp*2, 4, 6 and 7 expressions which coincides with absence of the choroid plexus (Theil *et al.*, 1999, Tole *et al.*, 2000). Finally, a recent study demonstrated that Wnt/β-catenin signaling directly regulates *Gli3* in the hippocampus (Hasenpusch-Theil *et al.*, 2012). In turn, *Gli3*$^{Pdn/Pdn}$ and *Gli3*$^{Xt/Pdn}$ mice also show reduction of cortical *Wnt*7*b* and *Wnt*8*b* expression (Kuschel *et al.*, 2003, Friedrichs *et al.*, 2008, Magnani *et al.*, 2012a) and it was shown that *Gli3* is required for *Wnt7b/8b* expression in the medial cortex (Grove *et al.*, 1998, Theil *et al.*, 2002).

Gli3$^{XtJ/XtJ}$ mutant mice also display an up-regulation of *Fgf*8 expression (Theil *et al.*, 1999). Up-regulation in the brain, eye, face and limb buds of *Gli3*$^{XtJ/XtJ}$ mutant mice is demonstrated for *Fgf*8 and Fgf signaling from E8.5 (Theil *et al.*, 1999, Aoto *et al.*, 2002). *Fgf*8 ectopic expression is shown in *Gli3*$^{Pdn/Pdn}$ and *Gli3*$^{Xt/Pdn}$ mice (Kuschel *et al.*, 2003, Magnani *et al.*, 2012a) suggesting a requirement of *Gli3* to confine *Fgf8* expression to the commissural plate (Theil *et al.*, 1999, Magnani *et al.*, 2012a). In turn, Fgf signaling negatively regulates Wnt/β-catenin signaling (Faedo *et al.*, 2010). These studies indicate a complex network between these signaling centers that is orchestrated either directly or indirectly by *Gli3*.

What is more, ectopic application of beads expressing Fgf8 induces subpallial markers and represses pallial specific genes in dorsal telencephalic tissue (Kuschel *et al.*, 2003). Briefly, in *Gli3*$^{XtJ/XtJ}$ mutant mice *Mash*1, *Dlx*2/5 and *Isl*1 ventral telencephalic markers are expanded dorsally with *Gli3*$^{Xt/Pdn}$ and *Gli3*$^{Pdn/Pdn}$ mutant mice showing gradually weaker phenotypes (Kuschel *et al.*, 2003). A recent study demonstrated that *Gli3* is required cell-autonomously to repress ventral telencephalic

gene expression in dorsal telencephalic cells (Quinn *et al.*, 2009). Thus, it is clear that dorso-ventral patterning of the telencephalon is affected in *Gli3* mutant mice.

Finally, *Gli3* has been implicated in cortical lamination. *Gli3*$^{XtJ/XtJ}$ cortex fails to develop a distinct marginal zone, subplate or cortical plate while there is aggregation of cells including Cajal-Retzius cells (Theil, 2005). Furthermore, loss of the apical-basal polarity of the cortical progenitor cells coincide with ectopic *Wnt7*b expression which is preceding the layering defects (Theil, 2005). Lamination defects are also exhibited in the intermediate compound mutant *Gli3*$^{Xt/Pdn}$. In particular, *Gli3* displays a role in maintaining the even distribution of Cajal-Retzius cells which also form aggregation in *Gli3*$^{Xt/Pdn}$ mutant mice (Friedrichs *et al.*, 2008). Furthermore, subplate neurons are largely absent in *Gli3*$^{Xt/Pdn}$ mutants (Magnani *et al.*, 2012b).

1.5.3.3 *Gli3* is a downstream effector of Shh signaling

Gli genes are downstream effectors of Shh signaling (see 1.1.2.1). Gli3 transcription factor act as activator in the presence of *Shh* and *Gli3* acts as a repressor in the absence of *Shh* (Matise and Joyner, 1999, Ruiz i Altaba, 1999). In more detail, in the absence of Shh Gli3 is cleaved in an ubiquitin/proteasome-dependent process into a short form (Gli3-83) which has transcriptional repressor activity (Gli3R) (Wang *et al.*, 2000, Tempe *et al.*, 2006). In the presence of Shh, the cleavage of Gli3 is inhibited and a full-length (Gli3-190) transcriptional activator form (Gli3A) is produced (Ruiz i Altaba, 1998, Sasaki *et al.*, 1999, Bai *et al.*, 2004). Gli3R and Gli3A are more prominent in the dorsal and ventral telencephalon, respectively (Fotaki *et al.*, 2006). Gli3 processing is controlled by the primary cilium, a subcellular structure protruding from the surface of the cell (Haycraft *et al.*, 2005, Huangfu and Anderson, 2005).

The balance between *Shh* and *Gli3* is crucial for dorso-ventral patterning of the telencephalon. In both *Shh* and *Gli3* mutants the ventral and dorsomedial telencephalon fails to form, respectively (Chiang *et al.*, 1996, Theil *et al.*, 1999). Analysis of *Shh*/*Gli3* double mutants by *Rallu et al.*, 2002b revealed a general

establishment of the dorso-ventral patterning of the telencephalon. Yet, this was contradicting with a later study in which in *Shh*/*Gli3* double mutants the dorsomedial telencephalon is not rescued and *Fgf* expression is expanded dorsally i.e. *Gli3* mutant phenotypes are maintained (Rash and Grove, 2007). These data point away from an involvement of *Shh* in the development of the dorsomedial telencephalic defects observed in *Gli3* mutants. In fact, the complex interactions between *Gli3* and the molecules described above constitute better candidates in patterning this region.

1.5.4 *Gli3* and axon tract formation

Gli3 has been implicated in major axon tract formation in the developing telencephalon. The severe early patterning defects observed in $Gli3^{Xt/Xt}$ cortex cause dysmorphogenesis and thereby significantly complicating the analyses of axon tract formation. Therefore, axon tract formation has been extensively studied in $Gli3^{Pdn/Pdn}$ mutants that represent excellent tools to study the Acrocallosal syndrome. The $Gli3^{Pdn/Pdn}$ mutants display CC agenesis and CC defects are caused by mislocation of the guidance cues at the CSB that originate during patterning stages (Naruse *et al.*, 1990, Magnani *et al.*, 2012a). Indeed, $Gli3^{Pdn/Pdn}$ mutants demonstrate an altered Fgf and Wnt/β-catenin signaling and up-regulation of *Slit*2 and interestingly $Gli3^{Pdn/Pdn}$; $Slit2^{-/-}$ double mutants show partial recovery of the midline defects (Magnani *et al.*, 2012a). These findings suggest a role for *Gli3* in positioning the midline guidance cues at the CSB during patterning stages and hence provide a link between patterning and CC development. However, as *Gli3* has a widespread and prolonged expression in the ventricular zone of the telencephalon, questions remain about the temporal and spatial requirements of *Gli*3 in CC development. I therefore will use *Gli3* mouse mutants as a model for better determining the temporal and spatial requirements of *Gli*3 during early patterning stages for CC formation and hence for better understanding the pathogenesis of Acrocallosal syndrome patients.

In addition, $Gli3^{Pdn/Pdn}$ mutants demonstrate aberrant corticothalamic/thalamocortical tract formation due to intrinsic inability of the $Gli3^{Pdn/Pdn}$ ventral telencephalon to

guide axons (Magnani *et al.*, 2010). Specifically, in *Gli3*$^{Pdn/Pdn}$ mutants the entry of the corticothalamic axons into the ventral telencephalon is delayed and thalamocortical axons form abnormal projections in the ventral telencephalon (Magnani *et al.*, 2010). DiI labelling and also neurofilament staining did not reveal corticothalamic axons at E14.5 (Magnani *et al.*, 2010). In addition, a recent study showed that in the *Gli3*$^{Xt/Pdn}$ compound mutant CTAs show severe outgrowth defects due to a nearly complete absence of subplate neurons which pioneer the corticothalamic tract (Magnani *et al.*, 2012b). Although these phenotypes emphasize the importance of *Gli3* for corticothalamic/thalamocortical tract formation, their severity might have obscured additional roles of *Gli3* in the developing cortex. In this thesis, I therefore wish to analyse the molecular mechanisms which lead to corticothalamic defects and hence deepen our understanding how transcription factors can control axon pathfinding in general and corticothalamic tract development in particular. It will also provide insights into the pathogenesis of the brain abnormalities seen in *GLI3* syndromes.

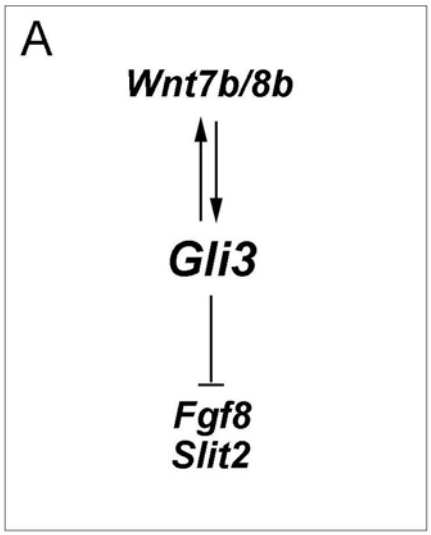

Figure 1-10: Schematic representation of the genetic interactions between *Gli3* and other signaling pathways.

(*A*) During patterning stages, *Gli3* restricts the expression of *Fgf8* and *Slit2* to the commissural plate and is required for *Wnt7b*/*8b* expression in the rostromedial cortex of control embryos thereby establishing the CSB and controlling a balance between Fgf and Wnt/β-catenin signaling. Arrows and lines indicate genetic interactions except for the direct regulation of *Gli3* expression by Wnt/β-catenin signaling (Hasenpusch-Theil *et al*. 2012).

1.6 Aims of thesis

The identification of axon pathfinding defects in *Gli3* mutants and the correlation between these defects and a consistent alteration in signalling and guidance molecules expression suggests a central role for *Gli3* in axon navigation. This leads to the possibility that *Gli3* is required in a specific sub-group of telencephalic progenitors for correct axon tract development. To test this possibility, different *Gli3* conditional mutant mice were analysed. Thus, for this thesis I address the following aims:

1. Investigate *Gli3's* role in cortical and septal progenitors as well as MGE progenitors for corpus callosum formation
2. Investigate whether *Gli3* expression in the dorsal telencephalon controls the entry of corticothalamic axons into the ventral telencephalon
3. Investigate *Gli3's* role in cortical progenitors for lateral olfactory tract formation

To address these aims, I made use of three Cre driver lines: *Zic4Cre* (Rubin *et al.*, 2010) and *Nkx2.1Cre* (Nobrega-Pereira *et al.*, 2008) and *Emx1Cre* (Gorski *et al.*, 2002). I specifically investigated axon tract formation by using transgenic mice, immunofluorescence and DiI tracing analysis. Informed by these results, I also examined the cellular and molecular mechanisms that led to axon pathfinding defects. To accomplish this, I performed various *in situ* hybridisation analyses and slice culture experiments.

2 Materials and Methods

2.1 Animals

2.1.1 Animal husbandry

Emx1Cre (Gorski *et al.*, 2002), *Zic4Cre* (Rubin *et al.*, 2010), *Nkx2.1Cre* (Nobrega-Pereira *et al.*, 2008), *Gli3$^{fl/fl}$* (Blaess *et al.*, 2008), *ROSA26CAG dual stop EGFP reporter (RCE)* (Sousa *et al.*, 2009) and *Golli-τauGFP* (Jacobs *et al.*, 2007) mice were kept on a mixed background and were interbred. *Emx1Cre;Gli3$^{fl/+}$*, *Zic4Cre;Gli3$^{fl/+}$*, *Nkx2.1Cre;Gli3$^{fl/+}$* and *Golli-τauGFP;Gli3$^{fl/+}$* mice were mated with *Gli3$^{fl/fl}$* mice to obtain *Emx1Cre;Gli3$^{fl/fl}$* and *ZicCre;Gli3$^{fl/fl}$*, *Nkx2.1Cre;Gli3$^{fl/fl}$* conditional mutant embryos and *Golli-τauGFP; Gli3$^{fl/fl}$* embryos. Likewise, *Emx1Cre;Gli3$^{fl/+}$* and *Nkx2.1Cre;Gli3$^{fl/+}$* mice were mated with *Gli3$^{fl/fl}$;RCE* females to obtain *Emx1Cre;Gli3$^{fl/fl}$;RCE* and *Nkx2.1Cre;Gli3$^{fl/fl}$;RCE* conditional mutant embryos. *Emx1Cre;Gli3$^{+/+}$ / Emx1Cre;Gli3$^{fl/+}$*, *Zic4Cre;Gli3$^{+/+}$ / Zic4Cre;Gli3$^{fl/+}$*, *Nkx2.1Cre;Gli3$^{+/+}$ / Nkx2.1Cre;Gli3$^{fl/+}$* and *Golli-τauGFP;Gli3$^{+/+}$ / Golli-τauGFP;Gli3$^{fl/+}$* embryos were used as controls as they showed no discernible phenotype. Below is a list of mice with the following genotypes that were used in each chapter:

- *Emx1Cre;Gli3$^{fl/+}$*, *Zic4Cre;Gli3$^{fl/+}$*, *Nkx2.1Cre;Gli3$^{fl/+}$* and *Nkx2.1Cre;Gli3$^{fl/+}$;RCE* control mice and *Emx1Cre;Gli3$^{fl/fl}$*, *Zic4Cre;Gli3$^{fl/fl}$*, *Nkx2.1Cre;Gli3$^{fl/fl}$* and *Nkx2.1Cre;Gli3$^{fl/fl}$;RCE* mutant mice (Chapter 3)

- *Emx1Cre;Gli3$^{fl/+}$*, *Golli-τauGFP;Gli3$^{fl/+}$* control mice and *Emx1Cre;Gli3$^{fl/fl}$*, *Golli-τauGFP;Gli3$^{fl/fl}$* mutant mice (Chapter 4)

- *Emx1Cre;Gli3$^{fl/+}$*, *Emx1Cre;Gli3$^{fl/+}$;RCE* control mice and *Emx1Cre;Gli3$^{fl/fl}$* *Emx1Cre;Gli3$^{fl/fl}$;RCE* mutant mice (Chapter 5)

All experimental procedures were performed in accordance with institutional guidelines and UK home office regulations. Mice were maintained in a 10/14 hour

dark/light cycle with food and water provided *ad libitum*. For timed mating, the morning the vaginal plug was detected was designated as E0.5 and the day of birth P0. For each stage and each marker, 3-5 embryos were analysed.

All the solutions mentioned below are enlisted in Table 2-7 at the end of this section.

2.1.2 **Mouse genotyping**

Mouse ear clips were collected and digested to confirm the genotype of each animal. Samples were digested in 100µl of Direct PCR Lysis Reagent (Viagen) containing 200µl/ml of proteinase K (Sigma) at 55°C for 2 hours while shaking in a thermomixer (Eppendorf) at 1400rpm. Incubation at 85°C for 45 minutes followed to inactivate the proteinase K solution. 1µl of DNA was used as a template in a PCR employing primers specific for *Gli3flox*, *Cre* (including *Emx1Cre*, *Zic4Cre*), *Nkx2.1-iCre*, *RCE* and *Golli-τauGFP* (see Table 2-1 and Table 2-2). The total volume for all PCR reactions was 25µl (see Table 2-1).

The thermal cycling conditions for the different genotyping protocols were as follows:

For the ***Gli3flox***: initial denaturing in 95°C for 5 minutes; 30 cycles of 95°C for 30 seconds, 62°C for 1 minute and 60°C for 1 minute; and finally a 10 minutes extension at 72°C.

For the ***Cre/ Nkx2.1-iCre***: initial denaturing in 94°C for 5 minutes; 35 cycles of 94°C for 30 seconds, 60°C for 45seconds and 72°C for 1 minute; and finally a 10 minutes extension at 72°C.

For the ***Golli τau-GFP***: initial denaturing in 95°C for 3 minutes; 30 cycles of 94°C for 30 seconds, 60°C for 30 seconds and 72°C for 30 seconds; and finally a 10 minutes extension at 72°C.

For the ***RCE***: initial denaturing in 95°C for 1 minute; 33 cycles of 94°C for 45 seconds, 59°C for 45 seconds and 72°C for 1 minute; and finally a 10 minutes extension at 72°C.

Amplification products were separated on a 2% (w/v) agarose gel (Web scientific) containing 1x TAE and visualized by staining with Webgreen (Web scientific). The products were visualised with ultraviolet light. The expected size of the bands can be seen in (Table 2-1).

Table 2-1: Genotyping protocol.

	Gli3flox	***Cre/Nkx2.1-iCre***	***Golli-τauGFP***	***RCE***
10mM dNTPs (Promega)	0.5µl	1/0.5µl	1µl	0.5µl
5x Taq Buffer (Promega)	5µl			
Taq DNA polymerase (Promega)	0.1µl			
H_2O	16.9µl	16/14.4µl	16.8µl	17.5µl
Oligonucleotides (Sigma)	0.75µl	1/2µl	0.5µl	1µl

Table 2-2: PCR primers for genotyping.

Allele	Primer	Sequence (5'-3')	Band size (bp)
Flox	Gli3-S1	-CTGGATGAACCAAGCTTTCCATC-	**Wt:200bp**
	Gli3-AS3	-CTGCTCAGTGCTCTGGGCTCC-	**Flox:500bp**
Emx1-Cre	CreForward	-ACCTGATGGACATGTTCAGGGA-	**308bp**
	CreReverse	-TCCGGTTATTCAACTTGCACCA-	
Zic4Cre	iCre250s	-GAGGGACTACCTCCTGTACC-	**630bp**
	iCre880as	-TGCCCAGAGTCATCCTTGGC-	
Nkx2.1-iCre	Nkx2.1-5'AscF1	TTGGCGCGCCTCTACCCACCTCTGGCCCTCC-	**600bp**
	iCre250 as	-AGGTACAGGAGGTAGTCCCTC-	
Golli-τGFP	GFP 3119	-GTCGGCCATGATATAGACGTT-	**1.1kb**
	TAU2070	-GAGAGGTGAATCTGGGAAATC-	
RCE	RCE-Rosa1	-CCCAAAGTCGCTCTGAGTTGTTATC-	**Wt:550bp**
	RCE-Rosa2	-GAAGGAGCGGGAGAAATGGATATG-	**Mt:350bp**
	RCE-Cag3	-CCAGGCGGGCCATTTACCGTAAG-	

2.1.3 **Tissue preparation**

On the day that embryos were required pregnant females were sacrificed by 1-chloro-2, 2, 2-trifluoroethyl difluoromethyl ether (Isoflurane, Merial, UK) inhalation overdose and subsequent cervical dislocation. The uterus was removed from the abdomen and the embryos removed from their deciduas and placed into cold 1x phosphate buffer saline (PBS, Table 2-7). The embryos were processed differently depending on age. The whole head of embryos was fixed in 4% paraformaldehyde in PBS until the age of E14.5 (PFA, Table 2-7) (Fisher). From E15.5 onwards, the brain of embryos was dissected from the skull and then fixed in 4%PFA. The fixation lasted from 3-4hours to overnight (O/N) depending on the tissue preparation technique. Once fixed, the brains/heads were washed in PBS O/N at 4^{o}C.

Postnatally, P7 pups were collected and intracardial perfusion was performed. Pups were sedated with intraperitoneal injection of 0.2ml (200mg/ml) of pentobarbital sodium (Euthatal, Merial, UK). Once the mouse was sedated, the rib cage was removed and the heart exposed. The right atrium was immediately cut and a butterfly needle was inserted into the left ventricle. PBS was administered with constant flow (4-5ml) and then replaced with 4% (w/v) perfusion paraformaldehyde (4-5ml) (Table 2-7). Testing tail's flexibility confirmed fixation. The brain was dissected from the skull and transferred to 4%PFA for 2-3hours.

For embryo/pup genotyping, tails from each embryo/pup were placed in a 1.5ml tube for DNA extraction followed by PCR (see Table 2-2).

2.1.4 **Tissue preparation and sectioning**

Vibroslicer sectioning was performed on brains fixed for 3-4 hours. Each brain was positioned in a mould with 4% LE Agarose (Lonza) /ddH2O, preincubated at 55^{o}C,

and left on ice to solidify. 100μm thick coronal sections were obtained with the use of a VT 1000S vibroslicer (Leica).

Cryosectioning was performed on brains fixed for 3-4 hours. Each brain/head was transferred into 30% sucrose (Fischer Scientific)/ PBS solution overnight for dehydration. Then, the brains/heads were transferred in 30%sucrose/OCT (Fischer Scientific) embedding matrix for 3-4 hours on a tumbler to allow even cover. The brain/heads were embedded in moulds containing 30%sucrose/OCT and frozen on dry ice. A CM3050S cryostat (Leica) was used to obtain 15-20μm coronal sections. The sections were mounted on Superfrost Plus slides (VWR) and dried overnight at 4^{o}C.

Microtome sectioning (paraffin sections) was performed on overnight fixed samples. Embryonic heads/brains remained in PBS overnight and transferred into 70% EtOH (Fischer) for at least 24 hours. The samples were embedded in wax using an automated tissue processor (Tissue-Tek,VIP, Sakura). A Leica RM2245 microtome was used to obtain 10-12.5μm coronal sections. The sections were mounted on Superfrost Plus slides and dried overnight at 37^{o}C.

2.2 Histological procedures

For all the histological procedures described below, the used primary and secondary antibodies are enlisted in Table 2-3 and Table 2-4 at the end of this section.

2.2.1 Cresyl violet staining

Brains were prepared as described above. Cryostat sections were washed in 1xPBS (3 times of 20 minutes each) and then washed in H_2O (2 minutes). Slides were incubated in potassium sulfite (Table 2-7) (15 minutes) at room temperature and then washed in H_2O (2 times of 1 minute each). Slides were immerged in cresyl violet solution (20 minutes) at room temperature, and then washed in acetate buffer (Table

2-7) (2 times of 1 minute each). Differentiation reaction was performed to eliminate the excess of cresyl violet from the sections for 30 seconds-2 minutes in differentiation solution (Table 2-7). Sections were then rehydrated through an alcohol series [50%EtOH, 70%EtOH, 90%EtOH and 100%EtOH for 1 minute each and then xylene for 10 minutes (2 times)] and then mounted in DPX (VWR).

2.2.2 **Immunohistochemistry analysis**

This analysis was performed on either paraffin or cryosections. Brains were prepared as described above (see 2.1.4). Paraffin sections were dewaxed in xylene (3 times of 7 minutes each) and then rehydrated through an alcohol series [100%EtOH (2 times of 2 minutes each), 96%EtOH, 90%EtOH, 70%EtOH and 50%EtOH (1 minute each)] and washed in PBS (5 minutes). For cryosections slides were washed in 1xPBS (3 times of 20 minutes each). From this step onwards paraffin and cryosections were handles in the same way and microwaved for 20 minutes (4 times of 5 minutes each) in 10mM sodium citrate buffer (pH=6) (Table 2-7) and then rested in citrate buffer for another 20 minutes. The slides were washed in PBS (5 minutes) and subsequently, endogenous peroxidase activity was blocked using 3% hydrogen peroxide in methanol (Fischer) (15 minutes). Sections were washed in PBS (2 times of 5 minutes each) with 0.1%Triton (BDH) in 1xPBS (PBT) for 5 minutes. Then, sections were sealed in ImmEdge fat pen (Vector) and incubated in blocking buffer (20% sheep serum (Sigma) in PBT) for 1 hour, followed by incubation in primary antibody diluted in 10% sheep serum/PBT (O/N) in a humid chamber. The following day, the slides were washed in PBS (3 times of 5 minutes each) and incubated in species specific biotinylated secondary antibody diluted in PBS for 1-4 hours in a humid chamber. The slides were subsequently washed in PBS (3 times of 5 minutes each) followed by incubation in **A**vidin and **B**iotinylated horseradish peroxidase macromolecular **C**omplex (**ABC**) (Vector) for 30 minutes. Slides were later washed in PBS (3 times of 5 minutes each) and peroxidase activity revealed using 3,3'-diaminobenzidine (DAB) (Sigma) as substrate. Reactions were stopped in

H_2O. Sections were dehydrated through an alcohol series and mounted as described before (see 2.2.1).

2.2.3 **Immunofluorescence analysis**

2.2.3.1 Immunofluorescence on cryosections

Brains were prepared as described above for cryosectioning (see 2.1.4). The slides were rinsed in PBS (3 times of 20 minutes each). Then, sections were encircled with ImmEdge fat pen and incubated in blocking buffer (20% sheep serum /PBS) for an hour in a humid chamber. Primary antibody incubation was carried out overnight at room temperature in a humid chamber diluted in 20% sheep serum /PBS. Next day, the sections were washed in PBS (3 times of 15 minutes each) and incubated with secondary antibodies diluted in 20% sheep serum /PBS for 2 hours at room temperature. Subsequently, the slides were washed in PBS (3 times of 10 minutes each) and immediately mounted with Mowiol (Sigma) (Table 2-7) containing 1, 4-diazabicyclo-2.2.2 octane (Dabco) (Sigma) to avoid bleaching. For counter staining TOPRO-3 (1:2000, Invitrogen) or Dapi (1:2000, Molecular Probes) was used.

2.2.3.2 Immunofluorescence on vibrotome sections

Brains were prepared as described above for vibrotome sectioning (see 2.1.4). Coronal sections (100µm thick) were collected in 24-well plate (Cellstar) and blocked (20% sheep serum/ PBS) for 1-2 hours at room temperature inside a humid chamber. The plate was placed on the tumbler to ensure even blocking. Blocking solution was replaced by primary antibody solution diluted in 10% sheep serum/PBS (O/N). Next day, the sections were washed in PBS (3 times of 10 minutes each) and incubated in secondary antibodies diluted in 10% sheep serum/ PBS for 2-4 hours in the humid chamber. Subsequently, the sections were washed in PBS (3 times of 5 minutes each) and mounted with Mowiol containing Dabco to avoid bleaching. For

counter staining TOPRO-3 (1:2000, Invitrogen) or Dapi (1:2000, Molecular Probes) was used.

2.2.3.3 Immunofluorescence on paraffin sections

Brains were prepared as described above for microtome sectioning (see 2.1.4). Paraffin sections were dewaxed in xylene (3 times of 7 minutes each) and then rehydrated through an alcohol series [100%EtOH (2 times of 2 minutes each), 96%EtOH, 90%EtOH, 70%EtOH and 50%EtOH (1 minute each)] and washed in PBS (1 minute). Paraffin sections were microwaved for 20 minutes (4 times of 5 minutes each) in 10mM sodium citrate buffer (pH=6) and then rested in citrate buffer for another 20 minutes. The slides were washed in PBS (5 minutes) followed by washing in PBT for 5 minutes and incubated in blocking solution (20% sheep serum /PBT) for 1hour in a humid box. Sections were incubated in primary antibody solution diluted in 20% sheep serum /PBS and left overnight at room temperature in the humid chamber. The following day, the slides were washed in PBT (3 times of 10 minutes each) and incubated in species-specific secondary antibodies diluted in 10% sheep serum/ PBT for 2-4 hours in the humid chamber. Subsequently, the slides were washed in PBS (3 times of 10 minutes each) and immediately mounted with Mowiol containing Dabco to avoid bleaching. For counter staining TOPRO-3 (1:2000, Invitrogen) or Dapi (1:2000, Molecular Probes) was used.

Table 2-3: Primary antibodies list.

Antigen:	Dilution:	Origin:	Histological procedure used in:	Supplier:
Calbindin (CB)	1/1000	rabbit	2.2.3.1	Swant
Calretinin (CR)	1/1000	rabbit	2.2.3	Swant
Cell adhesion molecule (L1)	1/1000	rat	2.2.2-2.2.3	Millipore
COUP-TF-interacting protein (Ctip2)	1/1000	rat	2.2.3	Abcam
Glial fibrillary acidic protein (GFAP)	1/1000	rabbit	2.2.2-2.2.3.1	DAKO
Gli3	1/3000	rabbit	2.5	Abcam
Green fluorescent protein (GFP)	1/1000	chicken	2.2.3	Abcam
Microtubule associated protein-2 (Map2)	1/1000	mouse	2.2.3.1	Sigma
Lot1	1/200	rat	2.2.3.3 (0.3%PBT used)	Provided by Tatsumi Hirata
Neurofilament (2H3)	1/50	mouse	2.2.3	DSHB
Nuclear factor 1-A type (Nf1a)	1/1000	rabbit	2.2.3.3	Active motif
Special AT-rich sequence-binding protein 2 (Satb2)	1/50	mouse	2.2.3	Abcam
T-box (Tbr1)	1/400	rabbit	2.2.3.1	Abcam
T-brain gene-2	1/1000	rabbit	2.2.3.3	Chemicon

Antigen:	Dilution:	Origin:	Histological procedure used in:	Supplier:
(Tbr2)				
Transient axonal glycoprotein-1 (4D7/Tag1)	1/100	mouse IgM	2.2.3.1	DSHB

Table 2-4: Secondary antibodies list.

Secondary antibody:	Dilution:	Origin:	Conjugated with:	Supplier:
Rabbit IgG	1/200	goat	Alexa-647	Invitrogen
Rat IgG	1/200	goat	Alexa-647	Invitrogen
Mouse IgG	1/200	goat	Alexa-647	Invitrogen
Rabbit IgG	1/100	goat	Cy3	Jackson/Dianova
Rat IgG	1/100	donkey	Cy3	Jackson/Dianova
Mouse IgG	1/100	donkey	Cy3	Jackson/Dianova
Mouse IgM	1/100	donkey	Cy3	Jackson/Dianova
Chicken IgG	1/100	donkey	Cy2	Jackson/Dianova
Rabbit IgG	1/200	donkey	Alexa-488	Invitrogen
Rabbit IgG	1/400	goat	Biotin	DAKO
Rabbit IgG	1/3000	goat	Horseradish peroxidase	DAKO

2.2.4 *In situ* hybridization

For *in situ* hybridisation analysis, the probes are enlisted in Table 2-5 at the end of this section. Probe synthesis is described in section 2.3.

2.2.5 *In situ* hybridization on paraffin sections

The sections were dewaxed in xylene (3 times of 7 minutes) and then, rehydrated in a descending EtOH series [50%xylene/ 50% EtOH (2 minutes), 100% EtOH (2 times of 2 minutes) and 96% EtOH, 90% EtOH, 70% EtOH, 50% EtOH (1 minute)]. The slides were washed in PBS (2 times of 5 minutes) and then incubated in 20µg/ml proteinase K in PBS at 37^{o}C (5 minutes). For the inactivation of proteinase K the slides were washed in 0.2% Glycine (Sigma) in PBS (5 minutes) and then washed in PBS (2 times of 5 minutes). Then, the slides were refixed in 4% PFA with 0.2% glutaraldehyde (Sigma) (20 minutes) and subsequently washed in PBS (2 times of 5 minutes). The sections were encircled with an ImmEdge fat pen and 80-90µl of Hybmix (Table 2-7) was added. Slides were incubated for 1-2 hours in a humid chamber containing 50%formamide/2* SSC (Table 2-7). Finally, the sections were incubated in RNA riboprobes, diluted in hybmix and denatured at 95^{o}C (5 minutes) at 68^{o}C overnight.

The slides were shortly washed in 2*SSC, followed by incubation in prewarmed 50% formamide/2*SSC (2 times of 15 minutes each) at 65^{o}C. Then, the slides were transferred to 0.1% Tween/PBS (3 times of 10 minutes) on a tumbler to allow even washing. Sections were incubated in B-Block (Table 2-7) at room temperature (1 hour). The sections were incubated in anti-digoxigenin-antibody (anti-Dig) (Roche) diluted in B-Block (1:1000) at 37^{o}C in a humid chamber (2 hours). Subsequently, the slides were washed in 0.1% Tween/PBS (3 times of 5 minutes each) and later in NTM (Table 2-7) (10 minutes). Finally, NBT/BCIP solution (Roche) was diluted in

NTM (1:50) and added on each slide. The staining reaction was left from 5 hours to O/N depending on the intensity of the reaction.

The slides were washed in PBS to stop the color reaction (1 hour) and subsequently in H_2O (10 minutes). The slides were left to dry and mounted in aquatex (Merck).

2.2.6 *In situ* hybridization on cryosections

The sections were prepared as described before (2.1.4) and warmed at room temperature (up to 30 minutes). The RNA probes were prepared as described below (see 2.3). The probe was thawed quickly and diluted in hybridization solution (Table 2-7). The diluted probe was denatured at 85^{o}C (at least 10 minutes) in the thermomixer while shaking (1400rpm) to mix thoroughly. The diluted probe (100-150µl) was added on the slides and incubated in a humid chamber including 50%formamide/2* SSC (O/N). Coverslips were placed on the slides to allow even distribution of the probe.

The slides were transferred in wash buffer (Table 2-7) prewarmed at 65^{o}C (15 minutes). Subsequently, they were transferred to a new box with prewarmed wash buffer and the incubation was continued for another 30 minutes (2 times). The sections were incubated further in 1x MABT (Table 2-7) at room temperature in a humid chamber (2 times of 30 minutes each at minimum). The sections were encircled with an ImmEdge fat pen and blocked (blocking solution, Table 2-7) at room temperature in a humid chamber (1 hour). The blocking solution was removed, and the slides are incubated in anti-digoxigenin-antibody (anti-Dig) diluted in blocking solution (1:1500) (O/N at room temperature or 4^{o}C).

The slides were washed in 1xMABT at room temperature while rocking (5 times of 20 minutes each). The sections were equilibrated in staining buffer (Table 2-7) (2 times of 10 minutes each) and subsequently, incubated in staining buffer with NBT (Table 2-7) in the dark at room temperature to develop the colour reaction. Washing

in PBS several times stopped the staining reaction. The slides were left to dry and mounted in aquatex.

Table 2-5: RNA probes list.

RNA probe:	Dilution on paraffin/cryosections:	Reference:	Restriction enzyme:	RNA polymerase:
Axin2	1:5	(Lustig *et al.*, 2002)	XbaI	T7
Ap-2e	1:5	(Feng *et al.*, 2009)	XbaI	SP6
Cux2	1:10	(Zimmer *et al.*, 2010)	NotI	T3
Dbx1	1:5/1:500	(Yun *et al.*, 2001)	EcoRI	T3
Dmrt5	1:5	(Saulnier *et al.*, 2012)	StuI	SP6
Emx1	1:5	(Simeone *et al.*, 1992)	EcoRI	SP6
EphrinA5	1:3	(Dufour *et al.*, 2006)	XbaI	T7
ER81		(Lin *et al.*, 1998)	SpeI	T7
Fabp7	1:10	(Genepaint. RNA probe 653)	NotI	SP6
Fgf8	1:5	(Crossley *et al.*, 2001)	BamHI	T7
Gli3	1:5	(NM_008130, Genbank, 132-5113bp)	NotI	T7
Id2	1:5	(Jen *et al.*, 1997)	EcoRI	T7
Lhx2	1:10/1:500	EST2101448	EcoRI	SP6
Liprinβ1	1:10	(Chou *et al.*, 2009)	BamHI	T7
Netrin1	1/10	(Genepaint_ NM_008744)	XhoI	SP6
Nrp2	1:10/1:500	(Chen *et al.*, 1997)	EcoRI	T7
Reelin	1:10	(D'Arcangelo *et al.*, 1995)	EcoRI	T3
Robo1	1:5	(Erskine *et al.*, 2000)	EcoRI	T7

RNA probe:	Dilution on paraffin/cryosections:	Reference:	Restriction enzyme:	RNA polymerase:
Sema3C	1:10	(Bagnard *et al.*, 2000)	EcoRI	T7
Sema3F	1:10	(Xu and Fan, 2008)	NotI	T7
Sema5B	1:10	(Matsuoka *et al.*, 2011)	XbaI	T3
Sfrp2	1:5/1:500	(Kim *et al.*, 2001)	XbaI	T7
Six3	1:10	(Oliver *et al.*, 1995)	XbaI	T7
Slc6a7	1:10	(Chou *et al.*, 2009)	BamHI	T7
Slit1	1:10/1:500	(Erskine *et al.*, 2000)	BamHI	T7
Slit2	1:5/1:500	(Erskine *et al.*, 2000)	XbaI	T7
Sox5	1:10	(Lefebvre *et al.*, 1998)	BamHI	T3
Sprouty2	1:5	(Minowada *et al.*, 1999)	SacII	T3
Tbx2.1	1:10	(Besse *et al.*, 2011)	NcoI	SP6
Tgfa	1:10	(Assimacopoulos *et al.*, 2003)	BamHI	SP6
Wnt7b	1:10	(Parr *et al.*, 1993)	ApaI	T3
Wnt8b	1:10	(Trommsdorff *et al.*, 1999)	XbaI	T3

2.3 Generation of DIG-labeled riboprobes

Plasmid DNA was **retransformed** using DH5α competent cells (Invitrogen) according to the manufacturer's instructions. The solution was spread evenly on a LB-agar plate containing an antibiotic depending on the antibiotic resistant gene of the plasmid, and left O/N at 37^{o}C. The next day, single colonies were picked and placed into 5ml LB broth medium containing the appropriate antibiotic. The tubes were incubated at 37^{o}C (approximately 16 hours). Then, the cultures were centrifuged to precipitate the cells, followed by plasmid DNA purification (according to the Qiagen spin miniprep kit). Control digests were performed after each transformation to verify the success of the protocol. The digested products were separated on a 1% (w/v) agarose gel (containing 1x TAE) and visualized by staining with Webgreen under UV inspection.

Linearization, via restriction enzyme digest, was performed at 37^{o}C for 4hours. The 20µl digest included 10µg plasmid, 1/10µl restriction enzyme buffer (Roche), 1/10µl restriction enzyme (Roche) and H_20. To purify the plasmid, 30µl of H_20 were added to the digest and an equal amount of phenol-chloroform (50µl) (Sigma). After thoroughly mixing the plasmid (2 minutes, Eppendorf at 13000rpm) the aqueous phase was separately collected. For plasmid precipitation, 3M NaAC (1/10 volume) was added together with 2.5 volumes of EtOH (100%) to the plasmid, which was thoroughly mixed and left at -20^{o}C (O/N). The plasmid was centrifuged for 10 minutes (2 minutes, Eppendorf at 13000rpm) and washed in 70%EtOH. After centrifugation, the pellet was dissolved in 5µl of H_2O.

After linearization the **probe synthesis** was performed according manufacturer's instructions (Roche). After the incubation at 37^{o}C (O/N), followed the addition of 67.5µl H_20, 12.5µl LiCl (3.25M) and 200µl EtOH(100%) to precipitate the RNA probe at -20^{o}C (30 minutes). The solution was centrifuged (20 minutes, Eppendorf at 13000rpm) and the pellet washed in 70%EtOH. The pellet was resuspended in 25µl Solution I (50% Formamide (Sigma)/ 2* SSC pH=4.5). To check the probe

synthesis, 2µl of the RNA were separated on a 1% (w/v) agarose gel and visualized by staining with Webgreen. The products were visualised with ultraviolet light.

2.4 Axonal tracing with DiI/DiA placements

For **callosal axons tracing**, single crystals of the lipophilic tracer DiI/DiA (Invitrogen) were placed along the anterior-posterior into the postnatal cortex (P7) of whole brains along the anterior-posterior axis of the cortex forming a single line. The injections were made immediately after perfusion (see 2.1.3) and the brains were kept in 4% PFA at 37^{o}C for 6-8weeks.

For **olfactory bulb injections**, the single crystals were placed into the olfactory bulb of E18.5 and P7 brains. The dyes were allowed to diffuse at room temperature for 12 weeks in 4%PFA.

After diffusion of the dyes, the brains were transferred in 4% LE agarose (Lonza) and sectioned on the vibrotome as described above (see 2.1.4). The sections were collected in 24-well plates and cleared in 1:1 glycerol (Melfond)/PBS solution (O/N) at 4^{o}C. Subsequently, the sections were further cleared in 9:1 glycerol/PBS solution containing TOPRO/Dapi (Molecular probes) (1/2000) nuclear counter staining (O/N) at 4^{o}C. The sections were mounted in 9:1 glycerol/PBS solution on Superfrost Plus slides sealed with nail polish and dried overnight at room temperature.

2.5 Western-blot analysis

Dorsal telencephali, from E12.5 control and *Emx1Cre;Gli3*$^{fl/fl}$ mutant brains, was snap frozen in liquid N_2 and stored, at -80^{o}C.

On the day, the tissue was weighted and left on dry ice until all the buffers were prepared. The buffers for each preparation were calculated accordingly i.e. for 10mg

of tissue 200µl BufferH [cOmplete protease inhibitor included (Roche), Table 2-7], 50µl 5xLaemmli buffer (Table 2-7) and 12.5µl β-mercaptoethanol (Millipore).

For **protein** extraction, after adding buffer H the tissue was homogenized on ice with the use of hand held homogeniser (Polytron or Dounce) and then further homogenisation took place with a 25G syringe after adding 5xLaemmli buffer. The samples were boiled (95^{o}C for 5 minutes) and 10-20µl were taken for determining the protein concentration. B-mercaptoethanol (Millipore) was added to a final concentration 5% of the total volume. The samples were boiled again for 20 minutes and aliquoted and stored at -20^{o}C.

Protein concentration was determined with the use of a Pierce BCA protein assay kit (Thermo Scientific). Bovine serum alvumin (BSA) (Promega) was diluted at 2mg/ml in 0.9% saline and 0.05% sodium azide and the diluted BSA standards were prepared according to (see Table 2-6).

To **prepare the BCA working reagent**, reagent A and B were mixed in a 5:1 ratio. Tubes for each standard and sample were prepared (5µl) and 100µl of BCA working reagent was added to each tube. The tubes were incubated at 37^{o}C (30 minutes) and subsequently the absorbance of each sample was measured at the nanodrop.

Table 2-6: Preparation of diluted alvumin (BSA) standards.

	BSA (2mg/ml):	BufferH:	Final concentration (ng/µl):
A	50µl	0µl	2000
B	25µl	25µl	1000
C	20µl	30µl	800
D	10µl	40µl	400
E	5µl	45µl	200
F	2.5µl	47.5µl	100
G	1.25µl	48.75µl	50
H	0.5µl	49.5µl	20
I	0.25µl	49.75µl	10
J	0µl	50µl	0

For **gel electrophoresis**, NuPAGE Novex 3-8% Tris-Acetate gels (Invitrogen) were used. 5-10µg protein of each sample was prepared for loading onto each well and the total volume was the same for all the loaded samples (adjusted based on sample buffer). 1/10 volume of the NuPAGE reducing agent and 1/4 volume NuPAGE LDS sample buffer was added to each sample which was then denatured by incubation at 70^{o}C for 10 minutes. NuPAGE Tris-Acetate SDS running buffer was prepared according to the manufacturers protocol (Invitrogen) and added to the PeqLab Minigel system. Electrophoresis was carried out at constant voltage (80V) for 2-2.5 hours.

Before transferring the protein to the polyvinylidene difluoride (PVDF) membrane (Invitrogen), the membrane was washed in 100% EtOH and equilibrated in 1xTransfer Buffer (Invitrogen) together with PVDF filter papers (Invitrolon). The PerfectBlue Semi-dry Electroblotter (PeqLab) was used for the transfer and the

following blot "sandwich" was assembled: 3 blotting papers, PVDF membrane, gel and finally 3 blotting papers. The transfer lasted for 1hr at room temperature (1 minigel: 160mA constant; 2 minigels: 400mA).

To detect proteins on cellulose PVDF, the membrane was stained with **ATX ponceau** red staining solution (Fluka) (5 minutes). The membrane was subsequently washed in H_2O several times until the bands were well defined. The membrane was washed in 1xPBS.

For the **western blot analysis**, the membrane was transferred into blocking solution (10% Sheep serum in 0.25%PBS/Tween20) and incubated at 4^{o}C for 1 hour under constant agitation. The membrane was washed in 0.25%PBS/Tween20 and incubated in primary antibody (Gli3 concentration 300μg/ml, see Table 2-3) diluted in blocking solution at 4^{o}C (O/N). Next day, the membrane was washed in 0.25%PBS/Tween20 (15 minutes) and subsequently, transferred in fresh 0.25%PBS/Tween20 (3 times of 5 minutes each). The membrane was incubated in horseradish peroxidase secondary antibody (see Table 2-3) diluted in blocking solution at room temperature (1 hour). The membrane was washed in 0.25%PBS/Tween20 (15 minutes and then in fresh solution for another 3 times for 5 minutes each). The membrane was incubated further in enhanced chemiluminescence (ECL plus solution) (GE Healthcare/Amersham), which was prepared according to the manufacturer's instructions, at room temperature (5 minutes). The excess solution was drained with filter paper and the membrane was wrapped in cling film for the exposure with films. The exposure time varied from 2 to 15minutes.

2.6 Slice transplant cultures

2.6.1 Preparation of media and solutions

All the media and solutions were prepared the day before the preparation of the slices. The media used during the culture were sterile and included:

Sterile filtered 1xKrebs (50ml): 1xKrebs (Table 2-7), 0.5ml Hepes (1M) (Sigma), 0.5ml Pen-strep (100%) (Sigma) and 0.1ml Gentamicin (20%) (Sigma).

Medium with serum (MEM) (50ml): 44ml MEM (Gibco), 5ml foetal bovine serum (Sigma), 0.5ml 50% glucose (Sigma) and 0.5ml Pen-strep (100%).

Serum free medium (Neurobasal) (50ml): 47.5ml Neurobasal (Gibco), 1ml B-27 supplement (Gibco), 0.5ml 50% glucose, 0.5ml Pen-strep (100%) and 0.5ml Glutamine (100%) (Gibco).

All the media were prepared under sterile conditions under the tissue culture hood to avoid any contamination. Low-melting point agarose (LMP) (Lonza) was prepared the day before the slice preparation in 4% concentration diluted in 1xPBS and left at 43^{o}C (O/N).

2.6.2 Slice preparation and transplant

The embryos were removed from the female (as described in 2.1.3) and kept in sterile filtered 1xKrebs on ice. The brains were dissected out of the embryos and control brains were separated from mutant brains. Subsequently, the selected brains were embedded in LMP agarose and the moulds were placed on 4^{o}C ice for hardening. The brains were cut in 300µl sections with a use of a vibrotome (Leica). The sections were collected in petri dishes containing sterile filtered 1xKrebs at 4^{o}C. The sections were transferred under the tissue culture hood to polycarbonate culture membranes (Whatman). Falcon organ tissue culture dishes (BD Biosciences, Falcon)

containing 1ml MEM medium. The dishes were placed in the incubator at 37^{o}C (1-2hours, 5% CO_2) and subsequently, changed into 1ml Neurobasal medium.

The transplants were cut with fine blades from the donor slice and transferred to the host slice with a 20µl pipette (see Chapter 4). The transplants were kept in the incubator at 37^{o}C (5% CO_2) for 3 days (72 hours) and then fixed in 4% PFA (O/N). Subsequently, the transplants were processed for further vibrotome sectioning (80µm) as described previously (see 2.1.4). Immunofluorescence analysis was performed on the sections as described before (see 2.2.3.2).

2.7 Microscopy

2.7.1 Light microscopy

Slides were visualized using a Leica DMLB upright compound microscope (Leica). Images were taken using an attached DFC480 digital camera and the images were processed using Adobe Photoshop CS2 (Adobe) image management software.

2.7.2 Fluorescence microscopy

Slides were visualized using a Leica DMRE compound microscope associated with the Leica TCS NT confocal system using Leica software to take images. Alternatively, staining was viewed using a Leica DMLB upright compound microscope with a TRITC filter. Images were taken using a Leica DSC480 digital camera and the images were processed using Adobe Photoshop CS2 (Adobe). High-resolution fluorescent microscopy was carried out using an inverted Zeiss LSM510 confocal system in the IMPACT facility, Centre of Integrative Physiology.

2.7.3 Statistical analysis

In Chapter 4 data were analyzed with the computer application GraphPad prism (Graphpad software). Analysis was performed on data collected from P7 brains of at least 3 embryos of each genotype. Mann-Whitney test was used to compare the absolute sizes and the relative length of neocortex and piriform cortex. Asterisks indicate $P< 0.05$.

Table 2-7: Table of solutions used in this thesis.

Solution:	Procedure (solutes and solvents):
Acetate buffer (see 2.2.1)	Set up 245ml H_2O and add 2.5ml 1M sodium acetate and 2.5ml 1M acetic acid
B-block(see 2.2.5)	Dissolve 1g Boehringer block in 45ml PBS/Tween20 on a hot plate stirrer (65^oC). Filter the solution, once it is cold, and add 5ml sheep serum. Aliquots were stored at -20^oC
Blocking solution (see 2.2.6)	5ml sheep serum, 5ml of 10% blocking reagent, 5ml 5xMABT and 10ml H_2O
Buffer H (see 2.5)	20mM Tris-HCl (pH=7.4) 40µl cOmplete protease inhibitor (Roche)
Citrate buffer (see 2.2.2, 2.2.3)	Set up 100mM sodium citrate buffer adjusted to pH=6 with 2N citric acid (29.41g Na_3citrate*2H_2O/ 1L)
Denhardt's (x100) (see 2.2.6)	2% BSA (w/v), 2% Ficoll (w/v) and 2% polyvinyl pyrolidone (w/v) in H_2O
Differentiation solution (see 2.2.1)	Set up 250ml H_2O and add 350µl glacial acetic acid
Hybmix (see 2.2.5)	Dissolve in water bath at 65^oC: 5ml Formamid, 2.5ml 20*SSC (pH=4.5), 100mg Boehringer block, 2ml H_2O. Once dissolved add 100µl 0.5M EDTA, 100µl 10% Tween20, 100µl CHAPS, 4µl Heparin (50mg/ml), 200µl tRNA (50mg/ml)
Hybridization solution(see 2.2.6)	Add 1ml 10x**Salt**, 5ml formamide, 2ml 50% dextran sulphate, 200µl tRNA (50mg/ml), **100µl 100xDenhardt's** and 900µl H_2O
Krebs (x10) (see 2.6)	Set up 73.6g NaCl 126mM, 1.87g KCl 2.5mM, 1.66g NaH_2PO_4–H_2O 1.2mM, 2.44g $MgCl_2$ 1.2mM, 3.68g $CaCl_2$ 2.1mM and add H_2O up to 1L
Laemmli (x5) (see 2.5)	0.125M Tris-HCl (pH=6.8) 10%SDS
MABT (x5) (see 2.2.6)	Add 58.05g Maleic acid, 32g NaOH and correct pH to 7.5 with NaOH before adding 43.8g NaCl, and 5ml 0.5% Tween20. Fill up to 1L with H_2O
Mowiol (see 2.2.2, 2.2.3)	Stir 2.4g Mowiol, 6g glycerol and 12ml H_2O into a 50ml conical flask at room temperature (O/N). Add 12ml 0.2M Tris (pH=8.5) and heat up to 50^oC for 1-2hrs (vortex occasionally). Centrifuge at 2000rpm for 15' and add 2.5% DABCO (Sigma). Aliquot and store at -20^oC

Solution:	Procedure (solutes and solvents):
NTM (see 2.2.5)	Set up 25ml 1M Tris-HCl (pH=9.5), 5ml 5M NaCl, 12.5ml 1M $MgCl_2$ and add H_2O up to 250ml
PBS (x10)	For 1L PBS (pH=7.4): 80.1g NaCl, 2g KCl, 2g KH_2PO_4, 11.6g $Na_2HPO_4*2H_2O$
PFA (4%) (see 2.1.3)	40g paraformaldehyde diluted in 1L PBS after heating (~2hours) and aliquoted in 50ml tubes and stored at -20^oC
PFA (perfusion) (see 2.1.3)	Add 800ml-prewarmed H_2O, 40g paraformaldehyde and 200µl 10N NaOH and stir on a heat plate until dissolved. Add 100ml 1M sodium phosphate buffer (pH=7.2-7.4) and fill up with H_2O up to 1L
Potassium sulphite (see 2.2.1)	Set up 50% potassium sulphite (w/v) in H_2O. Warm it up to help dissolve the saturated solution
Salt (x10) (see 2.2.6)	Add 114g NaCl, 14.04g Tris-HCl, 1.34g Tris base, 7.8g NaH_2PO_4*2 H_2O, 7.1g Na_2HPO_4, 100ml 0.5M EDTA and fill up to 1L with H_2O
SSC (x20) (see 2.2.5)	Add 175.3g NaCl, 88.2g Sodiumcitrate ($C_6H_6Na_3O_7$): 1) for pH 7.0 adjust by using NaOH 2) for pH 4.5 adjust by using 1M citric acid
Staining buffer (see 2.2.6)	Add 8ml 5M NaCl, 20ml 1M $MgCl_2$, 40ml 1M Tris-HCl (pH=9.5), 4ml 10% Tween20 and fill up to 400ml with H_2O
Staining buffer with NBT/BCIP (see 2.2.6)	Set up 95ml of the staining buffer (2ml 5M NaCl, 10ml 1M Tris-HCl and 83ml H_2O) (pH=9.5), add 9g polyvinyl alcohol and heat up until it starts boiling and becomes clear. Let it cool and add 4.5ml 1M $MgCl_2$, 90µl Tween20 and finally 1.8ml NBT/BCIP
TAE (x50)	Add 242g Tris Base, 57.1ml Acetic Acid and 100ml 0.5M EDTA (pH 8.0, adjust with NaOH)
Wash buffer (see 2.2.6)	Add 25ml of 20xSSC (pH=7), 250ml formamide, 500µl 0.1% Tween20 and 225ml H_2O

3 *Gli3* is required in Emx1^{+} progenitors for the development of the corpus callosum

3.1 Introduction

As described in Chapter 1, malformation of the corpus callosum (CC) is described in various clinical syndromes. However, the cellular and molecular mechanisms controlling CC development are yet to be fully understood. A key region controlling CC development is the corticoseptal boundary (CSB). The CSB is a critical intermediate target for callosal axons and contains several midline guidance cues. In brief, glial cells of the glial wedge and the indusium griseum are located adjacent to callosal axons (Shu and Richards, 2001) and prevent them from migrating into the septum by producing the repellent axon guidance molecule *Slit1/2* (Bagri *et al.*, 2002, Shu *et al.*, 2003, Unni *et al.*, 2012). GABAergic neurons, originating from the medial and caudal ganglionic eminence, populate the corpus callosum and channel axons across the midline by exerting attractive activity on callosal axons (Niquille *et al.*, 2009, Niquille *et al.*, 2013). Moreover, Calretinin+ and Calbindin+ neurons located in the indusium griseum and in the cingulate cortex express the *Sema*3C guidance factor, which is required for callosal development (Niquille *et al.*, 2009, Piper *et al.*, 2009). Calretinin+ neurons are also detected within the corpus callosum where they delineate its dorsal and ventral components (Niquille *et al.*, 2009). From these studies, the emerging picture is that the spatial position of the guidance cues at the CSB is critical for callosal axons navigation. Therefore, it is crucial to elucidate the molecular mechanisms that control their position.

Many human syndromes are associated with CC agenesis including Acrocallosal syndrome (Schinzel and Kaufmann, 1986). Acrocallosal syndrome patients carry mutations in the *GLI*3 gene that vary from single point mutations to large deletions and show complete agenesis of the CC (Elson *et al.*, 2002, Speksnijder *et al.*, 2013). The *Gli*3 hypomorphic mutant *Polydactyly Nagoya (Gli3$^{Pdn/Pdn}$)* displays CC agenesis and CC defects are caused by mislocation of the guidance cues at the CSB

that originate during patterning stages (Naruse *et al.*, 1990, Magnani *et al.*, 2012a). These findings suggest a role for *Gli3* in positioning the midline guidance cues at the CSB. Yet, questions remain about the temporal and spatial requirements of *Gli*3. *Gli3* is expressed from E8.5 onwards (Hui *et al.*, 1994) on either side of the CSB in both cortical and septal progenitors as well as in progenitors of the medial (MGE) and caudal ganglionic eminence from which the GABAergic guidepost neurons derive (Niquille *et al.*, 2009, Niquille *et al.*, 2013). This raised the possibility that *Gli*3 is required during patterning stages in cortical and/or septal telencephalic progenitor cells as well as in progenitors of the medial and caudal ganglionic eminence to control the positioning of the guidance cues and hence, CC formation.

The aims of this chapter were to study the above question by identifying the effects of *Gli3* inactivation in the dorsal telencephalon, septum or MGE on CC development and determining the potential *Gli3* controlled molecular mechanisms that regulate CSB formation. To address these aims, I made use of three different *Cre* driver lines i.e. *Zic4Cre* (Rubin *et al.*, 2010), *Nkx2.1Cre* (Nobrega-Pereira *et al.*, 2008) and *Emx1Cre* (Gorski *et al.*, 2002) which express the *Cre* gene in the septum, MGE and dorsal telencephalon, respectively. *Zic4*, *Nkx2.1* and *Emx1* gene expression has been reported in the septal, MGE and cortical progenitors, respectively, giving the unparalleled opportunity to inactivate *Gli3* selectively on the cortical and septal sides of the CSB as well as in the MGE (Schematic 1). Here, I show that deletion of *Gli3* in progenitors of the septum and of the medial ganglionic eminence has no obvious defects on callosal development. In contrast, loss of *Gli3* function in the cortex results in severe disorganization of guidepost cells and in the formation of a hypoplastic CC. Examination of early developmental stages further showed that early changes in Wnt/β-catenin and Fgf8 signaling lead to the premature formation of ectopic glial fibres and to ectopic *Slit1/2* expression in the septum.

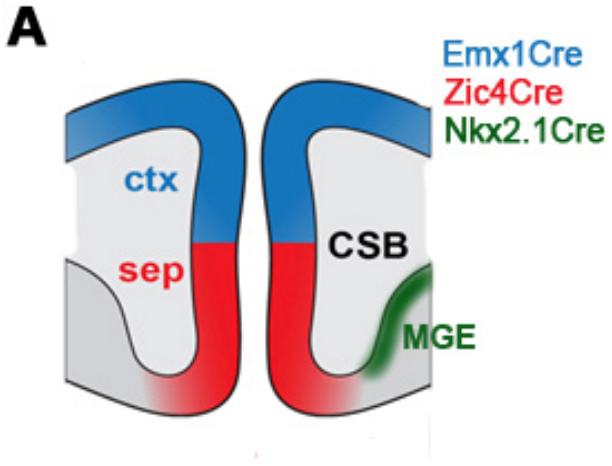

Schematic 8: Schematic illustrating *Zic4*, *Nkx2.1* and *Emx1* gene expression domain.

Schematic representation illustrating the expression of *Emx1Cre*, *Zic4Cre* and *Nkx2.1Cre* in the cortex, septum and MGE, respectively. Abbreviations: CSB, corticoseptal boundary; ctx, cortex; MGE, medial ganglionic eminence; sep, septum (adapted from Thomas Theil).

3.2 The corpus callosum forms normally following inactivation of *Gli3* in the septum or MGE

3.2.1 *Gli3* inactivation in the septum and the medial ganglionic eminence

As discussed above, *Gli3* is required for the correct positioning of the guidance cues and hence for CC development (Magnani *et al.*, 2012a). However, as *Gli3* is expressed widely in the developing forebrain including both cortical and septal progenitors as well as in MGE progenitors which give rise to GABAergic interneurons populating the corpus callosum, it remains unclear in which group of progenitor cells *Gli3* is required during callosal development. In order to address this question, I used the transgenic *Zic4Cre* (Rubin *et al.*, 2010) and *Nkx2.1Cre* (Nobrega-Pereira *et al.*, 2008) mouse lines in which *Cre* is expressed with *Zic4* and *Nkx2.1* regulatory elements from E10.5, respectively. These animals were mated with $Gli3^{fl/fl}$ animals in which two *loxP* sites flank exon 8 of *Gli3* and deletion of exon 8 by Cre recombinase result in a frameshift mutation upstream of the DNA binding domain (Blaess *et al.*, 2008). For the analysis presented in this chapter, $Zic4Cre;Gli3^{+/+}$/$Zic4Cre;Gli3^{fl/+}$ and $Nkx2.1Cre;Gli3^{+/+}$/$Nkx2.1Cre;Gli3^{fl/+}$ brains were used as controls while $Zic4Cre;Gli3^{fl/fl}$ and $Nkx2.1Cre;Gli3^{fl/fl}$ brain as mutants. Coronal sections of E12.5 control and mutant brains were analysed by *in situ* hybridisation to determine the efficiency and tissue-specificity of Cre-mediated deletion of *Gli3* during patterning stages in the regions of interest i.e. septum and MGE (Figure 3-1). A 4982 bp fragment comprising nucleotides 132–5113 of the mouse *Gli3* mRNA including exon 8 was used as a template for *Gli3* probe synthesis. This analysis revealed strong *Gli3* mRNA expression in the ventricular zone of both dorsal and ventral telencephalon of $Zic4Cre;Gli3^{fl/+}$ (Fig.3-1A) and $Nkx2.1Cre;Gli3^{fl/+}$(Fig.3-1C) embryos. In contrast, in $Zic4Cre;Gli3^{fl/fl}$ mutants *Gli3* expression was specifically abolished in the septum (Fig.3-1B) while in $Nkx2.1Cre;Gli3^{fl/fl}$ mutants *Gli3* mRNA deletion was selective in the MGE (Fig.3-1D). Thus, these conditional mutants demonstrate specific *Gli3* inactivation in a subset of telencephalic progenitor cells.

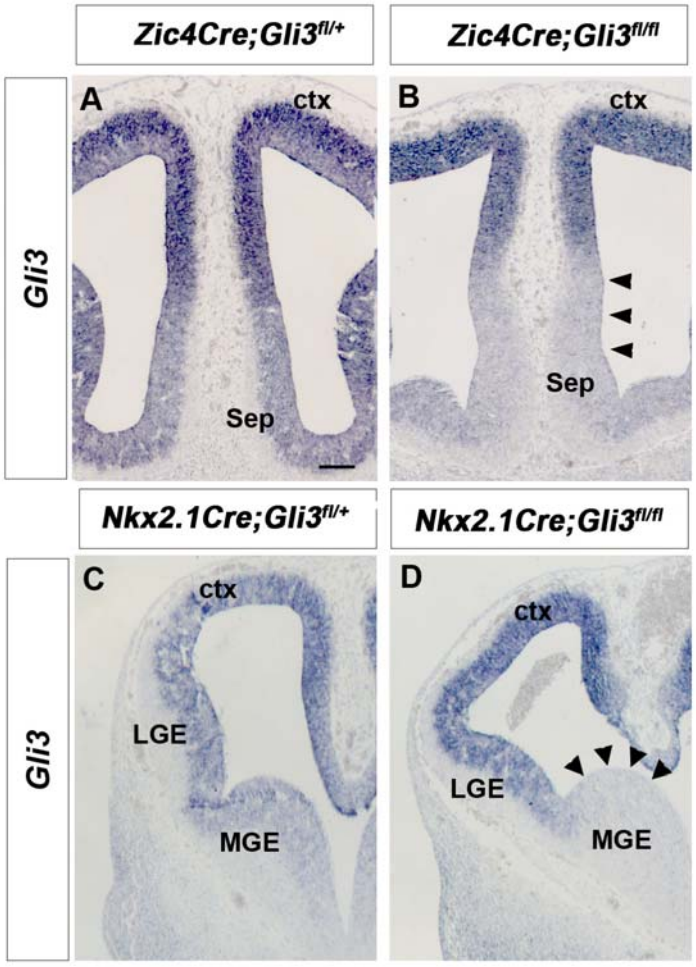

Figure 3-1: *Gli3* is inactivated in septal and MGE progenitors.

(A) *Gli3* is strongly expressed in the ventricular zone of both cortical and septal telencephalic regions (B) *Gli3* expression is abolished in the septum of *Zic4Cre;Gli3*$^{fl/fl}$ conditional mutants (arrow). (C) *Gli3* mRNA is strongly expressed at the cortex and lateral ganglionic eminence and at lower levels at the medial ganglionic eminence. (D) In *Nkx2.1Cre;Gli3*$^{fl/fl}$ mutants, progenitors residing at the MGE do not express *Gli3* (arrow). Abbreviations: ctx, cortex; LGE, lateral ganglionic eminence; MGE, medial ganglionic eminence; sep, septum. Scale bars: 100µm.

3.2.2 Formation of callosal tract and midline guidance cues is not obviously affected in *Zic4Cre;Gli3$^{fl/fl}$* and *Nkx2.1Cre;Gli3$^{fl/fl}$* mutants

Having established specific *Gli3* inactivation in *Zic4Cre;Gli3$^{fl/fl}$* and *Nkx2.1Cre;Gli3$^{fl/fl}$* mutants, I next examined the development of the CC and the formation of the midline guidance cues. I initially performed immunofluorescence analysis for the cell adhesion molecule L1, which is strongly expressed by axons (Persohn and Schachner, 1990) including callosal axons, on the rostrocaudal axis of E18.5 control, *Zic4Cre;Gli3$^{fl/fl}$* and *Nkx2.1Cre;Gli3$^{fl/fl}$* embryos (Figure 3-2). This analysis revealed the characteristic U-shaped pattern of the CC along the rostrocaudal axis of control brains (Fig.3-2A-C). Neither *Zic4Cre;Gli3$^{fl/fl}$* (Fig.3-2D-F) or *Nkx2.1Cre;Gli3$^{fl/fl}$* (Fig.3-2G-I) mutants revealed any obvious defects. To further examine the formation and positioning of the midline guidance cues in relation to the CC tract, I performed immunofluorescence analysis for L1 to label the callosal axons and glial fibrillary acidic protein (GFAP) to reveal the glial wedge (GW), the indusium griseum glia (IGG) and the midline zipper glia (MZG) (Fig.3-3A) (Shu *et al.*, 2003). In control brains, the IGG was located dorsally to the corpus callosum; GW was a bilateral symmetrical structure flanking CC at the CSB; and MZG was found ventrally to the CC at the septal midline (Fig.3-3A). The subcallosal sling was labelled for T-box brain 1 transcription factor (Tbr1) and intracellular calcium-binding protein Calretinin (CR) that marked glutamatergic neurons; and for calcium binding protein Calbindin (CB) that marked both glutamatergic and GABAergic neurons (Niquille *et al.*, 2009, Niquille *et al.*, 2013). In control brains, the expression of Tbr1 protein in the telencephalon was complex with Tbr1+ neurons found in the marginal zone, neocortical layer VI and subplate and also at the CSB dorsally to the CC and within the callosal tract (Fig.3-3B). CB+ and CR+ neurons were positioned dorsally to the CC at the indusium griseum and CR+ cells were also found within the callosal tract to delineate its path (Fig.3-3C-D). No apparent malformations of the callosal guidepost cells were seen in *Zic4Cre;Gli3$^{fl/fl}$* (Fig.3-3E-H) or *Nkx2.1Cre;Gli3$^{fl/fl}$* conditional mutants (Fig.3-3I-L).

The GABAergic neuronal population of the subcallosal sling originate from the MGE and caudal ganglionic eminence (Niquille *et al.*, 2009, Niquille *et al.*, 2013). These guidepost GABAergic neurons constitute attractive cues for callosal axons that converge towards the midline prior to the arrival of axons (Niquille *et al.*, 2013). Thus, I examined their formation and migration to the CSB by mating animals of the *Nkx2.1Cre* driver mouse line (Nobrega-Pereira *et al.*, 2008) with animals of the *ROSA26CAG dual stop EGFP reporter* (RCE) mouse line (Sousa *et al.*, 2009). In *Nkx2.1Cre;Gli3*$^{fl/+}$*;RCE* control and *Nkx2.1Cre;Gli3*$^{fl/fl}$*;RCE* conditional mutant brains, GFP is expressed after Cre mediated excision of the stop codon, that lies upstream of the *EGFP* reporter, in all *Nkx2.1* precursors (Sousa *et al.*, 2009). This lineage tracing of MGE derived GABAergic neurons was conducted by performing an immunofluorescence analysis for GFP on E18.5 *Nkx2.1Cre;Gli3*$^{fl/+}$*;RCE* and *Nkx2.1Cre;Gli3*$^{fl/fl}$*;RCE* conditional mutant brains (Figure 3-4). In *Nkx2.1Cre;Gli3*$^{fl/+}$*;RCE* control brains, GFP+ neurons had already migrated into the indusium griseum (Fig.3-4A) and within the callosal tract at the subcallosal sling (Fig.3-4C). Similarly, in *Nkx2.1Cre;Gli3*$^{fl/fl}$*;RCE* mutant brains GFP+ GABAergic neurons showed no apparent migration defects with GFP+ neurons present above and into the callosal tract (Fig.3-4 B, D). Taken together these experiments indicate that CC formation is not affected after specific *Gli3* inactivation in either the septum or the MGE.

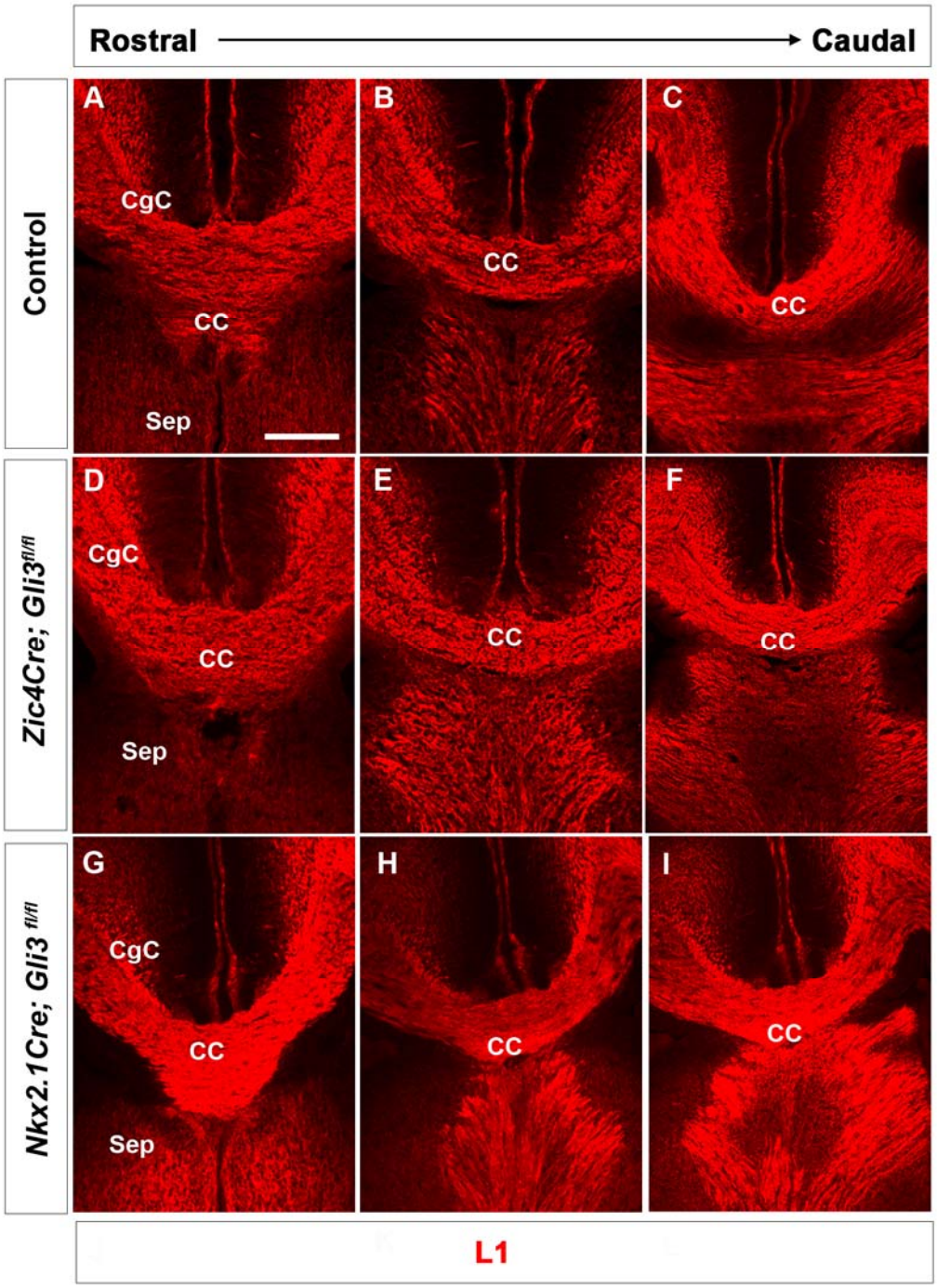
Rostral
Caudal
Control
Zic4Cre; Gli3fl/fl
Nkx2.1Cre; Gli3 fl/fl
A
B
C
D
E
F
G
H
I
CgC
CC
Sep
L1

Figure 3-2: No obvious defects are detected in CC development in *Zic4Cre;Gli3$^{fl/fl}$* or *Nkx2.1Cre;Gli3$^{fl/fl}$* mutants.

(A-I) L1 cell adhesion molecule labels axons of all three genotypes. (A-C) CC tract formation from rostral to caudal levels. (D-I) In *Zic4Cre;Gli3$^{fl/fl}$* or *Nkx2.1Cre;Gli3$^{fl/fl}$* mutants L1+ axons cross the midline along the rostrocaudal axis. Abbreviations: CC, corpus callosum; CgC, cingulate cortex; Sep, septum. Scale bars: 250μm.

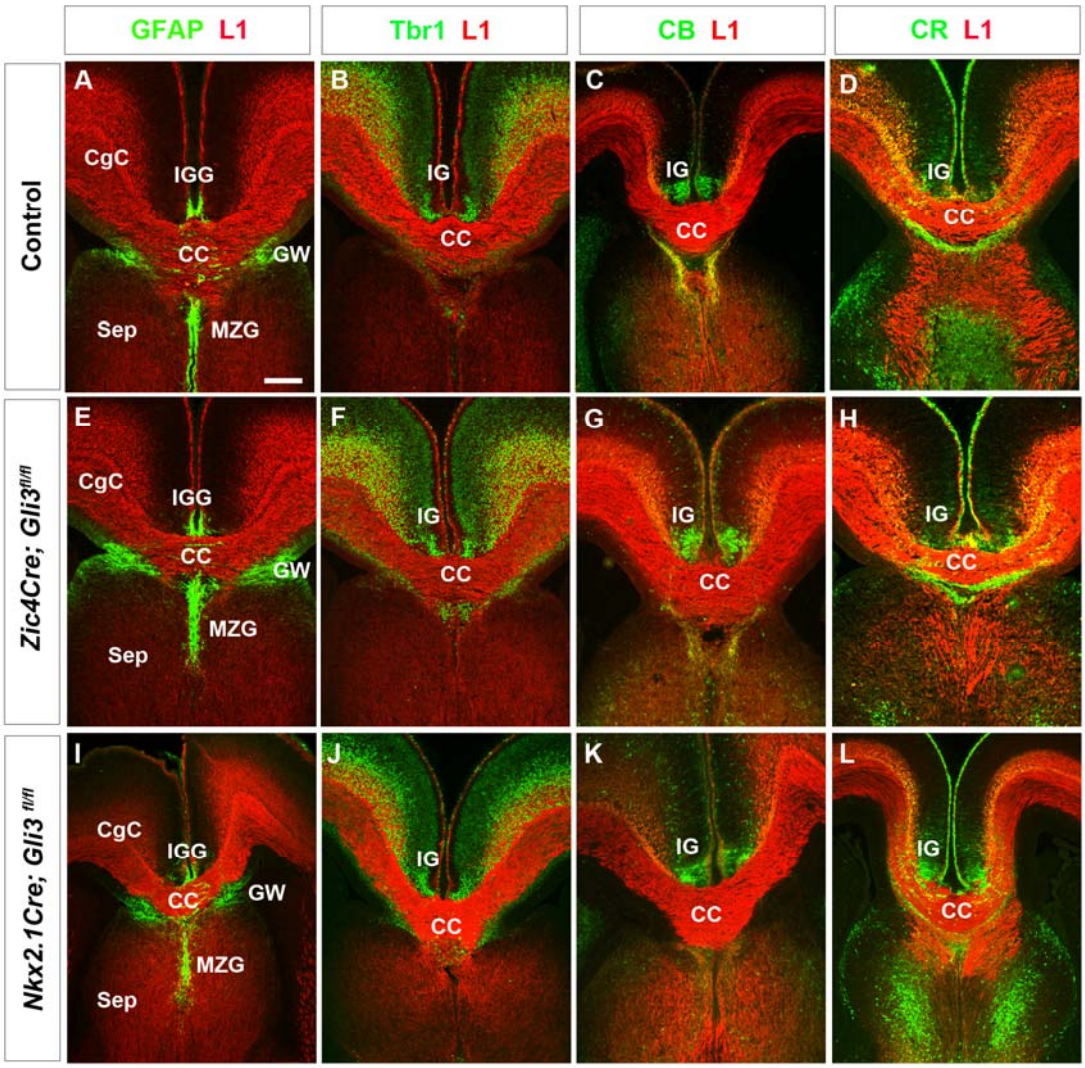

Figure 3-3: Corpus callosum and midline guidance cues form normally in *Zic4Cre;Gli3$^{fl/fl}$* and *Nkx2.1Cre;Gli3$^{fl/fl}$* mutants.(A-L) Immunofluorescence analysis for L1 revealed that callosal axons of all three genotypes cross the midline (A-L). Midline glial structures labelled with GFAP (A,E,I) and the callosal guidepost neurons labelled with Tbr1 (B,F,J), Calbindin (C,G,K) and Calretinin (D,H,L) show no obvious malformations in mutant brains. Abbreviations: CC, corpus callosum; CgC, cingulate cortex; GW, glial wedge; HC, hippocampal commissure; IGG, indusium griseum glia; IG, indusium griseum; MZG, midline zipper glia; Sep, septum. Scale bars: 250µm.

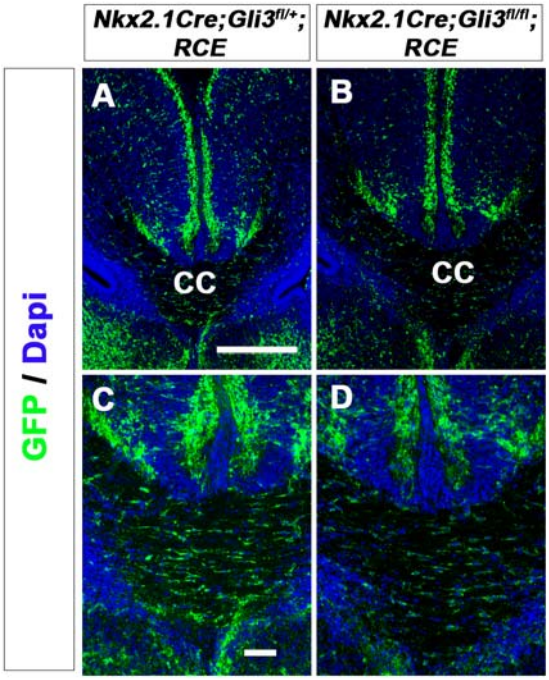

Figure 3-4: Lineage tracing analysis of guidepost cues originating from the MGE.

(A, C) GFP+ Nkx2.1-derived neurons are located above the corpus callosum as well as within the callosal tract in control brains (C, higher magnification). (B, D) GFP+ Nkx2.1-derived guidepost neurons acquire their normal position in *Nkx2.1Cre;Gli3$^{fl/fl}$;RCE* mutant brains. Abbreviations: CC, corpus callosum. Scale bars: A-B:250µm; C-D:50µm.

3.3 Deletion of *Gli3* in dorsal telencephalon causes callosal defects

3.3.1 Selective and gradual deletion of *Gli3* in *Emx1Cre;Gli3$^{fl/fl}$* conditional mutants

To determine whether *Gli3* is required in cortical progenitors dorsally to the CSB I used *Emx1-Cre* knock-in mice in which *Cre* expression is driven in the developing dorsal telencephalon from E9.5 (Gorski *et al.*, 2002). These animals were mated with *Gli3$^{fl/fl}$* animals to create *Gli3* conditional mutants as previously described. *Emx1Cre;Gli3$^{+/+}$*/*Emx1Cre;Gli3$^{fl/+}$* brains were used as controls for the study in this chapter, as neither showed any phenotype, and *Emx1Cre;Gli3$^{fl/fl}$* brains were used as mutants. To monitor *Gli3* inactivation, time course analysis of *Gli3* mRNA expression was performed on coronal sections of *Emx1Cre;Gli3$^{fl/+}$* and *Emx1Cre;Gli3$^{fl/fl}$* conditional mutant brains between E10.5-12.5 (Figure 3-5). In control brains, strong *Gli3* expression was seen in the ventricular zone of both the dorsal telencephalon and the lateral ganglionic eminence and lower levels were detected in the medial ganglionic eminence at all stages analysed (Fig.3-5.A-C). At E10.5 *Emx1Cre;Gli3$^{fl/fl}$* brains, *Gli3* expression was abolished from the medial cortex (Fig.3-5 D, arrowhead). Loss of *Gli3* expression gradually expanded to more lateral cortical regions during further development indicating that neocortical inactivation was complete by E12.5 (Fig.3-5E-F, arrowhead). The inactivation was specific as *Gli3* expression remained unaffected in the ventral telencephalon and the septum of *Emx1Cre;Gli3$^{fl/fl}$* brains (Fig.3-5D-F). To determine whether *Gli3* protein was also absent from the dorsal telencephalon, I performed western blot analysis.

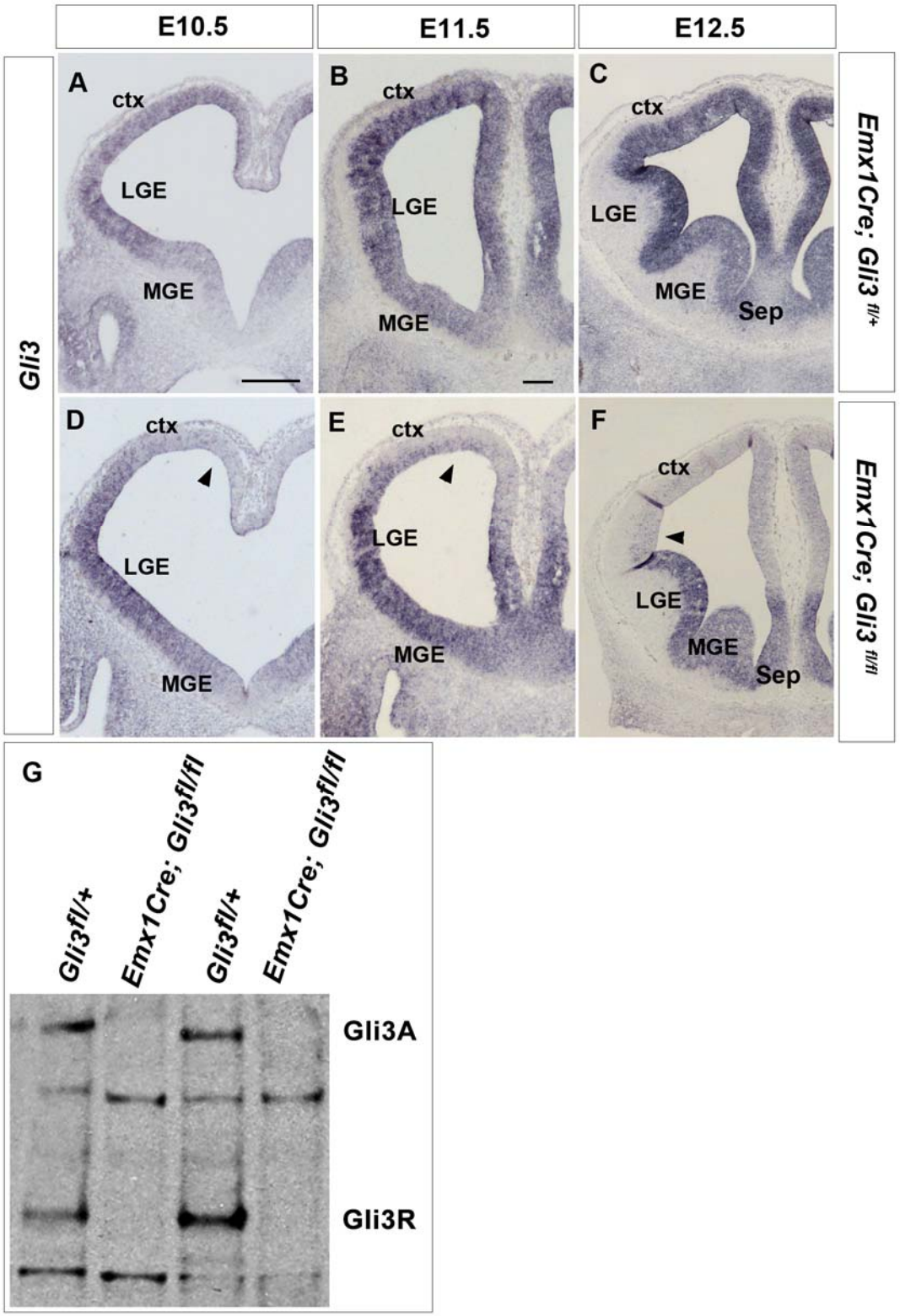
E10.5
E11.5
E12.5
Gli3
Emx1Cre; Gli3 fl/+
Emx1Cre; Gli3 fl/fl
A
B
C
D
E
F
ctx
LGE
MGE
Sep
G
Gli3fl/+
Emx1Cre; Gli3fl/fl
Gli3fl/+
Emx1Cre; Gli3fl/fl
Gli3A
Gli3R

Figure 3-5: *Gli3* is inactivated in the dorsal telencephalon of *Emx1Cre;Gli3$^{fl/fl}$* conditional mutants.

(A-C) Time course analysis of *Gli3* expression in control brains (E10.5-E12.5). *Gli3* is strongly expressed in both pallial and subpallial ventricular zone except in the MGE in which *Gli3* expression is lowered (C). (D-F) Selective and gradual deletion of *Gli3* in the dorsal telencephalon on *Emx1Cre;Gli3$^{fl/fl}$* conditional mutants. Inactivation begins from the medial cortex (D, arrowhead) and expands to the lateral cortex (E-F, arrowheads). (G) Western blot analysis of *Gli3* protein. Two Gli3 isoforms of about 170 and 88kDa, correspond to the Gli3 activator (Gli3A) and repressor (Gli3R) forms, respectively. In *Emx1Cre;Gli3$^{fl/fl}$* conditional mutants, Gli3A and Gli3R are absent. Abbreviations: ctx, cortex; LGE, lateral ganglionic eminence; MGE, medial ganglionic eminence. Scale bars: A, D:100µm; B-C, E-F:100µm.

Protein extracts from E12.5 dorsal telencephali of control embryos were examined using a Gli3 N-terminal antibody. Gli3 protein exists in two forms, a long 170 kDa full-length isoform and an 88 kDa isoform formed by cleavage of the full-length product, corresponding to the Gli3 activator (Gli3A) and repressor (Gli3R) forms, respectively (Wang *et al.*, 2000). The results showed bands at ~170kDa and 88 kDa, in extracts from control dorsal telencephalon that were absent in *Emx1Cre;Gli3*$^{fl/fl}$ tissue and correspond to the previously described full-length and cleaved isoforms, respectively (Fig.3-5G) (Wang *et al.*, 2000). The antibody also detected nonspecific bands of intermediate size and unknown identity as described in previous work (Magnani *et al.*, 2010) which were not affected by *Gli3* inactivation. Taken together these analyses confirmed that *Gli3* inactivation in the dorsal telencephalon was complete and specific by E12.5.

3.3.2 Corpus callosum and midline guidance cues are highly abnormal

Having established the specificity of *Gli3* inactivation in *Emx1Cre;Gli3*$^{fl/fl}$ mutants, I next examined CC development in E18.5 control and *Emx1Cre;Gli3*$^{fl/fl}$ mutants. I first carried out immunofluorescence analysis for the L1 axonal marker on coronal sections along the rostrocaudal axis (Figure 3-6). In control brains, L1+ callosal axons crossed the midline in a normal manner and in more caudal levels CC was located above the hippocampal commissure (Fig.3-6A-C). In contrast, *Emx1Cre;Gli3*$^{fl/fl}$ mutant brains showed aberrant callosal tract formation with many L1+ axons forming longitudinal callosal fascicles or Probst bundles. However, a few axons crossed the midline and formed a hypoplastic CC throughout the rostrocaudal axis (Fig.3-6D-F). Next, I investigated the formation and migration of the midline guidance cues in relation to the CC by performing a similar marker analysis to the one described above (Figure 3-7). In control brains, L1+ callosal axons crossed the midline normally in control brains (Fig.3-7A-C). In *Emx1Cre;Gli3*$^{fl/fl}$ mutants, however, the path of callosal axons was severely disrupted and ectopic axonal bundles were formed at several positions. Nonetheless, some callosal axons in the

conditional mutants approached the midline but formed a highly abnormal structure (Fig.3-7D-F). Tbr1+ and CB+ neurons were positioned dorsally to the CC and CB+ neurons were densely packed in the indusium griseum of control brains (Fig.3-7A-B). In *Emx1Cre;Gli3*$^{fl/fl}$ mutant brains, Tbr1+ and CB+ neurons acquired abnormal positions in the dorso-medial cortex, where they associated with the abnormal axon bundles and the hypoplastic CC (Fig.3-7D-E). GFAP labels the midline glial population at the IGG, GW and MZG in control brains (Fig.3-7C). In *Emx1Cre;Gli3*$^{fl/fl}$ mutant brains, the GFAP+ indusium griseum was expanded and abnormally associated with the hypoplastic CC while the glia wedge was present bilaterally ventral to the CC (Fig.3-7F). Thus, the CC is severely abnormal in E18.5 *Emx1Cre;Gli3*$^{fl/fl}$ mutant brains and midline guidance cues occupy aberrant positions.

The corpus callosum continues to develop postnatally with the callosal axons becoming myelinated and the tract increasing in size. As *Gli3*$^{Pdn/Pdn}$ mutants die perinatally, these mutants could not be used to determine a possible role for *Gli3* in later aspects of callosal development. In contrast, *Emx1Cre;Gli3*$^{fl/fl}$ conditional mutants are viable therefore offering the opportunity to study postnatal CC development in a *Gli3* mutant background. On that basis, I assessed CC development in postnatal day 7 (P7) control and *Emx1Cre;Gli3*$^{fl/fl}$ mutant brains (Figure 3-7). The overall midline morphology and CC was identified using Cresyl violet staining which labels Nissl substance in the cytoplasm of neurons. In control brains, the neuron-dense neocortical area appeared violet in contrast to the cell-sparse marginal zone. Moreover, the cell-sparse intermediate zone and the CC tract were also distinct (Fig.3-7G). In *Emx1Cre;Gli3*$^{fl/fl}$ mutants CC remained hypoplastic although it was increased in size (Fig.3-5J). To confirm whether callosal axons crossed the midline, DiI crystals were placed in control and mutant rostro-medial cortex (Fig.3-7H-I, K-L). DiI is a fluorescent lipophilic indocarbocyanine dye used as retrograde and anterograde neuronal tracer since it diffuses along the cellular membranes of cells including their axonal processes. In control brains, DiI crystal placement led to the anterograde labelling of a thick callosal bundle (Fig.3-7H, K). In contrast, in *Emx1Cre;Gli3*$^{fl/fl}$ mutants, although callosal axons did reach the midline, most of them formed Probst bundles (Fig.3-7K) and only a few actually

crossed to the contralateral side (Fig.3-7L). Taken together, these findings indicate that even though a number of axons are able to cross the midline in pre- and postnatal *Emx1Cre;Gli3*$^{fl/fl}$ conditional brains the CC is largely abnormal with the vast majority of the axons forming Probst bundles.

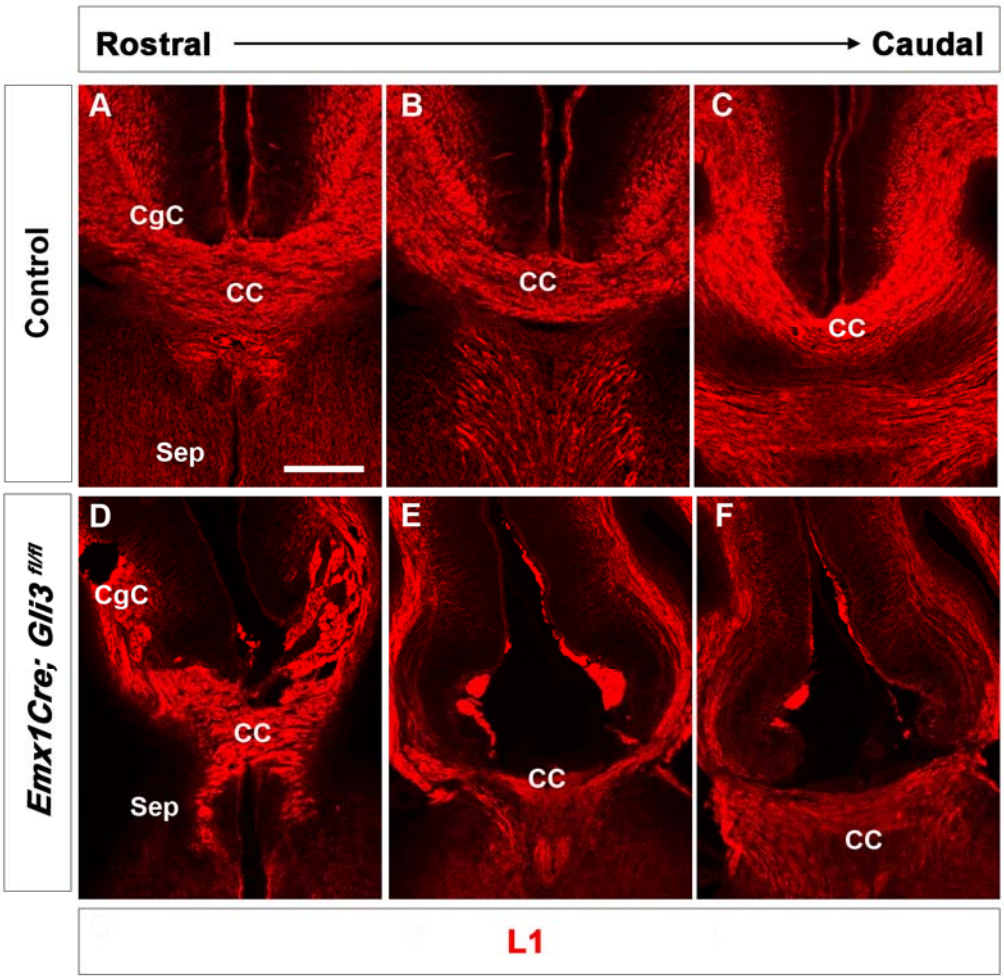

Figure 3-6: CC development is abnormal along the rostrocaudal axis of the *Emx1Cre;Gli3*$^{fl/fl}$ mutant brains.

(A-C) L1+ axons cross the midline along the rostrocaudal axis of control brains. CC is located above the hippocampal commissure in caudal levels. (D-F) *Emx1Cre;Gli3*$^{fl/fl}$ mutant brains show hypoplastic CC formation along the rostrocaudal axis with many L1+ axons forming probst bundles (n=6, with 100% penetrance). Abbreviations: CC, corpus callosum; CgC, cingulate cortex; Sep, septum. Scale bars: 250µm.

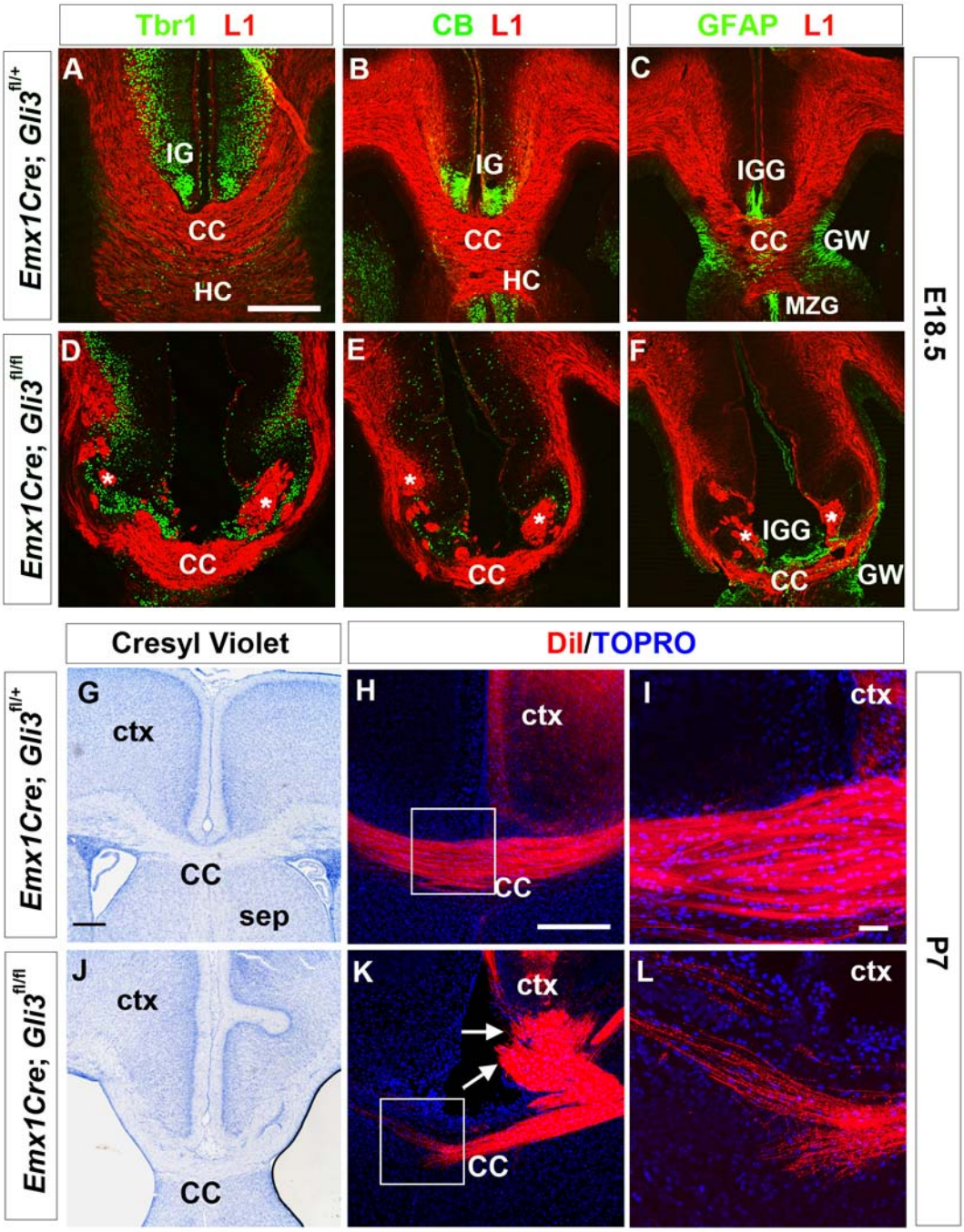
Tbr1 L1
CB L1
GFAP L1
Emx1Cre; Gli3fl/+
Emx1Cre; Gli3fl/fl
A
B
C
D
E
F
IG
CC
HC
IGG
GW
MZG
E18.5
Cresyl Violet
DiI/TOPRO
G
H
I
J
K
L
ctx
sep
P7

Figure 3-7: Callosal defects and severe disorganization of midline structures in *Emx1Cre;Gli3$^{fl/fl}$* conditional brains.

(A-C) L1+ axons cross the midline dorsally to the hippocampal commissure in control brains. (D-F) In *Emx1Cre;Gli3$^{fl/fl}$* mutants, callosal axons form probst bundles (asterisk) and the CC is hypoplastic. (A-B) Tbr1+ and CB+ midline neurons form bundles dorsally to the CC in control brains. (C) GFAP+ cells are located at the IGG, GW and the MZG. (D-E) Tbr1+ and CB+ midline neurons associate with the hypoplastic CC and the Probst bundles in *Emx1Cre;Gli3$^{fl/fl}$* mutants. (F) In *Emx1Cre;Gli3$^{fl/fl}$* mutants, the IGG is located dorsally to the hypoplastic CC but it is elongated. The GW is present on each side of the CC. (G) P7 control brains are stained with cresyl violet to visualize general midline morphology and CC. (J) In *Emx1Cre;Gli3$^{fl/fl}$* mutants, the CC is present but largely hypoplastic. (H-I) Anterograde labelling of a thick callosal axon bundle with DiI crystal placement. (K-L) In *Emx1Cre;Gli3$^{fl/fl}$* mutants, most axons form Probst bundles (arrow) and only few cross the midline. Abbreviations: CC, corpus callosum; ctx, neocortex; GW, glial wedge; HC, hippocampal commissure; IGG, indusium griseum glia; IG, indusium griseum; MZG, midline zipper glia; Sep, septum. Scale bars: A-F, H, K:250µm; G, J:100µm; I, l:50µm.

3.4 Callosal neuron specification is not affected in *Emx1Cre;Gli3$^{fl/fl}$* mutant brains

Emx1 is expressed in progenitor cells that will give rise to postmitotic callosal projection neurons as well as the midline guidance cues (Gorski *et al.*, 2002). Therefore, the CC defects in *Emx1Cre;Gli3$^{fl/fl}$* conditional mutants could result from neuronal misspecification or from defective formation of the midline guidance structures. To test the first possibility, cortical development was characterised (Li, 2011, Amaniti *et al.*, 2013). L1, 2011 conducted the following experiments under the supervision of EM. Amaniti. First, cortical thickness was measured along the rostrocaudal axis. At rostral levels of *Emx1Cre;Gli3$^{fl/fl}$* mutant brains the thickness of the cerebral cortex was not altered but at caudal levels the cortex was significantly thinner. Also, immunofluorescence analysis was performed for the special AT-rich sequence-binding protein 2 (Satb2) that labels callosal neurons in layers II/III (Alcamo *et al.*, 2008, Britanova *et al.*, 2008). The proportion of Satb2+ callosal neurons to the total number of neurons was not affected in mutant embryos. However, the distribution of Satb2+ neurons was altered and also differed along the rostrocaudal axis. At rostral levels, more Satb2+ neurons were detected in their final position in the upper cortical plate and subsequently fewer Satb2+ neurons were detected in the lower cortical plate of *Emx1Cre;Gli3$^{fl/fl}$* mutants. In contrast, a delay in cortical layering was detected at caudal levels since significantly more Satb2+ neurons were found in the lower cortical plate of mutant embryos (Li, 2011, Amaniti *et al.*, 2013).

Moreover, the IG and the GW express the chemorepellent *Slit1/2* which restricts callosal axons descent to the septum (Shu and Richards, 2001). Roundabout 1 (Robo1) is a transmembrane receptor implicated in transducing Slit signalling to callosal axons (Unni *et al.*, 2012). Brain commissural and decussating neurons, including callosal neurons, express Robo protein (Sundaresan *et al.*, 2004), and respond to *Slit1/2* both before and after they cross the midline (Bagri *et al.*, 2002, Shu *et al.*, 2003, Andrews *et al.*, 2006). Moreover, Robo1 knock-out mice show aberrant axonal pathfinding in the corpus callosum and hippocampal commissure

(Andrews *et al.*, 2006) rendering Robo1 an important axon guidance receptor. Thus, *in situ* hybridisation analysis was performed to analyse *Robo*1 expression and determine if callosal axons receptor was defective (Figure 3-8). In control brains, *Robo*1 is expressed within the cortical plate and the lateral ganglionic eminence (Fig.3-8A) (Marillat *et al.*, 2002). No obvious expression defects were detected in *Emx1Cre;Gli3*$^{fl/fl}$ mutant brains (Fig.3-8B). Taken together, these data indicate that Satb2+ callosal neurons are present in the cortex of *Emx1Cre;Gli3*$^{fl/fl}$ mutant brains and express Robo1 receptor. To which extent *Gli3* inactivation from the upper layer neurons has affected their specification and callosal axon formation is not examined in this thesis. Although, the contribution of cell autonomous effects in the CC phenotype observed in *Emx1Cre;Gli3*$^{fl/fl}$ mutant brains cannot be ruled out, I focused on examining the aberrant positioning of midline cues as a likely cause for the CC defects in *Emx1Cre;Gli3*$^{fl/fl}$ mutant brains.

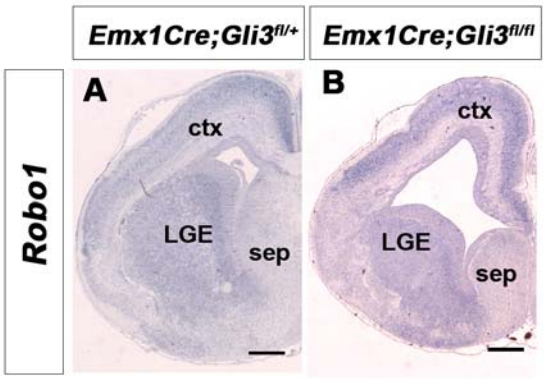

Figure 3-8: *Robo*1 expression is not affected in *Emx1Cre;Gli3*$^{fl/fl}$ mutant brains.

(A) In *Emx1Cre;Gli3*$^{fl/+}$ brains, *Robo*1 is expressed in the upper layers neurons of commissural and decussating axons and deep into the ganglionic eminence. (B) *Robo1* expression in cortical neurons is not affected in conditional mutants. Abbreviations: ctx, cortex; LGE, lateral ganglionic eminence; sep, septum. Scale bar: 100μm.

3.5 Midline abnormalities start to be found in *Emx1Cre;Gli3$^{fl/fl}$* conditional mutants at E12.5

Next, I investigated the causes of the midline defects. Several studies have shown a requirement of *Gli3* for the correct expression of several signalling molecules in the telencephalon, including several members of *Wnt* gene family and *Fgf8* (Grove *et al.*, 1998, Theil *et al.*, 1999, Tole *et al.*, 2000, Aoto *et al.*, 2002, Kuschel *et al.*, 2003, Magnani *et al.*, 2010). Moreover, since altered Fgf/Wnt/β–catenin signalling led to malformation of the CSB and subsequent misposition of midline guidance structures in E12.5 *Gli3$^{Pdn/Pdn}$* mutants (Magnani *et al.*, 2012a), I analysed Fgf/Wnt/β–catenin signalling by *in situ* hybridisation analysis in *Emx1Cre* conditional mutants. Initially, an anatomical comparison between E12.5 *Emx1Cre;Gli3$^{fl/+}$* and *Emx1Cre;Gli3$^{fl/fl}$* mutant brains revealed an elongation of the midline region and enlarged ventricles (Figure 3-9). Next, I focused on analysing Wnt ligands which were expressed at the midline i.e. *Wnt7b/8b* and the Wnt target gene *Axin2*. *Wnt7b* was expressed at cortical progenitors dorsally to the CSB and in preplate neurons and *Wnt8b* expression was confined to the dorso-medial telencephalon (Fig.3-9A-B). *Axin2* expression was confined at the CSB of control brains (Fig.3-9C). I n control brains *Fgf8* transcripts and that of its target gene *sprouty2* were confined to the commissural plate and to the septum, respectively (Fig.3-9D-E). In *Emx1Cre;Gli3$^{fl/fl}$* mutants, *Wnt7b* expression was clearly reduced in the cortical side of the CSB but not in preplate neurons (Fig.3-9F, arrow) while *Wnt8b* showed no obvious expression changes (Fig.3-9G). Moreover, *Axin2* expression is unaffected in *Emx1Cre;Gli3$^{fl/fl}$* mutant brains (Fig.3-9H). Finally, no obvious differences were detected between *Emx1Cre;Gli3$^{fl/+}$* and *Emx1Cre;Gli3$^{fl/fl}$* mutant brains regarding *Fgf*8 and *sprouty2* expression (Fig.3-9I-J). Thus, no apparent changes of signalling molecules were found in E12.5 *Emx1Cre;Gli3$^{fl/fl}$* mutant brains with the exception of *Wnt7b* which showed reduced expression. However, the unaffected *Axin2* expression indicates that the overall levels of Wnt/β–catenin signalling are not altered.

Midline glial structures are an important guidance cues for CC development, which appear severely disorganised in E18.5 and P7 *Emx1Cre* conditional mutants. Midline

glial structures are derived from differentiated radial glial cells that have translocated their bodies towards the pia (Pixley and de Vellis, 1984, Mission *et al.*, 1991). Radial glial cells (RGCs) extend an apical foot to the ventricular surface and a basal process to the pial membrane during their neurogenic phase. In E12.5 *Gli3*$^{Pdn/Pdn}$ mutants, RGCs form clusters in the dorso-medial telencephalon during their neurogenic phase, presaging the formation of ectopic glial clusters at later stages (Magnani *et al.*, 2012a). To determine whether this also happens in the *Emx1Cre* conditional mutants, I examined expression of the neurogenic RGC marker fatty acid binding protein 7 (*Fabp7*). In control brains, *Fabp7* was strongly expressed in the cortical side of the CSB and at the ganglionic eminences (Fig.3-9K). In *Emx1Cre;Gli3*$^{fl/fl}$ mutant brains, *Fabp7* expression was severely reduced in the midline (Fig.3-9M, arrow).

Finally, *Slit2* is an important axon guidance molecule that repels callosal axons from descending to the septum (Bagri *et al.*, 2002) and is expressed form E9.5 onwards at the commissural plate (Yuan *et al.*, 1999). Moreover, *Slit2* is already up-regulated in E12.5 *Gli3*$^{Pdn/Pdn}$ mutants causing a disorganization of midline guideposts (Magnani *et al.*, 2012a). To determine whether this also happens in the *Emx1Cre* conditional mutants, I examined expression of *Slit2*. In control brains, *Slit2* was expressed in the septum (Fig.3-9L) with no obvious defects detected in *Emx1Cre;Gli3*$^{fl/fl}$ mutant brains (Fig.3-9N). Overall, only subtle changes were found in the midline of *Emx1Cre* conditional mutant brains at E12.5. These changes involved a reduction in the cortical expression of *Wnt7b* and *Fabp7* at the CSB.

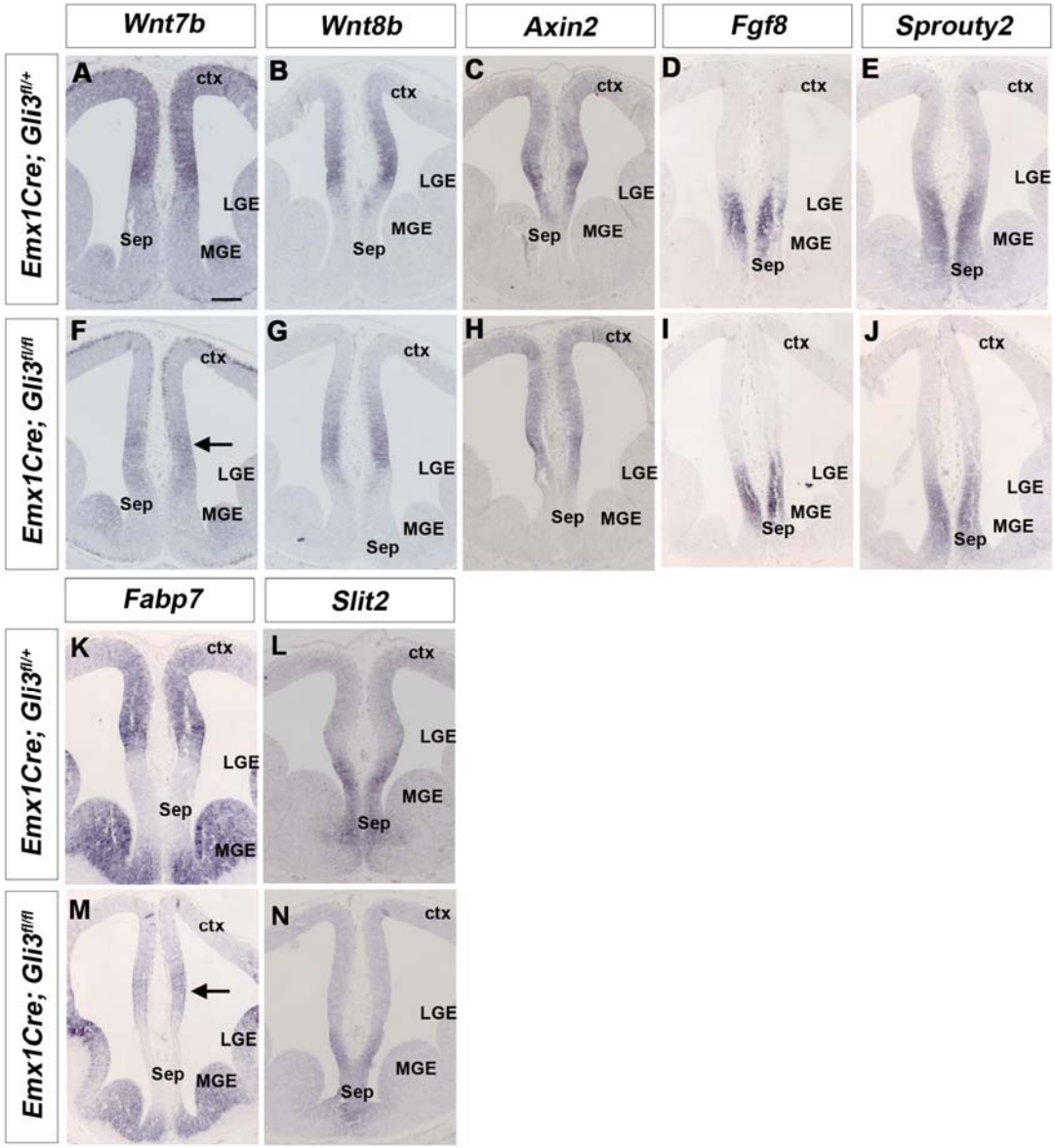
Wnt7b
Wnt8b
Axin2
Fgf8
Sprouty2
Emx1Cre; Gli3fl/+
Emx1Cre; Gli3fl/fl
A
B
C
D
E
F
G
H
I
J
ctx
LGE
MGE
Sep
Fabp7
Slit2
K
L
M
N

Figure 3-9: *Emx1Cre;Gli3*$^{fl/fl}$ conditional mutants display subtle patterning defects in the E12.5 telencephalic midline.

(A) *Wnt*7b is expressed in cortical progenitors and in preplate neurons. (F) In *Emx1Cre;Gli3*$^{fl/fl}$ mutants, *Wnt*7b expression is reduced in cortical progenitors dorsally to the CSB and shows weak expression in septal progenitors (arrow). (B, G) *Wnt8*b is expressed at the dorso-medial telencephalon of both control and in *Emx1Cre; Gli3*$^{fl/fl}$ mutant brains without obvious defects (C,H). *Axin*2 expression in dorso-medial cortex of control and mutant brains showed no obvious differences. (D,E) In control brains, *Fgf*8 and Fgf signalling is confined to the septum. (I, J) *Fgf*8 and *sprouty*2 expression in the septum show no obvious defects in *Emx1Cre; Gli3*$^{fl/fl}$ embryos. (K) Control embryos strongly express *Fabp*7 in the midline and the MGE. (M) In *Emx1Cre;Gli3*$^{fl/fl}$ mutants, *Fabp*7 expression is severely reduced in the dorso-medial cortex (arrow) and in a lesser extend in the MGE. (L, N) *Slit*2 expression in the septum shows no obvious difference between control and *Emx1Cre;Gli3*$^{fl/fl}$ mutant brains. Abbreviations: ctx, cortex; LGE, lateral ganglionic eminence; MGE, medial ganglionic eminence; sep, septum. Scale bars: 100µm.

3.6 The expression of signalling molecules is altered in E14.5 *Emx1Cre;Gli3*$^{fl/fl}$ conditional mutants

Given that only subtle changes were found in the midline of E12.5 conditional mutant brains, I tested whether CSB defects occur closer to the time at which callosal axons cross the midline (Figure 3-10). Fgf/Wnt/β–catenin signalling was examined by *in situ* hybridisation analysis. In E14.5 control embryos, *Wnt7b* and *Wnt8b* expression was restricted dorsally to the CSB (Fig.3-10A-C) while *Axin2* was expressed along the dorso-medial telencephalon (Fig.3-10C). In *Emx1Cre;Gli3*$^{fl/fl}$ mutant brains, *Wnt7b* and *Wnt8b* showed patchy expression at the CSB (Fig.3-10D, E). Despite these changes in *Wnt* gene expression, *Axin2* showed no apparent changes in its expression in *Emx1Cre;Gli3*$^{fl/fl}$ mutants brains (Fig.3-105F). *Fgf*8 expression and that of its target gene *sprouty*2 was analysed at rostral and caudal levels. In rostral sections of control brains, *Fgf*8 was expressed in the septum while *sprouty*2 expression was not discernible (Fig.3-10G, I). At more caudal levels, *Fgf*8 and *sprouty*2 expression were strong in the septal midline (Fig.3-10H-J). In contrast, at rostral levels of *Emx1Cre;Gli3*$^{fl/fl}$ mutant brains *Fgf8* (Fig.3-10M) and *sprouty*2 (Fig.3-10O) were strongly expressed and their expression even extended into the cortex where very little *Fgf8* and *sprouty2* expression was detected in control embryos. At caudal levels, *Fgf*8 and *sprouty*2 showed even more prominent expression (Fig.3-10N, P). These analyses therefore indicate severe changes in *Fgf* and *Wnt* gene expression in the dorso-medial telencephalon of E14.5 *Emx1Cre;Gli3*$^{fl/fl}$ mutants.

In *Gli3*$^{Pdn/Pdn}$ mutants, up-regulation of Fgf signalling underlies a clustering of RGCs marked by *Fabp7* expression (Magnani *et al.*, 2012a). Thus, changes in Fgf signalling in *Emx1Cre* conditional mutants could have also led to RGC clusters. To test this possibility *in situ* hybridisation analysis was performed for *Fabp7*. In control brains, *Fabp7* mRNA was strongly expressed at the ventricular zone of the midline and septum (Fig.3-10K). In contrast, in *Emx1Cre;Gli3*$^{fl/fl}$ mutant brains the cortical expression of *Fabp7* was reduced and clusters of cells expressing high levels of *Fabp7* were found traversing the cortex (Fig.3-10Q). Also, Fgf signalling regulates at

least partially the expression of the chemorepulsive molecule *Slit2* in the septum as shown by an *in vitro* study (Magnani *et al.*, 2012a) . In control *Emx1Cre* conditional brains, *Slit2* expression was confined to the prospective glial wedge and the septum (Fig.3-10L). In *Emx1Cre;Gli3*$^{fl/fl}$ mutants, I detected an expansion of *Slit2* expression in the dorso-medial telencephalon and an ectopic *Slit2* expression region at the centre of the septum (Fig.3-10R). Overall, these experiments demonstrate major changes in the expression and activity of several signalling molecules, a clustering of radial glial cells and misexpression of the axon guidance molecule *Slit2*.

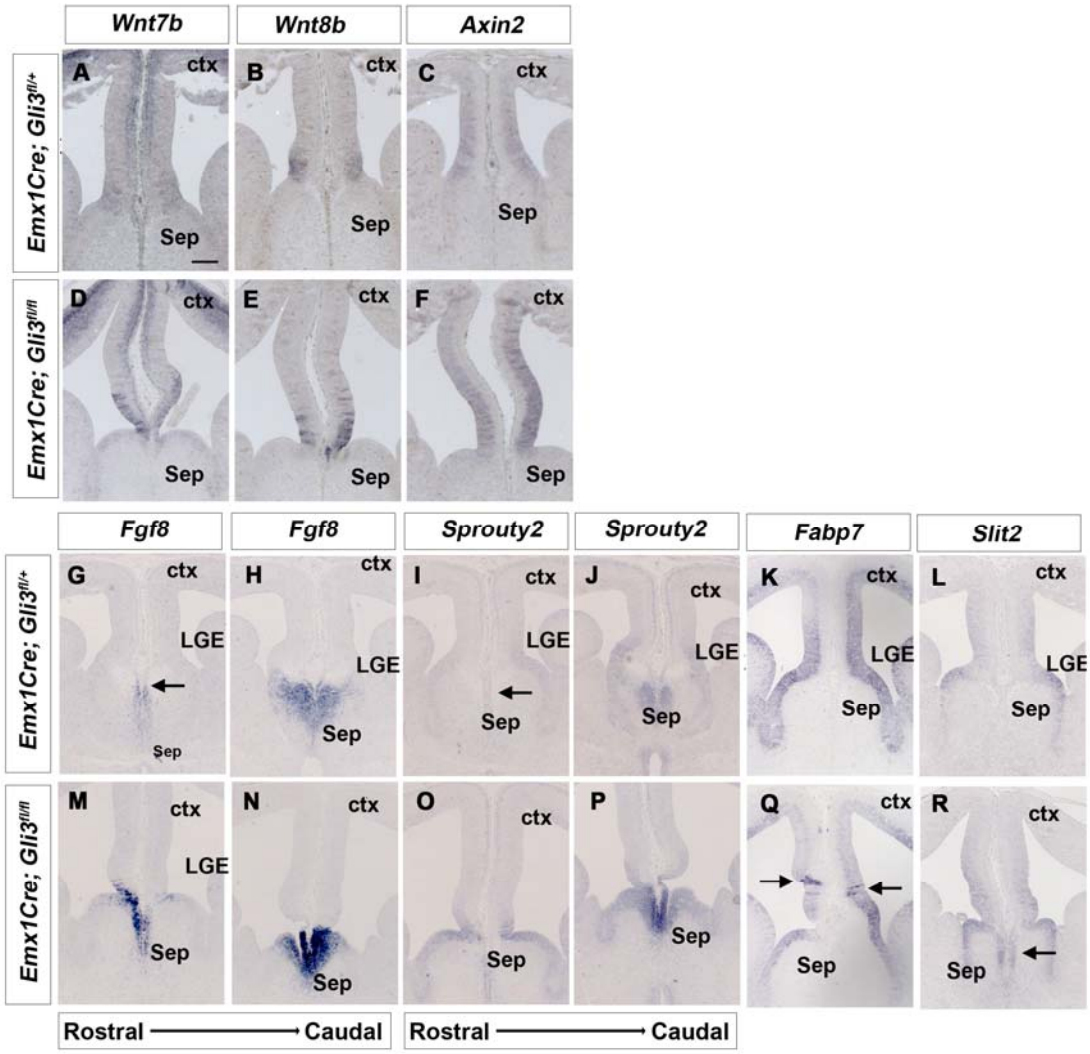
Wnt7b
Wnt8b
Axin2
Emx1Cre; Gli3fl/+
Emx1Cre; Gli3fl/fl
A
B
C
D
E
F
ctx
Sep
Fgf8
Fgf8
Sprouty2
Sprouty2
Fabp7
Slit2
G
H
I
J
K
L
M
N
O
P
Q
R
LGE
Rostral
Caudal

Figure 3-10: Patterning defects in the rostromedial telencephalon of E14.5 *Emx1Cre;Gli3*$^{fl/fl}$ conditional mutants.

(A-B) *Wnt7*b/*Wnt8*b expression is restricted to the dorso-medial telencephalon dorsally to the CSB of control embryos. (D-E) In *Emx1Cre;Gli3* $^{fl/fl}$ mutant brains, *Wnt7*b and *Wnt8*b show patchy expression which is expanded dorsally. (C) Wnt signalling is confined to the dorso-medial telencephalon. (F) *Axin*2 expression is normal in the elongated midline of mutant brains. (G-J) In control brains, *Fgf*8 expression and that of its target gene *sprouty*2 are confined to the CSB with weak expression at rostral levels and stronger expression at caudal levels (G and I, arrow). (M-P) In *Emx1Cre;Gli3* $^{fl/fl}$ mutant brains *Fgf*8 and *sprouty*2 expression is stronger expression at the CSB and dorsally expanded. (K) *Fabp*7 is expressed at high levels in the ventricular zone of the telencephalic midline and septum of control brains. (Q) *Emx1Cre;Gli3*$^{fl/fl}$ brains show reduced expression of *Fabp*7 with clusters of *Fabp*7 expressing cells in the midline. (L) *Slit*2 is expressed at the CSB of control brains. (R) In conditional mutants, *Slit*2 expression is expanded dorsally accompanied by an ectopic *Slit*2 expression in the septal midline (arrow). Abbreviations: ctx, cortex; LGE, lateral ganglionic eminence; sep, septum. Scale bars: 100μm

3.7 Commissural plate formation is not affected in *Emx1Cre;Gli3$^{fl/fl}$* mutant brains

Another key region for CC development is the commissural plate where the corpus callosum, the hippocampal and the anterior commissures normally cross the midline at E16.5 (Rakic, 1988). This region is delineated by several transcription factors including nuclear factor I family (Nf1a) (Shu T, 2003), empty spiracles homologs (Emx1) (Qiu *et al.*, 1996) and sine oculis-related homeobox 3 (Six3) (Oliver *et al.*, 1995). Six3 is an important regulator of early forebrain development and mice mutant for Emx1 or Nf1a lack the corpus callosum (Qiu *et al.*, 1996, Shu T, 2003). Correct formation of the commissural plate during patterning stages is essential for the prospective forebrain commissures development (Moldrich *et al.*, 2010). Moreover, in E12.5 *Gli3$^{Pdn/Pdn}$* mutants *Emx1* is lost in the cortex while *Six3* expression is expanded in the dorso-medial cortex (Kuschel *et al.*, 2003, Magnani *et al.*, 2012a). Nf1a is lost in the high level expression domain of the dorso-medial cortex while its septal expression is up-regulated (Magnani *et al.*, 2012a). Thus, I performed *in situ* hybridisation and immunofluorescence analysis for *Six3*, *Emx1* and Nf1a at two developmental stages i.e. E12.5 and E14.5 brains (Figure 3-11) to test if these changes occur in the *Emx1Cre* conditional mutants. In both E12.5 and E14.5 control brains, *Six*3 was expressed in the septum and the ventral telencephalon with a sharp expression boundary forming at the CSB (Fig.3-11A, G). *Emx*1 expression was restricted to cortical progenitors and formed a sharp boundary at the cortical side of the CSB (Fig.3-11B, H). Finally, Nf1a was strongly expressed at the dorso-medial cortex with lower expression levels at the septum (Fig.3-11C, I). In *Emx1Cre;Gli3$^{fl/fl}$* mutant brains of both stages no obvious defects were detected (Fig.3-10D-F, J-L). In contrast to *Gli3$^{Pdn/Pdn}$* mutants, the commissural plate formation shows no apparent malformation rendering it unlikely to be the cause for CC defects.

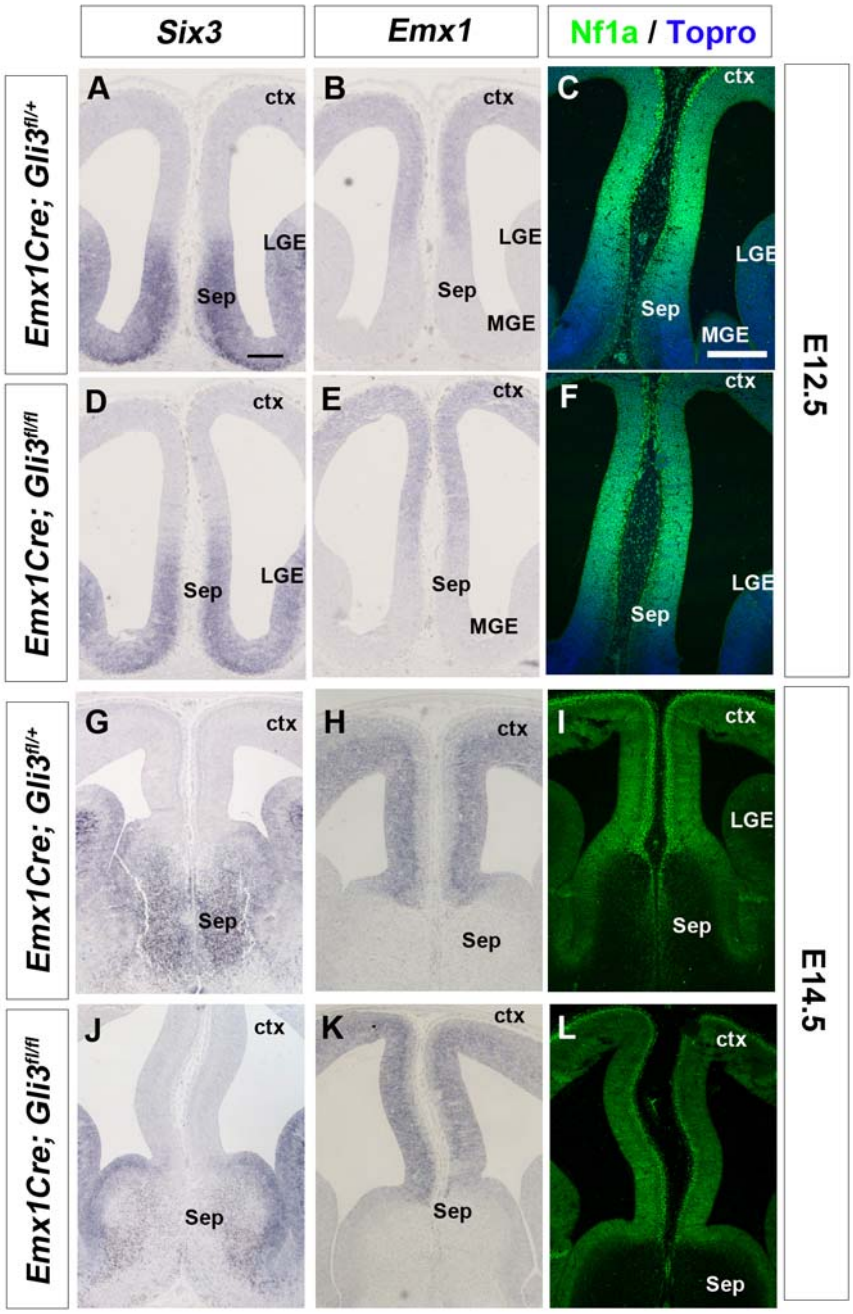
Six3
Emx1
Nf1a / Topro
Emx1Cre; Gli3fl/+
Emx1Cre; Gli3fl/fl
Emx1Cre; Gli3fl/+
Emx1Cre; Gli3fl/fl
E12.5
E14.5
A
B
C
D
E
F
G
H
I
J
K
L
ctx
LGE
MGE
Sep

Figure 3-11: Commissural plate formation shows no defects in E12.5 or E14.5 *Emx1Cre;Gli3*$^{fl/fl}$ mutant brains.

(A, G) *Six*3 is expressed in septal and ventral telencephalic progenitors. (B, H)*Emx*1 expression is restricted to cortical progenitors. (C, I) Strong Nf1a expression is observed in the dorso-medial cortex of control brains. Nf1a expression is weaker in the septum. (D-F, J-L) In *Emx1Cre;Gli3*$^{fl/fl}$ mutant brains of both stages no obvious expression defects of any marker was detected. Abbreviations: ctx, cortex; LGE, lateral ganglionic eminence; MGE, medial ganglionic eminence; sep, septum . Scale bar: A-L:100µm except C-F:250µm.

3.8 *Emx1Cre; Gli3*$^{fl/fl}$ mutants show midline defects at early stages of CC development

The defects observed during patterning stages could result in the aberrant positioning of the callosal guidepost cues as shown in *Gli3*$^{Pdn/Pdn}$ mutants. Callosal axons first cross the midline around E16.5 rendering this age the earliest time possible to analyse the positioning of midline guidance cues in relation to CC. Thus, I performed immunofluorescence analyses for the L1 axonal marker and for different midline guidance cues markers in E16.5 control and mutant embryos (Figure 3-12). In control brains, L1+ callosal axons had just started to cross the midline forming a tight bundle of axons (Fig.3-12A, C, K). In contrast, in *Emx1Cre;Gli3*$^{fl/fl}$ mutant brains L1+ axons reached the cingulate cortex, formed Probst bundles (Fig.3-12E, G, O arrow) and projected into the septum without crossing the midline (Fig.3-12E, G, M). Next, I examined the position of the midline guidance cues and their relevant position to callosal axons. In control brains, the Tbr1+, CB+ and CR+ guidepost neurons were present at the cingulate cortex, close to the early forming CC. Tbr1+, CB+ and CR+ guidepost neurons had already acquired their position in the prospective indusium griseum (Fig.3-12A-D, I, J). Also, L1+ axons appeared to be in close contact with both CR+ and Tbr1+ neurons located within their path (Fig.3-12B, J). In *Emx1Cre;Gli3*$^{fl/fl}$ mutants, the callosal guidepost neurons were present but only CR+ and not Tbr1+ neurons intermingle with the path of L1+ axons (Fig.3-12E, F, M, N). Moreover, only few CB+ neurons formed bundles on each side of the cingulate cortex dorsally to the CC (Fig.3-12G, H). Finally, fibres of nascent glial wedge cells which express GFAP started to extend towards the pial surface for their cell bodies to translocate and form the prospective IGG in control embryos (Fig.3-12K, L). In *Emx1Cre;Gli3*$^{fl/fl}$ mutants, ectopic GFAP+ glial projections were already traversing the cortex from the ventricular to the pia surface and L1+ axon path was intercepted (Fig.3-12O, P). Taken together these data indicate that ectopic GFAP+ fibres interrupt the path of L1+ callosal axons which form Probst bundles and do not cross the midline early in CC development. Thus, the midline guidance cues are already disorganised when the callosal axons approach the CSB.

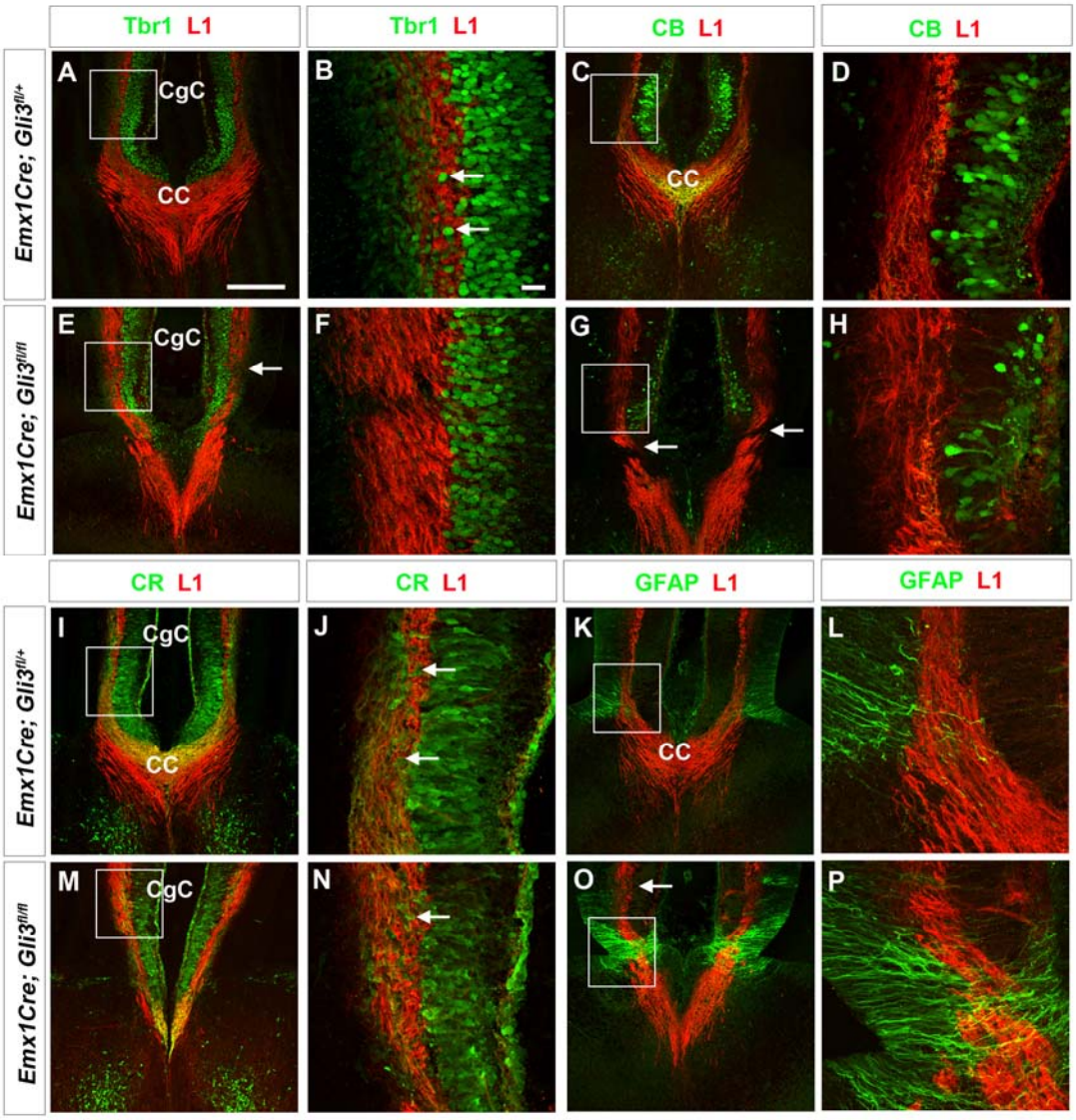
Tbr1 L1
Tbr1 L1
CB L1
CB L1
Emx1Cre; Gli3fl/+
A
CgC
CC
B
C
CC
D
Emx1Cre; Gli3fl/fl
E
CgC
F
G
H
CR L1
CR L1
GFAP L1
GFAP L1
Emx1Cre; Gli3fl/+
I
CgC
CC
J
K
CC
L
Emx1Cre; Gli3fl/fl
M
CgC
N
O
P

Figure 3-12: E16.5 *Emx1Cre;Gli3$^{fl/fl}$* mutant brains show midline defects.

(A-D, I-L) In control brains, L1+ axons cross the midline and form a tight axon bundle. (E-H, M-P) In contrast, some L1+ axons form probst bundles at the CSB (E,G and O, arrow) and do not cross the midline in *Emx1Cre;Gli3$^{fl/fl}$* mutant brains. Instead, some L1+ axons project towards the septum. (A-D, I-J) Tbr1+ , CB+ and CR+ guidance cues are located in the cingulate cortex above the L1+ axons. Tbr1+ and CR+ neurons intermingle with the L1+ callosal axons (B, J arrow). (E-H,M,N) In *Emx1Cre;Gli3$^{fl/fl}$* mutants, Tbr1+, CB+ and CR+ guidance cues occupy the correct region at the cingulate cortex but Tbr1+ neurons do not intermingle with the L1+ axons. Also, CB+ neuronal population is fewer at the IG region. (K,L) GFAP+ radial glial cells at the GW start to extend their processes to the pia surface. (O,P) In *Emx1Cre;Gli3$^{fl/fl}$* mutants, ectopic GFAP+ fibres transversely extend from the ventricular to the pia surface. Abbreviations: CC, corpus callosum; CgC, cingulate cortex .Scale bars: A, C, E, G, I, K, M and O:250µm; B, D, F, H, J, L, N and P: 25µm.

3.9 Fgf signalling and *Slit2* expression are altered in the *Emx1Cre;Gli3$^{fl/fl}$* mutant cingulate cortex at E16.5

3.9.1 Ectopic Fgf signaling and *Slit*2 expression in the septum

In addition to the control of RGC cell differentiation by Fgfs, a recent analysis had shown that Fgf signalling is required between E15.5 and E17.5 for the translocation of glial cells toward the indusium griseum (Smith *et al.*, 2006). Having demonstrated an up-regulation of Fgf signalling in the septum of E14.5 conditional mutant brains, I examined whether these changes persist and correlate with the aberrant CC tract observed two days later. *In situ* hybridisation analysis was performed for *Fgf8, sprouty2* on E16.5 control and *Emx1Cre;Gli3$^{fl/fl}$* mutant brains (Figure 3-13). In control brains, *Fgf8* was strongly expressed in the indusium griseum and at lower levels at the glial wedge (Fig.3-13A). *Sprouty2* expression was also present in the IG and the GW as well as in the cingulate cortex (Fig.3-13B). *Emx1Cre;Gli3$^{fl/fl}$* mutant brains showed that *Fgf8* expressing cells formed an abnormal ventrally elongated triangular structure which extended into the septum (Fig.3-13F, arrow). *Sprouty2* expression pattern in this region resembled that of *Fgf*8 (Fig.3-13G, arrow). Moreover, *sprouty2* expression appeared to be patchy in the GW region (Fig.3-13F). Thus, Fgf signalling is altered with *Fgf8*/*Sprouty2* expressing cells forming an abnormal structure in the septum.

The Slit genes *Slit1* and *Slit2* are chemorepulsive axon guidance molecules expressed in the IG and GW (Unni *et al.*, 2012). It has previously been shown that up-regulation of Fgf signalling controls *Slit2* expression (Magnani *et al.*, 2012a). Therefore, I carried out *in situ* hybridisation analysis for *Slit1* and *Slit2* to look for possible ectopic *Slit* expression. In control brains, *Slit1/2* were expressed by cells in the GW and the IG region in control brains and *Slit1* expression was also observed in the cortical plate (Fig.3-13C-D). However, in *Emx1Cre;Gli3$^{fl/fl}$* mutants, *Slit1/2* expressing cells formed a triangular structure in the septum similar to that seen with

Fgf8 and *sprouty*2 *in situs* (Fig.3-13H-I, arrow) with *Slit*1 expression showing no obvious defects in the cortical plate or septum. Thus, *Slit1/2* are ectopically expressed in *Emx1Cre;Gli3*$^{fl/fl}$ mutants.

Finally, the attractive axon guidance molecule *Sema3C* is expressed in CR+ glutamatergic neurons (Niquille *et al.*, 2009) and the intermediate zone (Piper *et al.*, 2009). Changes in *Sema3C* expression can trigger rapid responses that control the navigation of callosal axon growth cones as shown by *Sema3C* knock-out mice in which the corticofugal path is more compacted (Ruediger *et al.*, 2013). In *Emx1Cre;Gli3*$^{fl/fl}$ conditional brains I already demonstrated that CR+ neurons are present in E16.5 brains. Therefore, I examined the possibility that the expression of *Sema3C* was defective and hence callosal axons were not attracted to cross the midline. *In situ* hybridisation analysis demonstrated that *Sema3C* was strongly expressed within the intermediate zone and at the midline of control brains (Fig.3-13E). In *Emx1Cre;Gli3*$^{fl/fl}$ mutant brains, *Sema3C* was expressed within the intermediate zone but only a narrow *Sema3C* expression domain was found close to the CSB (Fig.3-13J). Collectively, these data reveal ectopic expression of *Fgf8*, *sprouty2* and *Slit1/2* in the septum coupled with a narrow *Sema3C* expression domain close to the CSB.

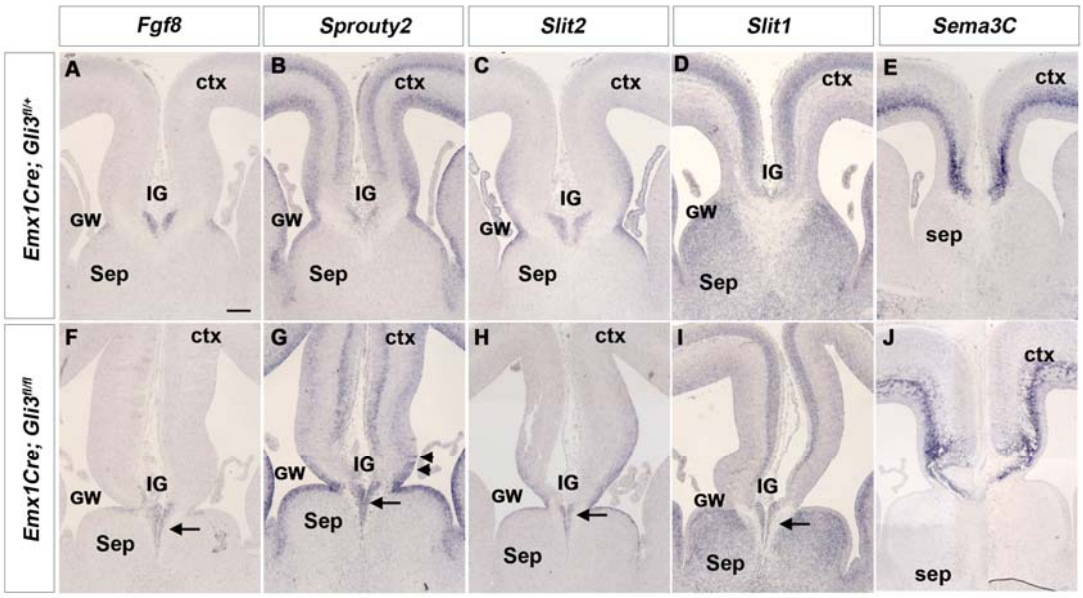

Figure 3-13: Defective Fgf signalling , *Slit*1/2 and *Sema*3C expression in the dorso-medial cortex of E16.5 *Emx1Cre;Gli3*$^{fl/fl}$ mutants.

(A) *Fgf*8 is expressed at the GW and the IG region, in control brains. (F) *Fgf*8 expression is restricted to the GW but *Fgf*8 expressing cells in the IG region form a triangular pattern that protrudes in the septum (arrow), in *Emx1Cre;Gli3*$^{fl/fl}$ mutants. (B) In control brains, S*prouty*2 is strongly expressed in the GW, the IG and in the cortex. (G) In *Emx1Cre;Gli3*$^{fl/fl}$ mutants, *Sprouty*2 expressing cells form a triangular pattern extending into the septum (arrow) and also show patchy *sprouty*2 expression at the GW (arrowheads). *Sprouty2* expression in the cortex seems unaffected. (C) In control embryos, *Slit*2 expression is confined to the IG region and the GW. (H) *Slit*2 expressing cells are protruding into the septum of *Emx1Cre;Gli3*$^{fl/fl}$ mutants (arrow). (D) *Slit*1 expression is detected in cortical and septal neurons, in the IG region and in the GW of control embryos. (I) In conditional mutants, *Slit*1 positive expression domain at the IG region extends into the septum (arrow). (E) In control brains, *Sema*3C is strongly expressed within the intermediate zone and the subventricular zone. (J) *Sema*3C show similar expression pattern in *Emx1Cre;Gli3*$^{fl/fl}$ mutants but its expression is disrupted in the midline. Note the fine *Sema*3C expression close to the CSB region. Abbreviations: ctx, neocortex; GW, glial wedge; IG, indusium griseum; Sep, septum. Scale bars: A-J:100µm.

3.9.2 Ectopic *Fgf8*+ cells do not express indusium griseum markers

The indusium griseum consists of astrocytes and glutamatergic neurons (Shu and Richards, 2001, Shu *et al.*, 2003, Richards *et al.*, 2004, Unni *et al.*, 2012). The up-regulation of *Slit* gene expression could indicate a ventral expansion or displacement of the indusium griseum. To examine this possibility, I performed *in situ* hybridisation analysis for *Slit2* and immunofluorescence analysis for GFAP and CR+ cells on adjacent coronal sections of E16.5 control and *Emx1Cre;Gli3*$^{fl/fl}$ mutant brains and overlaid these figures (Figure 3-14). As described above, GFAP and CR label glial cells and glutamatergic neurons of the indusium griseum, respectively (Fig.3-14A, C). *Slit2* expression on adjacent control sections revealed that *Slit*2 expressing cells in the IG (Fig.3-14B) did not co-express GFAP (Fig.3-14A, B). Some overlap was detected for *Slit2* expression and CR at the IG region of control brains (Fig.3-14C, D). In *Emx1Cre;Gli3*$^{fl/fl}$ mutants, there was a premature translocation of the glial cells which projected their processes transversely across the cortex (Fig.3-14E) with no GFAP+ cells located within the septum (Fig.3-14E, arrow). In contrast, some CR+ cells were located in the septum of the conditional mutants (Fig.3-14G). When I analysed *Slit2* expression on adjacent mutant sections, no overlap was detected between *Slit2* (Fig.3-14F, arrow) and GFAP (Fig.3-14E, arrow) and *Slit2* and CR expressing cell groups were adjacent to each other with no overlap in the septal midline (Fig.3-14H, green and black arrow). Taken together, the ectopic triangular structure is negative for IG markers.

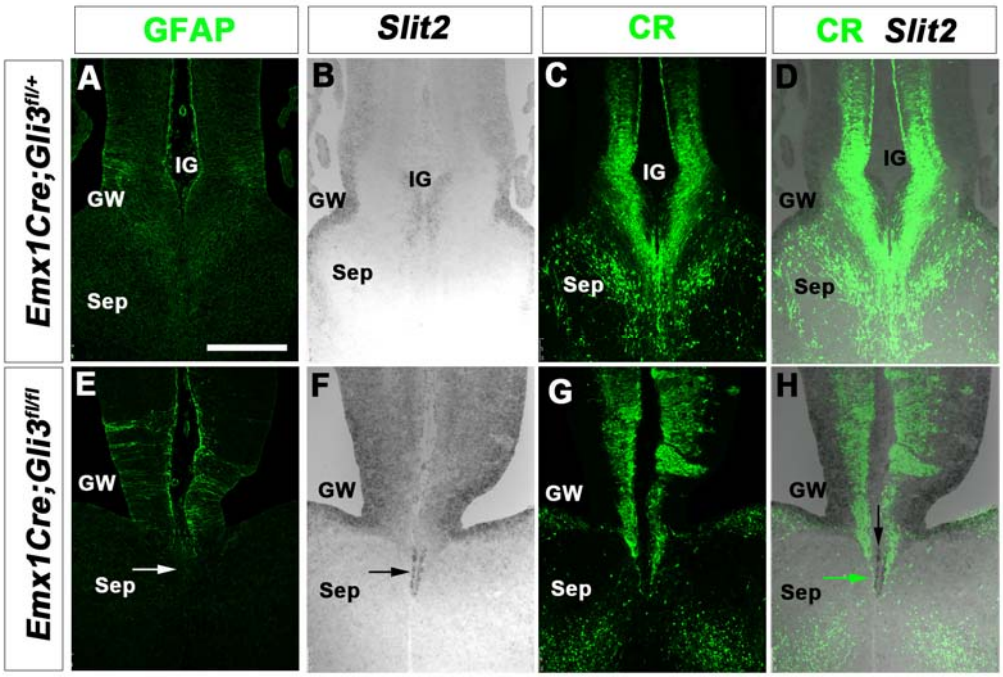

Figure 3-14: Cells of the triangular pattern do not express GFAP or CR.

(A-C, E-G) Immunofluorescence analysis for GFAP and CR and *in situ* hybridization for *Slit*2 on adjacent coronal sections of E16.5 control and *Emx1Cre;Gli3*$^{fl/fl}$ mutant brains. (A, B) In control brains, *Slit2* expression in the IG does not coincide with GFAP expression. (E, F) *Slit2* expression can be detected in the septal midline region (black arrow) while this region lacks GFAP expression (white arrow). (C, D) Overlay of *Slit2* and CR expression indicates a fine overlap between *Slit2* and CR at the IG region of control brains. (G, H) In *Emx1Cre;Gli3*$^{fl/fl}$ mutants, *Slit*2 (black arrow) and CR (green arrow) expression domains are distinct. Abbreviations: ctx, neocortex; GW, glial wedge; IG, indusium griseum; Sep, septum. Scale bar: 250µm

3.10 Discussion

Formation of the corpus callosum requires complex interactions between callosal axons and midline glial and neuronal guidepost cells positioned at the CSB. Since malformation of these guidance structures underlies agenesis of the corpus callosum, it is important to understand the molecular mechanisms that control their development. It has been demonstrated that *Gli*3 has a role in positioning the midline guidance cues at the CSB during patterning stages. Due to *Gli3*'s widespread expression, the aim of this chapter was to test whether *Gli*3 is required in cortical and/or septal telencephalic progenitor cells as well as in progenitors of the medial ganglionic eminence to control CC formation. Here, I provide evidence for a *Gli3* specific requirement in *Emx*1+ progenitor cells but not in the septum or in the medial ganglionic eminence for callosal development. Moreover, *Emx1Cre*;*Gli3*$^{fl/fl}$ embryos show ectopic *Fgf8* and *Slit1/2* expression in the septum and clusters of RGCs early in development.

3.10.1 Spatial and temporal requirements of *Gli3* for CC development

The CSB is a critical intermediate target for callosal axons containing the midline glial populations (Shu and Richards, 2001, Shu *et al.*, 2003) and the subcallosal sling (Silver *et al.*, 1982, Niquille *et al.*, 2009). Correct CSB formation is required for positioning these cues. Thus, understanding the mechanisms behind CSB formation is crucial. *Gli3* mouse mutants present excellent candidates to study CC formation since Acrocallosal syndrome patients carry mutations in the *GLI3* gene and show complete agenesis of the CC (Elson *et al.*, 2002, Speksnijder *et al.*, 2013). Moreover, a recent study on *Gli3*$^{Pdn/Pdn}$ hypomorphic mutant demonstrated that reduction of *Gli3* causes severe defects in CSB formation which subsequently interferes with the positioning of the guideposts and midline crossing of callosal axons (Magnani *et al.*, 2012a). Hence, I made use of three different conditional mutants to specifically

examine the role of *Gli3* in different parts of the telencephalon. *Gli3* deletion in the septum, as confirmed by *in situ* hybridisation analysis, caused no obvious callosal defects and highly likely indicated that *Gli3* is discernible in the septal region for CC development. Moreover, *Gli3* deletion in the medial ganglionic eminence caused no obvious callosal defects. My *in situ* hybridisation analysis confirmed that *Gli3* mRNA expression was lost from the MGE by E12.5 indicating that *Gli3* inactivation occurred at the time of CSB formation. Moreover, the lineage-tracing experiment for MGE derived GABAergic neurons of the subcallosal sling, which delineate callosal axons crossing, revealed normal migration and positioning of GFP+ cells at the CSB. Only recently, Niquille et al. 2013 demonstrated that GABAergic neurons of the subcallosal sling originate also from the caudal ganglionic eminence. *Gli3* is expressed by the progenitors of the caudal ganglionic eminence but none of the conditional mutants used in this study affected its expression in the caudal ganglionic eminence. These data demonstrate that although *Nkx2.1Cre*;*Gli3*$^{fl/fl}$ conditional mutants show specific inactivation, formation of the midline structures at the CSB is correct. This could be caused due to a "rescue" from caudal ganglionic eminence derived interneurons. Further experiments are needed to address the role of *Gli3* in caudal ganglionic eminence progenitors and hence, in CC development (see Chapter 6).

In contrast, *Gli3* deletion in the dorsal telencephalon using the *Emx1Cre* driver line (Gorski *et al.*, 2002) affected development of the corpus callosum. In prenatal and postnatal mutant brains, the CC appeared hypoplastic with many axons forming Probst bundles close to the midline while callosal axons projected to the septum early in CC development. For *Emx1Cre* conditional mutants, I performed extensive time course analysis for *Gli3* mRNA and Western blot analysis for Gli3 protein to ensure the specificity of the inactivation. In *Emx1Cre*;*Gli3*$^{fl/fl}$ conditional mutants *Gli3* was initially deleted from the medial cortex and progressively from more lateral cortical regions. *Gli3* inactivation was complete by E12.5 and *Gli3* protein was also absent at this age. Comparison with another *Gli3* conditional mutant provided some insights into the temporal requirements of *Gli3* expression in CC development. When *Gli3* was inactivated in *NestinCre*;*Gli3*$^{fl/fl}$ embryos after patterning is completed (E14.5)

(Wang *et al.*, 2011) a hypoplastic corpus callosum did form though this is due to apoptosis of callosal projection neurons at postnatal stages yet, no apoptosis is observed in *Emx1Cre*;*Gli3*$^{fl/fl}$ conditional mutants. In fact, my data suggest that the aberrant positioning of midline structures cause the CC malformation. In *Emx1Cre*;*Gli3*$^{fl/fl}$ mutant brains, the glial structures are severely disorganised and the neurons of the callosal sling acquire abnormal positions associating with the Probst bundles. Combining the temporal and spatial requirements of *Gli3*, these findings suggest that *Gli3* is required in dorsal telencephalic cells specifically at patterning stages to control CSB formation.

3.10.2 Defective organization of midline guidance cues underlie aberrant corpus callosum formation in *Emx1Cre*;*Gli3*$^{fl/fl}$ mutants

Gli3 is expressed in dorsal telencephalic progenitor cells that will give rise to both callosal neurons and to midline structures. Since *Emx1Cre* is active in both groups of progenitor cells, the CC defects in *Emx1Cre;Gli3*$^{fl/fl}$ conditional mutants could result from defective formation of the callosal neurons or of the midline guidance cues. Defects in callosal neurons could be caused by misspecification. Based upon Satb2 expression in layer II/III neurons, callosal neurons were specified normally in *Emx1Cre;Gli3*$^{fl/fl}$ conditional mutants and cortical thickness was not altered. The proportion of the upper layer cortical neurons to the total number of neurons was not affected. However, there are differences in the migration of callosal neurons in the *Emx1Cre;Gli3*$^{fl/fl}$ mutant brains. More Satb2+ neurons had already reached their final position in the upper cortical plate in rostral areas while migration of Satb2+ neurons was delayed and more Satb2+ neurons remained in the lower cortical plate in caudal sections (Li, 2011, Amaniti *et al.*, 2013). Overall, Satb2+ callosal neurons were specified normally and some callosal axons were capable of midline crossing despite a severe disorganization of the glial and neuronal guideposts.

However, while most callosal neurons reside in layer II/III, some are located in layer V/VI (Aboitiz and Montiel, 2003, Fame *et al.*, 2011). Formation and migration of layer V/VI callosal neurons was not analysed in this study leaving the possibility that defects in these neurons could cause the callosal defects in *Emx1Cre;Gli3*$^{fl/fl}$ mutant brains. To examine callosal neuron specification further, analyses for specific markers of layer V/VI will need to be performed. For example, *Cited2* or *Gfra2* are strongly expressed in callosal projection neurons in layers II/III/V of E18 brains and in layers V/VI of postnatal brains, respectively (Molyneaux *et al.*, 2007, Fame *et al.*, 2011). Moreover, *Mena* is expressed in layers II/III and V and is necessary for the formation of the corpus callosum by playing a role in actin cytoskeletal dynamics in neurons (Lanier *et al.*, 1999). Overall, analysis of these markers will provide a better understanding of the entire population of callosal neurons.

Intriguingly, the CC is formed in mice that show severe laminar organisation defects like the *reeler* and *p35* mutants (Caviness and Yorke, 1976, Kwon *et al.*, 1999). These mutants are generally characterised by an "outside-in" cortical migration and the formation of inverted layers (Caviness and Rakic, 1978, Rakic and Caviness, 1995, Chae *et al.*, 1997). Layering defects do not interfere with CC formation and the relatively normal formation of the CC indicates that axons project if the axon guidance cues are not affected. Therefore, the neuronal migration defects in *Emx1Cre;Gli3*$^{fl/fl}$ mutants are unlikely to be the primary cause for aberrant CC formation.

In contrast, defects in midline organization are likely to induce CC defects in *Gli3* mutants. The correct positioning of the neuronal and glial midline guidance cues is crucial for callosal axon navigation (Silver *et al.*, 1982, Shu *et al.*, 2003, Richards *et al.*, 2004, Lindwall *et al.*, 2007). On a cellular basis, in mutants that show a lack of guidance cues e.g. *Fgfr*1 mutants which lack the IGG (Smith *et al.*, 2006) or aberrant guidance cue formation e.g. *Slit2*$^{-/-}$ and *Slit1*$^{-/-}$*; Slit/2*$^{-/-}$ mutants in which the indusium griseum glia is shifted ventrally (Unni *et al.*, 2012) and *Bmp7*$^{-/-}$ null mutants in which midline glial structures formation is impaired (Sanchez-Camacho *et al.*, 2011), CC is malformed. In *Emx1Cre;Gli3*$^{fl/fl}$ mutant brains, radial glial cells of the glial wedge cells extend their processes prematurely and in ectopic positions to

the IG region and their fibres formed a potential barrier impermeable to callosal axons at this stage. Moreover, glutamatergic neurons of the subcallosal sling were disorganised and associated with the Probst bundles and the hypoplastic CC.

On a molecular basis, the known chemorepellent molecules *Slit1/2* are expressed by cells in the indusium griseum and glial wedge with *Slit1/2* mutants showing defective CC formation (Unni *et al.*, 2012). *Slit2* is ectopically expressed from E14.5 onwards in *Emx1Cre;Gli3*$^{fl/fl}$ mutants and *Slit2* expressing cells form an ectopic or displaced triangular structure in the midline region where callosal axons would normally cross. However, *Slit2* expressing cells in the septal midline do not overlap with GFAP and/or CR that label the glial and neuronal components of the indusium griseum, respectively. This finding suggests that these *Slit2* positive expressing cells are unlikely to be displaced indusium griseum cells.

It could be proposed, that *Slit1/2* up-regulation in these cells is a direct or indirect effect of *Gli*3 deletion. Interestingly, *Slit2* could be a downstream target of Fgf signalling given its co-expression with *sprouty2* (Yuan *et al.*, 1999) and its down-regulation in the septum of *Fgfr1* mutant mice (Tole *et al.*, 2006). Moreover, up-regulation of Fgf signalling regulates *Slit2* expression *in vitro* (Magnani *et al.*, 2012a). Alternatively, *Gli3* or transcription factors downstream of *Gli3* could repress *Slit2* expression in the dorsal telencephalon. Irrespective of the exact mechanism, the up-regulation of *Slit2* provides a link between early patterning and the coordination of midline development. In contrast, since Gli3R form predominates in the dorsal telencephalon (Fotaki *et al.*, 2006), deleting *Gli3* in *Emx1Cre;Gli3*$^{fl/fl}$ mutants would result in an up-regulation of *Slit*2. The latter argument supports a direct effect of *Gli3* deletion on *Slit2* expression.

Finally, *Sema3C* is expressed in the intermediate zone, possibly by pioneer callosal axons (Piper *et al.*, 2009) and also by CR+ neurons that contribute to the callosal axons projection towards the midline (Niquille *et al.*, 2009). *Sema3C* expression was present in the intermediate zone but just before the connection to the septum only a narrow line of *Sema3C* expression remained in *Emx1Cre;Gli3*$^{fl/fl}$ mutants. This finding suggests that a *Sema3C* attractive guidance signal is present at the defective

CSB providing an active cue for the axons to follow. Thus, it is unlikely that *Sema3C* misexpression is the primary cause for CC defects.

3.10.3 Malformation of CSB structures originate during patterning stages

In order to identify the origins of these cellular and molecular defects during CSB formation, I analyzed *Emx1Cre;Gli3*$^{fl/fl}$ mutant brains during patterning stages. The basis for this analysis was provided by previous analysis on *Gli3*$^{Pdn/Pdn}$ mutants which demonstrated that altered Fgf/Wnt/β–catenin signalling in E12.5 *Gli3*$^{Pdn/Pdn}$ mutants caused malformation of the CSB and a subsequent misposition of the midline guidance structures (Magnani *et al.*, 2012a). In *Emx1Cre;Gli3*$^{fl/fl}$ mutant brains, one of the earliest changes was the down-regulation of *Wnt7b* in E12.5 embryos followed by patchy expression two days later. At that time, *Fgf8* expression and Fgf signalling became drastically up-regulated similar to previous findings in *Gli3*$^{Pdn/Pdn}$ mutants. Moreover, at E16.5 when callosal axons started to cross the midline *Fgf8* expressing cells formed an ectopic triangular structure in the midline region where callosal axons would normally cross. Interestingly, Fgf signalling controls radial glial cell differentiation (Kang *et al.*, 2009, Sahara and O'Leary, 2009) and is required for the formation of radial glial cell clusters in *Gli3*$^{Pdn/Pdn}$ embryos (Magnani *et al.*, 2012a). This suggests that the premature translocation of GFAP+ fibres in the conditional mutants is highly likely the outcome of patchy *Fabp7* expression at E14.5 caused by an up-regulation of Fgf signalling. Nevertheless, in E18.5 *Emx1Cre;Gli3*$^{fl/fl}$ mutant brains callosal axons have already circumvented the ectopic GFAP+ fibres and form a hypoplastic CC. This is in direct contrast to E18.5 *Gli3*$^{Pdn/Pdn}$ embryos in which ectopic glial fascicles span the width of the cortex and provide a barrier to the migration of callosal axons which in return try to circumvent them, in order to cross the midline, but eventually fail.

Taken together, these data demonstrate cellular and molecular defects in guidance cues that normally control CC formation that originate during patterning stages

which in combination are causing the CC malformation. *Gli3* deletion causes an up-regulation of *Fgf8* expression and Fgf signalling in the septal midline during patterning stages. In return, up-regulation of Fgf signalling is demonstrated to control *Slit2* expression and cluster formation of radial glial cells. Ultimately, the ectopic chemorepellent activity of *Slit1/2* in the septal midline and ectopic GFAP+ fibres at the CSB form a temporal boundary to callosal axons. Thus, *Gli3* is positioned in the centre of a complex network that regulates midline guidance cues position at the CSB and hence, CC formation. How *Gli3* regulates this network and whether *Gli3* effect on this network is direct or indirect remains to be elucidated (further discussed in Chapter 6).

3.11 Summary

Despite the fact that the anatomical development of the corpus callosum is well defined, the molecular mechanisms that govern the navigation of callosal axons remain to be fully resolved. Many guidance cues are implicated in this temporally and spatially tightly controlled process. *GLI3* is mutated in human syndromes that reveal agenesis of the CC. Thus, *Gli3* mouse mutants represent excellent models to analyse *Gli3*'s role in CC development. In this chapter I have extensively presented the cellular and molecular mechanisms that are likely to result in the callosal phenotype of *Emx1Cre;Gli3*$^{fl/fl}$ conditional mutants while *Gli3* expression in septal or MGE progenitors is discernible for correct CC formation. These results support previous findings from *Gli3*$^{Pdn/Pdn}$ hypomorphic mutants confirming a central role of *Gli3* during patterning stages for correct guideposts positioning and hence CC formation. My results from the conditional mutants extend these findings and provide a basis to identify genes expressed at the midline that are regulated directly or indirectly by *Gli3*.

4 Expansion of the piriform cortex contributes to the corticothalamic pathfinding defects in *Gli3*^{cKO} conditional mutants

4.1 Introduction

The corticothalamic/thalamocortical network is crucial for the synchronisation of the highly integrated units of the cortex and thalamus. The thalamocortical tract conveys sensory information to the cortex and cortical innervation of the thalamus is highly important since the corticothalamic tract conveys processed sensory information to the thalamic neurons to influence activity patterns and sensory responses. These tracts are laid down during embryonic development. Briefly, corticofugal axons reach the pallial-subpallial boundary (PSPB) at around E14.5 in the mouse (Molnar and Cordery, 1999, Auladell *et al.*, 2000, Jacobs *et al.*, 2007). After a waiting period, corticothalamic axons (CTAs) cross the PSPB in a radiate and widespread manner and extend deeply into the ventral telencephalon. CTAs project as a tight bundle through the internal capsule at 15.5 and subsequently cross the diencephalic-telencephalic boundary and innervate the thalamus (Molnar and Cordery, 1999, Auladell *et al.*, 2000, Jacobs *et al.*, 2007). Thalamocortical projections (TCAs) follow a reciprocal pathway to the cortex extending through the same territories until they reach the intermediate zone of the cortex and innervate cortical layer IV. Although, the paths followed by CTAs and TCAs are well understood, our understanding of the molecular mechanisms underlying the pathfinding of these projections is only beginning to emerge.

Guidance of CTAs/TCAs through the ventral telencephalon involves at least three different steps: (i) pioneer axons which constitute early projecting axons provide a scaffold for the corticofugal and thalamocortical axons in order to orientate their direction of growth and reach their targets (Metin and Godement, 1996, Molnar *et*

al., 1998); (ii) a permissive corridor positive for *Isl1* and *Ebf1* cells that guide TCAs through the ventral telencephalon (Lopez-Bendito *et al.*, 2006); and (iii) the handshake hypothesis which suggests that CTAs and TCAs meet in the ventral telencephalon and guide each other to their target areas (Molnar and Blakemore, 1995b). In contrast, much less is known about the preceding step to the guidance of CTAs through the ventral telencephalon. In fact, the guidance cues that direct CTAs to enter the ventral telencephalon are still not fully elucidated. One key region to study these cues is the PSPB, as in this region CTAs experience a waiting period, change direction by sharply turning medially and change territory by radiating into the subpallium. Surprisingly, CTAs are defasciculated at the PSPB and striatum and radiate into the ventral telencephalon over a widespread domain in contrast to their tightly fasciculated path in other regions. Combinatorial expression of several guidance cues navigates CTAs through the PSPB into the ventral telencephalon. *Sema3A* expression at the cortical plate repels corticofugal axons which in return are attracted by *Sema3C* in the intermediate zone (Bagnard *et al.*, 1998, Skaliora *et al.*, 1998), *Sema3E*/*PlexinD1* (Deck *et al.*, 2013) have been implicated in mediating the waiting period of the corticofugal axons while the chemoattractant activity of *Netrin-1* can turn CTAs towards the ventral telencephalon (Metin *et al.*, 1997). However, the molecular mechanisms that regulate the wide entrance of CTAs into the subpallium are not fully understood.

Mouse mutants that show corticothalamic/thalamocortical defects represent an excellent opportunity to study these mechanisms. *Gli3* has a known role in dorsoventral regionalization of the telencephalon (Theil *et al.*, 1999, Tole *et al.*, 2000, Rallu *et al.*, 2002b, Kuschel *et al.*, 2003, Quinn *et al.*, 2009) and in axon pathfinding (Magnani *et al.*, 2010, Magnani *et al.*, 2012a, Magnani *et al.*, 2012b, Amaniti *et al.*, 2013). In fact, in the *Gli3* hypomorphic mouse mutant *Polydactyly Nagoya* ($Gli3^{Pdn/Pdn}$) entry of the corticothalamic axons into the ventral telencephalon is delayed (Magnani *et al.*, 2010) while in the $Gli3^{Xt/Pdn}$ compound mutant, which carry the *Gli3* null allele *extra-toes* ($Gli3^{Xt}$) over the hypomorphic $Gli3^{Pdn}$ allele, CTAs show severe outgrowth defects due to a nearly complete absence of subplate neurons (Magnani *et al.*, 2012b). These severe axon outgrowth defects of $Gli3^{Xt/Pdn}$

mutants may obscure additional roles of *Gli3* in axon pathfinding. Therefore, I investigated the possibility that *Gli3* expression in the dorsal telencephalon controls the entry of corticothalamic axons into the ventral telencephalon.

The aims of this chapter were to identify the effects of *Gli3* inactivation in the dorsal telencephalon on CTA tract formation and characterize the potential cellular and molecular mechanisms by which *Gli3* regulates CTA entry into the ventral telencephalon. To address these aims, I utilized the *Emx1Cre* driver line (Gorski *et al.*, 2002) to specifically inactivate *Gli3* in cortical progenitors (as previously described in Chapter 3). Here, I show that in *Emx1Cre*;*Gli3*$^{fl/fl}$ embryos, CTAs do grow but leave the cortex in a narrow, restricted domain. Analyses of cortical lamination revealed that corticofugal projection neurons are formed. Surprisingly, the rhinal fissure, which separates the lateral neocortex from the piriform cortex, is shifted medially, indicating a medial expansion of the piriform cortex. Transplantation experiments showed that this expanded piriform cortex is repulsive for the growth of corticothalamic axons thereby restricting their entry zone into the ventral telencephalon. Moreover, the repulsive activity of the piriform cortex is at least partially mediated by *Sema5B,* which acts as a chemorepellent on corticothalamic axons and whose expression is shifted medially in the mutants (Lett *et al.*, 2009). Finally, the expression analysis of various cortical progenitor markers suggest that the expansion of the piriform cortex arises from an expansion of the ventral pallial progenitor domain.

4.2 The corticothalamic tract is impaired in *Gli3*^{cKO} mutants

To study the role of *Gli3* in axon tract formation different mouse mutants have previously been analyzed including the *Gli3*$^{Pdn/Pdn}$ and *Gli3*$^{Xt/Pdn}$ mutants while the severe patterning defects in *Gli3*$^{Xt/Xt}$ prevent fibre tract analysis. *Gli3*$^{Pdn/Pdn}$ and *Gli3*$^{Xt/Pdn}$ mutants showed a delay in the entry of CTAs into the ventral telencephalon and axon outgrowth defects, respectively (Magnani *et al.*, 2010, Magnani *et al.*,

2012b). This latter phenotype made it impossible to dissect further roles of *Gli3* in corticothalamic pathfinding using $Gli3^{Xt/Pdn}$ mutants. Therefore, I used the $Emx1Cre;Gli3^{fl/fl}$ mutants to dissect *Gli3*'s role in the dorsal telencephalon for CTA pathfinding. As in Chapter 3, *Emx1Cre* animals were mated with $Gli3^{fl/fl}$ to generate $Emx1Cre;Gli3^{fl/fl}$ mutants that were used in this study. For this chapter, $Emx1Cre;Gli3^{+/+}$ and $Emx1Cre;Gli3^{fl/+}$ brains showed no obvious phenotype and were therefore used as controls for comparison with $Emx1Cre;Gli3^{fl/fl}$ mutant brains. For simplicity, $Emx1Cre;Gli3^{+/+}$/$Emx1Cre;Gli3^{fl/+}$ and $Emx1Cre;Gli3^{fl/fl}$ brains will be referred to as control and $Gli3^{cKO}$ mutant brains, respectively. Initially, I examined axon tract formation by performing an immunohistochemistry analysis of the pan-axonal marker neurofilament on E18.5 control and $Gli3^{cKO}$ mutant brains (Figure 4-1). In control brains, neurofilament marked the cortical intermediate zone in which axons projected as a tight axon bundle. At the PSPB, the neurofilament+ axons radiated into the striatum over a widespread region and formed a tight bundle again in the internal capsule and close to the diencephalic-telencephalic boundary (Fig.4-1A). In $Gli3^{cKO}$ mutants, the intermediate zone appeared thinner with only a few axons present in the ventral telencephalon (Fig.4-1D). Surprisingly, the neurofilament+ axons formed a tight axon bundle at the PSPB and the dorsal most part of the striatum with a separate bundle projecting ventrally (Fig.4-1D). Neurofilament+ axons reached the thalamus in $Gli3^{cKO}$ mutants similar to control brains. These data indicate defects in the formation of the corticothalamic/thalamocortical tract however; it is unclear whether these defects were specific to the corticothalamic and/or thalamocortical tract.

To address this question, $Emx1Cre;Gli3^{fl/+}$ mice were mated with the *Golli-τauGFP* transgenic mouse line. In *Golli-τauGFP* transgenic mice, the *Golli* promoter of the myelin basic protein (MBP) gene drives expression of a τauGFP fusion protein in a subset of subplate (SP) and layer VI neurons (Jacobs *et al.*, 2007). Due to the τau sequences, the τauGFP fusion protein localizes to the cell bodies of these neurons and to axonal projections (Jacobs *et al.*, 2007). This transgene therefore provides an excellent tool to label the axonal trajectories of these neurons. In *control;Golli-τGFP* brains, GFP+ axons were present in the cortex, entered the subpallium in a

widespread manner, crossed the diencephalic-telencephalic boundary and innervated the thalamus (Fig.4-1B). In more caudal sections, GFP+ axons clearly innervated the thalamus (Fig.4-1C). In *Gli3*^{cKO}*;Golli-τGFP* mutants, GFP+ axons only entered into the dorsal most part of striatum from a restricted region (Fig4-1E, arrow) while a separate axon bundle descended along the PSPB (Fig4-1E, arrowhead). In caudal sections, GFP+ axons crossed the diencephalic-telencephalic boundary and innervated the thalamus (Fig.4-1F). Finally, DiI crystals were placed in the thalamus to label CTAs and TCAs specifically. DiI is a fluorescent lipophilic indocarbocyanine dye used as a retrograde and anterograde neuronal tracer since it diffuses along the cellular membranes of cells including their axonal processes. For this experiment, DiI was used to anterogradely label the CTAs and examine their trajectory by placing a DiI crystal in the cortex (Fu, 2012). In control brains, CTAs formed a tight bundle that entered the striatum and projected towards the thalamus (Fig.4-1G). Back-labelled cell bodies in the thalamus indicated retrograde labelling of TCA projections. In accordance with the results described above, in *Gli3*^{cKO} mutants CTAs entered the striatum through a restricted region and projected along the dorsal most part of the striatum (Fig.4-1J). Yet, some DiI labelled axons reached and innervated the thalamus (Fig.4-1J). These data provide further evidence for the aberrant pathfinding of CTAs with corticofugal axons entering the ventral telencephalon through a restricted region and navigating mainly in the dorsal most part of the striatum (Fu, 2012).

The TCAs supply the cortex with innervation from the thalamus and convey sensory information to the neocortex for processing. Thus, the TCAs formation is also crucial for the cortex/thalamus unit. Moreover, according to the "handshake hypothesis", TCAs and CTAs guide each other to grow into the cortex and thalamus, respectively (Molnar and Blakemore, 1995b). As CTAs show pathfinding defects in *Gli3*^{cKO} mutants, this raised the possibility that TCA tract formation was also affected. To examine their formation, TCAs were labelled anterogradely by placing a DiI crystal in the thalamus (Fu, 2012). This experiment was performed with two different approaches. With the first approach, a coronal section through the thalamus was performed on control brains before DiI placement, thereby separating the caudal

thalamus from the cortex. In control brains, DiI crystal placement revealed that TCAs extended in the ventral telencephalon and reached the cortex (Fig.4-1H). In contrast, TCAs projected through the ventral telencephalon of *Gli3*^{cKO} mutants but did not enter the cortex. In fact, the TCAs were deflected ventrally (Fig.4-1K). With the second approach, a DiI crystal was placed in the thalamus of a midsagittal section which leaves all thalamus connected to the telencephalon. As before, TCAs projected through the ventral telencephalon to the cortex in control brains (Fig.4-1I). In contrast, in *Gli3*^{cKO} mutants TCAs traversed the subpallium but many axons turned ventrally, perpendicular to their normal trajectory, as they approached the PSPB while a tight bundle projected to the cortex (Fig.4-1L). Overall, this analysis revealed severe CTA and TCA pathfinding defects in *Gli3*^{cKO} embryos. Many axons abnormally project along the PSPB and only a few CTAs and TCAs, which are derived from neurons in the caudal thalamus, leave and enter the cortex, respectively. Strikingly, exit from and entry into the cortex is restricted to a small area in the dorsalmost part of the PSPB.

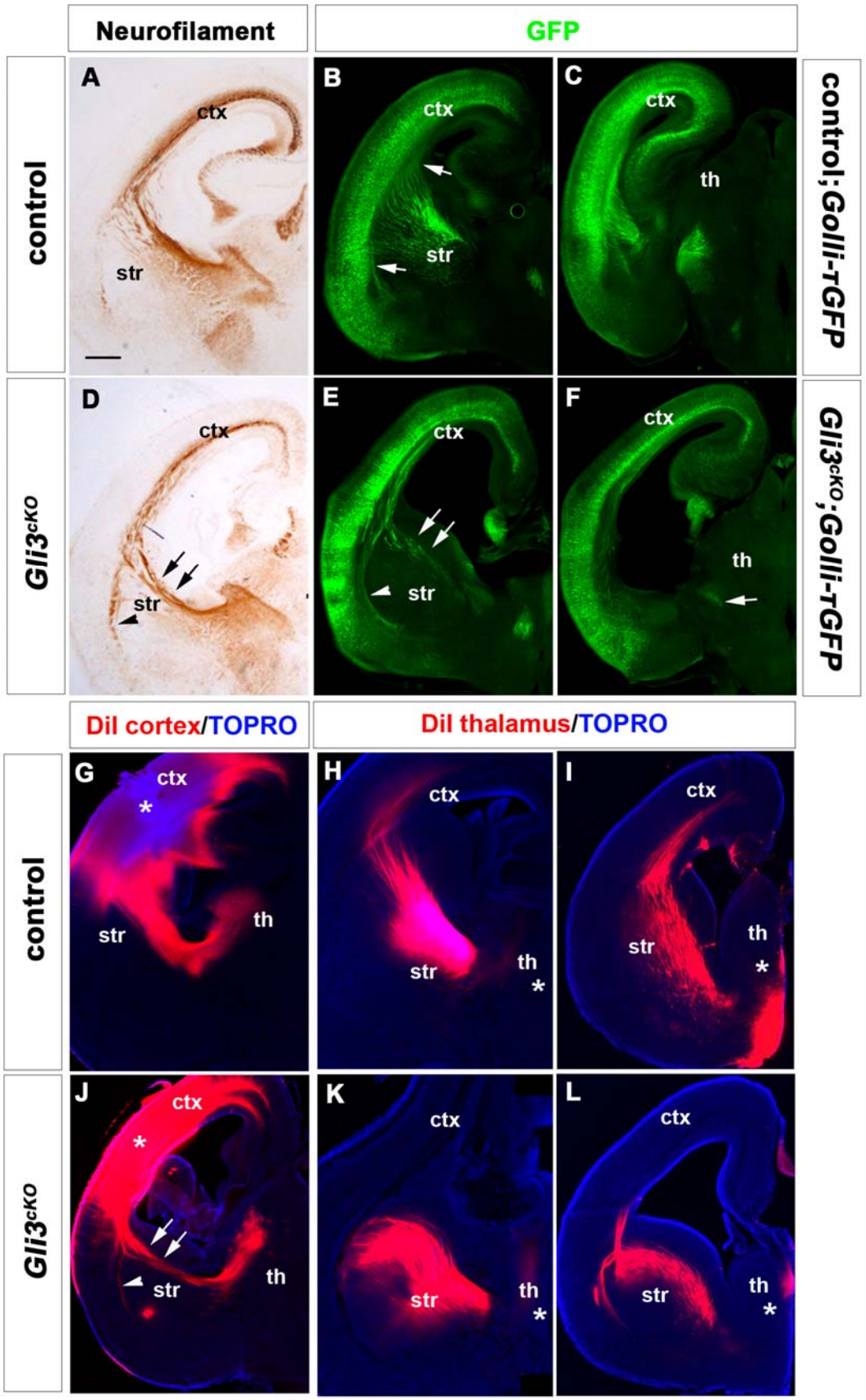
Neurofilament
GFP
control
Gli3cKO
control;Golli-tGFP
Gli3cKO;Golli-tGFP
A
B
C
D
E
F
ctx
str
th
Dil cortex/TOPRO
Dil thalamus/TOPRO
G
H
I
J
K
L
*

Figure 4-1: Corticothalamic and thalamocortical defects in *Gli3*^{cKO} mutants.

(A) Neurofilament staining reveals the intermediate zone and axon bundles entering the striatum, in control brains. (D) In *Gli3*^{cKO} mutants, neurofilament+ axons are present in the dorsal most part of the striatum (arrow) and some axon bundles project along the PSPB (arrowhead). (B-C) Rostral to caudal analysis of *Golli-τauGFP*+ subplate and layer VI axon projections. Note, the widespread entrance of corticofugal axons (E-F) In *Gli3*^{cKO} mutants, GFP+ axons extend into the ventral telencephalon and form one bundle that project at the dorsal most part of the striatum (arrow) and another that descend along the PSPB (arrowhead). Some axons innervate the thalamus at more caudal sections (arrow). (G) DiI placement at the cortex reveals the CTAs trajectory in control brains. (J) In *Gli3*^{cKO} mutants, few axons project to the thalamus (arrow) while another bundle descends ventrally (arrowhead). (H-I) DiI crystal placement in the thalamus by using different techniques. DiI placement in coronal sections (H) and midsagittal (I) sections reveal the TCAs trajectory in control brains. (K-L) Most thalamic axons project to the ventral telencephalon but do not enter the cortex with only few axons entering the cortex in the midsagittal section. Asterisk shows DiI placement. Abbreviations: ctx, cortex; str, striatum; th, thalamus. Scale bars: 250μm.

4.3 *Gli3* inactivation is specific and thalamic development is not obviously affected

Neurons in the cortex and thalamus extend axons that form the corticothalamic or thalamocortical tract, respectively. Cellular defects in either population of neurons could underlie the axonal defects described above. This is particularly important since CTAs and TCAs guide each other (Molnar and Blakemore, 1995b). Although the use of the *Emx1Cre* driver line should not cause any defects in the thalamus, I carried out *in situ* hybridisation analysis for *Gli3* to exclude the possibility that unspecific inactivation of *Gli3* leads to patterning defects in the thalamus and consequent TCA pathfinding defects (Figure 4-2). For this analysis E12.5 control and $Gli3^{cKO}$ brains were examined since *Gli3* inactivation in the cortex is complete at that time point. In control brains *Gli3* was strongly expressed in cortical and ventral telencephalic progenitors as well as in the proliferating neuroepithelium of the thalamus (Fig.4-2A). In $Gli3^{cKO}$ mutants, *Gli3* was specifically inactivated in the dorsal telencephalon *Gli3* expression in the thalamus was not obviously affected (Fig.4-2B). In addition to having established that *Gli3* inactivation is specific to the cortex, thalamic development was further examined by analysing the expression of several thalamic genes with important roles in thalamic development (Fu, 2012). This analysis was performed by Chao Fu in her MSc dissertation under my supervision and I briefly summarize her results below. The thalamic expression of the transcription factors *Ngn2*, *Pax6*, *Gbx2* and *Lhx2* was analysed. These markers are expressed in the ventricular zone of the cortex and the thalamus or prethalamus (*Pax6*) (Fig.4-2C-F) with no obvious defects in $Gli3^{cKO}$ mutant brains (Fig.4-2G-J). Collectively, these findings indicate specific *Gli3* inactivation in the dorsal telencephalon and no apparent malformation in thalamic development. Thus, it is unlikely that the thalamocortical axon defects in conditional mutants are caused by thalamic defects.

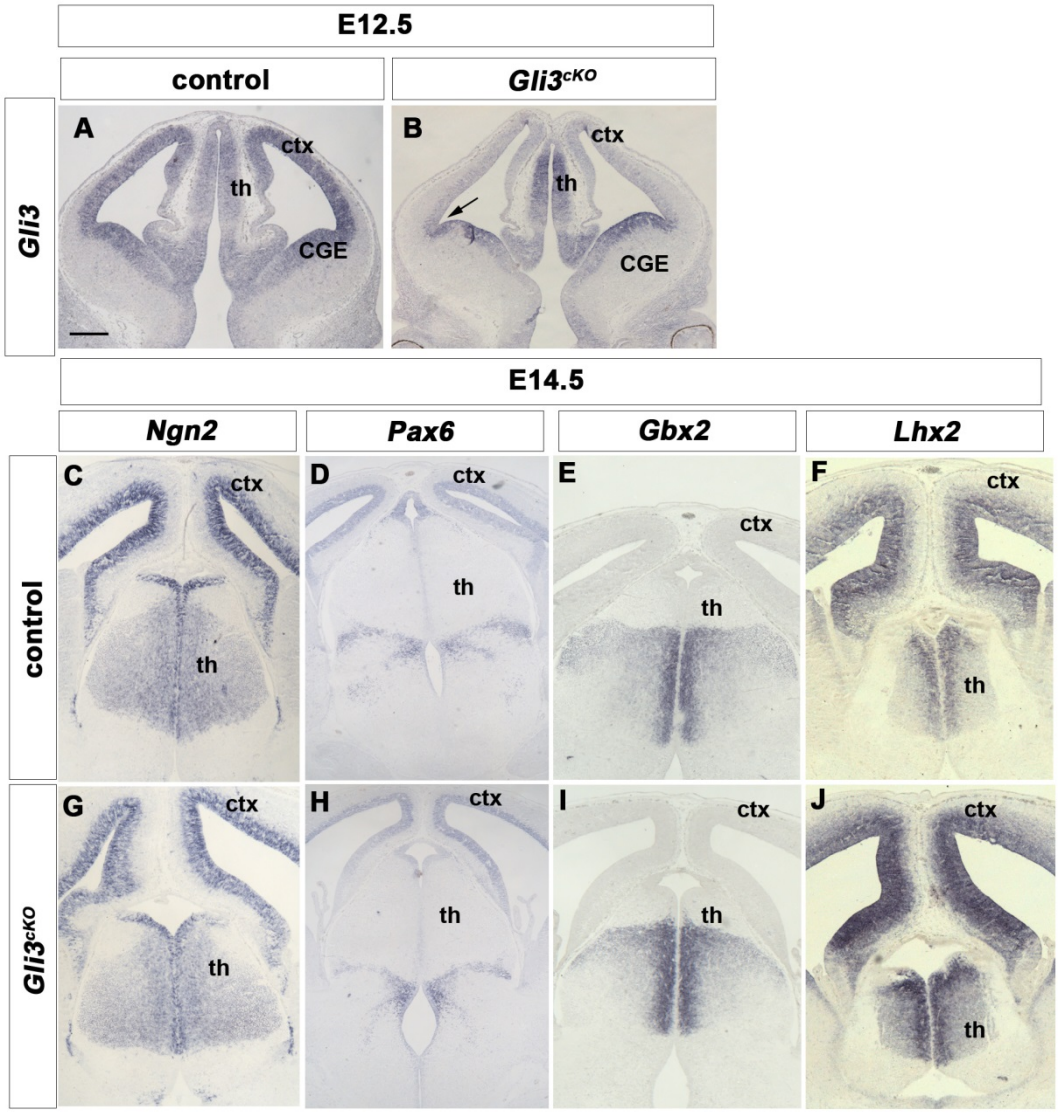

Figure 4-2: *Gli3* specific inactivation and thalamic markers show no obvious defects.

(A) *Gli3* is expressed in dorsal and ventral telencephalic progenitors. *Gli3* mRNA is expressed in the thalamus. (B) *Gli3* specific inactivation in the dorsal telencephalon (arrow). *Gli3* expression remains stable in the thalamus of $Gli3^{cKO}$ mutants. (C-F) In situ hybridisation showing expression of different transcription factors used as thalamic markers. (G) No obvious defects are detected in $Gli3^{cKO}$ mutants. Abbreviations: ctx, neocortex; CGE, caudal ganglionic eminence; th, thalamus. Scale bars: 100µm.

4.4 Corticofugal projection neurons in the medial neocortex are specified correctly

Neocortical progenitors give rise to corticofugal neurons that will extend axons towards the ventral telencephalon. Thus, misspecification of these neurons could explain the CTA pathfinding defects. To analyze this possibility, I performed *in situ* hybridization for the sex determining region Y-box 5 (*Sox5*) transcription factor which has been shown to specify corticofugal projection patterns (Figure 4-3) (Kwan *et al.*, 2008, Lai *et al.*, 2008). In E18.5 control brains, *Sox5* labelled subplate and layer V/VI neurons. *Sox5* expression extended from the dorso-medial neocortex above the corpus callosum to the lateral neocortex ventrally to the angle region (Fig.4-3A). In $Gli3^{cKO}$ mutant brains, *Sox5* was expressed in the dorso-medial cortex without obvious changes but, *Sox5* expression did not extend ventrally to the angle region (Fig.4-3B). These data indicated that corticofugal neurons are specified in the medial neocortex but revealed an absence of *Sox5* expressing cells in the lateral neocortex.

Having observed this defect in *Sox5* expression, I further examined the specification of corticofugal projection neurons by analysing the expression of COUP-TF interacting protein 2 (Ctip2). In $Ctip2^{-/-}$ mutants the formation of the corticospinal tract is affected with axons exhibiting defects in fasciculation, growth and pathfinding (Arlotta *et al.*, 2005). Ctip2 labelled corticospinal neurons which are part of corticofugal neurons in layer V (Arlotta *et al.*, 2005, Molyneaux *et al.*, 2007) and also layer II neurons in the piriform cortex which resides in the ventro-lateral telencephalon. In fact, the transition from layer V cortical neurons to layer II piriform neurons indicated the position of the rhinal fissure a sulcus that is conserved across mammalian species and separates neocortex from the paleocortical piriform cortex (Fig.4-3C-D) (Ariens-Kapers *et al.*, 1936). In $Gli3^{cKO}$ mutants, Ctip2+ cells were present in cortical layer V (Fig.4-3E-F). However, the medial expression of Ctip2 was diminished laterally and its piriform expression in layer II increased medially (Fig.4-3E-F). To further distinguish between neocortex and piriform cortex, I carried out immunofluorescence analyses to further infer the position of the rhinal fissure.

To this end, expression of the callosal determinant Satb2 and Tbr1, which label subplate and layer VI corticothalamic projection neurons (Hevner *et al.*, 2001) were analysed. Moreover, Tbr1 marks piriform cortex layer II and the olfactory tubercle. In control brains, double labelling with Satb2 and Tbr1 revealed the position of Tbr1+ neurons in the deeper cortical layers underneath the Satb2+ callosal projection neurons of layers II/III and IV (Fig.4-3G). From this analysis the position of the rhinal fissure can be inferred and it is characterised by a tissue indentation as well as by the transition of Tbr1 expression from layer VI cortical neurons to layer II piriform neurons (Fig.4-3H). In *Gli3*^{cKO} mutants, Tbr1+ and Satb2+ cells occupied their correct laminar position in the neocortex and in the piriform cortex, but the rhinal fissure position was shifted medially (Fig.4-3J). In fact, Satb2+ cells were absent beyond the angle region and Tbr1 labelled both layer VI and piriform cortex layer II neurons thereby indicating the rhinal fissure (Fig.4-3I). Taken together, these data suggest that corticofugal projection neurons form and occupy their correct laminar position in medial neocortex but that the lateral neocortex is affected by a medial expansion of the piriform cortex.

This prominent contrast between medial and lateral neocortex raised the possibility that cortical lamination is affected in *Gli3*^{cKO} mutant brains along the medio-lateral axis. To further analyse lamination in *Gli3*^{cKO} mutants two markers were analysed: the cut-like homeodomain transcription factor (*Cux2*) and *reelin* which are expressed in pyramidal cells in layer II/III (Nieto *et al.*, 2004) and Cajal-Retzius cell (D'Arcangelo *et al.*, 1995, Meyer *et al.*, 1999), respectively. In control brains, *Cux2* and *reelin* expression were present at layer II/III and the marginal zone (Fig.4-4A-B, E-F), respectively, and extended into the lateral neocortex beyond the angle region (Fig.4-4A, E). No obvious defects were detected in the expression of *Cux2* and *reelin* in the medial cortex of *Gli3*^{cKO} mutant brains (Fig.4-4C-D, G-H) but *Cux2* and *reelin* expression was restricted at the lateral neocortex and did not extend beyond the angle region (Fig.4-4D, H). Interestingly, these data demonstrate that upper layer neurons and corticofugal projection neurons are specified in the medial cortex but they are not present in the lateral cortex of *Gli3*^{cKO} mutant brains.

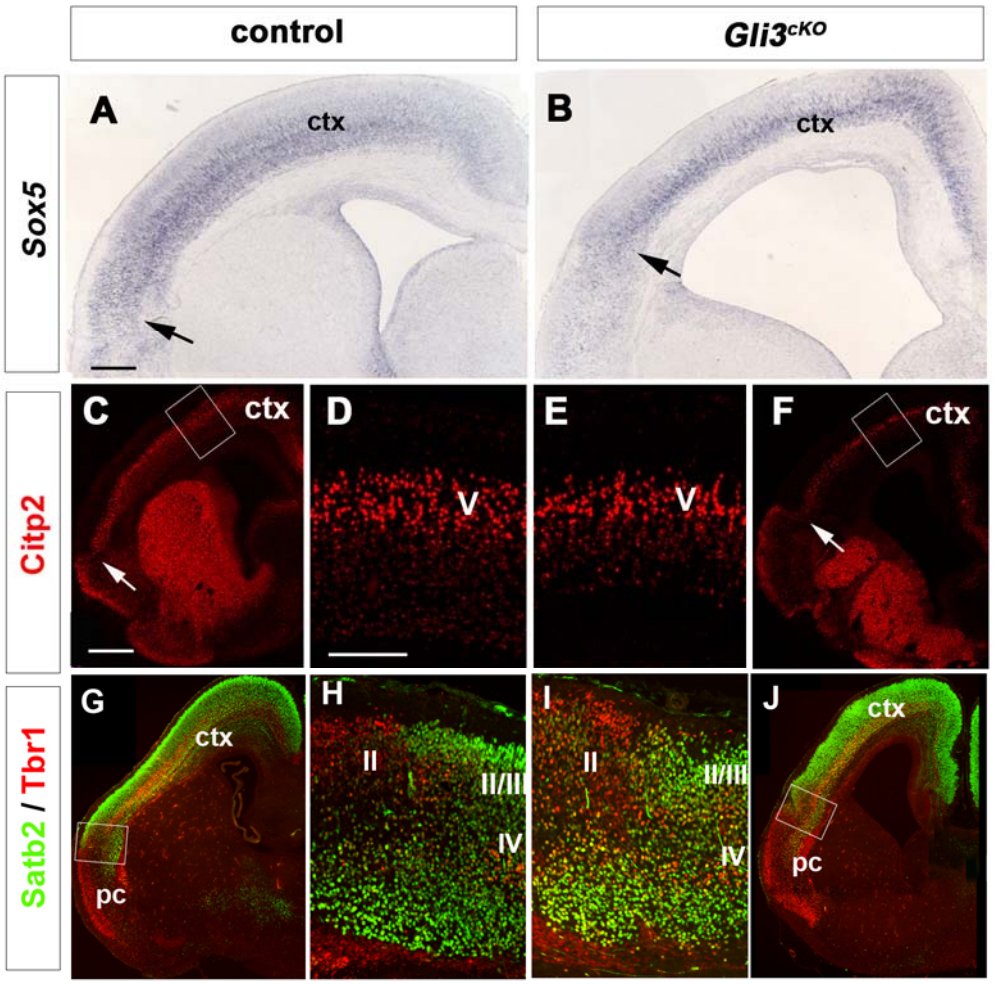
control
Gli3cKO
Sox5
Citp2
Satb2 / Tbr1
A
B
C
D
E
F
G
H
I
J
ctx
V
pc
II
II/III
IV

Figure 4-3: Corticofugal projection neurons are formed but the piriform cortex is expanded in E18.5 *Gli3*^{cKO} mutants.

(A) *Sox5* is expressed in SP and layer V/VI neurons and its expression extends throughout the neocortex of control embryos. (B) In *Gli3*^{cKO} mutants, neocortical *Sox5* expression stops at the level of the dorsal most striatum. The arrow demarcates the lateral end of the *Sox5* expression domain in the neocortex. (C-F) Ctip2 labels corticospinal motor neurons in layer V of the neocortex and layer II neurons in the piriform cortex in control and *Gli3*^{cKO} embryos (arrows indicate the boundary between these two expression domains). In *Gli3*^{cKO} mutants, the neocortical expression of Ctip2 was diminished laterally and its piriform expression increased medially. (G-J) Double immunofluorescence staining for Tbr1 and Satb2. In control and *Gli3*^{cKO} embryos, Tbr1 is strongly expressed in subplate and layer VI corticothalamic projection neurons and in layer II neurons of the piriform cortex whereas Satb2 expression is restricted to callosal projection neurons of layers II/III and IV. The transition between the Satb2+ neocortex and Satb2- piriform cortex (magnifications in H and I) marks the position of the rhinal fissure. In *Gli3*^{cKO} embryos, this fissure is shifted medially.. Abbreviations: ctx, neocortex; pc, piriform cortex. Scale bars: A-B:100µm; C-J: 250µm.

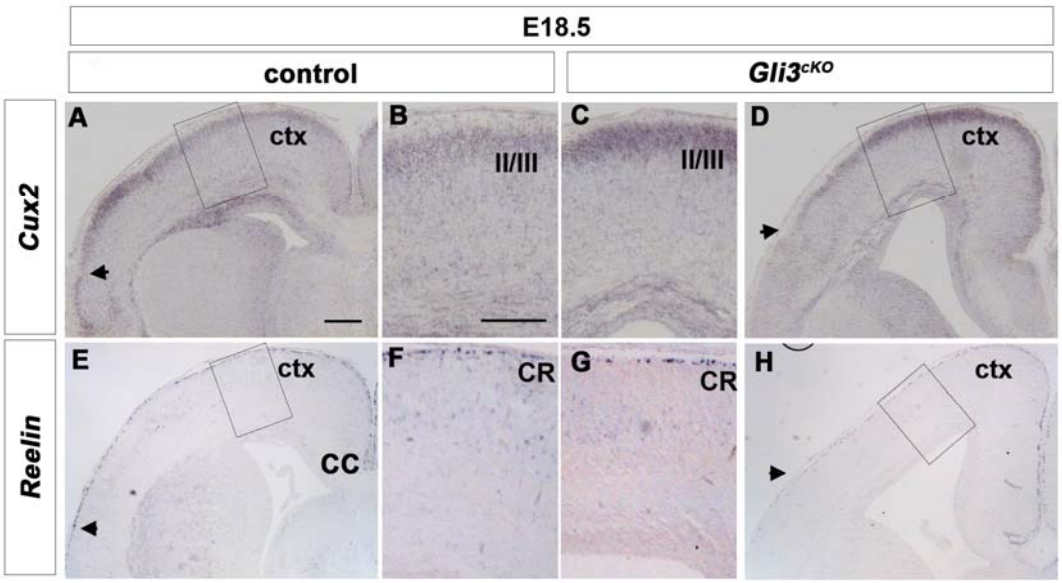

Figure 4-4: Upper layer neurons are not present in the lateral neocortex of *Gli3*^{cKO} mutants.

(A-B) *Cux2*+ neurons occupy layers II/III and extend into the lateral neocortex. (C-D) In *Gli3*^{cKO} mutants, *Cux2*+ neurons occupy similar position in the medial neocortex although they are not expressed below the angle region (arrow). (E-F) *Reelin* is characteristic for Cajal-Retzius neurons in the marginal zone. (G-H) Cajal-Retzius cells are present in the medial cortex but not ventrally to the angle region (arrow). Abbreviations: ctx, neocortex; CC, corpus callosum; CR, Cajal-Retzius cells. Scale bars: 100μm.

4.5 The piriform cortex is expanded in *Gli3^{cKO}* mutants

Although the markers used so far indicate an expansion of the piriform cortex, they are not specific to this structure. A recent study used *Slc6a7* (Hoglund *et al.*, 2005) and *Liprin-β1* (Kriajevska *et al.*, 2002) as markers to label specifically the piriform cortex in postnatal brains when laminar organisation of the piriform cortex is mature (Sarma *et al.*, 2011). In contrast to *Gli3* null mutants (*Gli3$^{Xt/Xt}$*) (Vyas *et al.*, 2003) and *Gli3$^{Xt/Pdn}$* mutants (Magnani *et al.*, 2012b) which die perinatally, *Gli3^{cKO}* conditional mutants are viable after birth and provided an unparalleled opportunity to study the formation of the postnatal piriform cortex in a *Gli3* mutant background. To confirm piriform cortex expansion, I performed *in situ* hybridization analysis for *Slc6a7* (Hoglund *et al.*, 2005) and *Liprin-β1* (Kriajevska *et al.*, 2002) to specifically label the piriform cortex on P7 coronal sections of control and *Gli3^{cKO}* mutant brains (Figure 4-5). In control brains, *Slc6a7* and *Liprin-β1* revealed the piriform cortex at the lateral side of the telencephalon (Fig.4-5A-B, E-F) with the rhinal fissure positioned at the dorsal end of the piriform cortex (Fig.4-5A-B, E-F, arrow). In *Gli3^{cKO}* mutants, *Slc6a7* and *Liprin-β1* were expressed just below the rhinal fissure but their expression domains appeared expanded (Fig.4-5C-D, G-H). To confirm a possible alteration in the length of the piriform cortex or neocortex, I measured and compared the absolute size and the relative size of piriform cortex and neocortex in control and *Gli3^{cKO}* mutant brains. The absolute size of the piriform cortex and neocortex was measured in order to establish if they were expanded or decreased in length, respectively. The size of the piriform cortex was measured as the length of the *Slc6a7* expression domain while the neocortical size corresponded to the *Slc6a7* negative area from the dorsal end point of *Slc6a7* expression to the medial end of the dorsal cortex defined by the cortical curve in this region (Fig.4-5I, insert). In *Gli3^{cKO}* mutants, the neocortex and piriform cortex were significantly reduced and enlarged in absolute size, respectively (Fig.4-5I, insert). The relative size of the piriform cortex and neocortex was measured to take into account a potential change in the overall size of the mutant cortex. For this the relative size is defined as the ratio

between the size of piriform cortex or neocortex to the total cortical size (Fig.4-5J). The total cortical size was defined as the combined lengths of piriform cortex and neocortex. This analysis showed that in *Gli3*^{cKO} mutants, the neocortex was significantly reduced and the piriform cortex enlarged in relative size, respectively (Fig.4-5I-J). The latter experiment suggests that the piriform cortex is expanded in comparison to the total cortical length. Collectively, these data confirm an expansion of the piriform cortex.

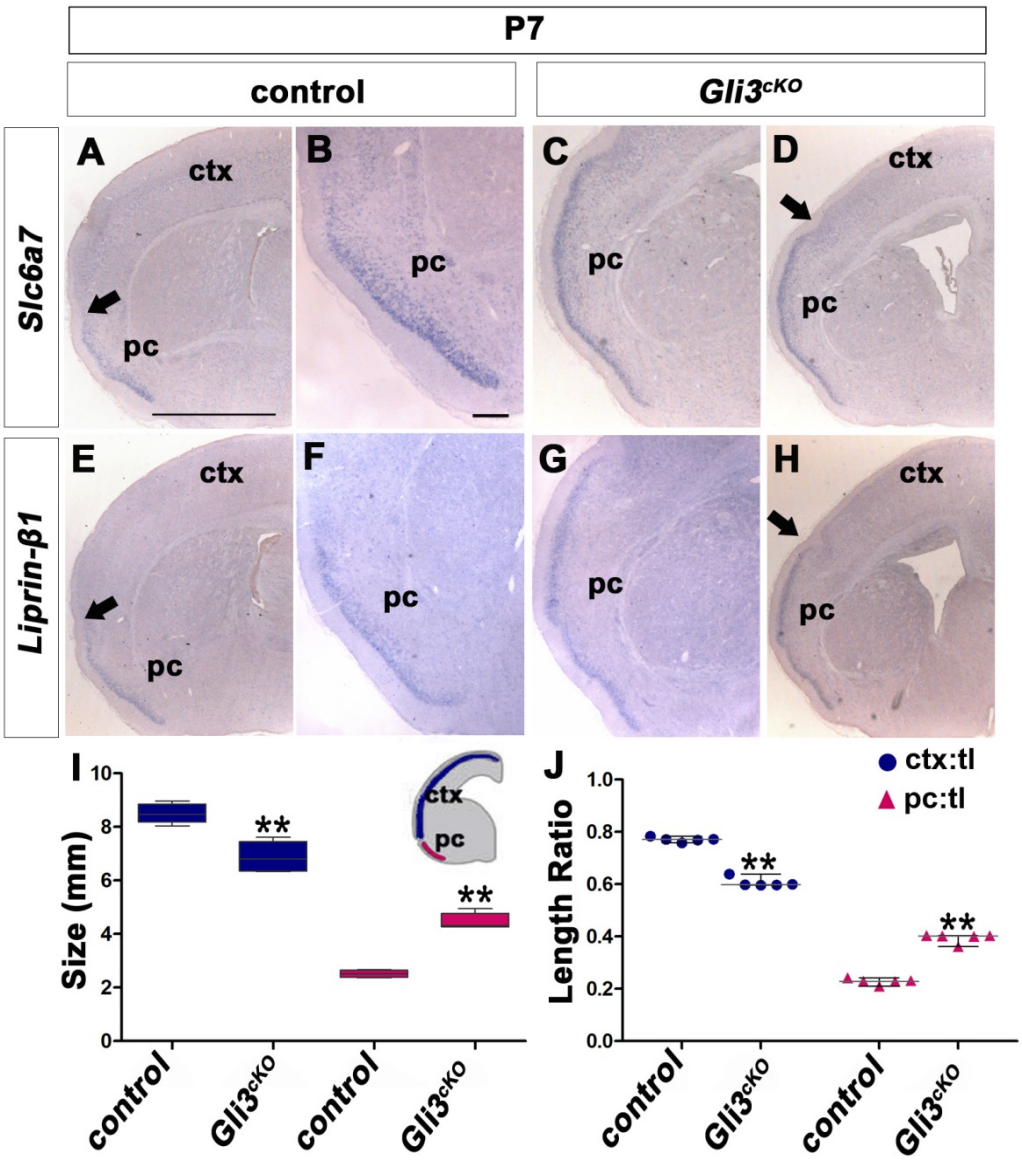
P7
control
Gli3cKO
Slc6a7
Liprin-β1
A
B
C
D
E
F
G
H
ctx
pc
I
J
Size (mm)
Length Ratio
ctx:tl
pc:tl
**
control
Gli3cKO

Figure 4-5: Piriform cortex is expanded in *Gli3*^{cKO} mutant brains.

(A, B, E and F) *Slc6a7* and *Liprinβ1* expression marks the piriform cortex in control brains. Note the rhinal fissure (arrow). (C, D, G, H) Expression of *Slc6a7* and *Liprinβ1* is dorsally expanded in *Gli3*^{cKO} mutants. (I) Measuring the size of the cortex confirmed that the neocortex and piriform cortex of *Gli3*^{cKO} mutants is significantly diminished and enlarged, respectively. (J) Measuring the relative size of piriform cortex and neocortex in comparison to entire cortical size confirmed that the piriform cortex is enlarged and the neocortex reduced in size. Abbreviations: ctx, neocortex; pc, piriform cortex; tl, total cortical size. Asterisks (**) denote statistically significant changes with $p \leq 0.01$. Scale bars: A, D, E and H: 50µm; B, C, F and G: 100µm.

.

4.6 Expansion of the piriform cortex spatially and temporally coincides with corticofugal pathfinding defects

In *Gli3*^{cKO} mutants, the extended piriform cortex occupies the area where CTAs would normally change direction and turn to radiate into the ventral telencephalon. This extension could therefore affect the navigation of CTAs into the striatum. Thus, I investigated a potential spatial correlation between E18.5 control and conditional mutant brains when CTA entry into the striatum is complete. I used *Golli-τGFP Gli3* conditional mutants and performed double immunofluorescence analysis for Ctip2 and GFP to reveal the relative position of the rhinal fissure and the area where corticofugal axons leave the cortex, respectively. In control brains, GFP+ axons turned medially and entered the striatum in a widespread manner whereby the rhinal fissure provided a good landmark for the ventral most axonal exit point (Fig.4-6A-B, E-F). In contrast, in *Gli3*^{cKO}*;Golli-τGFP* mutants GFP+ axons encountered the rhinal fissure at the angle region (Fig.4-4C-D, G-H). The position of the medially shifted rhinal fissure correlated with entry point of the GFP+ axons into the striatum (Fig.4-4G, arrow). Thus, the expansion of the piriform cortex spatially correlates with the restricted region through which corticofugal axons leave the cortex.

The axon pathfinding defects above described and the piriform cortex expansion were examined at late embryonic stages. However, CTAs project and reach the PSPB by E14.5 and after a brief waiting period they extend into the ventral telencephalon (Auladell *et al.*, 2000, Jacobs *et al.*, 2007). This raises the possibility that the CTAs encounter the expanded piriform cortex much earlier in development while they are still descending towards the PSPB. To test this possibility, I carried out immunofluorescence and *in situ* hybridisation analysis on E14.5 control and *Gli3*^{cKO} mutant brains to investigate whether the piriform cortex is already expanded when corticofugal axons start to cross the PSPB. I performed *in situ* hybridisation analysis for the paleocortical marker *Neuropilin-2* (*Nrp2*) on E14.5 control and *Gli3*^{cKO} mutant brains (Figure 4-7). In control brains, *Nrp2* labeled the paleocortex including

the piriform cortex and the olfactory tubercle (Fig.4-7A). *Nrp2* expression formed a sharp boundary at the lateral neocortex (Fig.4-7A, arrow). In *Gli3*^{cKO} mutants, *Nrp2* expanded medially into the region normally occupied by lateral neocortex (Fig.4-7D). I next examined Tbr1 expression which labels newly formed cortical neurons. In E14.5 control brains, Tbr1+ cells formed a dense population at the cortical plate and a lower-density population at the presumptive piriform cortex and the endopiriform nucleus (Ceci *et al.*, 2012) (Fig.4-7B-C). In *Gli3*^{cKO} mutants, Tbr1+ cells occupied similar positions. However, the transition between the dense Tbr1+ neocortical population and the low-density Tbr1+ piriform cortex and endopiriform nucleus population had shifted medially (Fig.4-7E-F). Thus, by using *Nrp2* and Tbr1 markers I could demonstrate that the piriform cortex appears expanded medially in E14.5 *Gli3*^{cKO} mutants.

To further analyse whether expansion of the piriform cortex correlated with the corticofugal guidance defects, I performed immunofluorescence analysis for *Golli-τauGFP* (Jacobs *et al.*, 2007) and TAG-1 (Cntn2 – Mouse Genome Informatics), a member of the subfamily of immunoglobulin (Ig)-like proteins (Denaxa *et al.*, 2001) to label the early corticofugal axons (Figure 4-7). In control;*Golli-τGFP* brains, GFP+ fibres and TAG-1+ axons, which had reached the PSPB were detected in the intermediate zone. At the PSPB GFP+ fibres and TAG-1+ axons turned medially (Fig.4-7G-I). In contrast, in *Gli3*^{cKO};*Golli-τGFP* mutants GFP+ and TAG-1+ axons were present in the intermediate zone of neocortex (Fig.4-7J-L) but no GFP+ or TAG-1+ axons had reached the PSPB (Fig.7J, higher magnification). In fact, TAG-1+ axons reached the angle region and did not project further into the lateral neocortex (Fig.4-7L). Overall, these findings suggest that the corticofugal pathfinding defects coincide both spatially and temporarily with expansion of the piriform cortex raising the possibility that the expanded piriform cortex restricts the exit zone of the corticofugal axons.

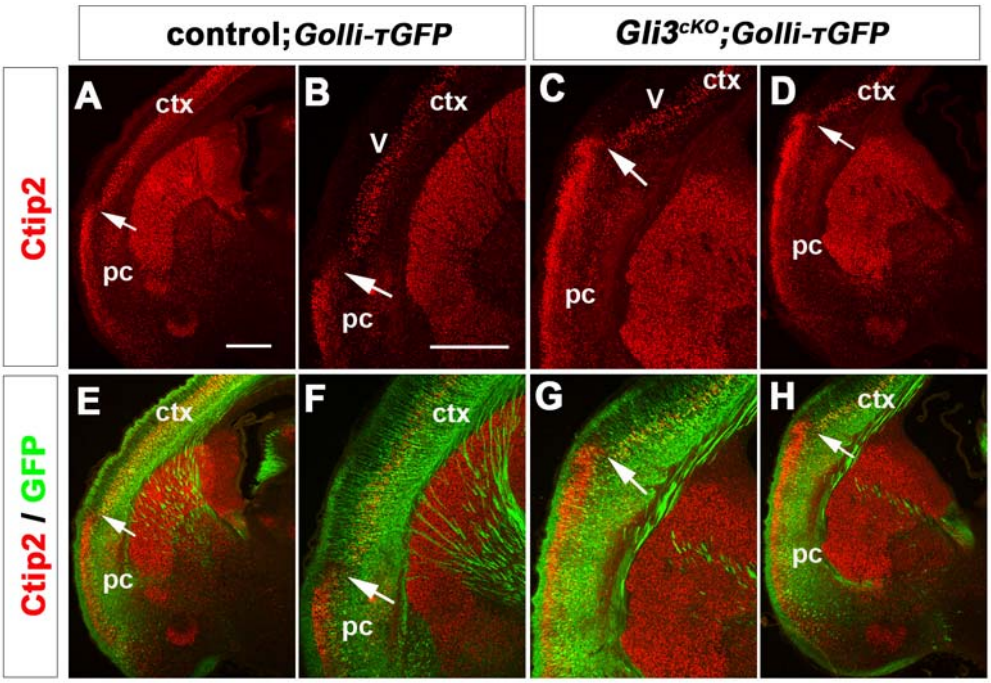

Figure 4-6: Piriform cortex is expanded in E18.5 *Gli3*^{cKO} brains.

(A-B) Ctip2+ neurons occupy neocortical layer V and paleocortical layer II. Note the shift between layers indicated by the rhinal fissure (arrow). (C-D) In *Gli3*^{cKO} mutants, the rhinal fissure is positioned more dorsally. (E-F) Double immunofluorescence for Ctip2 and GFP+ corticofugal axons. Note the ventral exit point of the GFP+ axons at the rhinal fissure (arrow). (G-H) In *Gli3*^{cKO} mutants, GFP+ axons encounter the rhinal fissure more dorsally close to the angle point region (arrow). Abbreviations: ctx, neocortex; pc, piriform cortex. Scale bars:250µm.

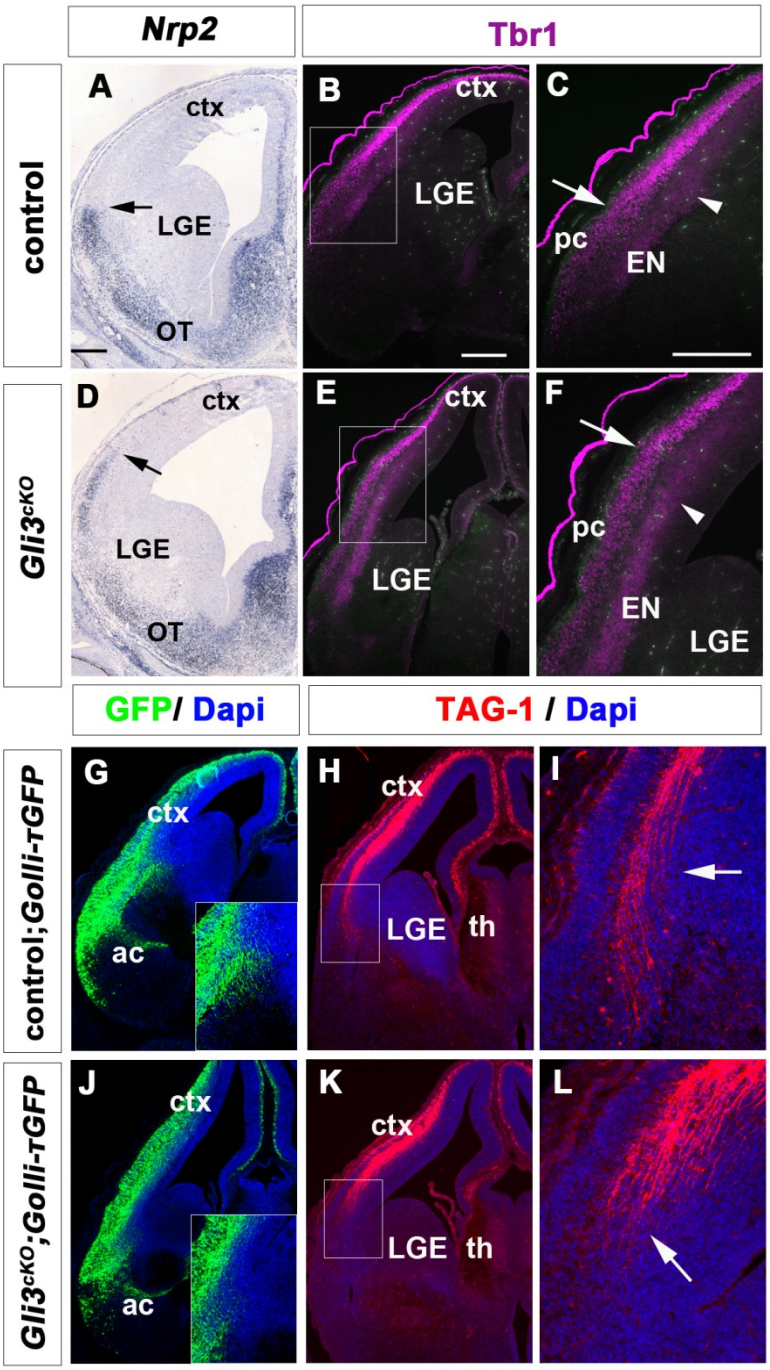
Nrp2
Tbr1
control
A
ctx
LGE
OT
B
ctx
LGE
C
pc
EN
Gli3cKO
D
ctx
LGE
OT
E
ctx
LGE
F
pc
EN
LGE
GFP/ Dapi
TAG-1 / Dapi
control;Golli-tGFP
G
ctx
ac
H
ctx
LGE
th
I
Gli3cKO;Golli-tGFP
J
ctx
ac
K
ctx
LGE
th
L

Figure 4-7: Piriform cortex expansion coincides with early corticofugal defects.

(A) *Nrp2* expression marks the presumptive piriform cortex and the olfactory tubercle but is absent from neurons in the lateral neocortex in control embryos. (D) In *Gli3*^{cKO} embryos, *Nrp2* expression is expanded medially. The arrows in (A) and (D) indicate the dorsal limit of the *Nrp2* expression domain. (B-C; E-F) Tbr1 is expressed in cortical projection neurons and neurons of the presumptive piriform cortex and in the endopiriform nucleus (EN) of control (B,C) and *Gli3*^{cKO} embryos (E,F). In mutant embryos, Tbr1 expression in the presumptive piriform cortex and in the EN are expanded medially. The arrows indicate the transition between these two Tbr1 expression domains, (C) and (F) are higher magnifications of the boxed areas in (B) and (E). (G-L) GFP (G,J) and TAG-1 (H,I,K,L) immunofluorescence analysis to reveal the trajectory of corticofugal axons. In control embryos, GFP+ and TAG-1^{+} axons (arrow in I) turn medially upon reaching the PSPB (G-I) whereas these axons are prematurely stalled at the angle region in mutants (J-L). Abbreviations: ac, anterior commissure; ctx, cortex; EN, endopiriform nucleus; LGE, lateral ganglionic eminence; OT, olfactory tubercle; th, thalamus.Scale bars: A, D:100μm; B, C, E, F and G-L:250μm.

4.7 The expanded piriform cortex inhibits the growth of corticofugal axons

In order to examine whether expansion of the piriform cortex causes the CTA pathfinding defects, I conducted a series of explant cultures and slice transplant experiments between *control*;*Golli-τGFP* and *Gli3^{cKO};Golli-τGFP* mutant brains (Figure 4-8). Initially, explant cultures were performed to assess whether these pathfinding defects would be recapitulated under culture conditions. Coronal sections of E14.5 *control*;*Golli-τauGFP* and *Gli3^{cKO};Golli-τGFP* brains were cultured for 72 hours, then fixed and immunostained for GFP. In *control*;*Golli-τGFP* sections, GFP+ axons fasciculated and radiated into the ventral telencephalon (Fig.4-8A-B). In contrast, in *Gli3^{cKO};Golli-τGFP* brains GFP+ axons did not project into the striatum (Fig.4-8C-D). Therefore, the data from the explant cultures revealed a similar but more severe phenotype to the one observed *in vivo*. Next, *control*;*Golli-τGFP*- piriform cortex and lateral neocortex -a region corresponding to the expanded piriform cortex in *Gli3^{cKO}* mutant brains- were homotopically transplanted into *control*;*Golli-τGFP*+ sections to examine whether GFP+ axons would project under these transplant conditions and assess the experiment's validity (Fig.4-8E, G). GFP+ axons grew into the ventral telencephalon (n=8/11) maintaining their normal projection pattern (Fig.4-8F). Since the transplantation did not interfere with axon growth, I next tested whether the expanded piriform cortex of *Gli3^{cKO}* mutants would interfere with the growth of control corticofugal axons. To examine this possibility, *Gli3^{cKO};Golli-τGFP*- expanded piriform cortex was homotopically transplanted into the *control*;*Golli-τGFP*- piriform cortex and lateral neocortical region (Fig.4-8H, J). Under these conditions, GFP+ axons did not project into the striatum (n=8/10) (Fig.4-8I) indicating that the expanded piriform cortex is not permissive to corticofugal growth. Finally, *control*;*Golli-τGFP*- piriform cortex and lateral neocortex were homotopically transplanted into the *Gli3^{cKO};Golli-τGFP*+ expanded piriform cortex area with the aim being to rescue the axonal defects of *Gli3^{cKO}* mutant brains (Fig.4-8K, M). With this replacement experiment, I observed GFP+ axons projecting but they followed the PSPB ventrally and failed to enter the

striatum indicating a partial rescue (n=13/16) (Fig.4-8 L). Taken together, these experiments demonstrate that the expanded piriform cortex can inhibit the growth of CTAs into the ventral telencephalon.

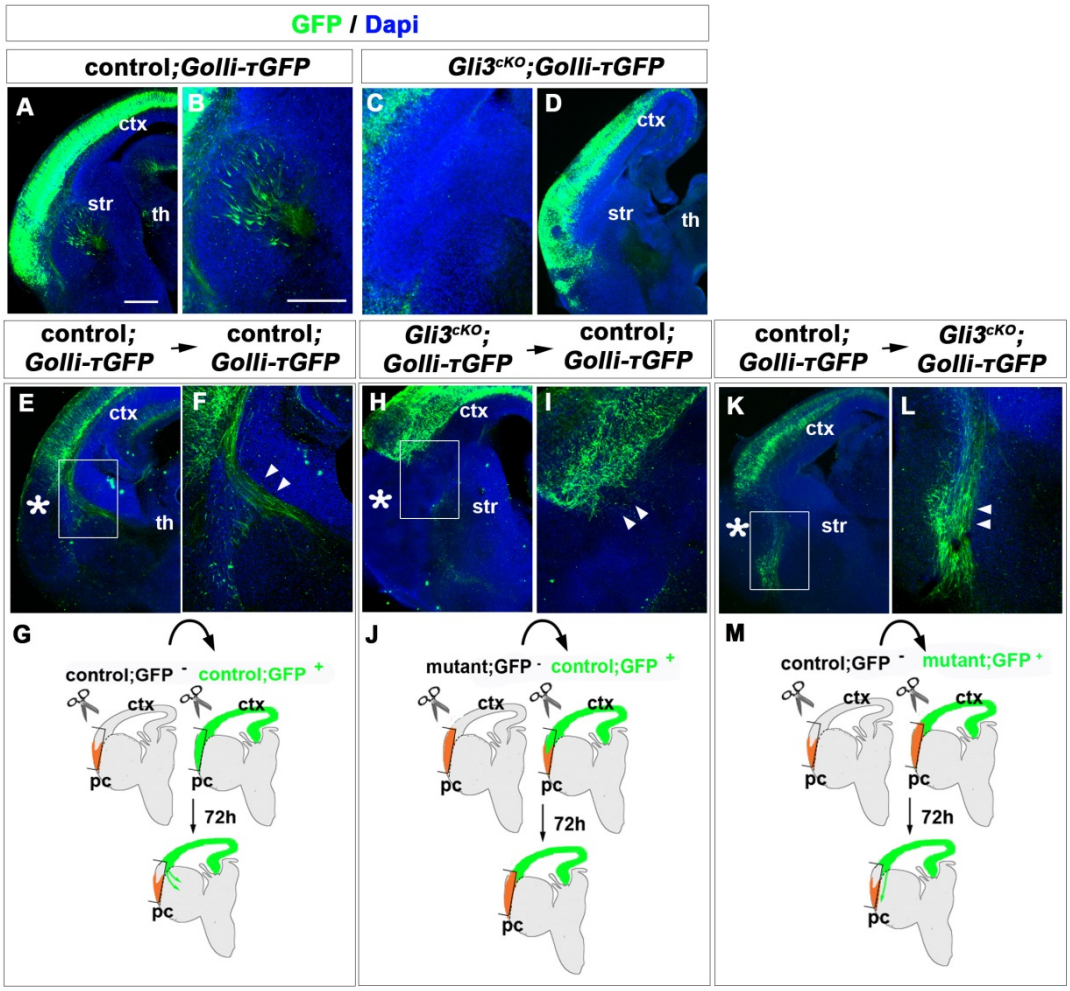

Figure 4-8: The expanded piriform cortex inhibits the growth of corticofugal axons.

(A-D) After 3 days in culture, explants of *control;Golli-τGFP*+ E14.5 brains showed corticofugal axons projecting into the striatum (A,B) while *Gli3^{cKO};Golli-τGFP*+ did not show axons growing into the striatum (C,D). (E-G) Homotopic transplantation of *control;Golli-τGFP*- lateral cortex including neocortical and piriform cortex tissue into *control;Golli-τGFP*+ cortex also led to corticofugal axons entering the striatum (arrowheads in F). (H-J) No axon outgrowth was observed after transplanting *Gli3^{cKO};Golli-τGFP*- lateral cortex into *control;Golli-τGFP*+ cortex. (K-M) Replacement of the expanded piriform cortex of *Gli3^{cKO};Golli-τGFP*+ mutants with *control;Golli-τGFP*- lateral cortex led to growth of corticofugal axons along the PSPB (arrowheads in L) but not into the striatum (n=13/16). (G, J, M) Schematic representation of the homotopic transplants conducted. Abbreviations: ctx, neocortex; pc, piriform cortex; str, striatum; th, thalamus. Scale bar: A-M:250µm.

4.8 *Sema5B* expression coincides with the expansion of the piriform cortex

To address the possible molecular basis for the inhibitory activity of the piriform cortex on the navigation of corticofugal axons, we searched for chemorepellent axon guidance molecules expressed in the piriform cortex. In fact, *Sema5B* expression flanks the projection of descending cortical axons which appear to avoid the *Sema5B* expression domain. *In vivo* knock-down of *Sema5B* and *in vitro* experiments suggest that *Sema5B* has a chemorepulsive activity for cortical axons, while thalamocortical axons where not inhibited (Lett *et al.*, 2009). *Sema5B* is also expressed in the piriform cortex and its ability to specifically repel cortical axons raises the possibility that it is a good candidate to explain how the piriform cortex can inhibit corticofugal axons growth. I therefore I performed *in situ* hybridisation for *Sema5B* on E14.5 control and $Gli3^{cKO}$ mutant brains (Figure 4-9). In control brains, *Sema5B* expression was restricted to the ventricular zone of neocortex and caudal ganglionic eminence, the piriform cortex and the endopiriform nucleus (Skaliora *et al.*, 1998) (Fig.4-9A-B). *Sema5B* expression also showed a gap between the expression domains in the cortical ventricular zone and in the endopiriform nucleus in control brains (Fig.4-9A-B, arrowhead). In $Gli3^{cKO}$ mutants, *Sema5B* was expressed in the dorsal and ventral telencephalic ventricular zone. However, the *Sema5B* expression in the piriform cortex and endopiriform nucleus was shifted medially restricting the gap between the cortical ventricular zone and the endopiriform nucleus expression domains (Fig.4-8C-D, arrowhead). Thus, the restricted entry of corticofugal axons into the striatum could be caused by this shift in *Sema5B* expression. To find further support for this possibility, I performed TAG-1 immunofluorescence analysis to label the early corticofugal axons and *Sema5B in situ* hybridisation on adjacent sections. In control brains, overlay of these markers revealed that TAG-1+ axons were detected in the intermediate zone and projected towards the gap between expression domains in the cortical ventricular zone and in the endopiriform nucleus, where they turned medially towards the PSPB (Fig.4-8E-F, I-J). In contrast, in $Gli3^{cKO}$ mutants TAG-1+ axons were detected in the intermediate zone and did not project further from the angle

region. At this region the axons encountered the shifted *Sema5B* expression domain (Fig.4-8G-H, K-L). Taken together these data indicate that early corticofugal axon defects coincide with the shifted *Sema5B* expression domain.

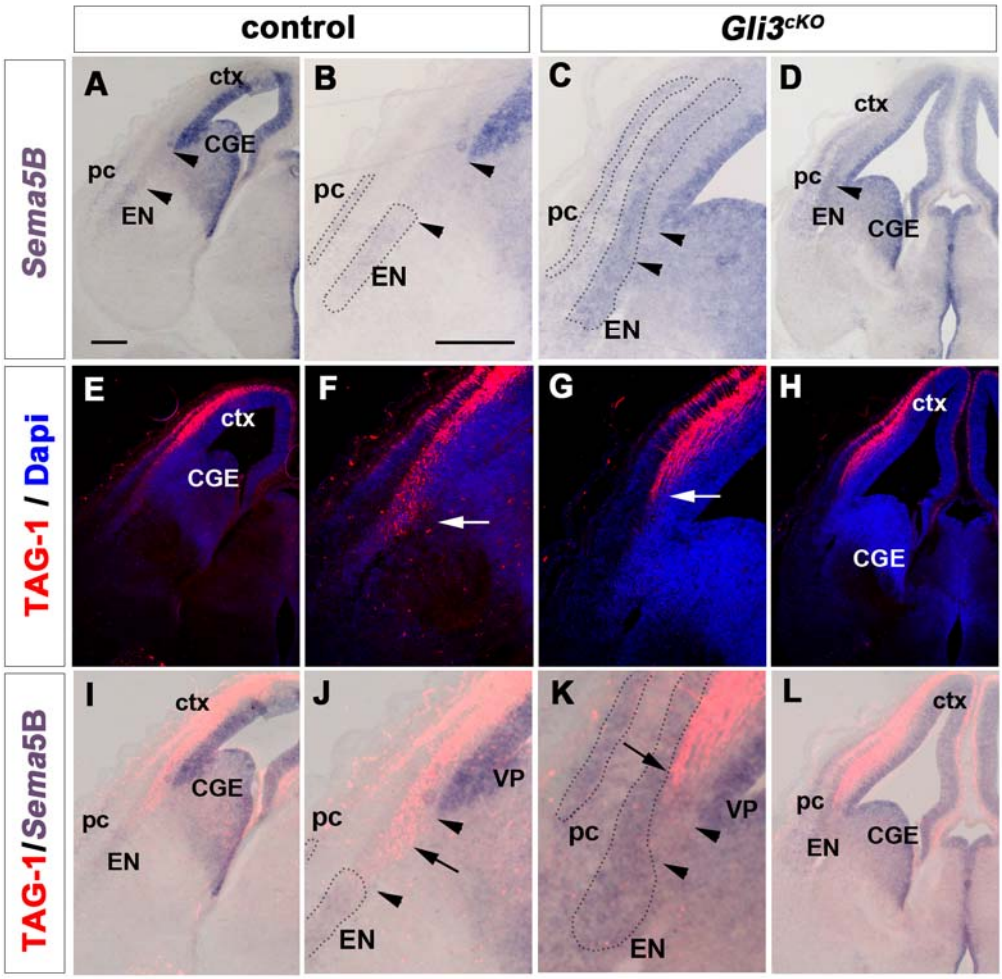
control
Gli3cKO
Sema5B
TAG-1 / Dapi
TAG-1/Sema5B
A
B
C
D
E
F
G
H
I
J
K
L
ctx
CGE
pc
EN
VP

Figure 4-9: *Sema5B* show a repulsive activity to TAG-1+ corticofugal axons.

(A-B) *Sema5B* is expressed in the ventricular zone of the neocortex and of the caudal ganglionic eminence and in neurons of the piriform cortex and of the endopiriform nucleus (dotted area). The arrowheads in (A) indicate the gap between the cortical ventricular zone and the endopiriform nucleus expression domain. (C-D) These expression patterns are maintained in *Gli3*^{cKO} mutants but the piriform and endopiriform nucleus expression is expanded laterally leaving only a small gap (arrowhead) between the two expression domains (dotted area). (E-H) TAG-1+ axons turn towards the PSPB in control embryo but stop their descent in the lateral neocortex of *Gli3*^{cKO} brains. Arrows in (F and G) indicate the end point of axon migration. (I-L) Overlay of the stainings presented in (A-H). In control embryos, TAG-1+ axons projected ventrally (arrow) till they reached the *Sema5B* expression domain in the EN (arrow). In conditional mutants TAG-1+ axons already encounter the expanded *Sema5B* expression domain at the level of the angle region (arrow). Arrowheads in (J,K) indicate the gap between EN and cortical VZ. Abbreviations: ctx, neocortex; CGE, caudal ganglionic eminence; EN, endopiriform nucleus; VP, ventral pallium; pc, piriform cortex. Scale bar: A-L:250µm.

4.9 Regionalization defects in *Gli3*^{cKO} mutants

Finally, I investigated how *Gli3* inactivation in the cortex leads to the expansion of the piriform cortex in *Gli3*^{cKO} mutants. From medial to lateral the dorsal telencephalon will give rise to the medial pallium, the dorsal pallium, the lateral pallium and the ventral pallium. The latter contributes to a specific subpopulation of cells in the deeper layers of the piriform cortex (Hirata *et al.*, 2002). The ventral pallium is the ventral most part of the cortex and is delineated on its ventral side by the PSPB, which plays a key role in corticothalamic pathfinding (Lopez-Bendito and Molnar, 2003). *Gli3* is expressed in dorsal telencephalic progenitor cells and since the progenitor domain of the ventral pallium (VP) resides within this region, defective VP development in *Gli3*^{cKO} mutants might underlie the expansion of the piriform cortex. To examine VP formation, I performed *in situ* hybridization analyses for secreted frizzled-related protein-2 (*Sfrp2*) (Kim *et al.*, 2001), transforming growth factor-alpha (*Tgfα*) (Assimacopoulos *et al.*, 2003) and developing brain homeobox-1 (*Dbx1*) (Yun *et al.*, 2001) which label VP progenitors (Figure 4-10). In control brains, *Sfrp2, Tgfα* and *Dbx1* expression were restricted to the ventral pallium (Fig.4-10A-C). In *Gli3*^{cKO} mutants, *Sfrp2* and *Tgfα* expression were moderately expanded dorsally while *Dbx1* expression was detected throughout the neocortical ventricular zone (Fig.4-10D-F). These data revealed an expansion of the VP in *Gli3*^{cKO} mutant brains. To further determine the origins of this striking *Dbx1* up-regulation, I performed a time course analysis of *Dbx*1 expression (Figure 4-11). Strong *Dbx*1 expression was found at the ventral pallium of E11.5 control brains (Fig.4-11A) but *Dbx*1 became sparser from E13.5 onwards (Fig.4-11B-C). In *Gli3*^{cKO} mutant brains, *Dbx*1 expression was already up-regulated at E11.5 in the lateral pallium but more medial pallial regions did not express *Dbx1* (Fig.4-11D). From E11.5 to E14.5, I observed a progressive up-regulation of *Dbx1* in the cortical ventricular zone and by E14.5 *Dbx1* expression encompasses the entire cortical ventricular zone. (Fig.4-11E-F). Collectively, these data indicate a medial expansion of the ventral pallium together with a surprising up-regulation of *Dbx1* expression.

I also investigated whether other transcription factors, known to control the development of the piriform cortex, are affected in *Gli3*^{cKO} mutants. Conditional inactivation of *LIM* homeobox protein-2 (*Lhx2*) in the dorsal telencephalon results in an ectopic formation of the piriform cortex (Chou *et al.*, 2009). Also, doublesex related gene-5 (*Dmrt*5) null mutants show a lateral expansion of the piriform cortex (Saulnier *et al.*, 2012). It is possible that *Gli3*'s inactivation in the dorsal telencephalon has an effect on *Lhx2* and/or *Dmrt5* expression. Thus, I examined the expression of these transcription factors in E14.5 control and *Gli3*^{cKO} mutants (Figure 4-12). In control brains, *Dmrt5* expression was restricted to cortical progenitors while *Lhx*2 was expressed in dorsal and ventral progenitors (Fig.4-12A-B). In contrast in *Gli3*^{cKO} mutants, both *Dmrt5* and *Lhx*2 expression was reduced in the ventricular zone of the lateral neocortex (Fig.4-12C-D). Taken together, these data suggest that *Gli3* is required in cortical progenitors early in development to repress VP gene expression by regulating *Lhx2* and *Dmrt5* expression in the lateral neocortex.

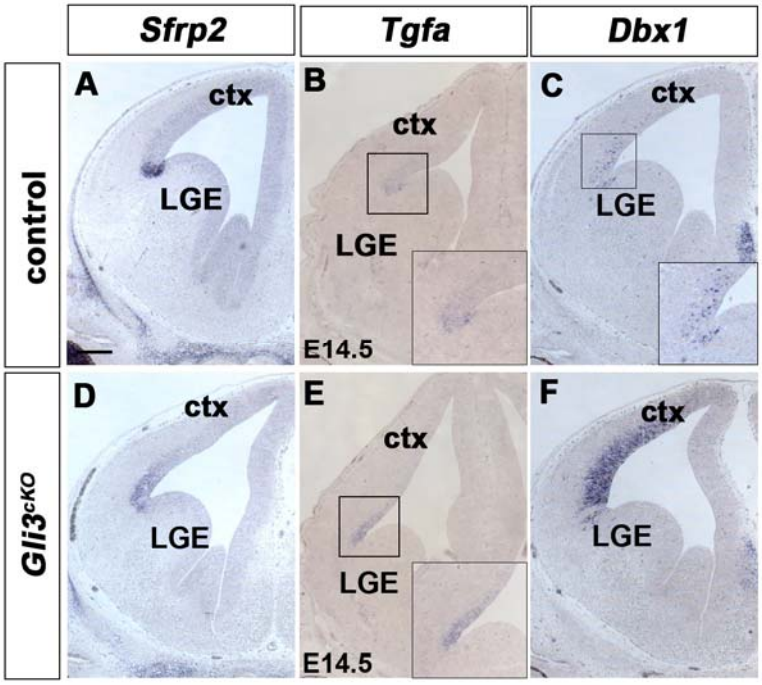

Figure 4-10: Ventral pallium is expanded in the cortical ventricular zone of *Gli3*^{cKO} mutants.

(A-C) *Sfrp2, Tgfα* and *Dbx1* are expressed at the ventral pallium. (F-H) In *Gli3*^{cKO} mutants, the expression of *Sfrp2, Tgfα* and *Dbx1* is expanded dorsally. Note the striking intensified expression of *Dbx*1. Abbreviations: ctx, neocortex; LGE, lateral ganglionic eminence.Scale bars: A-J:100μm.

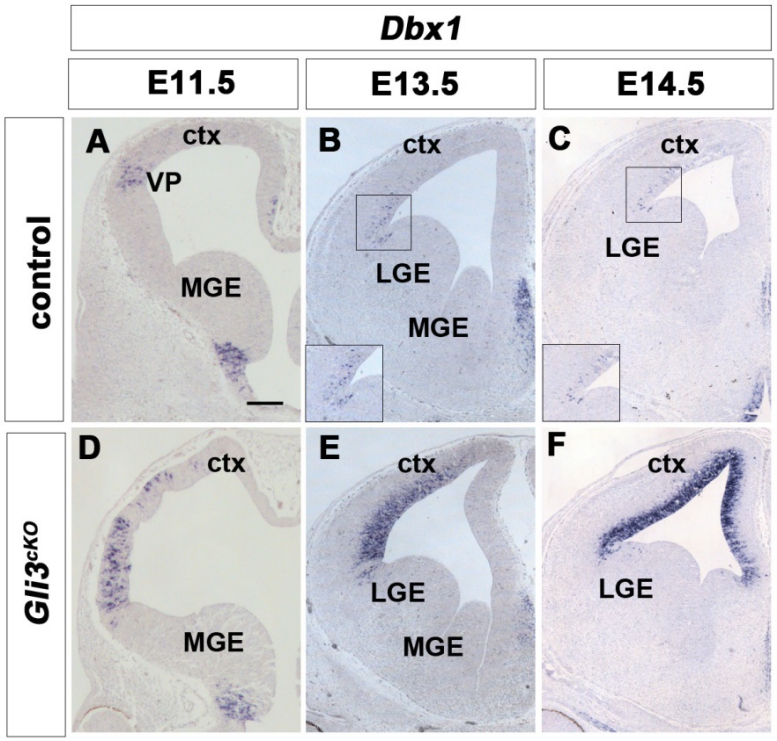

Figure 4-11: *Dbx1* expression is up-regulated in the cortical ventricular zone of *Gli3*^{cKO} mutants.

(A-C) *Dbx1* expression is confined to the ventral pallium of control embryos at all stages analysed. (D-F) *Dbx1* expression is gradually up-regulated in the cortex of *Gli3*^{cKO} embryos. While this up-regulation is confined to the lateral neocortex at E11.5, it encompasses the complete cortical VZ at E14.5.Abbreviations: ctx, neocortex; LGE, lateral ganglionic eminence; MGE, medial ganglionic eminence; VP, ventral pallium. Scale bar: A-F:100µm.

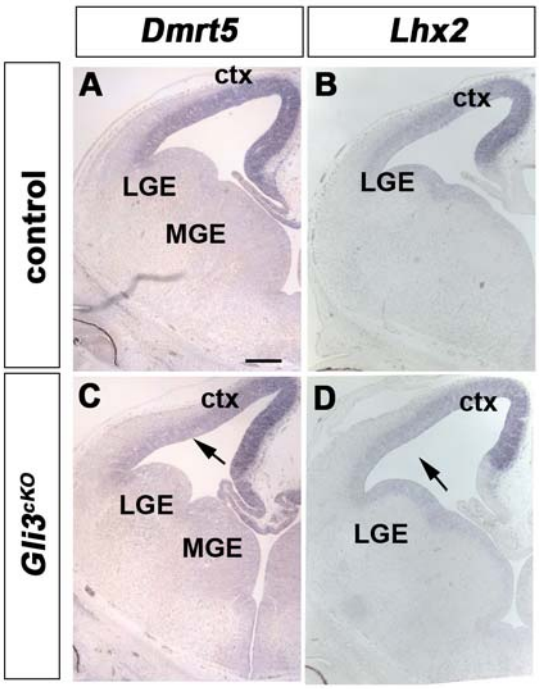

Figure 4-12: *Dmrt*5 and *Lhx*2 expression are reduced at the lateral neocortex of *Gli3*^{cKO} mutant brains.

(A-B) *Dmrt5* expression in cortical progenitors and *Lhx2* expression in dorsal and ventral telencephalic progenitors. (C-D) In *Gli3*^{cKO} mutants, *Dmrt5* and *Lhx2* expression is restricted to the medial telencephalon while being down-regulated at the lateral neocortex (arrow). Abbreviations: ctx, neocortex; LGE, lateral ganglionic eminence; MGE, medial ganglionic eminence. Scale bar: A-F:100μm.

4.10 Discussion

Here, I investigated the possibility that *Gli3* expression in the dorsal telencephalon controls the entry of corticothalamic axons into the ventral telencephalon. *Gli3* conditional mouse mutants show only few CTAs and TCAs leaving and entering the cortex, respectively, while exit from and entry into the cortex is restricted to a small area in the dorsalmost part of the PSPB. Moreover, I demonstrated that *Gli3* is required in cortical progenitor cells to regulate the absolute size and relative size of the piriform cortex, which in turn provides, at least partially, the spatial and temporal requirements for CTAs to project from the cortex to the ventral telencephalon. In $Gli3^{cKO}$ embryos the ventral pallial progenitor domain and the piriform cortex, which is derived from the VP, expand medially. This expansion coincides with an extended expression of *Sema5B*, a known chemorepellent for CTAs, thereby restricting the entry zone of corticofugal axons into the ventral telencephalon.

4.10.1 Chemorepulsion of the piriform cortex regulates spatial and temporal pathfinding of corticothalamic axons

The entry of CTAs into the ventral telencephalon represents a key step in formation of the corticothalamic tract. The migration of CTAs from the cortex to the ventral telencephalon is guided by a complex combination of attractive and/or repulsive guidance cues produced at either the pallial or subpallial side of the PSPB (Polleux *et al.*, 1998, Lett *et al.*, 2009, Oeschger *et al.*, 2012, Deck *et al.*, 2013). Strikingly, CTAs enter the striatum in a broad domain along the PSPB and radiate into the ventral telencephalon. How this broad entry into the striatum is spatially regulated remains an important but largely unexplored aspect of CTA pathfinding.

In $Gli3^{cKO}$ mutants, CTAs entered the striatum through a restricted area at the PSPB close to the angle region and formed a tight axon bundle at the dorsalmost part of the striatum. The PSPB has a known key role in corticothalamic pathfinding (Lopez-

Bendito and Molnar, 2003) due to being an important decision point where corticofugal axons turn sharply from their original trajectory to enter into the subpallium (Molnar and Cordery, 1999), possibly by the expression of corticofugal guidance cues like Netrin-1, Sema3C or Sema5A (Jones, 2002). Many mutants including *Tbr1*, *Emx2*, *Pax6*$^{Sey/Sey}$, and *Gbx2* mutants, show corticofugal pathfinding defects at the PSPB including the formation of aberrant tract formation that projects ventrally or even more severe defects with lack of projecting axons into the ventral telencephalon (Hevner *et al.*, 2002, Lopez-Bendito and Molnar, 2003). Therefore, the restricted entrance of the CTAs into the ventral telencephalon in *Gli3*^{cKO} mutants could have been caused by PSPB defects. However, *Gli3*^{cKO} mutants showed only subtle PSPB defects (Saisana, 2010). Briefly, analysis of the expression of the cortical markers Pax6 and *Ngn2* and of the subpallial markers Gsh2 and *Dlx2* which showed sharp expression boundaries at the PSPB in E12.5 control brains, demonstrated that these expression patterns were largely maintained in *Gli3*^{cKO} mutants although there was some intermingling of cortical and LGE progenitor cells (Saisana, 2010). However, the extent of this intermingling is similar to that found in *Gli3*$^{Pdn/Pdn}$ embryos, which don't show any change in the exit domain of corticofugal axons (Magnani *et al.*, 2010). Although, it cannot be excluded that PSPB defects contribute to this phenotype, I investigated other causes for the entry defects of CTA pathfinding.

Misspecification of corticofugal projection neurons would provide a cellular cause for the CTA pathfinding defects. In *Gli3*^{cKO} mutants my findings suggest that corticofugal projection neurons form and occupy their correct laminar position in medial neocortex but that the lateral neocortex is affected by a medial expansion of the piriform cortex coinciding with absence of corticofugal neurons. Moreover, as shown in Chapter 3 expression of the *Robo1* receptor which has an important role in mediating the guidance of the CTAs is not affected. Hence the major defects were observed at the lateral neocortex and two possibilities were further analysed. These possibilities provided evidence for separate but possibly combinatorial causes for the CTA defects in *Gli3*^{cKO} mutants. Regarding the first possibility, subplate neurons are amongst the earliest born cortical neurons and play a crucial role in pioneering the

corticothalamic tract (McConnell *et al.*, 1989, Jacobs *et al.*, 2007). A recent study reported that *Gli3*$^{Xt/Pdn}$ mutants, which show axonal growth defects, lack subplate neurons (Friedrichs *et al.*, 2008, Magnani *et al.*, 2012b) raising the possibility that their development is also affected in the *Gli3*^{cKO} mutants. In line with this, in *Gli3*^{cKO} mutants a distinct subplate layer was only evident in medial neocortex but not in lateral neocortex suggesting that the formation of the subplate layer is affected in the lateral cortex of *Gli3*^{cKO} mutants (Fu, 2012). This defect suggest that *Gli3*^{cKO} mutants might lack corticothalamic pioneers in the lateral neocortex and hence, an important axon guidance cue that could contribute to the broad entrance of CTAs into the ventral telencephalon.

Secondly, my expression analysis indicated a medial expansion of the piriform cortex from early development stages while my transplantation experiments demonstrated that the expanded piriform cortex was repulsive to the growth of corticofugal axons and growth of CTAs was restored after replacing the expanded piriform cortex with control lateral cortex. However, under these latter conditions, CTAs projected along the PSPB similar to the situation in *Gli3*^{cKO} mutants. These experiments support an emerging picture that the piriform cortex, at least partially regulates the spatial and temporal entrance of CTAs into the subpallium. Projections of CTAs along the PSPB *in vitro* suggests additional cell-autonomous defects in cortical projection neurons or combinatorial defects including cell-autonomous and/or PSPB, subplate defects. A contribution of the piriform cortex to regulating the entry domain of the CTAs was also supported on a molecular basis by the expanded expression of *Sema5B*. *Sema5B* expression is repulsive to cortical axons but not thalamic axons (Lett *et al.*, 2009) suggesting that the expanded *Sema5B* expression domain renders the lateral cortex non-permissive to early corticofugal axons. In control embryos, the *Sema5B* expression domains in the germinal zones of the cortex and ventral telencephalon were well separated from its expression domains in the piriform cortex and endopiriform nucleus creating a gap for corticofugal axons to reach the PSPB and enter the ventral telencephalon. In contrast, due to the expansion of the piriform cortex, only a small *Sema5B* negative area (gap) remained between the cortical ventricular zone and the endopiriform nucleus in *Gli3*^{cKO} embryos.

Consequently, early corticofugal axons encountered *Sema5B* expressing cells right at the angle region. Collectively these data suggest a mechanism by which the piriform cortex may, at least in part, regulate the size of the CTA entry zone into the ventral telencephalon by *Sema5B* expression.

Finally, in $Gli3^{cKO}$ mutants CTAs entered the ventral telencephalon through a restricted region and only navigated through the dorsalmost part of the striatum while other axons projected ventrally at the PSPB. TCAs migrated through the striatum and some TCAs projected to the cortex while others were deflected ventrally at the PSPB. Thus, both corticothalamic and thalamocortical defects were observed in $Gli3^{cKO}$ mutants although *Gli3* inactivation was specific to the dorsal telencephalon and *Gli3* expression in the ventral telencephalon (Amaniti *et al.*, 2013) was not affected rendering a disorganization of ventral telencephalic guidance cues unlikely. Moreover, *Gli3* and several transcription factors were expressed without obvious defects in the thalamus. Therefore, aberrant thalamocortical tract formation is unlikely to be due to thalamic disorganization. Another possible explanation for the defects in the thalamocortical tract is provided by the handshake hypothesis (Molnar and Blakemore, 1995b). At the PSPB and in the ventral telencephalon CTAs interact with TCAs, which migrate in the opposite direction and according to the handshake hypothesis (Molnar and Blakemore, 1995b) guide each other into their target area in the thalamus and cortex, respectively. Recent work also demonstrated that thalamic axons require cortical axons in order to cross the PSPB and reach the cortex even if the cortex itself is attractive to thalamic axons (Chen *et al.*, 2012). Hence, aberrant TCA pathfinding defects in embryos are likely to be secondary to CTA defects. Although this is a reasonable explanation, fundamental questions remain as to how CTAs and TCAs interact and fasciculate with each other (Molnar and Blakemore, 1995a) and what are those signals which are involved in this process.

4.10.2 *Gli3* regulates lateral/piriform cortex fate

Despite the importance of the piriform cortex (see Chapter 1) there has been very little progress in understanding its specification and its separation from the adjacent neocortex. *Gli3*, a transcription factor with a known role in dorsoventral patterning in the telencephalon (Theil *et al.*, 1999, Tole *et al.*, 2000, Aoto *et al.*, 2002, Kuschel *et al.*, 2003, Magnani *et al.*, 2010), has been implicated in specification of the piriform cortex. For example, in $Gli3^{Xt/Xt}$ null mutants, the piriform cortex is specified even though dorsal telencephalic regionalisation is severely disrupted (Vyas *et al.*, 2003). Also, in the $Gli3^{Xt/Pdn}$ intermediate mutants the piriform cortex is medially expanded (Magnani *et al.*, 2012b). Yet, in these studies, the molecular mechanisms by which *Gli3* regulates this process have not been addressed.

The detailed analyses of the $Gli3^{cKO}$ mutants provide important clues to the molecular requirements of *Gli3* function in this process. Since the piriform cortex is derived at least partially from ventral pallium progenitors, I analysed the expression of several ventral pallium markers and identified a moderate medial expansion of the *Sfrp2* and *TGFα* expression domains and a striking up-regulation of *Dbx1* throughout the cortical germinal layer in $Gli3^{cKO}$ mutants. *Dbx1* has previously been implicated in delineating the ventral pallium domain (Yun *et al.*, 2001, Assimacopoulos *et al.*, 2003, Vyas *et al.*, 2003). These findings are consistent with the idea that progenitors of the lateral most neocortex but not those of more medial neocortex have been transformed to a ventral pallial fate. This suggests that at this stage lateral cortex progenitors are still plastic and their neocortical/paleocortical fate is not determined.

Moreover, *Gli3* expression could regulate lateral cortex progenitors fate either directly or indirectly. The Gli3 repressor form (Gli3R) is prominent in the dorsal telencephalon (Fotaki *et al.*, 2006) and *Gli3* inactivation in the dorsal telencephalic progenitors could cause an up-regulation of directly regulated genes. $Gli3^{cKO}$ mutants showed a moderate medial expansion of the *Sfrp2* and *TGFα* expression domains. In contrast, I observed striking up-regulation of *Dbx1* throughout the cortical germinal

layer in *Gli3*^{cKO} mutants as early as E11.5 brains. It is conceivable that *Gli3* directly controls the expression of *Dbx1*, *Sfrp2* and *TGFα*, however, the time course and the extent of their up-regulation argues against this possibility especially as the *Dbx1* up-regulation occurs from lateral to medial opposite to the *Gli3* inactivation gradient. Although, the latter possibility cannot be excluded, I favoured the indirect effect of *Gli3* on VP expression. *Gli3* could regulate ventral pallium development indirectly by controlling the expression of *Lhx2* and *Dmrt5*. Conditional inactivation of *Lhx2* in cortical progenitor cells leads to a duplication of the piriform cortex (Chou *et al.*, 2009) while loss of *Dmrt5* function results in a similar expansion of the piriform cortex as in *Gli3*^{cKO} embryos (Saulnier *et al.*, 2012). The down-regulation of both factors in the lateral cortex of *Gli3*^{cKO} mutants suggests an indirect role of *Gli3* for ventral pallium development. Therefore, my findings place *Gli3* upstream of these transcription factors and imply a key role for *Gli3* in controlling the relative size of neocortex and piriform cortex.

Finally, *Gli3* is a downstream effector of *Shh* signalling (Murone *et al.*, 1999). A recent study described that an up-regulation of *Shh* expression and *Shh* signalling in the ventral telencephalon of *Gli3*$^{Pdn/Pdn}$ is linked to severe patterning defects including a dorsal shift of the PSPB and a ventralization of the lateral ganglionic eminence (Magnani *et al.*, 2010). This raises the possibility that the expansion of the piriform cortex is downstream of *Shh* signalling. Yet, *Shh* expression and Shh signalling are not affected in *Gli3*^{cKO} mutants (Saisana, 2010). In mice lacking Shh (*Shh*$^{-/-}$) the dorsal telencephalic midline, cortical hem and hemispheres are formed but in *Gli3* null mutants and in mutants that both copies of *Shh* are removed from *Gli3*-null mice, dorsal telencephalic defects persist, dorsal telencephalic development is arrested and the ventral telencephalon expands dorsally (Theil *et al.*, 1999, Tole *et al.*, 2000, Rash and Grove, 2007). The latter study, provided evidence for a *Shh*-independent role for *Gli3* in patterning the dorsal telencephalon (Rash and Grove, 2007). A similar Shh-independent role for *Gli3* could be suggested in specifying piriform cortex development.

4.11 Summary

In this chapter, I have extensively presented the *Gli3* controlled defects that highly likely result in the CTAs phenotype in $Gli3^{cKO}$ mutants. Briefly, *Gli3* conditional mouse mutants show only few CTAs and TCAs leaving and entering the cortex, respectively, while exit from and entry into the cortex is restricted to a small area in the dorsalmost part of the PSPB. Moreover, I demonstrated that *Gli3* is required in cortical progenitor cells to regulate the size of the piriform cortex by regulating the ventral pallial progenitor domain which is expanded medially. The piriform cortex provides, at least partially, the spatial and temporal requirements for CTAs to project from the cortex to the ventral telencephalon by expressing *Sema5B*, a known chemorepellent for CTAs. The expansion of the piriform cortex in $Gli3^{cKO}$ mutant embryos thereby restricts the entry zone of corticofugal axons into the ventral telencephalon. These results support and extend previous findings on the central role of *Gli3* for axon tract formation. My results from the $Gli3^{cKO}$ mutants provide a basis to identify the *Gli3* controlled molecular mechanisms and gene network that regulate ventral pallium fate.

5 The expanded piriform cortex may have contributed to the medial shift of the LOT in *Emx1Cre*;*Gli3* conditional mutants

5.1 Introduction

Olfaction plays a central role in the behavior of mammals. The brain receives input from the olfactory bulb for processing. Three major cell types reside within the olfactory bulb (OB): projection neurons (mitral and tufted cells), local inhibitory interneurons (periglomerular and granule cells) and glia (Shipley and Ennis, 1996). The mitral and tufted cells extend axons to the telencephalon forming the lateral olfactory tract (LOT). LOT axons project over the cortical surface to colonise olfactory cortex structures including the piriform cortex (see Introduction) (Derer *et al.*, 1977, Hirata and Fujisawa, 1999). The piriform cortex is the principal olfactory cortical area that receives monosynaptic input from the olfactory bulb, through the LOT. It has been suggested that intrinsic properties of olfactory projection neurons regulate axon outgrowth while environmental cues from the telencephalon control axon navigation to the different olfactory cortex structures (Jimenez *et al.*, 2000, Saha *et al.*, 2007, de Castro, 2009). An interesting study has established that single cortical neurons receive combinatorial input from multiple olfactory receptor neurons, which are positioned in the nasal cavity (Zou *et al.*, 2001). Thus, lateral olfactory tract formation and the specificity of cortical innervation is a fundamental step for the transmission of olfactory information (Shipley and Ennis, 1996, Stettler and Axel, 2009, Gottfried, 2010).

Several guidance molecules and transcription factors regulate different aspects of LOT formation (see Introduction), one of which is the zinc finger transcription factor Gli3. $Gli3^{Xt/Xt}$ null mutants and $Gli3^{Pdn/Pdn}$ hypomorphic mutants show no discernible olfactory bulb protrusion but form an olfactory bulb like (OB-like) structure consisting of specific cells in ectopic, more dorsal positions (Besse *et al.*, 2011). $Gli3^{Xt/Xt}$ lack the LOT (Johnson, 1967) while $Gli3^{Pdn/Pdn}$ show apoptosis of precursor

mitral cells in the OB-like structure (Naruse and Keino, 1995) with residual surviving mitral cells creating a slender LOT (Naruse *et al.*, 1990, Naruse and Keino, 1995). In *Gli3*$^{Xt/Xt}$ mutants telencephalic guidance cues for LOT formation are also severely affected with the lot cells being widely distributed over the entire dorsal telencephalon in small clusters (Tomioka *et al.*, 2000). These severe defects in both intrinsic and environmental cues severely complicate the analysis of the role of *Gli3* in lateral olfactory tract formation. Thus, in this chapter I made use of the *Emx1Cre;Gli3*$^{fl/fl}$ conditional mutants which show milder axon pathfinding defects in comparison to other *Gli3* mutants. My aim was to investigate the role of *Gli3* in LOT formation and in the colonisation of the olfactory cortex by LOT axons especially based on my previous findings (see Chapter 4). To address this aim, I characterised LOT formation, LOT axon branching and piriform cortex development in *Emx1Cre;Gli3*$^{fl/fl}$ conditional mutants. Here, I show that the expanded piriform cortex in *Emx1Cre*;*Gli3*$^{fl/fl}$ embryos (see Chapter 4) is innervated by LOT axons which also appear to be medially shifted with LOT collaterals aberrantly colonising the piriform cortex. Moreover, an OB-like structure was formed in the brain of conditional mutants that consisted of mitral cells but did not protrude from the surface of the telencephalon. No obvious defects were found in the expression of telencephalic guidance cues in E12.5 mutants. Time course analysis confirmed an expansion of the paleocortical primordium from E13.5 onwards, coinciding with the arrival of the LOT axons. Hence, it is possible that the expanded piriform cortex contributed to the medial shift of the LOT.

5.2 Laminar organization of the expanded piriform cortex is correct in *Gli3*^{cKO} mutants

Gli3$^{Xt/Xt}$ null mutants (Vyas *et al.*, 2003) and *Gli3*$^{Xt/Pdn}$ (Magnani *et al.*, 2012b) mutants show an extension of the paleocortex and piriform cortex, respectively, coupled with severe patterning defects including loss of some dorsal telencephalic structures (Theil *et al.*, 1999, Tole *et al.*, 2000, Kuschel *et al.*, 2003). These severe regionalization defects significantly complicate the analysis of the formation of the

trilaminar piriform cortex. *Emx1Cre;Gli3*$^{fl/fl}$ conditional mutants offer an excellent opportunity to study this since they show an expansion of the piriform cortex (see Chapter 4) but lack the severe patterning defects observed in *Gli3*$^{Xt/Xt}$ or *Gli3*$^{Xt/Pdn}$ mutants (see Chapter 3, 4). This is particularly interesting since aberrant lamination of the expanded piriform cortex might have affected olfactory bulb input to the cortex. Hence, to further investigate piriform cortex laminar organization I performed an immunofluorescence analyses for Ctip2 and Calretinin (CR) on E18.5 *Emx1Cre;Gli3*$^{+/+}$/*Emx1Cre;Gli3*$^{fl/+}$ (control) and *Emx1Cre;Gli3*$^{fl/fl}$ (*Gli3*^{cKO}) mutant brains (Figure 5-1). Ctip2 labels layer V neurons in the neocortex and layer II neurons in the piriform cortex (Arlotta *et al.*, 2005). The intracellular calcium-binding protein Calretinin (CR) labels mitral cell axons which comprise the LOT (Bulfone *et al.*, 1998) (Fig.5-1A-B). In control brains, the transition of Ctip2+ staining from layer V to layer II revealed the position of the rhinal fissure (Ariens-Kapers *et al.*, 1936) (Fig.5-1A, arrow). Ctip2+ cells were positioned in layer II of the piriform cortex and the CR+ LOT was located in the ventro-lateral telencephalon, ventral to the Ctip2+ layer (Fig.5-1A-B). In *Gli3*^{cKO} mutants, CR+ LOT axons were present and Ctip2+ layer II neurons had expanded medially as indicated by the rhinal fissure (Fig.5-1C-D, arrow). Combined analysis for CR, microtubule associated protein-2 (Map2) and nuclear counterstain (Dapi) enabled further delineation of the piriform cortex layers in E18.5 brains. In controls, CR identified mitral cell axons, Map2 stained dendrites that span across layer I and dense Dapi+ cell bodies occupied layer II (Fig.5-1E-F) (Sarma *et al.*, 2011). In *Gli3*^{cKO} mutants, the LOT was present and the laminar organization of the piriform cortex was maintained without obvious defects (Fig.5-1G-H). Overall, the expanded piriform cortex receives input from the olfactory bulb and its lamination shows no apparent malformations in E18.5 *Gli3*^{cKO} mutant brains.

The thickness of the piriform cortex increases during early postnatal stages and functional connectivity is shaped between the piriform cortex, the olfactory bulbs and other paleocortical structures. Having already established that piriform cortex is expanded in P7 brains (see Chapter 4), I further analyzed the laminar organization of the piriform cortex of postnatal day 7 (P7) control and *Gli3*^{cKO} mutants. I performed

immunofluorescence analysis for upper layer marker Satb2 (Alcamo *et al.*, 2008, Britanova *et al.*, 2008) and for the deep layer neocortical markers Tbr1 (Hevner *et al.*, 2001) and Ctip2. In control brains, Satb2+ neurons were present in layers II/III of the neocortex but absent from the piriform cortex and Tbr1 stained layer VI neocortical neurons and layer II neurons of the piriform cortex and the olfactory tubercle (Pedraza and De Carlos, 2012) (Fig.5-2A). On the ventro-lateral side of the telencephalon where the rhinal fissure was located, Satb2 expression was reduced and Tbr1 labelling changed from neocortical layer VI to piriform cortex layer II (Fig.5-2B). In *Gli3*^{cKO} mutant brains, Satb2 and Tbr1 staining was maintained without apparent malformation in the neocortex (Fig.5-2D). However, the rhinal fissure was shifted medially as indicated by the reduction in Satb2 expression and the transition of Tbr1+ neurons from neocortical layer VI to layer II of the piriform cortex (Fig.5-2C). In addition, Ctip2 labeled layer V neocortical neurons and layer II neurons of the piriform cortex in control brains (Fig.5-2E-F). In P7 *Gli3*^{cKO} mutant brains the pattern is maintained but the rhinal fissure was shifted medially (Fig.5-2G-H). Collectively, piriform cortex lamination showed no obvious defects in P7 *Gli3*^{cKO} mutant brains but the rhinal fissure was shifted medially.

Based on the fact that synaptic networks between the piriform cortex and other paleocortical structures are being established at P7, I examined CR, Map2 and Dapi expression that enable further examination of the piriform cortex layers. In P7 control brains, CR+ mitral cell axons extended further from the LOT to layer Ia, but not further into layer Ib (Schwob and Price, 1984b), in order to synapse with dendrites and pyramidal cells (Haberly and Behan, 1983). The dendritic marker Map2 labeled layer Ia and Ib and Dapi marked the dense population of cells in layer II (Sarma *et al.*, 2011) (Fig.5-2I-J). In *Gli3*^{cKO} mutant brains, CR+ LOT axons were disorganized and extended beyond layer Ia to layer Ib and some to layer II (Fig.5-2K-L). Moreover, Map2+ dendrites were not discernible in layer Ia but were present in layer Ib (Fig.5-2K). Layer II cells were present without obvious defects although a few CR+ axons projected aberrantly into layer II (Fig.5-2K-L). Collectively, these data indicate that laminar organization of the piriform cortex shows no obvious defects in E18.5 or P7 *Gli3*^{cKO} mutant brains. However, in both prenatal and postnatal

brains the LOT is present innervating the expanded piriform cortex while in postnatal brains LOT axons project aberrantly into layers Ib and II.

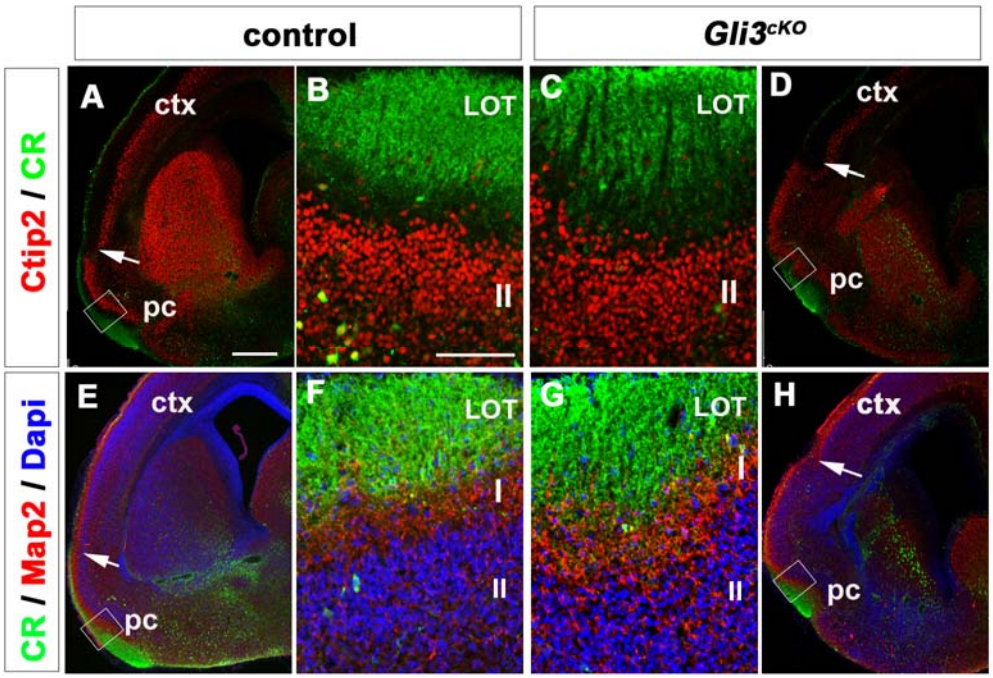

Figure 5-1: The expanded piriform cortex in E18.5 *Gli3*^{cKO} mutants showed no obvious lamination defects, however the LOT is shifted medially.

(A) Ctip2 labels neocortical neurons in layer V and layer II neurons in the piriform cortex of E18.5 control brains. CR labels mitral cell axons comprising the LOT. (B) Higher magnification revealing that Ctip2+ cells in layer II are positioned below the CR+ axons of the LOT. (C) In *Gli3*^{cKO} mutants, Ctip2+ cells occupy layer II at the piriform cortex below the CR+ axons without obvious defects. (D) Ctip2+ layer II neurons are expanded medially and the position of the LOT is shifted medially. (E-H) Laminar organization of the piriform cortex visualized by immunofluorescence analysis of CR, Map2 and Dapi. (E-F) CR labels the LOT axons; Map2 identifies dendrites in layer I and the dense population of cells in layer II is stained with Dapi. (G-H) In *Gli3*^{cKO} mutants, no obvious defects are observed in piriform cortex lamination. (A, D, E, H) Arrow indicates the rhinal fissure and the shift from neocortical to piriform cortex region. Abbreviations: ctx, neocortex; LOT, lateral olfactory tract; pc, piriform cortex. Scale bars:A-H:250µm.

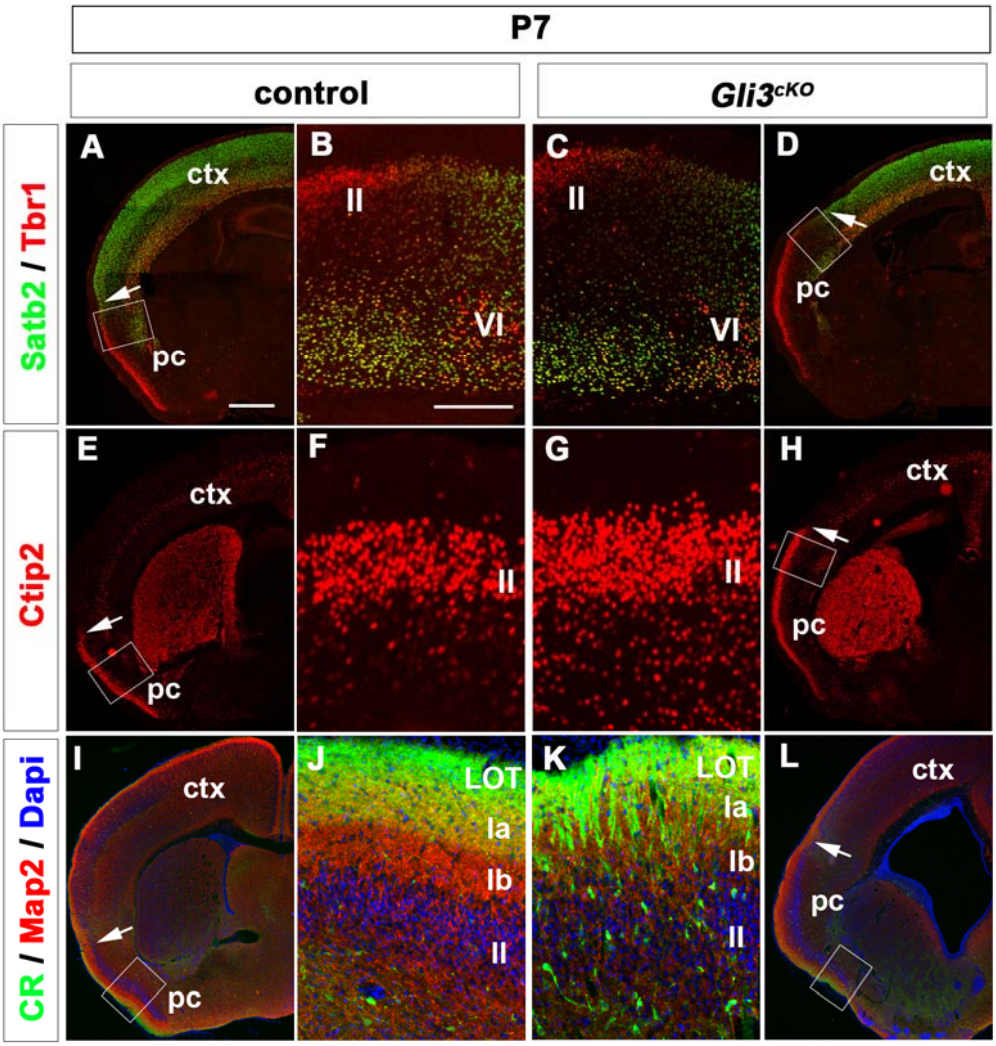
P7
control
Gli3cKO
Satb2 / Tbr1
Ctip2
CR / Map2 / Dapi
A
B
C
D
E
F
G
H
I
J
K
L
ctx
pc
II
VI
LOT
Ia
Ib

Figure 5-2 Formation of the LOT and axon collaterals is disorganized in P7 *Gli3*^{cKO} brains.

(A) In P7 control brains, Satb2 is expressed in layer II/III neocortical neurons and Tbr1 in layer VI neocortical neurons and layer II neurons of the piriform cortex. (B) Magnification of the transition from neocortex to piriform cortex. Satb2 expression is reduced and Tbr1 labeling changes from layer VI to II. (C-D) In *Gli3*^{cKO} brains, Satb2 and Tbr1 labeling in neocortex or piriform cortex show no obvious defects. Note that the transition between neocortex and piriform cortex is shifted medially but does occur without defects. (E-F) Ctip2+ neurons are positioned in layer II of the piriform cortex. (G-H) In *Gli3*^{cKO} brains, Ctip2+ neurons show similar position but layer II is expanded medially. (I-L) Laminar organization of the piriform cortex visualized by immunofluorescence analysis of CR, Map2 and Dapi. (I-J) CR+ LOT axons extend to layer Ia; Map2 dendrites are present in layer Ia and Ib and Dapi+ cells occupy layer II. (K-L) CR+ LOT axons extend in layer Ia and a few CR+ axons aberrantly project in layer Ib and II. Map2+ dendrites are not discernible in layer Ia but are present is layer Ib. Layer II shows no obvious defects. (A, D, E, H, I, L) Arrow indicates the rhinal fissure and the shift from neocortical to piriform cortex region. Abbreviations: ctx, neocortex; LOT, lateral olfactory tract; pc, piriform cortex. Scale bars: A-L:250μm.

5.3 Morphogenesis of the OB is disrupted in *Gli3^{cKO}* mutants but mitral cells are specified

Projection neurons in the OB extend axons that form the LOT that innervate the piriform cortex. Since the *Emx1Cre* driver line has been reported to drive Cre activity in the OB (Gorski *et al.*, 2002), I crossed the *Emx1Cre* mouse line with the *ROSA26CAG dual stop EGFP reporter* (RCE) mouse line (Sousa *et al.*, 2009) to produce *Emx1Cre;Gli3$^{fl/fl}$;RCE* animals and confirm that Cre recombination had occurred in the OB (Figure 5-3A). In these animals, GFP is expressed after Cre mediated excision of the stop sequence that lies upstream of the *EGFP* reporter, in all *Emx1*-expressing cells in the OB. For this analysis E14.5 control and *Gli3^{cKO}* brains were examined since *Gli3* inactivation in the cortex is complete and the OB is discernible at that stage. In E14.5 *control;RCE* brains, GFP reporter expression was obvious in the neocortex and in the OB primordium (Fig.5-3B, D). In *Gli3^{cKO};RCE* conditional mutants, GFP reporter expression was present in both neocortex and the barely discernible OB-like primordium (Fig.5-3C, E). From these data it can be inferred that *Gli3* was inactivated in the OB primordium.

Previous findings in other *Gli3* mutants reveal the formation of an OB-like structure (Naruse and Keino, 1995, Besse *et al.*, 2011). Based on these findings and the lack of an OB protuberance in *Gli3^{cKO}* brains, it could be suggested that early OB developmental defects have affected early mitral cell specification and axon outgrowth in the OB primordium. To further test if OB specification occurred despite the lack of morphogenetic development of the OB, I performed immunofluorescence analysis for transcription factor Tbr1 (Bulfone *et al.*, 1998) and *in situ* hybridization analysis for the activating enhancer binding protein-2e *AP2e* (Feng *et al.*, 2009), inhibitor of DNA binding-2 (*Id2*) (Jen *et al.*, 1997, Bulfone *et al.*, 1998) to mark mitral cells (Figure 5-4). In E14.5 control brains, Tbr1, *AP2e* and *Id2* expression labeled the rostral tip of the OB primordium and marked mitral cells at this age (Fig.5-4A-B, E-F, I-J). In *Gli3^{cKO}* brains, Tbr1, *AP2e* and *Id2* expression labeled a thick band at the rostral tip of the OB-like primordium (Fig.5-4C-D, G-H, K-L). Since the OB does not protrude in *Gli3^{cKO}* brains, I further tested specification of OB

cell types by examining the formation of the inner OB layers consisting of interneurons (Shipley and Ennis, 1996). In control brains, *in situ* hybridization analysis for ETS transcription factor (*ER81*) (Stenman *et al.*, 2003, Cave *et al.*, 2010) revealed the interneuron progenitors in the granule cell layer and in cortical progenitors (Fig.5-4M-N). In *Gli3*^{cKO} mutants, *ER81* expression was present in both cortex and in the OB-like primordium with *ER81* expressing cells forming a discernible cell layer. However, some *ER81* expressing cells formed ectopic clusters in the outer mitral cell layer (Fig.5-4O-P). In summary, *Gli3*^{cKO} mutants form an OB-like structure that is specified and contains mitral cells and interneurons despite the lack of protrusion.

The previous analysis confirmed the formation of an OB-like structure at early developmental stages in *Gli3*^{cKO} mutants. However, I wanted to further investigate mitral cell formation later in development when the piriform cortex is already expanded and its connection with the OB, through the mitral cell projections, established. To investigate this possibility, I performed immunofluorescence analysis for T-box transcription factor Tbr2 (also known as Eomes) in both E18.5 control and *Gli3*^{cKO} brains (Figure 5-5). In control brains, Tbr2 was expressed at lower levels in granular layer interneurons of the OB and in basal progenitors of the cortex (Fig.5-5A) and strongly expressed in differentiated OB projection neurons with mitral cells forming a distinct layer (Fig.5-5D-E). Two different phenotypes were observed in *Gli3*^{cKO} conditional brains regarding OB laminar organization yet both lack a protruding OB (Fig.5-5B-C). *Gli3*^{cKO} brains showed a mild phenotype with Tbr2+ cells forming a discernible layer in the OB-like structure (n=2/3) (Fig.5-5B, F) and a strong phenotype with Tbr2+ cells forming a big large cluster within the OB-like structure (n=1/3) (Fig.5-5C, H). For both phenotypes of *Gli3*^{cKO} and control brains, Tbr2+ cells have a large and round nucleus, a feature characteristic of mitral cells (Fig.5-5E, G, I). To confirm the presence of mitral projection neurons, I further examined the expression of the *Tbx2.1*, a T-box transcription factor gene, specifically expressed in mitral cells (Faedo *et al.*, 2010). *Tbx2.1* was expressed at the mitral cell layer in control brains (Fig.5-5J-K). In *Gli3*^{cKO} mutant brains *Tbx*2.1 was expressed at either a discernible mitral cell layer or a cluster of cells, confirming the previous

results (Fig.5-5L-O). Thus, the mitral cells that will project axons through the LOT to the telencephalon are specified, yet some *Gli3*^{cKO} mutants display OB lamination defects with mitral cells forming a large cluster.

.

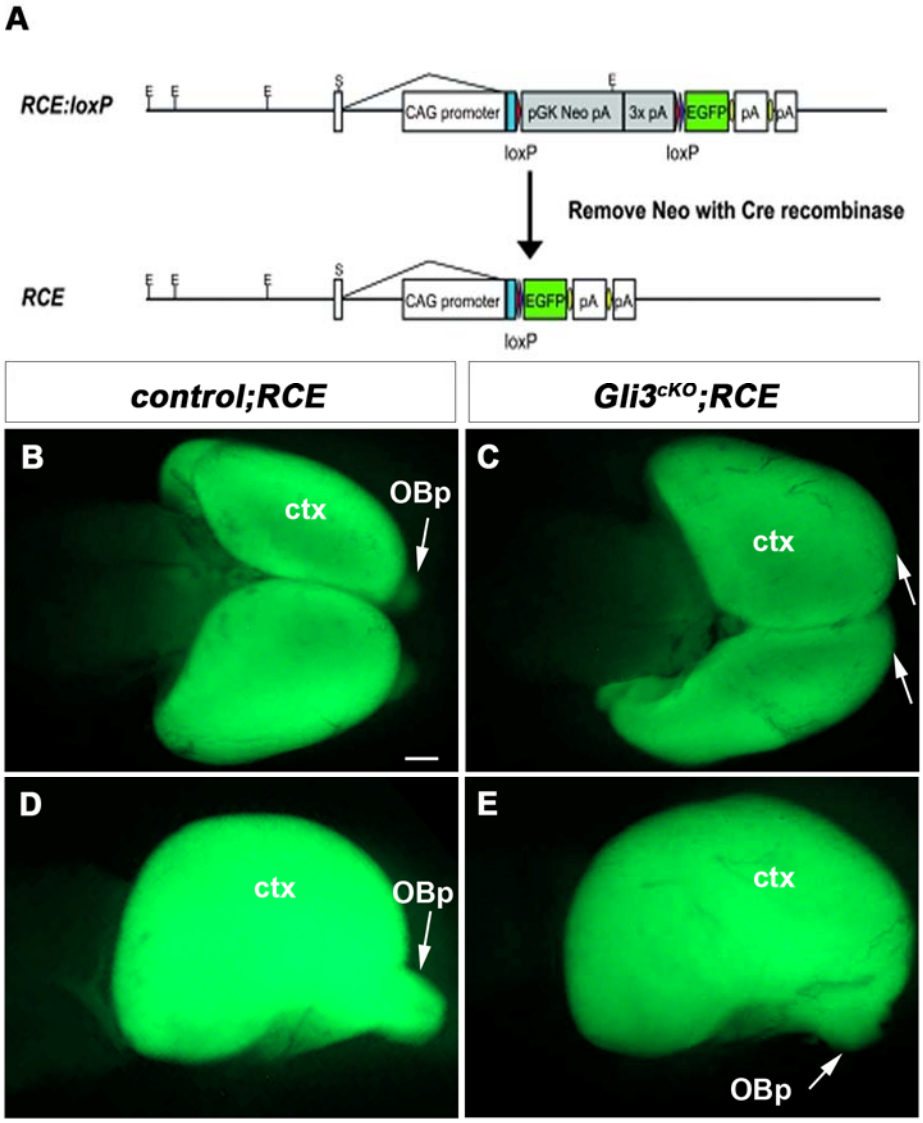

Figure 5-3: Cre-mediated recombination occurs in the neocortex and OB-like structure of E14.5 *Gli3^{cKO};RCE* brains.

(A) *ROSA26CAG dual stop EGFP reporter* (RCE) mouse line used (B, D) GFP reporter in an E14.5 *control;RCE* brain. Both neocortex and olfactory bulb primordium are GFP+ indicating where Cre is active. (C, E) GFP reporter on a E14.5 *Gli3^{cKO};RCE* mutant brain. Note the lack of OB protuberance and the formation of a GFP+ OB-like structure. Abbreviations: ctx, neocortex; OBp, olfactory bulb primordium. Scale bar: A-D:250µm.

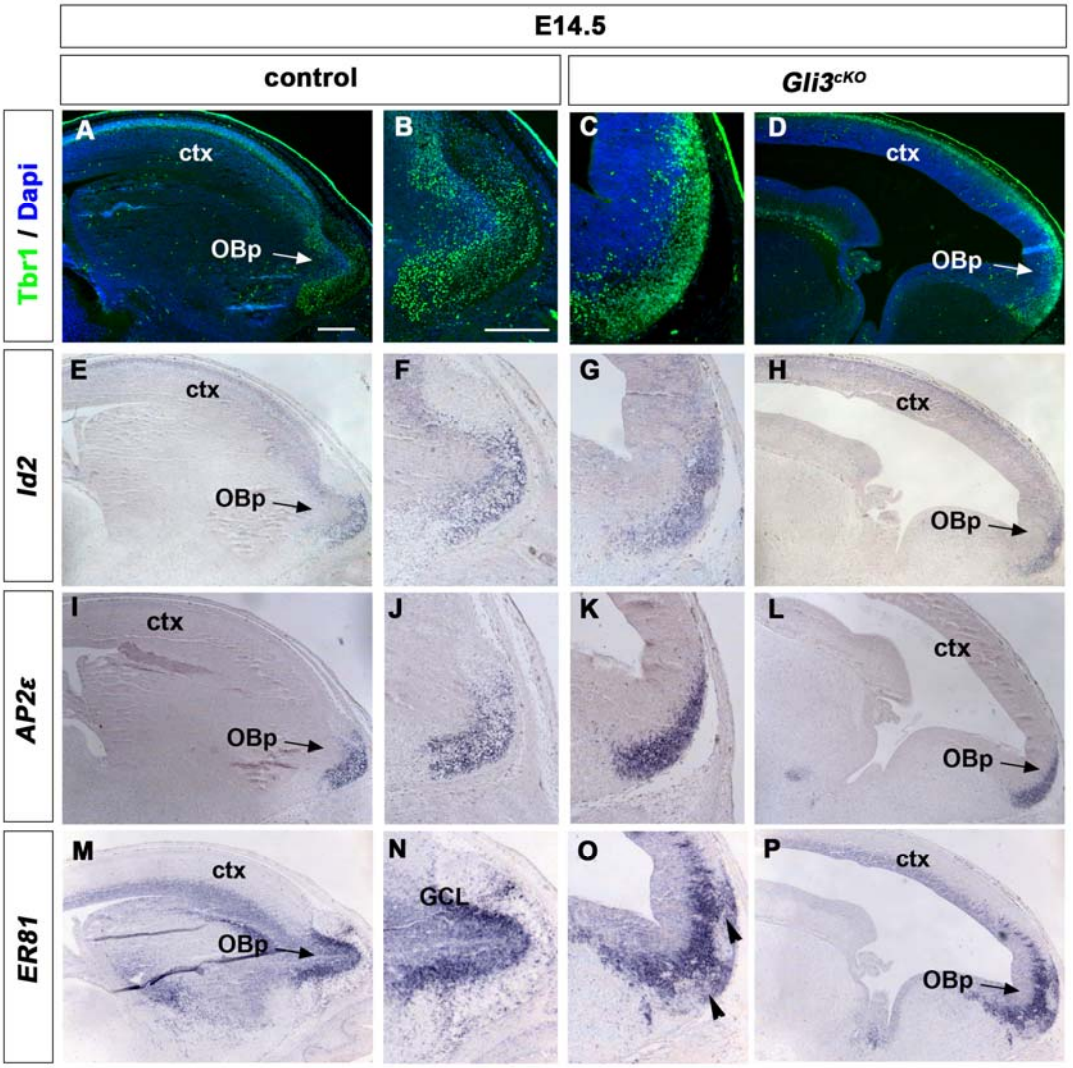

Figure 5-4: Mitral and granule cell layers are formed in the early OB-like primordium.

(A-B, E-F, I-J) *In situ* hybridisation analysis reveals that Tbr1, *Id2* and *Ap2e* expression is restricted to OB projection neurons and specifically mitral cells at the rostral tip of the OB. (C-D, G-H, K-L) In *Gli3*^{cKO} mutants, Tbr1, *Id2* and *Ap2e* expression form a thick band at the rostral tip of the OB-like primordium. (M-N) *ER81* expression is observed in interneuron progenitors in the granule cell layer of the OB primordium. (O-P) In *Gli3*^{cKO} mutants, *ER81* expression is present in a distinct cell layer of the OB-like primordium. The *ER81*+ inner cell layer is extended into the outer mitral cell layer (arrowhead). Abbreviations: ctx, neocortex; OBp, olfactory bulb primordium. Scale bars: A-P:250µm.

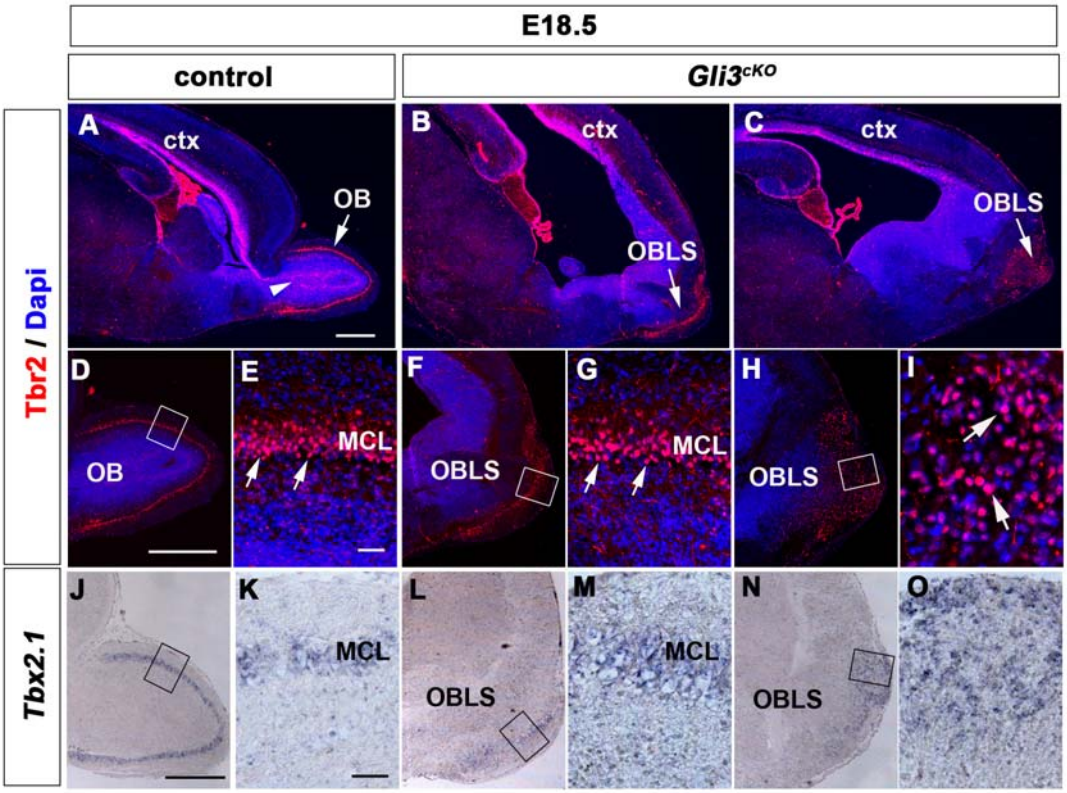

Figure 5-5: Mitral cells are present in an OB-like structure in *Gli3*^{cKO} mutant brains.

(A) The OB is formed at the anterior end of the telencephalon. (B-C) *Gli3*^{cKO} brains form an OB-like structure that does not protrude from the brain. (A, D, E) Tbr1+ cells are present in the cortical ventricular zone, mitral and granule cell layer (arrowhead) of the OB. Note the characteristic round shape of the mitral cells (E, arrow). (B-I) In *Gli3*^{cKO} brains, Tbr2+ cells form a discernible mitral cell layer or a cluster in the OB-like structure. Note that Tbr2+ cells share the characteristic round shape of the mitral cells in *Gli3*^{cKO} brains (G and I, arrow). (J-K) *Tbx2.1* expression is restricted to mitral cells in control brains. (L-O) In *Gli3*^{cKO} brains, *Tbx2.1* expressing mitral cells are present in the OB-like structure and either form a layer or a cluster. Abbreviations: ctx, neocortex; MCL, mitral cell layer; OB, olfactory bulb; OBLS, olfactory bulb like structure. Scale bars:A-D, F and H:250µm; E, G and I:50µm; J, L and N:100µm; K, M and O:50µm.

5.4 The lateral olfactory tract innervates the expanded piriform cortex in *Gli3*^{cKO} mutants

In mice, mitral cell axons reach the telencephalon at around E13.5 and LOT collaterals begin to colonize the piriform cortex three days later at around E16.5 (Sugisaki *et al.*, 1996, Hirata and Fujisawa, 1999). As previously described, *Gli3*^{cKO} mutant brains form an OB-like structure and an expanded piriform cortex from E14.5 onwards (see Chapter 4). Hence, I analysed the degree of innervation of the expanded piriform cortex by examining LOT formation in *Gli3*^{cKO} mutant brains. I anterogradely labelled LOT axons by placing a crystal of the lipophilic tracer DiI in the olfactory bulb of E18.5 control and *Gli3*^{cKO} mutant brains (Figure 5-6). I first assessed formation of the OB, where the DiI crystal was placed. In control brains, the OB protrudes at the anterior end of the telencephalon (Fig.5-6B). DiI crystal placement in the OB of control brains reveals the position of the LOT in the ventro-lateral side of the telencephalon and the collateral branches that are sent off by mitral cell axons to innervate the olfactory cortex (Fig.5-6A-C). In contrast, *Gli3*^{cKO} conditional brains form only a small OB protrusion i.e. an OB-like structure (Fig.5-6D). In *Gli3*^{cKO} brains, the LOT is formed and the axons extended collateral branches. However, the LOT appeared less densely packed and its position is shifted medially in the mutants (Fig.5-6E-F). These data show the formation of an OB-like structure and reveal that the LOT is subtly shifted medially in E18.5 *Gli3*^{cKO} mutant brains.

The functional connectivity of the piriform cortex continues to develop during postnatal stages. Therefore, I further examined LOT formation at P7 using DiI tracer to label mitral cell axons anterogradely. In P7 control brains, the OB clearly protrudes and the LOT site occupies a more extended region with dense collateral branches in layer III of the piriform cortex (Fig.5-6G-I) (Chou *et al.*, 2009). In P7 *Gli3*^{cKO} brains, the OB-like structure is more prominent than at prenatal stages, yet an OB protrusion is not fully formed (Fig.5-6J). Although the LOT is formed, the extension of collateral branches in the piriform cortex is disorganized with only a barely discernible gap between the LOT and layer III in *Gli3*^{cKO} brains (Fig.5-6K).

Interestingly, mitral cell axons and their branches occupy a medially expanded region (Fig.5-6L). Moreover, an aberrant formation of an axon bundle that projects into the ventral telencephalon is also reported (Fig.5-6L, arrow). This is interesting since afferent input from the OB and target invasion of mitral cell axons coincides with the previously described piriform cortex expansion. Collectively, these experiments established that mitral cell axons extend through the LOT to the telencephalon and project collaterals in $Gli3^{cKO}$ mutants. The site of target invasion by mitral cell axons and formation of the LOT is expanded medially reflecting the expansion of the piriform cortex. Hence, the LOT is formed and mitral cell axons seem to recognize and innervate the expanded piriform cortex region.

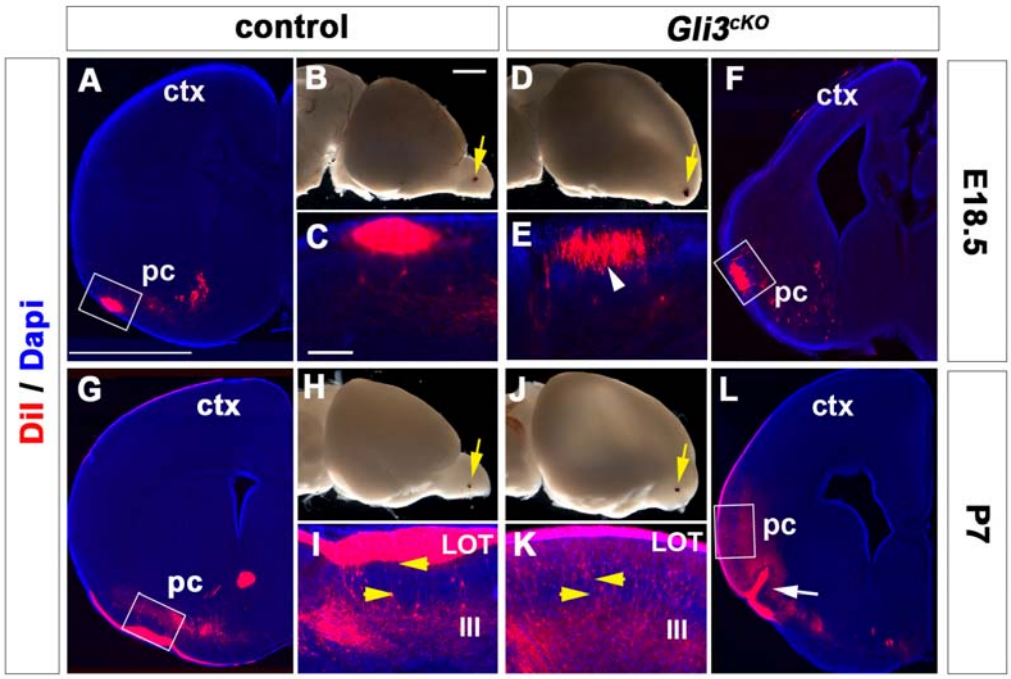

Figure 5-6: Afferent input from the olfactory bulb is expanded medially.

(B, D, H, J) DiI crystal placement in the olfactory bulb (OB) and OB-like structure of control (B, D) and *Gli3*^{cKO} brains (H, J), respectively (arrow). In P7 *Gli3*^{cKO} brains (J), OB protrusion is more prominent in comparison to E18.5 *Gli3*^{cKO} brains (D), however OB development is only partial. (A, C, G, I) Anterograde labeling of LOT axons and their collateral branches in E18.5 (A, C) and P7 (G, I) control brains. In P7 brains (G, I), the LOT occupies the outer piriform cortex layers and LOT axons extend collateral branches in layer III. Note the distinct gap between LOT and layer III (I, arrowheads). (E, F) In E18.5 *Gli3*^{cKO} brains, LOT position is shifted medially and the LOT formation appears striped (arrowhead). (K) The LOT is present in the correct position. A dense population of collateral branches is present in layer III with a barely discernible gap between the LOT and layer III (K, arrowheads). (L) Mitral cell axons and their collateral branches occupy a medially expanded region in P7 *Gli3*^{cKO} brains. Note the aberrant formation of an axon bundle that projects into the ventral telencephalon (L, arrow). Abbreviations: ctx, neocortex; LOT, lateral olfactory tract; pc, piriform cortex. Scale bars: A, G, F and L:50mm; B, D, H and J:0.5mm;C-E, I-K:250µm.

5.5 Normal localization of guidance cues in E12.5 *Gli3*^{cKO} mutant telencephalon

The overall positioning of the LOT trajectory is controlled by a unique population of cells called "lot cells" that restrict the trajectory of the developing LOT (Sato *et al.*, 1998, Tomioka *et al.*, 2000) and secreted signalling molecules e.g. *Sema3F* that provide repulsive cues (de Castro *et al.*, 1999, Nguyen-Ba-Charvet *et al.*, 2002, Ito *et al.*, 2008). In *Gli3*$^{Xt/Xt}$ mutants, lot cells are widely distributed over the entire dorsal telencephalon in small clusters (Tomioka *et al.*, 2000). I therefore investigated lot cell formation in *Gli3*^{cKO} mutants, to determine whether lot cell migration defects may provide an explanation for the medial expansion of the LOT axons. Immunofluorescence analysis using lot1 antibody was initially performed on E12.5 brains when lot cells are first detectable (Tomioka *et al.*, 2000) and have just migrated to the prospective LOT site. In control brains, immunofluorescence analysis for lot1 revealed the position of lot cells, which flank the prospective LOT site at the ventro-lateral aspect of the telencephalon (Fig.5-7A-B). In *Gli3*^{cKO} mutants, no obvious defects were detected in the position of lot1+ cells at this age (Fig.5-7C-D). The location of lot cells was also analyzed two days later when the mitral cell axons have arrived at the LOT site. In control brains, lot1+ cells were present surrounding the LOT axons while more lot1+ cells are located in deeper layers (Fig.5-7E-F). In *Gli3*^{cKO} brains, lot1+ cells flanked the LOT axons (Fig.5-7H). However, fewer lot1+ cells were located deeper in the tissue (Fig.5-7G-H). Overall, at both ages analyzed lot cells were positioned in the correct position surrounding the LOT axons but in E14.5 *Gli3*^{cKO} brains fewer lot cells are present in deeper layers.

Lot cell migration is controlled by several guidance cues including *Netrin-1*, which guides lot cells to surround the LOT site (Kawasaki *et al.*, 2006) and *EphrinA5*, which prevents lot cells migrating into the subpallium (Nomura *et al.*, 2006). Thus, I performed *in situ* hybridization analysis for *Netrin-1* and *EphrinA5* in E12.5 control and mutant brains. In control brains, *Netrin*-1 and *EphrinA5* expression was restricted to the neuroepithelium of the ganglionic eminences and *Netrin*-1 expression extended to the surface of the olfactory tubercle (Fig.5-7I-J, M-N). In

Gli3^{cKO} mutants, no obvious defects were detected in the expression domains of *Netrin-1* and *EphrinA5* (Fig.5-7K-L, O-P). Collectively these data indicate that lot cells are positioned around the LOT axons and the guidance cues that control their migration early in development show no obvious defects.

Finally, *Sema3F* provide repulsive cues to the LOT axons. *Sema3F* prevents LOT axons from invading the cortical plate and the ganglionic eminences (de Castro *et al.*, 1999). An alteration in *Sema3F* expression would potentially explain the aberrant axon bundle that invades the ventral telencephalon (Fig.5-6). *In situ* hybridization was performed to analyze *Sema3F e*xpression in E12.5 control and *Gli3*^{cKO} mutants. In control brains, *Sema3F* is expressed at deep levels of the subpallium surrounding the LOT region (Fig.5-8A-B). In *Gli3*^{cKO} mutants, the subpallial expression of *Sema3F* is similar to that in control brains (Fig.5-8C-D). In summary, LOT guidance cues show no obvious defects in E12.5 *Gli3*^{cKO} mutants.

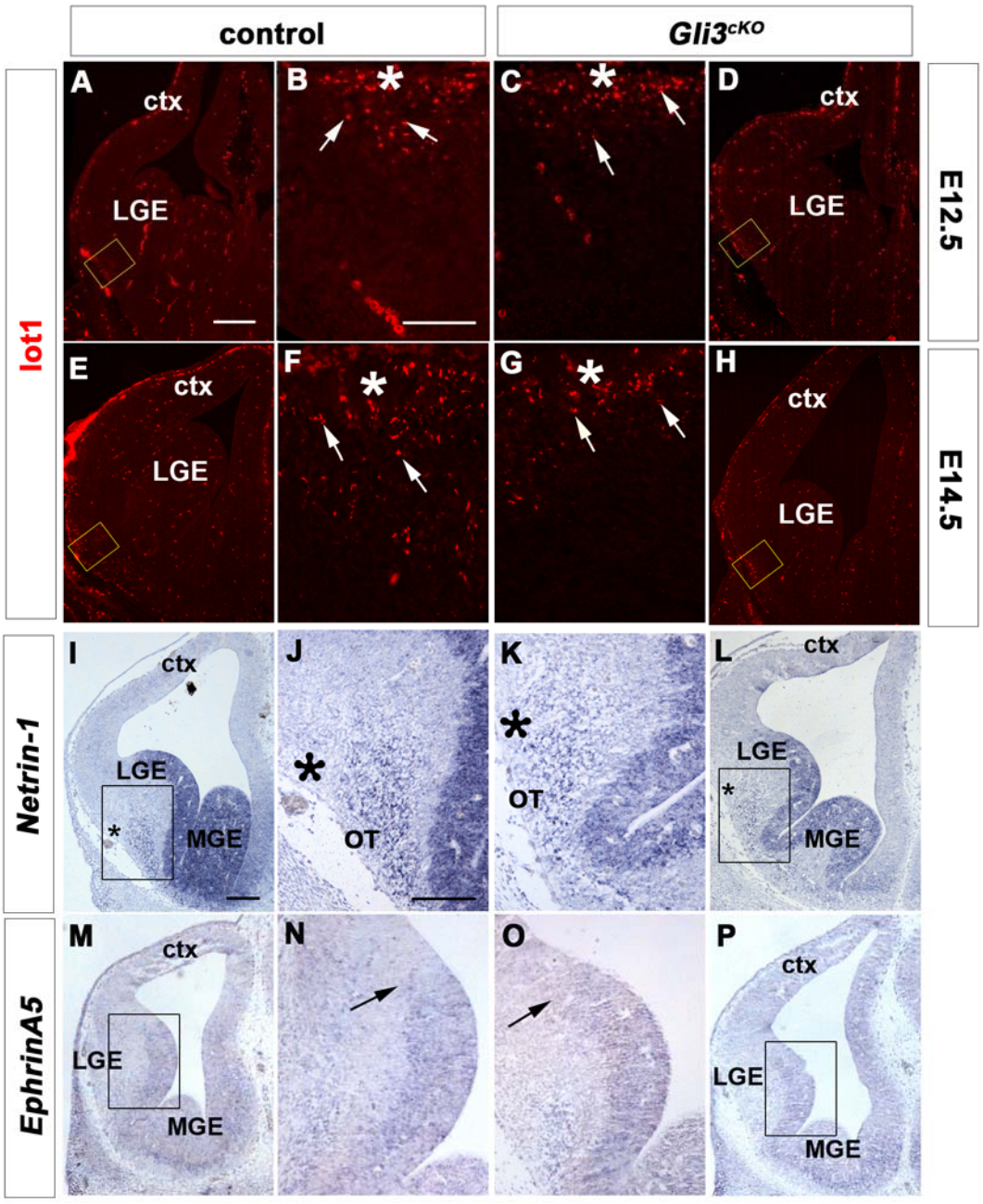
control
Gli3cKO
Iot1
E12.5
E14.5
Netrin-1
EphrinA5
A
B
C
D
E
F
G
H
I
J
K
L
M
N
O
P
ctx
LGE
MGE
OT
*

Figure 5-7: Lot cells are present flanking the LOT axons in *Gli3*^{cKO} mutant brains.

(A-H) Immunofluorescence analysis for lot1 was used to mark lot cells in E12.5 and E14.5 control and *Gli3*^{cKO} mutant brains. (A-B) In E12.5 brains, lot1+ cells have migrated to the future LOT site (B, arrow). (E-F) Similarly in E14.5 control brains, lot1+ cells flank the LOT site while more lot1+ cells are present to the region below the LOT site. (C-D) In E12.5 *Gli3*^{cKO} mutants, lot1+ cells flank the prospective LOT site with no obvious defects (C, arrow). (G-H) In E14.5 *Gli3*^{cKO} mutants, lot cells flank the LOT axons without obvious defects (G, arrow). Note that fewer lot1+ cells are present below the LOT site. (I-J, M-N) *In situ* hybridization demonstrates that *Netrin-1* and *EphrinA5* expression is restricted to the neuroepithelium of the ganglionic eminences in control brains. Note *Netrin-1* expression at the olfactory tubercle. (K-L, O-P) In *Gli3*^{cKO} mutants, *Netrin*-1 and *EphrinA5* expression show no obvious defects. Abbreviations: ctx, neocortex; LGE, lateral ganglionic eminence; MGE, medial ganglionic eminence. Scale bars: A-P:250μm; I-T: 100μm. Asterisks (*) indicate the prospective LOT position in E12.5 brains and the LOT site in E14.5 brains.

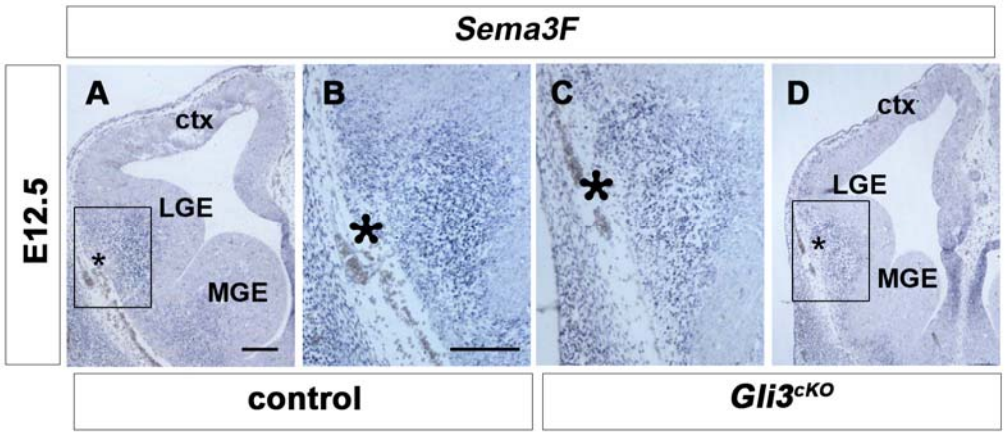

Figure 5-8: *Sema3F* expression showed no obvious defects in E14.5 *Gli3*^{cKO} conditional mutants.

(A-B) *Sema3F* expression is confined deep in the subpallium of E12.5 control brains. (C-D) *Sema3F* show similar expression pattern in *Gli3*^{cKO} mutants. Abbreviations: ctx, neocortex; LGE, lateral ganglionic eminence; MGE, medial ganglionic eminence. Scale bars: A-H:100μm. Asterisks (*) indicate the prospective LOT position in E12.5 brains

5.6 Expansion of the paleocortex precedes entry of mitral cell axons to their target region

Cues produced by the piriform cortex are suggested to control colonization of the telencephalon by LOT axons (Soussi-Yanicostas *et al.*, 2002). Hence, altered piriform cortex formation early in development could result in defective formation of the LOT and extension of collateral branches. To test this possibility, I performed an *in situ* hybridisation analysis for *Nrp2*, a paleocortical marker, to analyse the development of the presumptive piriform cortex in both control and $Gli3^{cKO}$ mutants before the arrival of the LOT axons (Figure 5-9). In E12.5 control brains, *Nrp2* was expressed in the presumptive paleocortex forming a prominent *Nrp2*+ domain (Fig.5-8A-B). In E12.5 $Gli3^{cKO}$ mutants, *Nrp2* expression showed no apparent defects (Fig.5-9C-D). Overall, the presumptive paleocortex show no obvious defects in E12.5 $Gli3^{cKO}$ mutant brains which is in contrast to the already observed expansion of the piriform cortex in E14.5 mutant brains (see Chapter 4).

LOT axons arrive at the telencephalon around E13.5 and the dramatic expansion of the piriform cortex occurs between E12.5 to E14.5 in mutant brains. Therefore, I was interested in investigating the correlation between LOT formation and piriform cortex development in E13.5 $Gli3^{cKO}$ mutant brains. Initially, immunofluorescence analysis was performed for calretinin (CR) to label the LOT axons (Bulfone *et al.*, 1998) in both control and $Gli3^{cKO}$ mutant brains. In control brains, CR+ axons extended to the LOT site at the ventro-lateral aspect of the telencephalon (Fig.5-9E). Similarly in $Gli3^{cKO}$ mutants, CR+ axons occupy the LOT site (Fig.5-9H). In order to establish the relation between LOT and the presumptive piriform cortex, I performed immunofluorescence analysis for the postmitotic marker Map2 and Tbr1 and an *in situ* hybridization analysis for *Nrp2* for both control and mutant brains. In control brains, Map2+ cells were positioned above the Tbr1+ cells (Fig.5-9F) and $Gli3^{cKO}$ mutant brains shared a similar organization (Fig.5-9I). However, *Nrp2* expression in adjacent sections reveals that in control brains the region above the LOT was *Nrp2* negative (Fig.5-9G) while in $Gli3^{cKO}$ mutants it ectopically expressed *Nrp2* (Fig.5-

9J). Overall, these data indicate that in E13.5 *Gli3*^{cKO} mutant brains the presumptive piriform cortex is already expanded when the mitral cell axons first arrive at the LOT site.

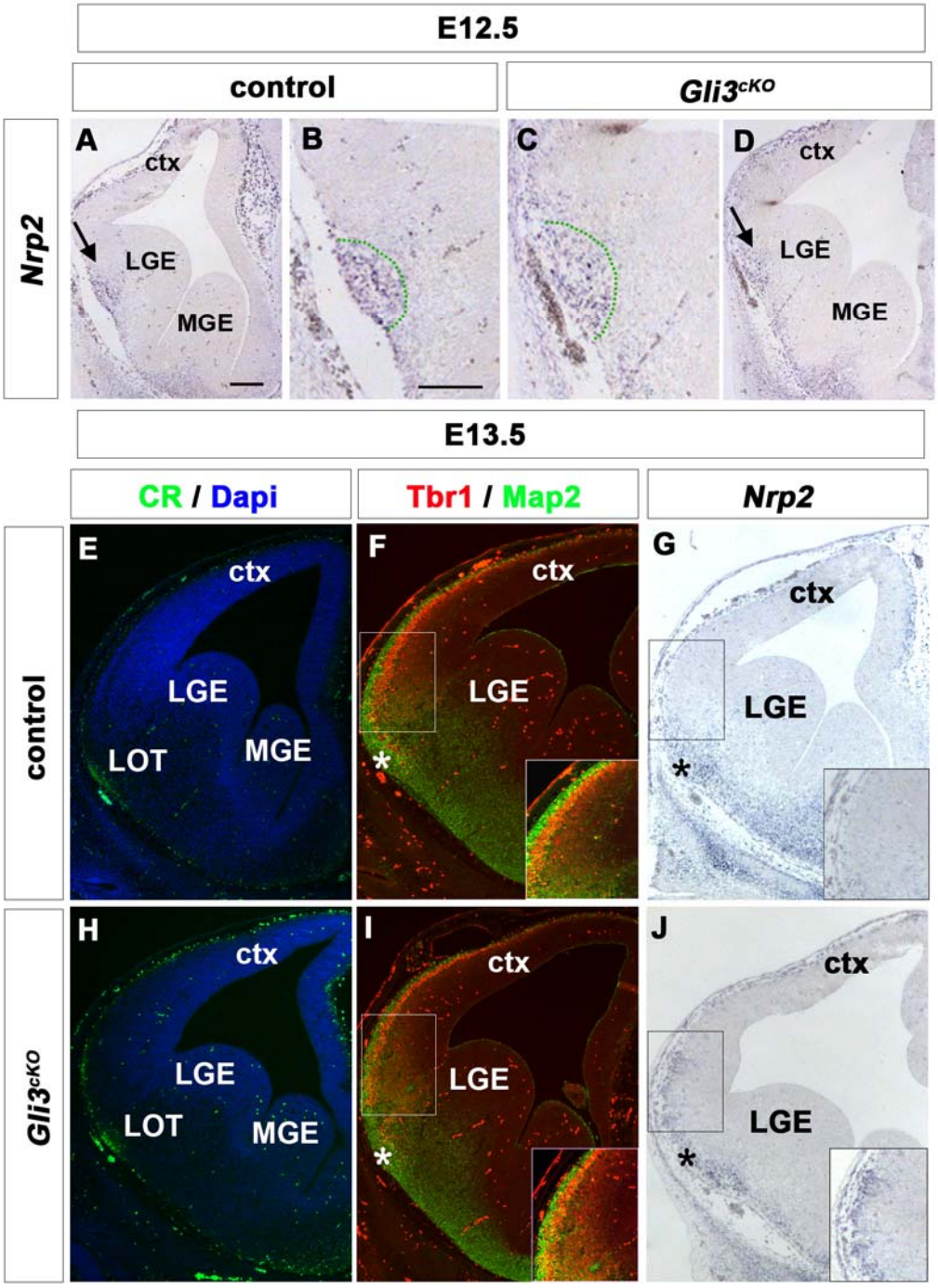
E12.5
control
Gli3cKO
Nrp2
A
ctx
LGE
MGE
B
C
D
ctx
LGE
MGE
E13.5
CR / Dapi
Tbr1 / Map2
Nrp2
control
E
ctx
LGE
LOT
MGE
F
ctx
LGE
*
G
ctx
LGE
*
Gli3cKO
H
ctx
LGE
LOT
MGE
I
ctx
LGE
*
J
ctx
LGE
*

Figure 5-9: The *Nrp2* positive domain is already expanded when mitral cell axons arrive at the LOT position in E13.5 *Gli3*^{cKO} mutants.

(A-B) *Nrp2* is expressed at the presumptive paleocortex (arrow) and has a restricted positive domain in E12.5 control brains (B, green dotted region). (C-D) *Nrp2* positive domain is similar to control brains in E12.5 *Gli3*^{cKO} mutants (D, arrow) and show no obvious defects (C, dotted green domain). (E, H) CR+ mitral cell axons extend to the LOT site in E13.5 control and *Gli3*^{cKO} mutants. (B, E) Tbr1+ neurons are positioned above the MAP2+ cells in control (F, index) and *Gli3*^{cKO} mutant brains (I, index). (G) *Nrp2* expression is restricted to the paleocortex. Note the area above the LOT (*) is *Nrp2* negative (G, index). (J) *Nrp2* expression is expanded medially. The region above the LOT (*) is *Nrp2* positive. Abbreviations: ctx, neocortex; LGE, lateral ganglionic eminence; LOT, lateral olfactory tract; MGE, medial ganglionic eminence. Scale bars: A-J:100μm.

5.7 Discussion

The aim of this chapter was to investigate LOT formation and LOT collaterals colonisation in the *Gli3*^{cKO} conditional mutant. Use of the conditional mutant allowed me to circumvent the severe phenotypes of other *Gli3* mutants. Here, I show that the expanded piriform cortex in *Emx1Cre*;*Gli3*$^{fl/fl}$ embryos (see Chapter 4) is innervated by LOT axons which appear to be also medially shifted with LOT collaterals aberrantly colonising the expanded piriform cortex. Moreover, an OB-like structure was formed in the brain of conditional mutants that consisted of mitral cells but did not protrude from the surface of the telencephalon. No obvious defects were found in the expression of telencephalic guidance cues in E12.5 mutants. Time course analysis confirmed an expansion of the paleocortical primordium from E13.5 onwards, coinciding with the arrival of the LOT axons. Hence, it is possible that the expanded piriform cortex contributed to the medial shift of the LOT.

5.7.1 LOT formation and axonal branching is disorganized in *Gli3*^{cKO} mutants

A combination of cellular and environmental defects have been reported in *Gli3*$^{Xt/Xt}$ and *Gli3*$^{Pdn/Pdn}$ mouse mutants that show severe LOT formation defects varying from lack of LOT to slender LOT formation (Johnson, 1967, Naruse *et al.*, 1990, Naruse and Keino, 1995). In both cases the LOT defects can be explained by defective formation of the OBs (Besse *et al.*, 2011). Moreover, *Gli3*$^{Xt/Xt}$ mutants show severe telencephalic patterning defects that do not allow the evaluation of possible additional roles of *Gli3* regarding LOT formation for example lot guidepost cell clusters (Tomioka *et al.*, 2000). *Emx1Cre;Gli3*$^{fl/fl}$ conditional mutants show milder axon pathfinding defects in comparison to other *Gli3* mutants and their analysis allowed the better understanding of the *Gli3* controlled mechanisms underlying LOT formation. Mitral cells project axons through the LOT pathway to the telencephalon as early as E12.5 and these axons reach the LOT site at E13.5 (Schwob and Price,

1984a, Sugisaki *et al.*, 1996). LOT axons project collateral branches that innervate the olfactory cortex from E15.5 onwards and the piriform cortex first receives olfactory bulb input at E16.5 (Hirata and Fujisawa, 1999). Here, I show that in E18.5 *Gli3*^{cKO} brains the LOT site is present and the mitral cell axons extend collateral branches to the already expanded piriform cortex and other olfactory structures. In P7 *Gli3*^{cKO} brains, the medial expansion of the LOT is prominent. Moreover, axons abnormally branch/extend into the inner piriform cortex layers that are normally populated by dendrites. Thus, in *Gli3*^{cKO} mutants the LOT is formed yet colonization defects are observed especially in postnatal brains. One way to address this issue is to analyze mitral cell specification.

5.7.2 **Mitral cells are specified in *Gli3*^{cKO} mutants**

Various transcription factors have been implicated in mitral cell specification and axon outgrowth. For example, in *Tbr1* null mutants the mitral cells are missing and so is the LOT (Bulfone *et al.*, 1998) and in *Lhx2* null mutants the mitral cells are specified but no LOT axons project to the telencephalon (Saha *et al.*, 2007). Here, I provide evidence that in *Gli3*^{cKO} brains the mitral cells are specified despite the formation of a highly abnormal OB-like structure. In fact, the OB-like primordium occupies a region that resembles its normal position but is not protruding. This result is in contrast to *Gli3*$^{Xt/Xt}$ and *Gli3*$^{Pdn/Pdn}$ mouse mutants where the OB-like structure is ectopically formed in more dorsal regions. Despite the formation of the OB-like structure and to further elucidate and compare these results to the other *Gli3* mutants, further experiments are required to determine the time point that *Gli3* is inactivated in the OB primordium in *Gli3*^{cKO} mutant brains.

Moreover, E18.5 *Gli3*^{cKO} mutant brains have two distinct phenotypes with one forming a mitral cell layer and another forming a cluster of mitral cells at the OB-like structure. The later phenotype is possibly the result of the defective OB-like primordium that was observed earlier in development. Yet, displaced OBs have also been reported in *Pax6* mutants in which LOT projections nevertheless form (Jimenez

et al., 2000). Thus, a lack of the OB protuberance does not by itself explain LOT mislocalization especially since mitral cells are specified and project axons.

5.7.3 Guidance molecules and guidepost cells in *Gli3^{cKO}* mutants

Several telencephalic guidance cues have been implicated in the formation of the LOT and the intracortical connections of the olfactory cortex. Regarding LOT formation these cues involve the lot guidepost cells (Sato *et al.*, 1998, Tomioka *et al.*, 2000) and various guidance molecules with repulsive activity such as *Sema3F* (de Castro *et al.*, 1999) or with attractant activity such as *Sema3B* (de Castro *et al.*, 1999). Here, I provide evidence that in *Gli3^{cKO}* mutant brains lot cells formation and migration to the prospective LOT site is correct however in E14.5 *Gli3^{cKO}* mutant brains, less lot cells are found in deeper layers. Moreover, expression of the *Netrin-1* and *EphrinA5* guidance cues that determine the final position of lot cells (Kawasaki *et al.*, 2006, Nomura *et al.*, 2006) show no obvious defects. In fact, lot cells position was analysed as early as E12.5 before the arrival of the LOT axons and at E14.5 *Gli3^{cKO}* mutant brains. In none of those stages, lot cell clusters were observed as in *Gli3$^{Xt/Xt}$* mutants (Tomioka *et al.*, 2000). In addition the secreted cue *Sema3F* was analysed in *Gli3^{cKO}* mutant brains. In E12.5 mutant brains *Sema3F* expression showed no obvious defects. Strikingly, none of the guidance cues analysed in the *Gli3^{cKO}* mutant brains showed any defects. This result could be explained either because this analysis was performed at an early stage or because these guidance cues do not cause the medial shift of the LOT and the disorganised LOT axon branching. Further experiments are required to address the above possibilities (see Chapter 6).

5.7.4 Medial expansion of the LOT coincides with piriform cortex expansion

The molecular cues that trigger the formation of the LOT axon collaterals and their extension toward the olfactory cortex target are largely unknown. Guidance cues expressed at the piriform cortex have been reported to enhance axonal branching. For example Anosmin-1 is reported to have a chemoattractant activity towards mitral cell axons *in vitro* and axon branches *in vivo* (Soussi-Yanicostas *et al.*, 2002).

In this study, mitral cell axons project normally to the telencephalon of E13.5 *Gli3*^{cKO} brains. At this stage LOT axons encounter an already medially expanded paleocortex. Strikingly, the expanded piriform cortex expresses *Sema5B* in *Gli3*^{cKO} mutant brains from this early developmental stage (Chapter 4). Sema5A/5B constitute one class of membrane spanning Semaphorin proteins whose signal is modulated by proteoglycans through an unidentified receptor (Bagnard *et al.*, 1998, Kantor *et al.*, 2004). Specifically, Sema5A acts as an attractant for axons expressing heparin sulphate proteoglycans and as repellents for axons expressing chondroitin sulphate proteoglycans (Kantor *et al.*, 2004). Although the role of proteoglycans in *Sema5B* activity is not known, *Sema5B* has recently been described to act as a repellent towards corticofugal axons but not thalamic axons (Lett *et al.*, 2009). Moreover, *Sema5A/5B* has been reported to have a key role in establishing synaptic connectivity during postnatal retinal development with loss of *Sema5A/5B* causing the aberrant innervation of retinal layers by neurites (Matsuoka *et al.*, 2011). This supports the idea that the expanded expression of *Sema5B* in *Gli3*^{cKO} mutant brains (see Chapter 4) could lead to the disorganised LOT axon branching through aberrant activity. However, additional experiments will need to be conducted to verify this hypothesis (see Chapter 6).

Finally, the medial expansion of the LOT coincides with the already discussed piriform cortex expansion into the lateral neocortical region (see Chapter 4). So far, only conditional inactivation of *Lhx2* -a LIM homeodomain transcription factor- in the dorsal telencephalon results in the formation of an ectopic piriform cortex that

shows connectivity to the olfactory bulbs (OB) (Chou *et al.*, 2009). This is in direct contrast to *Lhx2* null mutants in which mitral cells are specified but cannot project axons and lot guidepost cells form clusters at the dorsal telencephalon (Saha *et al.*, 2007). The formation of lot cell clusters resembles the phenotype observed in $Gli3^{Xt/Xt}$ mutants. These findings together with the fact that *Lhx2* expression is down-regulated in the lateral neocortex of $Gli3^{cKO}$ brains (see Chapter 4) could suggest a direct or indirect role of *Gli3* in regulating *Lhx2* expression and hence piriform cortex and LOT formation.

5.8 Summary

In this chapter, I have extensively examined LOT formation and axon branching to the olfactory cortex and especially to the piriform cortex. Briefly, in $Gli3^{cKO}$ mutant brains I showed a medial shift of the LOT site and the aberrant projection of LOT collaterals in postnatal conditional mutant brains with the early expansion of piriform cortex presenting a possible explanation to the aberrant target invasion of LOT axons. These results support and extend previous findings on the central role of *Gli3* for axon tract formation and especially LOT development. My results from the $Gli3^{cKO}$ mutants provide a basis to identify genes expressed at the piriform cortex that guide LOT axons and based on that enhance our current knowledge regarding axon branching.

6 Final discussion and future work

The work presented in this thesis encompasses a descriptive analysis of the formation of the major axon tracts in the telencephalon of *Gli3* conditional mutant mice and a functional investigation into *Gli3's* role in axon pathfinding. Different experimental approaches were combined to dissect the axon pathfinding defects in the mutants and the mechanisms underlying this defective development. The use of *Gli3* conditional mutant mice provided the advantage that the severe regionalisation defects observed in other *Gli3* mutants were not present, allowing us to further our understanding of the link between patterning and axon pathfinding. Here, I discuss the results presented in each chapter and propose future experiments.

6.1 Further analysis of the regulatory role of *Gli3* in development of the corpus callosum

6.1.1 Brief summary of chapter three

During CC development, a number of strategically located glial and neuronal guidepost structures guide callosal axons across the midline at the corticoseptal boundary (CSB). Correct positioning of these guideposts requires the normal activity of *Gli3* and *Gli3* mutations result in callosal defects in humans and mice. *Gli3* is widely expressed during critical stages of forebrain development but the precise temporal and spatial requirements for *Gli3* function in callosal development remained unclear. Here, I used a conditional mouse mutant approach to inactivate *Gli3* in specific regions of the developing telencephalon in order to delineate the domain(s) in which *Gli3* is required for normal development of the corpus callosum. Inactivation of *Gli3* in the septum or in the medial ganglionic eminence had no effect on CC formation, however inactivating *Gli3* in the developing cerebral cortex led to the formation of a severely hypoplastic CC at E18.5 due to a severe disorganization of midline guideposts. Glial wedge cells translocate prematurely and *Slit1/2* are ectopically expressed in the septum. These changes coincide with altered Fgf and

Wnt/β-catenin signalling during CSB formation. Collectively, these data demonstrate a crucial role for *Gli3* in cortical progenitors to control CC formation and indicate how defects in CSB formation affect the positioning of callosal guidepost cells.

6.1.2 **Future directions**

One of the key findings presented in Chapter three was that *Gli3* deletion in the medial ganglionic eminence (MGE) and hence, the MGE derived interneurons, caused no obvious callosal defects. My *in situ* hybridisation analysis confirmed that *Gli3* mRNA expression was lost from the MGE by E12.5, indicating that *Gli3* inactivation occurred at the time of CSB formation. Moreover, lineage-tracing for MGE derived GABAergic neurons of the subcallosal sling, which delineate the crossing of callosal axons, revealed normal migration and positioning of GFP+ cells at the CSB. Only recently, Niquille et al. 2013 demonstrated that GABAergic neurons of the subcallosal sling also originate from the caudal ganglionic eminence (Niquille *et al.*, 2013). *Gli3* is expressed by the progenitors of the caudal ganglionic eminence but none of the conditional mutants used in this study affected its expression there. These data demonstrate that although *Nkx2.1Cre*;*Gli3*$^{fl/fl}$ conditional mutants show specific inactivation, formation of the midline structures at the CSB is correct. This could be caused due to a "rescue" by caudal ganglionic eminence derived interneurons. One way to address the above possibility would be to inactivate *Gli3* in the progenitors of both MGE and CGE domains that will give rise to GABAergic neurons. The formation of the CC and callosal sling populations could then be examined. This type of experiment will require the use of Cre driver line in which the promoter would be expressed in ventricular zone cells of the ventral telencephalon. One possible Cre line to address the above question is the Dlx5/6 mouse line (Kohwi *et al.*, 2007) since *Dlx5* and *Dlx6* genes provide attractive means for the identification of precursors (i.e., immature but postmitotic cells) destined to give rise to interneurons. However, inactivation in postmitotic cells might be a late stage to observe any defects since *Gli3* is expressed in progenitors.

Moreover, my findings provided some insights into the temporal requirements of *Gli3* expression in CC development. I performed extensive time course analysis for *Gli3* mRNA and Western blot analysis for Gli3 protein to ensure the specificity of the inactivation. In *Emx1Cre*;*Gli3*$^{fl/fl}$ conditional mutants *Gli3* was initially deleted from the medial cortex and progressively from more lateral cortical regions. *Gli3* inactivation was complete by E12.5 and Gli3 protein was also absent at this age, which caused the formation of a hypoplastic CC due to a severe disorganization of midline guideposts. In *NestinCre*;*Gli3*$^{fl/fl}$ embryos in which *Gli3* is inactivated after patterning is completed (E14.5) a hypoplastic CC also formed, though in this case, the hypoplasia was due to apoptosis of callosal projection neurons (Wang *et al.*, 2011). Although CC formation was well characterised in this study, *Gli3* inactivation was not extensively analysed and data are only provided from E14.5 brains. A combined analysis of these conditional mutants regarding the time points of *Gli3* inactivation will provide an in depth knowledge of the temporal requirements of *Gli3* for CC formation.

Alternatively, to identify a critical period for *Gli3* function before E10.5, the *CAGG;Cre-ER* mouse line (Hayashi and McMahon, 2002) could be analysed in which the *Cre–ER* fusion protein activity can be regulated by administrating tamoxifen. Tamoxifen could be administered at early stages in development. Preliminary analysis of mouse brains after administering tamoxifen at E8.5 showed a phenotype similar to *Gli3*$^{Xt/Xt}$ mutants with severe patterning defects rendering it impossible to study CC development (unpublished data T Theil). To circumvent the above mentioned defects tamoxifen could be administered a day later at E9.5. Yet, it is conceivable that the CC phenotype resulting from this administration would be similar to the *Gli3*^{cKO} conditional mutants I used in this thesis. Therefore, although a crucial requirement of *Gli3* early in development is clear the combined analysis of the *Gli3*^{cKO} and *NestinCre*;*Gli3*$^{fl/fl}$ conditional mutants might be sufficient for identifying a critical period for the identification of *Gli3* target genes implicated in CC development during patterning.

Lastly, the findings in this chapter combined with the previous analyses in Gli3$^{Pdn/Pdn}$ mutants reveal a role for Gli3 in the development of the corpus callosum as part of a

gene network. My findings demonstrate cellular and molecular defects in guidance cues that normally control CC formation. These defects originate during patterning stages and, in combination, cause the CC malformation. *Gli3* deletion causes an up-regulation of *Fgf8* expression and of Fgf signalling in the septal midline during patterning stages (Amaniti *et al.*, 2013). In turn, up-regulation of Fgf signalling was shown to control *Slit2* expression and formation of radial glial cell clusters (Magnani *et al.*, 2012a). Ultimately, the ectopic chemorepellent activity of *Slit1/2* in the septal midline and ectopic GFAP+ fibres at the CSB form a temporal boundary to callosal axons (Amaniti *et al.*, 2013). Thus, *Gli3* is positioned in the centre of a complex network that regulates the position of midline guidance cues at the CSB and hence, *Gli3* controls the formation of the corpus callosum. In fact, an important question that has not yet being addressed is the molecular mechanisms by which Gli3 controls the formation of the CC through this network. How *Gli3* regulates this network and whether *Gli3*'s effect on this network is direct or indirect also remains to be elucidated. Therefore, the most important open question will be to aim at identifying genes regulated by *Gli3* and comprehend the network involving *Gli3*, *Fgf8* and *Wnt* genes. To that end, it is necessary to identify the genes, transcription factors or signalling molecules regulated by *Gli3*. One way to address this question is to initially perform microarray analysis and investigate the changes in gene expression. To investigate further which genes *Gli3* regulates directly or indirectly further experiments need to be performed such as ChIP analysis to identify genes bound by Gli3 protein. Finally, *in vivo* transgenic reporter assays will further elucidate the functionality of these sites. Such analyses would further determine the direct role of *Gli3* in CC development and provide a better insight on the defects in GLI3 syndrome patients.

6.2 Further analysis of the regulatory role of *Gli3* in corticothalamic/thalamocortical tract formation

6.2.1 Brief summary of chapter four

The corticothalamic and thalamocortical tracts play essential roles in the communication between the cortex and thalamus. During development, the axons that form these tracts have to follow a complex path to reach their target areas. While much attention has been paid to the mechanisms regulating their passage through the ventral telencephalon, very little is known about how the developing cortex contributes to corticothalamic/thalamocortical tract formation. *Gli3* has important roles in corticothalamic and thalamocortical pathfinding. Here, I conditionally inactivated *Gli3* in dorsal telencephalic progenitors to determine its role in corticothalamic tract formation. In *Emx1Cre;Gli3*$^{fl/fl}$ mutants, only a few corticothalamic axons entered the striatum, in a restricted dorsal domain. This restricted entry correlated with a medial expansion of the piriform cortex. Transplantation experiments showed that the expanded piriform cortex repelled corticofugal axons. Moreover, expression of *Sema5B*, a chemorepellent for corticofugal axons produced by the piriform cortex, was similarly expanded. Finally, time course analysis revealed an expansion of the ventral pallial progenitor domain which gives rise to the piriform cortex. Hence, control of lateral cortical development by *Gli3* at the progenitor level is crucial for corticothalamic pathfinding.

6.2.2 Future directions

One of the key findings presented in Chapter 4 was a mechanism by which the piriform cortex may regulate the size of the CTA entry zone into the ventral telencephalon, at least in part by controlling *Sema5B* expression. The piriform cortex is repulsive to the growth of corticofugal axons as shown by transplantation assays. This analysis also revealed that growth of CTAs is restored in *Gli3*^{cKO} embryos after

replacing the mutant expanded piriform cortex with control lateral cortex. However, under these conditions, CTAs project along the PSPB similar to the situation in *Gli3*^{cKO} mutants, suggesting that there may be additional cell-autonomous defects in cortical projection neurons. Further experiments are needed to assess the molecular basis of such a cell-autonomous effect. Analysis of various transcription factors such as Tbr1, Ctip2 and Sox5 revealed the formation of corticofugal neurons in the correct layer while analysis of the expression of Robo1 receptor showed no obvious defects (Hevner *et al.*, 2001, Arlotta *et al.*, 2005, Lopez-Bendito *et al.*, 2007, Kwan *et al.*, 2008, Lai *et al.*, 2008). In the absence of *Ctip2* and *Tbr1* subcerebral projection neurons exhibit defects in fasciculation, out-growth, pathfinding and migration, respectively (Hevner *et al.*, 2001, Arlotta *et al.*, 2005) while, *Sox5* regulates migration and identity of deep-layer neurons (Kwan *et al.*, 2008, Lai *et al.*, 2008). Although the previous analysis pointed towards non-cell autonomous defects, further support to this argument can be provided by a cortical transplantation assay. In order to address the question whether CTA pathfinding defects are caused by cell autonomous defects of corticofugal neurons, cortical tissue from a conditional mutant section could be homotopically transplanted into a control section (as described in chapter 4). In contrast, the reverse experiment - transplanting control cortical tissue into a mutant section - will address environmental defects (as described in chapter 4). This experiment will provide a solid basis for identifying *Gli3*'s role in CTAs pathfinding.

Nevertheless, *Sema5B* expression is expanded and has known repulsive activity towards the CTAs (Lett *et al.*, 2009). Although, the chemorepellent activity of *Sema5B* is known, the Sema5B receptor(s) remain unknown. For the Sema5B homologue, Sema5A, it has previously been shown that while plexinB3 has been shown to function as a receptor for Sema5A in heterologous cells (Artigiani *et al.*, 2004), an alternative, unknown receptor appears to function in neurons (Kantor *et al.*, 2004). Whether Sema5B has also multiple receptors in different cells is unknown but identification of the later could provide a potential additional cause of the defects I observed. The challenging task of identifying the Sema5B receptor is further complicated by the fact that the Sema5 proteins interact with proteoglycans. In fact,

Sema5A and Sema5B are transmembrane proteins which have been shown to bind to heparin and chondroitin sulfate proteoglycans (Kantor *et al.*, 2004) and act as permissive or inhibitory cue to axon outgrowth depending on these local matrix proteoglycans (Kantor *et al.*, 2004). Overall, identifying the Sema5s receptor will help us understand how Sema5B regulates axon pathfinding and hence, CTA tract formation. It is also conceivable that other guidance molecules produced by the piriform cortex contribute to its ability to repel CTAs in combination with Sema5B or separately. To date, other guidance molecules with that type of activity in the piriform cortex are not known and screening experiments could be conducted to identify such factors.

Lastly, although the piriform cortex arises at the lateral extreme of the dorsal telencephalon, there has been very little progress in understanding its specification and its separation from the adjacent neocortex. My findings of an expansion of the piriform cortex in $Gli3^{cKO}$ embryos and the molecular analyses conducted might shed some light on these issues. An expansion of the piriform cortex has previously been observed in $Gli3^{Xt/Xt}$ null mutants and in the *Gli3* compound mutant $Gli3^{Xt/Pdn}$ (Vyas *et al.*, 2003, Magnani *et al.*, 2012b). These findings further emphasize *Gli3*'s importance in the development of the piriform cortex but the molecular mechanisms underlying this control were not investigated. My analyses revealed a moderate medial expansion of the *Sfrp2* and *TGF*α expression domains and a striking up-regulation of *Dbx1* was observed throughout the cortical germinal layer in $Gli3^{cKO}$ mutants (as discussed in Chapter 4). These findings are therefore consistent with the idea that progenitors of the lateral most neocortex but not those of more medial neocortex have been transformed to a ventral pallium fate. As the Gli3 repressor form predominates in the developing cortex, it is conceivable *Gli3* could regulate ventral pallium expression indirectly by controlling the expression of *Lhx2* and *Dmrt5* (as discussed in chapter 4). The down-regulation of both factors specifically in the lateral cortex of $Gli3^{cKO}$ mutants provides an explanation for the expansion of the piriform cortex in these animals. Therefore, my findings place *Gli3* upstream of these transcription factors and imply a key role for *Gli3* in controlling the relative size of neocortex and piriform cortex.

Future studies should aim to identify the mechanism(s) by which *Gli3* controls this process at the molecular level. Forming the different boundaries between regions involves cell-cell interactions and the establishment of gene expression patterns. These boundaries form at the progenitor level and in fact this is the time point when *Gli3* is actually expressed. Thus, a well-used experiment to address the above aim will be to perform microarray analysis to identify differentially expressed genes at the progenitor level. Since the pallium-subpallium boundary is not morphologically discernible between E10.5 and E12.5 for identical tissue dissection, the experiment could be performed by mating the $Gli3^{cKO}$ conditional mutants with the ROSA26-EGFP reporter (see chapter 5) to label cortical tissue. This analysis combined with bioinformatic and gene expression analyses will further elucidate *Gli3* regulated genes in the pallium.

6.3 Further analysis of the role of the piriform cortex in the lateral olfactory tract formation

6.3.1 Brief summary of chapter five

Lateral olfactory tract formation and the specificity of cortical innervation is a fundamental step to allow the transmission of olfactory information. Several guidance molecules and transcription factors including *Gli3* regulate different aspects of LOT formation. Severe defects in both intrinsic and environmental cues in the *Gli3* null and hypomorphic mutants severely complicate the analysis of the role of *Gli3* in lateral olfactory tract formation. I made use of a conditional mutant which shows milder axon pathfinding defects in comparison to other *Gli3* mutants with the aim to investigate the role of *Gli3* in LOT formation and colonisation of the olfactory cortex. I found that the expanded piriform cortex in $Gli3^{cKO}$ embryos is innervated by LOT axons, which also appear to be expanded medially, with LOT collaterals colonising the expanded piriform cortex. Moreover, an OB-like structure that consisted of mitral cells but did not protrude from the surface of the telencephalon was formed in the brain of conditional mutants. No obvious defects were found in the expression of telencephalic guidance cues in E12.5 mutants. Time course analysis confirmed an expansion of the paleocortical primordium from E13.5 onwards, coinciding with the arrival of the LOT axons. Hence, it is possible that the expanded piriform cortex contributed to the medial expansion of the LOT.

6.3.2 Future directions

In order to extend the characterization of LOT formation in *Gli3* mutants and to further investigate the role of the piriform cortex, a more detailed analysis into the effects of the expansion of the piriform cortex on LOT formation needs to be carried out. The data presented in Chapter 5 demonstrate a potential role for the piriform

cortex in LOT formation, suggesting that the expanded piriform cortex could contribute to aberrant colonization by LOT collaterals. It is also conceivable that intrinsic mitral cell defects might contribute to the above phenotype. However, LOT axons do extend arguing against this hypothesis. To distinguish between cell intrinsic and environmental effects from the telencephalon, an *in vitro* explant culture presents an excellent tool. Several studies have reported the role of different transcription factors in LOT formation using transplantation experiments. Most notably, the study by Saha *et al.*, 2007 that analyzed the role of *Lhx2* in LOT formation and proposed an *Lhx2* dual role in both the OB as well as in the telencephalon (Saha *et al.*, 2007) provided a paradigm how to dissect the roles of transcription factors in LOT formation. In this study, an *in vitro* explant culture experiment determined whether the projection neurons are capable of forming an LOT. Although there is no defect in LOT axon formation in $Gli3^{cKO}$ mutants, I propose using this technique to test for the environmental nature of the defects. In particular, mutant olfactory bulb like structure (OBLS) explants will be juxtaposed to wild-type lateral telencephalic preparations, and wild-type OB explants will be juxtaposed to mutant lateral telencephalic recipient explants. The outcome will provide solid information on the nature of the LOT defects observed in $Gli3^{cKO}$ mutants.

Moreover, none of the guidance cues analysed in the $Gli3^{cKO}$ mutant brains showed any defects. This result was not unexpected since the LOT axons reach the telencephalon in $Gli3^{cKO}$ mutants without showing pathfinding defects but aberrant colonisation of the expanded piriform cortex. Yet, the expanded piriform cortex remains their normal target region. This result could be explained either because this analysis was performed at an early stage (E12.5) or because these guidance cues do not cause the expansion of the LOT or the disorganised LOT axon branching. To test the first possibility, the expression of the guidance molecules analysed in chapter 5 i.e. *Sema3F*, *Netrin1* and *EphrinA5* should be further analysed at different time points.

In addition, another guidance molecule, Anosmin-1, has recently been identified which promotes the outgrowth of and attracts OB axons (Soussi-Yanicostas *et al.*, 2002). Anosmin-1 is expressed in the piriform cortex and attracts the collateral

branches of OB axons *in vivo*. Thus, the expression of Anosmin-1 should be studied in future experiments as it represents a good candidate for the LOT defects I observed. Future studies should aim to analyse other candidates such as the EphA and EphB receptors and their ligands. EphA and EphB receptors have been known for mediating the projections of retinal ganglion cells to the optic tectum or the superior colliculus and control the formation of branches along the termination zones. For example, topographic branch formation and arborization is inhibited by EphrinAs along retinal ganglion cell axons posteriorly to the termination zones (Yates *et al.*, 2001). A detailed analysis of EphA and EphB receptors and their ligands expression will determine whether they are expressed in our region of interest i.e. olfactory bulb and piriform cortex and will potentially unravel new cues that contribute to the expanded innervation of the piriform cortex by LOT.

A crucial defect observed in the telencephalon of $Gli3^{cKO}$ mutants is the expansion of the piriform cortex and the concomitant expansion of *Sema5B* expression. As previously described, *Sema5B* is necessary for repulsion of cortical axons (Lett *et al.*, 2009) and is also expressed in the olfactory bulb (Lett *et al.*, 2009). However, the type of cells expressing *Sema5B* in the OB remains to be further described and identifying these cells in $Gli3^{cKO}$ mutants is fundamental in order to address a potential role of *Sema5B* in axon branching. It has been reported that Sema5A/B knock-out mice show defects in retinal ganglion cells that lead to neurite mistargeting (Matsuoka *et al.*, 2011). Also, Sema5B is a transmembrane protein that, in addition to the typically inhibitory sema domain, possesses seven thrombospondin repeats (Adams *et al.*, 1996). This is intriguing as thrombospondins are permissive for axon outgrowth and enhance synaptogenesis, suggesting a bifunctional role for Sema5B (Christopherson *et al.*, 2005). Since LOT collaterals aberrantly colonise the piriform cortex in $Gli3^{cKO}$ mutants, this raises the possibility that *Sema5B* has a previously undescribed effect on LOT axon guidance and collateral colonisation, as the one described in retinal ganglion cells. One way to address this question would be to perform culture OB explants from an early stage of LOT development (E13.5) in the presence of *Sema5B*-expressing or control cells. Further, organotypic slice cultures could be used to determine whether *Sema5B* can perturb the pathfinding of

LOT axons and/or enhance the formation of collaterals in their normal environment. One way to do that will be to place Sema5B-expressing or control cells directly on slices along the pathway normally established by LOT axons in the telencephalon. It is also crucial to determine what the in vivo role of *Sema5B* is. Thus, I propose to use the *Sema5B* knock out mutant or a knock down of Sema5B with short hairpin RNA (shRNA) vectors as recently described in Lett *et al*., 2009 in order to elucidate its role in LOT formation. The use of shRNA will cause a much more restricted phenotype if any, with the advantage being the generation of a mosaic environment with cells expressing normal *Sema5B* expression levels next to cells with reduced levels. The use of the *Sema5B* knock out mutant would be equally informative as it can be used for "rescue" experiments after mating the later animals with $Gli3^{cKO}$ mutants. These experiments would offer additional insight into the role of *Sema5B* in axon guidance and provide a better understanding of LOT tract formation.

While this data will provide a valuable data set for the interpretation of the defects, a much more thorough investigation should be conducted regarding the inactivation of *Gli3* in the OB. In chapter 5, the use of the *RCE* mouse line suggested that *Gli3* is inactivated in the OB-like structure. As an extension of the work presented here, I propose using *in situ* hybridisation analysis to determine the *Gli3* mRNA expression at various developmental stages from E11.5-E14.5. This analysis would provide a better understanding of the temporal requirements of *Gli3* during OB formation.

6.4 Synopsis

The main focus of this thesis was on the development of three major axon tracts including the corpus callosum, the corticothalamic/thalamocortical tract and the lateral olfactory tract. Axon tract development is under the control of genes and in this thesis I focused on analysing axon pathfinding in *Gli3* conditional mutants. The corpus callosum and the corticothalamic/thalamocortical tract showed severe pathfinding defects, while the lateral olfactory tract axons and their branches reached the telencephalon but aberrantly colonised the expanded piriform cortex. Although,

no strong conclusions can be drawn regarding the LOT axons and further experiments are required (see 6.1.3), the observed corpus callosum and corticothalamic/thalamocortical pathfinding defects offer the opportunity to study and compare axon pathfinding in different regions of the brain in the same mutant.

What is striking for both axon tracts in *Gli3*^{cKO} mutants is that the aberrant pathfinding is highly likely caused by patterning defects that gave rise to environmental defects and hence, providing a unified picture of *Gli3* function. Regarding the CC my findings demonstrated a crucial role for *Gli3* in the dorsal telencephalon to control corpus callosum formation and indicated that defects in the formation of the CSB affect the positioning of callosal guidepost cells. These defects coincide with altered Fgf and Wnt/β-catenin signalling during CSB formation and ectopic *Slit2* expression in the septum as early as E14.5. Moreover, conditional inactivation of *Gli3* in dorsal telencephalic progenitors led to few corticothalamic axons leaving the cortex in a restricted lateral neocortical domain. This restricted entry is at least partially caused by an expansion of the piriform cortex which forms from an enlarged progenitor domain of the ventral pallium and an expanded *Sema5B* expression. The most obvious link between these two phenotypes is an early defect in patterning caused by the loss of *Gli3* in the dorsal telencephalon, which as a transcription factor can control different genetic programs depending on its site and time of expression.

Thus, an important question in the field of axon tract formation still remains. How can a transcription factor like *Gli3*, which is solely expressed in the progenitors, cause axon pathfinding defects at later stages of development? In this context it is useful to mention that a gene is not a protein. The level, timing and position of the protein expression are also critical. For example, *Engrailed* transcription factors are known for regulating the expression of guidance cues that pattern retinal axon terminals in the dorsal midbrain. *Engrailed1/2* is believed to induct EphrinAs that repel axon growth in a concentration-dependent manner (Brunet *et al.*, 2005) while Engrailed is also influencing the behaviour of axons directly (Wizenmann *et al.*, 2009). What is more, in *Drosophila*, once cells form, interactions take place between

the cells mediated by the segment polarity genes including *Engrailed* and proteins that are constituents of the Wingless and Hedgehog signal transduction pathways. The diffusion of these proteins is thought to provide the gradients by which the cells acquire their identities. It is then possible that other transcription factors such as *Gli3* act in a similar multifunctional way.

Another possibility is that a transcription factor controls the formation and positioning of guidance cues at patterning stages as shown in this thesis. For example, *Gli3* deletion causes an up-regulation of *Fgf8* expression and Fgf signalling in the septal midline during patterning stages. In return, up-regulation of Fgf signalling is demonstrated to control *Slit2* expression and cluster formation of radial glial cells. Ultimately, the ectopic chemorepellent activity of *Slit1/2* in the septal midline and ectopic GFAP+ fibres at the CSB form a temporal boundary to callosal axons. Or *Gli3* deletion is possibly causing a down-regulation of *Dmrt5* and/or *Lhx2,* which in turn cause the expansion of the ventral pallium markers. In both tracts, whether this cascade of events is directly or indirectly controlled by *Gli3* is not known. Nevertheless, this highlights fundamental differences in the ways different regions exploit different genes.

Studies from other transcription factors reinforce the idea that a transcription factor expressed at a progenitor level can potentially control axon pathfinding. For example, it is known that Pax6 is critically important for the establishment of the PSPB while also levels of Pax6 expression are critically important for cortical progenitor proliferation (Stoykova *et al.*, 1996, Stoykova *et al.*, 2000, Manuel *et al.*, 2007, Georgala *et al.*, 2011). Moreover, *Pax6*$^{-/-}$ mutants show axon guidance defects which different studies have shown to be the cause of either the role of Pax6 in projecting cells (Pratt *et al.*, 2000) or in the ventral telencephalic environment (Simpson *et al.*, 2009). However, which target genes Pax6 regulates to control the formation of axon tracts and if these genes are the same for different tracts remains to be elucidated.

At present, too little is known about the targets of *Gli3*. Further work is needed to discover targets of *Gli3* are and whether and how they change during development.

In this respect, my work will form the basis for the future identification of Gli3 target genes as it helped to identify the spatial requirements for *Gli3* function in axon tract development. A greater knowledge of the primary gene targets of *Gli3* and an understanding of how its downstream networks are regulated will help to understand how a transcription factor controls axon pathfinding at a molecular level

6.5 Concluding remarks

The development of highly complex structures such as the brain relies on the precisely coordinated activity of different signalling pathways and transcription factors. Axon tracts convey information between the different brain regions rendering their correct formation crucial. While a number of transcription factors have been implicated in axon pathfinding, the role of *Gli3* has not yet been fully elucidated. Importantly, previous studies taken together with my findings suggest a key role for *Gli3* during patterning stages for axon pathfinding. Based on these observations, there is a link between a role for *Gli3* in patterning and corpus callosum and corticothalamic/thalamocortical. Thus, I investigated this link for these by utilising *Gli3* conditional mutants. Here, I provide evidence for a *Gli3* specific requirement in *Emx*1+ progenitor cells but not in the septum or in the medial ganglionic eminence for callosal development. Also, I have extensively presented the *Gli3* controlled defects that highly likely result in the CTAs phenotype in $Gli3^{cKO}$ mutants and proposed that an expansion of the piriform cortex contributes to the corticothalamic pathfinding defects in $Gli3^{cKO}$ conditional mutants. Finally, I have extensively examined LOT formation and axon branching to the olfactory cortex and especially to the piriform cortex and suggested the expanded expression of *Sema5B* in $Gli3^{cKO}$ mutant brains could lead to the disorganised LOT axon branching through an unknown mechanism. While these analyses provide valuable insight into the cellular processes, it is crucial to extend these findings by understanding the *Gli3* controlled molecular mechanisms for axon pathfinding and reveal how alteration of its expression contributes to connectivity defects.

Bibliography

Aboitiz, F. & Montiel, J. 2003. One hundred million years of interhemispheric communication: the history of the corpus callosum. *Brazilian journal of medical and biological research = Revista brasileira de pesquisas medicas e biologicas / Sociedade Brasileira de Biofisica ... [et al.],* 36**,** 409-420.

Adams, R. H., Betz, H. & Puschel, A. W. 1996. A novel class of murine semaphorins with homology to thrombospondin is differentially expressed during early embryogenesis. *Mech Dev,* 57**,** 33-45.

Alcamo, E. A., Chirivella, L., Dautzenberg, M., Dobreva, G., Farinas, I., Grosschedl, R. & Mcconnell, S. K. 2008. Satb2 regulates callosal projection neuron identity in the developing cerebral cortex. *Neuron,* 57**,** 364-77.

Allendoerfer, K. L. & Shatz, C. J. 1994. The subplate, a transient neocortical structure: its role in the development of connections between thalamus and cortex. *Annu Rev Neurosci,* 17**,** 185-218.

Amaniti, E. M., Hasenpusch-Theil, K., Li, Z., Magnani, D., Kessaris, N., Mason, J. O. & Theil, T. 2013. Gli3 is required in Emx1+ progenitors for the development of the corpus callosum. *Developmental Biology,* 376**,** 113-24.

Anderson, J. S., Druzgal, T. J., Froehlich, A., Dubray, M. B., Lange, N., Alexander, A. L., Abildskov, T., Nielsen, J. A., Cariello, A. N., Cooperrider, J. R., Bigler, E. D. & Lainhart, J. E. 2011. Decreased interhemispheric functional connectivity in autism. *Cereb Cortex,* 21**,** 1134-46.

Anderson, S. A., Kaznowski, C. E., Horn, C., Rubenstein, J. L. & Mcconnell, S. K. 2002. Distinct origins of neocortical projection neurons and interneurons in vivo. *Cereb Cortex,* 12**,** 702-9.

Andrews, W., Liapi, A., Plachez, C., Camurri, L., Zhang, J., Mori, S., Murakami, F., Parnavelas, J. G., Sundaresan, V. & Richards, L. J. 2006. Robo1 regulates the development of major axon tracts and interneuron migration in the forebrain. *Development (Cambridge, England),* 133**,** 2243-2252.

Angevine, J. B., Jr. & Sidman, R. L. 1961. Autoradiographic study of cell migration during histogenesis of cerebral cortex in the mouse. *Nature,* 192**,** 766-8.

Aoto, K., Nishimura, T., Eto, K. & Motoyama, J. 2002. Mouse GLI3 regulates Fgf8 expression and apoptosis in the developing neural tube, face, and limb bud. *Developmental biology,* 251**,** 320-332.

Ariani, F., Hayek, G., Rondinella, D., Artuso, R., Mencarelli, M. A., Spanhol-Rosseto, A., Pollazzon, M., Buoni, S., Spiga, O., Ricciardi, S., Meloni, I., Longo, I., Mari, F., Broccoli, V., Zappella, M. & Renieri, A. 2008. FOXG1 is responsible for the congenital variant of Rett syndrome. *Am J Hum Genet,* 83**,** 89-93.

Aribandi, M. 2011. *Imaging in Agenesis of the Corpus Callosum* [Online]. [Accessed].

Ariens-Kapers, C., Huber, G. & Crosby, E. 1936. *The comparative anatomy of the nervous system of the vertebrates including man,* New York, Macmillan.

Arlotta, P., Molyneaux, B. J., Chen, J., Inoue, J., Kominami, R. & Macklis, J. D. 2005. Neuronal subtype-specific genes that control corticospinal motor neuron development in vivo. *Neuron,* 45**,** 207-221.

Artigiani, S., Conrotto, P., Fazzari, P., Gilestro, G. F., Barberis, D., Giordano, S., Comoglio, P. M. & Tamagnone, L. 2004. Plexin-B3 is a functional receptor for semaphorin 5A. *EMBO Rep,* 5**,** 710-4.

Assimacopoulos, S., Grove, E. A. & Ragsdale, C. W. 2003. Identification of a Pax6-dependent epidermal growth factor family signaling source at the lateral edge of the embryonic cerebral cortex. *J Neurosci,* 23**,** 6399-403.

Auladell, C., Perez-Sust, P., Super, H. & Soriano, E. 2000. The early development of thalamocortical and corticothalamic projections in the mouse. *Anat Embryol (Berl),* 201**,** 169-79.

Bagnard, D., Chounlamountri, N., Puschel, A. W. & Bolz, J. 2001. Axonal surface molecules act in combination with semaphorin 3a during the establishment of corticothalamic projections. *Cereb Cortex,* 11**,** 278-85.

Bagnard, D., Lohrum, M., Uzeil, D., Puschel, A. W. & Bolz, J. 1998. Semaphorins act as attractive and repulsive guidance signals during the development of cortical projections. *Development,* 125**,** 5043-5053.

Bagnard, D., Thomasset, N., Lohrum, M., Puschel, A. W. & Bolz, J. 2000. Spatial distributions of guidance molecules regulate chemorepulsion and chemoattraction of growth cones. *J Neurosci,* 20**,** 1030-5.

Bagri, A., Marin, O., Plump, A. S., Mak, J., Pleasure, S. J., Rubenstein, J. L. & Tessier-Lavigne, M. 2002. Slit proteins prevent midline crossing and determine the dorsoventral position of major axonal pathways in the mammalian forebrain. *Neuron,* 33**,** 233-48.

Bai, C. B., Stephen, D. & Joyner, A. L. 2004. All mouse ventral spinal cord patterning by hedgehog is Gli dependent and involves an activator function of Gli3. *Dev Cell,* 6**,** 103-15.

Bayer, S. A., Altman, J., Russo, R. J., Dai, X. F. & Simmons, J. A. 1991. Cell migration in the rat embryonic neocortex. *J Comp Neurol,* 307**,** 499-516.

Bedard, A. & Parent, A. 2004. Evidence of newly generated neurons in the human olfactory bulb. *Brain Res Dev Brain Res,* 151**,** 159-68.

Bedeschi, M. F., Bonaglia, M. C., Grasso, R., Pellegri, A., Garghentino, R. R., Battaglia, M. A., Panarisi, A. M., Di Rocco, M., Balottin, U., Bresolin, N., Bassi, M. T. & Borgatti, R. 2006. Agenesis of the corpus callosum: clinical and genetic study in 63 young patients. *Pediatr Neurol,* 34**,** 186-93.

Besse, L., Neti, M., Anselme, I., Gerhardt, C., Rã¼Ther, U., Laclef, C. & Schneider-Maunoury, S. 2011. Primary cilia control telencephalic patterning and morphogenesis via Gli3 proteolytic processing. *Development (Cambridge, England),* 138**,** 2079-2088.

Bhanot, P., Brink, M., Samos, C. H., Hsieh, J. C., Wang, Y., Macke, J. P., Andrew, D., Nathans, J. & Nusse, R. 1996. A new member of the frizzled family from Drosophila functions as a Wingless receptor. *Nature,* 382**,** 225-30.

Bishop, K. M., Goudreau, G. & O'leary, D. D. 2000. Regulation of area identity in the mammalian neocortex by Emx2 and Pax6. *Science (New York, N.Y.),* 288**,** 344-349.

Blaess, S., Stephen, D. & Joyner, A. L. 2008. Gli3 coordinates three-dimensional patterning and growth of the tectum and cerebellum by integrating Shh and Fgf8 signaling. *Development (Cambridge, England),* 135**,** 2093-2103.

Bonatz, E., Descartes, M. & Tamarapalli, J. R. 1997. Acrocallosal syndrome: a case report. *J Hand Surg [Am],* 22**,** 492-4.

Bopp, D., Burri, M., Baumgartner, S., Frigerio, G. & Noll, M. 1986. Conservation of a large protein domain in the segmentation gene paired and in functionally related genes of Drosophila. *Cell,* 47**,** 1033-40.

Borello, U., Cobos, I., Long, J. E., Mcwhirter, J. R., Murre, C. & Rubenstein, J. L. 2008. FGF15 promotes neurogenesis and opposes FGF8 function during neocortical development. *Neural Dev,* 3**,** 17.

Briata, P., Diblas, E., Gulisano, M., Mallamaci, A., Iannone, R., Boncinelli, E. & Corte, G. 1996. EMX1 homeoprotein is expressed in cell nuclei of the developing cerebral cortex and in the axons of the olfactory sensory neurons. *Mechanisms of Development,* 57**,** 169-180.

Britanova, O., De Juan Romero, C., Cheung, A., Kwan, K. Y., Schwark, M., Gyorgy, A., Vogel, T., Akopov, S., Mitkovski, M., Agoston, D., Sestan, N., Molnã¡R, Z. & Tarabykin, V. 2008. Satb2 is a postmitotic determinant for upper-layer neuron specification in the neocortex. *Neuron,* 57**,** 378-392.

Brunet, I., Weinl, C., Piper, M., Trembleau, A., Volovitch, M., Harris, W., Prochiantz, A. & Holt, C. 2005. The transcription factor Engrailed-2 guides retinal axons. *Nature,* 438**,** 94-8.

Bulfone, A., Wang, F., Hevner, R., Anderson, S., Cutforth, T., Chen, S., Meneses, J., Pedersen, R., Axel, R. & Rubenstein, J. L. 1998. An olfactory sensory map develops in the absence of normal projection neurons or GABAergic interneurons. *Neuron,* 21**,** 1273-1282.

Carney, R. S., Alfonso, T. B., Cohen, D., Dai, H., Nery, S., Stoica, B., Slotkin, J., Bregman, B. S., Fishell, G. & Corbin, J. G. 2006. Cell migration along the lateral cortical stream to the developing basal telencephalic limbic system. *The Journal of neuroscience : the official journal of the Society for Neuroscience,* 26**,** 11562-11574.

Cave, J. W., Akiba, Y., Banerjee, K., Bhosle, S., Berlin, R. & Baker, H. 2010. Differential Regulation of Dopaminergic Gene Expression by Er81. *Journal of Neuroscience,* 30**,** 4717-4724.

Caviness, V. S., Jr. & Rakic, P. 1978. Mechanisms of cortical development: a view from mutations in mice. *Annu Rev Neurosci,* 1**,** 297-326.

Caviness, V. S., Jr. & Yorke, C. H., Jr. 1976. Interhemispheric neocortical connections of the corpus callosum in the reeler mutant mouse: a study based on anterograde and retrograde methods. *J Comp Neurol,* 170**,** 449-59.

Ceci, M. L., Pedraza, M. & De Carlos, J. A. 2012. The embryonic septum and ventral pallium, new sources of olfactory cortex cells. *PLoS One,* 7**,** e44716.

Chae, T., Kwon, Y. T., Bronson, R., Dikkes, P., Li, E. & Tsai, L. H. 1997. Mice lacking p35, a neuronal specific activator of Cdk5, display cortical lamination defects, seizures, and adult lethality. *Neuron,* 18**,** 29-42.

Chen, H., Chedotal, A., He, Z., Goodman, C. S. & Tessier-Lavigne, M. 1997. Neuropilin-2, a novel member of the neuropilin family, is a high affinity receptor for the semaphorins Sema E and Sema IV but not Sema III. *Neuron,* 19**,** 547-59.

Chen, Y., Magnani, D., Theil, T., Pratt, T. & Price, D. J. 2012. Evidence that descending cortical axons are essential for thalamocortical axons to cross the pallial-subpallial boundary in the embryonic forebrain. *PLoS One,* 7**,** e33105.

Chiang, C., Litingtung, Y., Lee, E., Young, K. E., Corden, J. L., Westphal, H. & Beachy, P. A. 1996. Cyclopia and defective axial patterning in mice lacking Sonic hedgehog gene function. *Nature,* 383**,** 407-13.

Cholfin, J. A. & Rubenstein, J. L. 2007. Patterning of frontal cortex subdivisions by Fgf17. *Proc Natl Acad Sci U S A,* 104**,** 7652-7.

Chou, S. J., Perez-Garcia, C. G., Kroll, T. T. & O'leary, D. D. 2009. Lhx2 specifies regional fate in Emx1 lineage of telencephalic progenitors generating cerebral cortex. *Nat Neurosci,* 12**,** 1381-9.

Christopherson, K. S., Ullian, E. M., Stokes, C. C., Mullowney, C. E., Hell, J. W., Agah, A., Lawler, J., Mosher, D. F., Bornstein, P. & Barres, B. A. 2005. Thrombospondins are astrocyte-secreted proteins that promote CNS synaptogenesis. *Cell,* 120**,** 421-33.

Clasca, F., Angelucci, A. & Sur, M. 1995. Layer-specific programs of development in neocortical projection neurons. *Proc Natl Acad Sci U S A,* 92**,** 11145-9.

Corbin, J. G., Gaiano, N., Machold, R. P., Langston, A. & Fishell, G. 2000. The Gsh2 homeodomain gene controls multiple aspects of telencephalic development. *Development,* 127**,** 5007-20.

Crossley, P. H., Martinez, S., Ohkubo, Y. & Rubenstein, J. L. 2001. Coordinate expression of Fgf8, Otx2, Bmp4, and Shh in the rostral prosencephalon during development of the telencephalic and optic vesicles. *Neuroscience,* 108**,** 183-206.

Crossman, A. R. & Neary, D. 2010. *Neuroanatomy: An illustrated colour text*, Elsevier.

D'arcangelo, G., Miao, G. G., Chen, S. C., Soares, H. D., Morgan, J. I. & Curran, T. 1995. A protein related to extracellular matrix proteins deleted in the mouse mutant reeler. *Nature,* 374**,** 719-23.

Danesin, C., Peres, J. N., Johansson, M., Snowden, V., Cording, A., Papalopulu, N. & Houart, C. 2009. Integration of telencephalic Wnt and hedgehog signaling center activities by Foxg1. *Developmental cell,* 16**,** 576-587.

De Carlos, J. A. & O'leary, D. D. 1992. Growth and targeting of subplate axons and establishment of major cortical pathways. *J Neurosci,* 12**,** 1194-211.

De Castro, F. 2009. Wiring Olfaction: The Cellular and Molecular Mechanisms that Guide the Development of Synaptic Connections from the Nose to the Cortex. *Frontiers in neuroscience,* 3**,** 52.

De Castro, F., Hu, L., Drabkin, H., Sotelo, C. & Chã©Dotal, A. 1999. Chemoattraction and chemorepulsion of olfactory bulb axons by different secreted semaphorins. *The Journal of neuroscience : the official journal of the Society for Neuroscience,* 19**,** 4428-4436.

Deck, M., Lokmane, L., Chauvet, S., Mailhes, C., Keita, M., Niquille, M., Yoshida, M., Yoshida, Y., Lebrand, C., Mann, F., Grove, E. A. & Garel, S. 2013. Pathfinding of corticothalamic axons relies on a rendezvous with thalamic projections. *Neuron,* 77**,** 472-84.

Defelipe, J. 2011. The evolution of the brain, the human nature of cortical circuits, and intellectual creativity. *Frontiers in neuroanatomy,* 5**,** 29.

Denaxa, M., Chan, C. H., Schachner, M., Parnavelas, J. G. & Karagogeos, D. 2001. The adhesion molecule TAG-1 mediates the migration of cortical interneurons from the ganglionic eminence along the corticofugal fiber system. *Development,* 128**,** 4635-44.

Derer, P., Caviness, V. S., Jr. & Sidman, R. L. 1977. Early cortical histogenesis in the primary olfactory cortex of the mouse. *Brain Res,* 123**,** 27-40.

Devor, M. 1976. Fiber trajectories of olfactory bulb efferents in the hamster. *J Comp Neurol,* 166**,** 31-47.

Diamond, I. T., Jones, E. G. & Powell, T. P. 1969. The projection of the auditory cortex upon the diencephalon and brain stem in the cat. *Brain Res,* 15**,** 305-40.

Doetsch, F., Caille, I., Lim, D. A., Garcia-Verdugo, J. M. & Alvarez-Buylla, A. 1999. Subventricular zone astrocytes are neural stem cells in the adult mammalian brain. *Cell,* 97**,** 703-16.

Dorus, S., Anderson, J. R., Vallender, E. J., Gilbert, S. L., Zhang, L., Chemnick, L. G., Ryder, O. A., Li, W. & Lahn, B. T. 2006. Sonic Hedgehog, a key development gene, experienced intensified molecular evolution in primates. *Hum Mol Genet,* 15**,** 2031-7.

Dou, C. L., Li, S. & Lai, E. 1999. Dual role of brain factor-1 in regulating growth and patterning of the cerebral hemispheres. *Cereb Cortex,* 9**,** 543-50.

Dufour, A., Egea, J., Kullander, K., Klein, R. & Vanderhaeghen, P. 2006. Genetic analysis of EphA-dependent signaling mechanisms controlling topographic mapping in vivo. *Development,* 133**,** 4415-20.

Echelard, Y., Epstein, D. J., St-Jacques, B., Shen, L., Mohler, J., Mcmahon, J. A. & Mcmahon, A. P. 1993. Sonic hedgehog, a member of a family of putative signaling molecules, is implicated in the regulation of CNS polarity. *Cell,* 75**,** 1417-30.

Ekstrand, J. J., Domroese, M. E., Feig, S. L., Illig, K. R. & Haberly, L. B. 2001. Immunocytochemical analysis of basket cells in rat piriform cortex. *J Comp Neurol,* 434**,** 308-28.

Elson, E., Perveen, R., Donnai, D., Wall, S. & Black, G. C. 2002. De novo GLI3 mutation in acrocallosal syndrome: broadening the phenotypic spectrum of GLI3 defects and overlap with murine models. *Journal of Medical Genetics,* 39**,** 804-806.

Erskine, L., Williams, S. E., Brose, K., Kidd, T., Rachel, R. A., Goodman, C. S., Tessier-Lavigne, M. & Mason, C. A. 2000. Retinal ganglion cell axon guidance in the mouse optic chiasm: expression and function of robos and slits. *J Neurosci,* 20**,** 4975-82.

Faedo, A., Borello, U. & Rubenstein, J. L. 2010. Repression of Fgf signaling by sprouty1-2 regulates cortical patterning in two distinct regions and times. *J Neurosci,* 30**,** 4015-23.

Fame, R. M., Macdonald, J. L. & Macklis, J. D. 2011. Development, specification, and diversity of callosal projection neurons. *Trends in neurosciences,* 34**,** 41-50.

Feng, W., Simoes-De-Souza, F., Finger, T. E., Restrepo, D. & Williams, T. 2009. Disorganized olfactory bulb lamination in mice deficient for transcription factor AP-2 epsilon. *Molecular and Cellular Neuroscience,* 42**,** 161-171.

Florian, C., Bahi-Buisson, N. & Bienvenu, T. 2012. FOXG1-Related Disorders: From Clinical Description to Molecular Genetics. *Mol Syndromol,* 2**,** 153-163.

Fotaki, V., Yu, T., Zaki, P. A., Mason, J. O. & Price, D. J. 2006. Abnormal positioning of diencephalic cell types in neocortical tissue in the dorsal telencephalon of mice lacking functional Gli3. *J Neurosci,* 26**,** 9282-92.

Fothergill, T., Donahoo, A. L., Douglass, A., Zalucki, O., Yuan, J., Shu, T., Goodhill, G. J. & Richards, L. J. 2013. Netrin-DCC Signaling Regulates Corpus Callosum Formation Through Attraction of Pioneering Axons and by Modulating Slit2-Mediated Repulsion. *Cereb Cortex*.

Fouquet, C., Di Meglio, T., Ma, L., Kawasaki, T., Long, H., Hirata, T., Tessier-Lavigne, M., Chã©Dotal, A. & Nguyen-Ba-Charvet, K. T. 2007. Robo1 and robo2 control the development of the lateral olfactory tract. *The Journal of neuroscience : the official journal of the Society for Neuroscience,* 27**,** 3037-3045.

Friedrichs, M., Larralde, O., Skutella, T. & Theil, T. 2008. Lamination of the cerebral cortex is disturbed in Gli3 mutant mice. *Dev Biol,* 318**,** 203-14.

Fu, C. 2012. *The role of Gli3 in thalamocortical/corticothalamic axons pathfinding.* MSc, University of Edinburgh.

Fuccillo, M., Rallu, M., Mcmahon, A. P. & Fishell, G. 2004. Temporal requirement for hedgehog signaling in ventral telencephalic patterning. *Development,* 131**,** 5031-40.

Fukuchi-Shimogori, T. & Grove, E. A. 2001. Neocortex patterning by the secreted signaling molecule FGF8. *Science,* 294**,** 1071-4.

Fukuchi-Shimogori, T. & Grove, E. A. 2003. Emx2 patterns the neocortex by regulating FGF positional signaling. *Nature neuroscience,* 6**,** 825-831.

Furuta, Y., Piston, D. W. & Hogan, B. L. 1997. Bone morphogenetic proteins (BMPs) as regulators of dorsal forebrain development. *Development,* 124**,** 2203-12.

Galceran, J., Miyashita-Lin, E. M., Devaney, E., Rubenstein, J. L. & Grosschedl, R. 2000. Hippocampus development and generation of dentate gyrus granule cells is regulated by LEF1. *Development,* 127**,** 469-82.

Garel, S., Huffman, K. J. & Rubenstein, J. L. R. 2003. Molecular regionalization of the neocortex is disrupted in Fgf8 hypomorphic mutants. *Development,* 130**,** 1903-1914.

Georgala, P. A., Manuel, M. & Price, D. J. 2011. The generation of superficial cortical layers is regulated by levels of the transcription factor Pax6. *Cerebral cortex (New York, N.Y. : 1991),* 21**,** 81-94.

Ghosh, A., Antonini, A., Mcconnell, S. K. & Shatz, C. J. 1990. Requirement for subplate neurons in the formation of thalamocortical connections. *Nature,* 347**,** 179-81.

Ghosh, A. & Shatz, C. J. 1993. A role for subplate neurons in the patterning of connections from thalamus to neocortex. *Development (Cambridge, England),* 117**,** 1031-1047.

Gorski, J. A., Talley, T., Qiu, M., Puelles, L., Rubenstein, J. L. & Jones, K. R. 2002. Cortical excitatory neurons and glia, but not GABAergic neurons, are produced in the Emx1-expressing lineage. *J Neurosci,* 22**,** 6309-14.

Gottfried, J. A. 2010. Central mechanisms of odour object perception. *Nature reviews. Neuroscience,* 11**,** 628-641.

Gotz, M. & Huttner, W. B. 2005. The cell biology of neurogenesis. *Nat Rev Mol Cell Biol,* 6**,** 777-88.

Grindley, J. C., Hargett, L. K., Hill, R. E., Ross, A. & Hogan, B. L. 1997. Disruption of PAX6 function in mice homozygous for the Pax6Sey-1Neu mutation produces abnormalities in the early development and regionalization of the diencephalon. *Mech Dev,* 64**,** 111-26.

Grove, E. A., Tole, S., Limon, J., Yip, L. & Ragsdale, C. W. 1998. The hem of the embryonic cerebral cortex is defined by the expression of multiple Wnt genes and is compromised in Gli3-deficient mice. *Development,* 125**,** 2315-25.

Guillery, R. W. 1967. Patterns of fiber degeneration in the dorsal lateral geniculate nucleus of the cat following lesions in the visual cortex. *J Comp Neurol,* 130**,** 197-221.

Gunhaga, L., Jessell, T. M. & Edlund, T. 2000. Sonic hedgehog signaling at gastrula stages specifies ventral telencephalic cells in the chick embryo. *Development,* 127**,** 3283-93.

Guo, F., Maeda, Y., Ma, J., Xu, J., Horiuchi, M., Miers, L., Vaccarino, F. & Pleasure, D. 2010. Pyramidal neurons are generated from oligodendroglial progenitor cells in adult piriform cortex. *The Journal of neuroscience : the official journal of the Society for Neuroscience,* 30**,** 12036-12049.

Haberly, L. & Behan, M. 1983. Structure of the piriform cortex of the opossum. III. Ultrastructural characterization of synaptic terminals of association and olfactory bulb afferent fibers. *J Comp Neurol,* 219**,** 448-60.

Hansen, D. V., Lui, J. H., Parker, P. R. & Kriegstein, A. R. 2010. Neurogenic radial glia in the outer subventricular zone of human neocortex. *Nature,* 464**,** 554-561.

Hasenpusch-Theil, K., Magnani, D., Amaniti, E. M., Han, L., Armstrong, D. & Theil, T. 2012. Transcriptional analysis of Gli3 mutants identifies Wnt target genes in the developing hippocampus. *Cereb Cortex,* 22**,** 2878-93.

Haubensak, W., Attardo, A., Denk, W. & Huttner, W. B. 2004. Neurons arise in the basal neuroepithelium of the early mammalian telencephalon: a major site of neurogenesis. *Proc Natl Acad Sci U S A,* 101**,** 3196-201.

Hayasaka, I., Nakatsuka, T., Fujii, T., Naruse, I. & Oda, S. 1980. Polydactyly Nagoya, Pdn: A new mutant gene in the mouse. *Jikken Dobutsu,* 29**,** 391-5.

Hayashi, S. & Mcmahon, A. P. 2002. Efficient recombination in diverse tissues by a tamoxifen-inducible form of Cre: a tool for temporally regulated gene activation/inactivation in the mouse. *Dev Biol,* 244**,** 305-18.

Haycraft, C. J., Banizs, B., Aydin-Son, Y., Zhang, Q., Michaud, E. J. & Yoder, B. K. 2005. Gli2 and Gli3 localize to cilia and require the intraflagellar transport protein polaris for processing and function. *PLoS Genet,* 1**,** e53.

Hayhurst, M., Gore, B. B., Tessier-Lavigne, M. & Mcconnell, S. K. 2008. Ongoing sonic hedgehog signaling is required for dorsal midline formation in the developing forebrain. *Dev Neurobiol,* 68**,** 83-100.

He, Z. & Tessier-Lavigne, M. 1997. Neuropilin is a receptor for the axonal chemorepellent Semaphorin III. *Cell,* 90**,** 739-51.

Hebert, J. M., Mishina, Y. & Mcconnell, S. K. 2002. BMP signaling is required locally to pattern the dorsal telencephalic midline. *Neuron,* 35**,** 1029-41.

Hevner, R. F., Miyashita-Lin, E. & Rubenstein, J. L. 2002. Cortical and thalamic axon pathfinding defects in Tbr1, Gbx2, and Pax6 mutant mice: evidence that cortical and thalamic axons interact and guide each other. *J Comp Neurol,* 447**,** 8-17.

Hevner, R. F., Shi, L., Justice, N., Hsueh, Y., Sheng, M., Smiga, S., Bulfone, A., Goffinet, A. M., Campagnoni, A. T. & Rubenstein, J. L. 2001. Tbr1 regulates differentiation of the preplate and layer 6. *Neuron,* 29**,** 353-66.

Hill, R. E., Favor, J., Hogan, B. L., Ton, C. C., Saunders, G. F., Hanson, I. M., Prosser, J., Jordan, T., Hastie, N. D. & Van Heyningen, V. 1991. Mouse small eye results from mutations in a paired-like homeobox-containing gene. *Nature,* 354**,** 522-5.

Hirata, T. & Fujisawa, H. 1999. Environmental control of collateral branching and target invasion of mitral cell axons during development. *Journal of Neurobiology,* 38**,** 93-104.

Hirata, T., Fujisawa, H., Wu, J. Y. & Rao, Y. 2001. Short-range guidance of olfactory bulb axons is independent of repulsive factor slit. *The Journal of neuroscience : the official journal of the Society for Neuroscience,* 21**,** 2373-2379.

Hirata, T., Nomura, T., Takagi, Y., Sato, Y., Tomioka, N., Fujisawa, H. & Osumi, N. 2002. Mosaic development of the olfactory cortex with Pax6-dependent and -independent components. *Brain research. Developmental brain research,* 136**,** 17-26.

Hogan, B. L., Horsburgh, G., Cohen, J., Hetherington, C. M., Fisher, G. & Lyon, M. F. 1986. Small eyes (Sey): a homozygous lethal mutation on chromosome 2 which affects the differentiation of both lens and nasal placodes in the mouse. *J Embryol Exp Morphol,* 97**,** 95-110.

Hoglund, P. J., Adzic, D., Scicluna, S. J., Lindblom, J. & Fredriksson, R. 2005. The repertoire of solute carriers of family 6: identification of new human and rodent genes. *Biochem Biophys Res Commun,* 336**,** 175-89.

Huangfu, D. & Anderson, K. V. 2005. Cilia and Hedgehog responsiveness in the mouse. *Proc Natl Acad Sci U S A,* 102**,** 11325-30.

Hughes, J. R. 2007. Autism: the first firm finding = underconnectivity? *Epilepsy & behavior : E&B,* 11**,** 20-24.

Huh, S., Hatini, V., Marcus, R. C., Li, S. C. & Lai, E. 1999. Dorsal-ventral patterning defects in the eye of BF-1-deficient mice associated with a restricted loss of shh expression. *Dev Biol,* 211**,** 53-63.

Hui, C. C., Slusarski, D., Platt, K. A., Holmgren, R. & Joyner, A. L. 1994. Expression of three mouse homologs of the Drosophila segment polarity gene cubitus interruptus, Gli, Gli-2, and Gli-3, in ectoderm- and mesoderm-derived tissues suggests multiple roles during postimplantation development. *Dev Biol,* 162**,** 402-13.

Ingham, P. W. & Mcmahon, A. P. 2001. Hedgehog signaling in animal development: paradigms and principles. *Genes Dev,* 15**,** 3059-87.

Ito, K., Kawasaki, T., Takashima, S., Matsuda, I., Aiba, A. & Hirata, T. 2008. Semaphorin 3F confines ventral tangential migration of lateral olfactory tract

neurons onto the telencephalon surface. *The Journal of neuroscience : the official journal of the Society for Neuroscience,* 28**,** 4414-4422.

Itoh, N. & Ornitz, D. M. 2004. Evolution of the Fgf and Fgfr gene families. *Trends Genet,* 20**,** 563-9.

Jacobs, E. C., Campagnoni, C., Kampf, K., Reyes, S. D., Kalra, V., Handley, V., Xie, Y. Y., Hong-Hu, Y., Spreur, V., Fisher, R. S. & Campagnoni, A. T. 2007. Visualization of corticofugal projections during early cortical development in a tau-GFP-transgenic mouse. *Eur J Neurosci,* 25**,** 17-30.

Jen, Y., Manova, K. & Benezra, R. 1997. Each member of the Id gene family exhibits a unique expression pattern in mouse gastrulation and neurogenesis. *Dev Dyn,* 208**,** 92-106.

Jimenez, D., Garcia, C., De Castro, F., Chã©Dotal, A., Sotelo, C., De Carlos, J. A., Valverde, F. & Lã³pez-Mascaraque, L. 2000. Evidence for intrinsic development of olfactory structures in Pax-6 mutant mice. *The Journal of comparative neurology,* 428**,** 511-526.

Johnson, D. R. 1967. Extra-toes: a new mutant gene causing multiple abnormalities in the mouse. *J Embryol Exp Morphol,* 17**,** 543-81.

Johnston, J. J., Olivos-Glander, I., Killoran, C., Elson, E., Turner, J. T., Peters, K. F., Abbott, M. H., Aughton, D. J., Aylsworth, A. S., Bamshad, M. J., Booth, C., Curry, C. J., David, A., Dinulos, M. B., Flannery, D. B., Fox, M. A., Graham, J. M., Grange, D. K., Guttmacher, A. E., Hannibal, M. C., Henn, W., Hennekam, R. C., Holmes, L. B., Hoyme, H. E., Leppig, K. A., Lin, A. E., Macleod, P., Manchester, D. K., Marcelis, C., Mazzanti, L., Mccann, E., Mcdonald, M. T., Mendelsohn, N. J., Moeschler, J. B., Moghaddam, B., Neri, G., Newbury-Ecob, R., Pagon, R. A., Phillips, J. A., Sadler, L. S., Stoler, J. M., Tilstra, D., Walsh Vockley, C. M., Zackai, E. H., Zadeh, T. M., Brueton, L., Black, G. C. & Biesecker, L. G. 2005. Molecular and clinical analyses of Greig cephalopolysyndactyly and Pallister-Hall syndromes: robust phenotype prediction from the type and position of GLI3 mutations. *Am J Hum Genet,* 76**,** 609-22.

Johnston, J. J., Olivos-Glander, I., Turner, J., Aleck, K., Bird, L. M., Mehta, L., Schimke, R. N., Heilstedt, H., Spence, J. E., Blancato, J. & Biesecker, L. G. 2003. Clinical and molecular delineation of the Greig cephalopolysyndactyly contiguous gene deletion syndrome and its distinction from acrocallosal syndrome. *Am J Med Genet A,* 123**,** 236-42.

Jones, E. G. 2002. Thalamic circuitry and thalamocortical synchrony. *Philos Trans R Soc Lond B Biol Sci,* 357**,** 1659-73.

Jones, E. G. & Powell, T. P. 1968. The projection of the somatic sensory cortex upon the thalamus in te cat. *Brain Res,* 10**,** 369-91.

Just, M. A., Cherkassky, V. L., Keller, T. A. & Minshew, N. J. 2004. Cortical activation and synchronization during sentence comprehension in high-functioning autism: evidence of underconnectivity. *Brain,* 127**,** 1811-21.

Kandel, E., Schwartz, M. L. & Jessell, T. M. 2000. *Principles of neural science*, McGraw Hill.

Kang, S., Allen, J., Graham, J. M., Jr., Grebe, T., Clericuzio, C., Patronas, N., Ondrey, F., Green, E., Schaffer, A., Abbott, M. & Biesecker, L. G. 1997.

Linkage mapping and phenotypic analysis of autosomal dominant Pallister-Hall syndrome. *J Med Genet,* 34**,** 441-6.

Kang, W. F., Wong, L. C., Shi, S. H. & Herbert, J. M. 2009. The Transition from Radial Glial to Intermediate Progenitor Cell Is Inhibited by FGF Signaling during Corticogenesis. *Journal of Neuroscience,* 29**,** 14571-14580.

Kantor, D. B., Chivatakarn, O., Peer, K. L., Oster, S. F., Inatani, M., Hansen, M. J., Flanagan, J. G., Yamaguchi, Y., Sretavan, D. W., Giger, R. J. & Kolodkin, A. L. 2004. Semaphorin 5A is a bifunctional axon guidance cue regulated by heparan and chondroitin sulfate proteoglycans. *Neuron,* 44**,** 961-75.

Kawano, Y. & Kypta, R. 2003. Secreted antagonists of the Wnt signalling pathway. *Journal of Cell Science,* 116**,** 2627-2634.

Kawasaki, T., Ito, K. & Hirata, T. 2006. Netrin 1 regulates ventral tangential migration of guidepost neurons in the lateral olfactory tract. *Development (Cambridge, England),* 133**,** 845-853.

Kim, A. S., Anderson, S. A., Rubenstein, J. L., Lowenstein, D. H. & Pleasure, S. J. 2001. Pax-6 regulates expression of SFRP-2 and Wnt-7b in the developing CNS. *J Neurosci,* 21**,** RC132.

Kohtz, J. D., Baker, D. P., Corte, G. & Fishell, G. 1998. Regionalization within the mammalian telencephalon is mediated by changes in responsiveness to Sonic Hedgehog. *Development,* 125**,** 5079-89.

Kohwi, M., Petryniak, M. A., Long, J. E., Ekker, M., Obata, K., Yanagawa, Y., Rubenstein, J. L. & Alvarez-Buylla, A. 2007. A subpopulation of olfactory bulb GABAergic interneurons is derived from Emx1- and Dlx5/6-expressing progenitors. *J Neurosci,* 27**,** 6878-91.

Kriajevska, M., Fischer-Larsen, M., Moertz, E., Vorm, O., Tulchinsky, E., Grigorian, M., Ambartsumian, N. & Lukanidin, E. 2002. Liprin beta 1, a member of the family of LAR transmembrane tyrosine phosphatase-interacting proteins, is a new target for the metastasis-associated protein S100A4 (Mts1). *J Biol Chem,* 277**,** 5229-35.

Kriegstein, A. R. & Gotz, M. 2003. Radial glia diversity: a matter of cell fate. *Glia,* 43**,** 37-43.

Kuschel, S., Ruther, U. & Theil, T. 2003. A disrupted balance between Bmp/Wnt and Fgf signaling underlies the ventralization of the Gli3 mutant telencephalon. *Developmental biology,* 260**,** 484-495.

Kwan, K. Y., Lam, M. M., Krsnik, Z., Kawasawa, Y. I., Lefebvre, V. & Sestan, N. 2008. SOX5 postmitotically regulates migration, postmigratory differentiation, and projections of subplate and deep-layer neocortical neurons. *Proc Natl Acad Sci U S A,* 105**,** 16021-6.

Kwan, K. Y., Sestan, N. & Anton, E. S. 2012. Transcriptional co-regulation of neuronal migration and laminar identity in the neocortex. *Development (Cambridge, England),* 139**,** 1535-1546.

Kwon, Y. T., Tsai, L. H. & Crandall, J. E. 1999. Callosal axon guidance defects in p35(-/-) mice. *J Comp Neurol,* 415**,** 218-29.

Lai, T., Jabaudon, D., Molyneaux, B. J., Azim, E., Arlotta, P., Menezes, J. R. & Macklis, J. D. 2008. SOX5 controls the sequential generation of distinct corticofugal neuron subtypes. *Neuron,* 57**,** 232-47.

Lanier, L. M., Gates, M. A., Witke, W., Menzies, A. S., Wehman, A. M., Macklis, J. D., Kwiatkowski, D., Soriano, P. & Gertler, F. B. 1999. Mena is required for neurulation and commissure formation. *Neuron,* 22**,** 313-25.

Lee, S. M., Tole, S., Grove, E. & Mcmahon, A. P. 2000. A local Wnt-3a signal is required for development of the mammalian hippocampus. *Development,* 127**,** 457-67.

Lefebvre, V., Li, P. & De Crombrugghe, B. 1998. A new long form of Sox5 (L-Sox5), Sox6 and Sox9 are coexpressed in chondrogenesis and cooperatively activate the type II collagen gene. *EMBO J,* 17**,** 5718-33.

Lett, R. L., Wang, W. & O'connor, T. P. 2009. Semaphorin 5B is a novel inhibitory cue for corticofugal axons. *Cerebral cortex (New York, N.Y. : 1991),* 19**,** 1408-1421.

Li, Z. 2011. *The role of Gli3 in the lamination of the cerebral cortex.* MSc, University of Edinburgh.

Lin, J. H., Saito, T., Anderson, D. J., Lance-Jones, C., Jessell, T. M. & Arber, S. 1998. Functionally related motor neuron pool and muscle sensory afferent subtypes defined by coordinate ETS gene expression. *Cell,* 95**,** 393-407.

Lindwall, C., Fothergill, T. & Richards, L. J. 2007. Commissure formation in the mammalian forebrain. *Curr Opin Neurobiol,* 17**,** 3-14.

Lopez-Bendito, G., Cautinat, A., Sanchez, J. A., Bielle, F., Flames, N., Garratt, A. N., Talmage, D. A., Role, L. W., Charnay, P., Marãn, O. & Garel, S. 2006. Tangential neuronal migration controls axon guidance: a role for neuregulin-1 in thalamocortical axon navigation. *Cell,* 125**,** 127-142.

Lopez-Bendito, G., Flames, N., Ma, L., Fouquet, C., Di Meglio, T., Chedotal, A., Tessier-Lavigne, M. & Marãn, O. 2007. Robo1 and Robo2 cooperate to control the guidance of major axonal tracts in the mammalian forebrain. *The Journal of neuroscience : the official journal of the Society for Neuroscience,* 27**,** 3395-3407.

Lopez-Bendito, G. & Molnar, Z. 2003. Thalamocortical development: how are we going to get there? *Nat Rev Neurosci,* 4**,** 276-89.

Luders, E., Thompson, P. M. & Toga, A. W. 2010. The development of the corpus callosum in the healthy human brain. *J Neurosci,* 30**,** 10985-90.

Lustig, B., Jerchow, B., Sachs, M., Weiler, S., Pietsch, T., Karsten, U., Van De Wetering, M., Clevers, H., Schlag, P. M., Birchmeier, W. & Behrens, J. 2002. Negative Feedback Loop of Wnt Signaling through Upregulation of Conductin/Axin2 in Colorectal and Liver Tumors. *Mol. Cell. Biol.,* 22**,** 1184-1193.

Macdonald, R., Barth, K. A., Xu, Q. L., Holder, N., Mikkola, I. & Wilson, S. W. 1995. Midline Signaling Is Required for Pax Gene-Regulation and Patterning of the Eyes. *Development,* 121**,** 3267-3278.

Magnani, D., Hasenpusch-Theil, K., Benadiba, C., Yu, T., Basson, M. A., Price, D. J., Lebrand, C. & Theil, T. 2012a. Gli3 Controls Corpus Callosum Formation by Positioning Midline Guideposts During Telencephalic Patterning. *Cereb Cortex*.

Magnani, D., Hasenpusch-Theil, K., Jacobs, E. C., Campagnoni, A. T., Price, D. J. & Theil, T. 2010. The Gli3 hypomorphic mutation Pdn causes selective

impairment in the growth, patterning, and axon guidance capability of the lateral ganglionic eminence. *J Neurosci,* 30**,** 13883-94.

Magnani, D., Hasenpusch-Theil, K. & Theil, T. 2012b. Gli3 Controls Subplate Formation and Growth of Cortical Axons. *Cereb Cortex*.

Malatesta, P., Hack, M. A., Hartfuss, E., Kettenmann, H., Klinkert, W., Kirchhoff, F. & Gotz, M. 2003. Neuronal or glial progeny: regional differences in radial glia fate. *Neuron,* 37**,** 751-64.

Manuel, M., Georgala, P. A., Carr, C. B., Chanas, S., Kleinjan, D. A., Martynoga, B., Mason, J. O., Molinek, M., Pinson, J., Pratt, T., Quinn, J. C., Simpson, T. I., Tyas, D. A., Van Heyningen, V., West, J. D. & Price, D. J. 2007. Controlled overexpression of Pax6 in vivo negatively autoregulates the Pax6 locus, causing cell-autonomous defects of late cortical progenitor proliferation with little effect on cortical arealization. *Development,* 134**,** 545-55.

Manuel, M. & Price, D. J. 2005. Role of Pax6 in forebrain regionalization. *Brain Res Bull,* 66**,** 387-93.

Marillat, V., Cases, O., Nguyen-Ba-Charvet, K. T., Tessier-Lavigne, M., Sotelo, C. & Chedotal, A. 2002. Spatiotemporal expression patterns of slit and robo genes in the rat brain. *J Comp Neurol,* 442**,** 130-55.

Martynoga, B., Morrison, H., Price, D. J. & Mason, J. O. 2005. Foxg1 is required for specification of ventral telencephalon and region-specific regulation of dorsal telencephalic precursor proliferation and apoptosis. *Developmental Biology,* 283**,** 113-27.

Mason, I. 2007. Initiation to end point: the multiple roles of fibroblast growth factors in neural development. *Nat Rev Neurosci,* 8**,** 583-96.

Matise, M. P. & Joyner, A. L. 1999. Gli genes in development and cancer. *Oncogene,* 18**,** 7852-9.

Matsuoka, R. L., Chivatakarn, O., Badea, T. C., Samuels, I. S., Cahill, H., Katayama, K., Kumar, S. R., Suto, F., Chedotal, A., Peachey, N. S., Nathans, J., Yoshida, Y., Giger, R. J. & Kolodkin, A. L. 2011. Class 5 transmembrane semaphorins control selective Mammalian retinal lamination and function. *Neuron,* 71**,** 460-73.

Maynard, T. M., Jain, M. D., Balmer, C. W. & Lamantia, A. S. 2002. High-resolution mapping of the Gli3 mutation extra-toes reveals a 51.5-kb deletion. *Mamm Genome,* 13**,** 58-61.

Mcconnell, S. K. 1995. Constructing the cerebral cortex: neurogenesis and fate determination. *Neuron,* 15**,** 761-8.

Mcconnell, S. K., Ghosh, A. & Shatz, C. J. 1989. Subplate neurons pioneer the first axon pathway from the cerebral cortex. *Science,* 245**,** 978-82.

Mcconnell, S. K., Ghosh, A. & Shatz, C. J. 1994. Subplate pioneers and the formation of descending connections from cerebral cortex. *J Neurosci,* 14**,** 1892-907.

Medina, L., Legaz, I., Gonzalez, G., De Castro, F., Rubenstein, J. L. & Puelles, L. 2004. Expression of Dbx1, Neurogenin 2, Semaphorin 5A, Cadherin 8, and Emx1 distinguish ventral and lateral pallial histogenetic divisions in the developing mouse claustroamygdaloid complex. *J Comp Neurol,* 474**,** 504-23.

Metin, C., Deleglise, D., Serafini, T., Kennedy, T. E. & Tessier-Lavigne, M. 1997. A role for netrin-1 in the guidance of cortical efferents. *Development,* 124**,** 5063-74.

Metin, C. & Godement, P. 1996. The ganglionic eminence may be an intermediate target for corticofugal and thalamocortical axons. *J Neurosci,* 16**,** 3219-35.

Meyer, G., Goffinet, A. M. & Fairen, A. 1999. What is a Cajal-Retzius cell? A reassessment of a classical cell type based on recent observations in the developing neocortex. *Cereb Cortex,* 9**,** 765-75.

Meyers, E. N., Lewandoski, M. & Martin, G. R. 1998. An Fgf8 mutant allelic series generated by Cre- and Flp-mediated recombination. *Nat Genet,* 18**,** 136-41.

Miller, B., Chou, L. & Finlay, B. L. 1993. The early development of thalamocortical and corticothalamic projections. *J Comp Neurol,* 335**,** 16-41.

Minowada, G., Jarvis, L. A., Chi, C. L., Neubuser, A., Sun, X., Hacohen, N., Krasnow, M. A. & Martin, G. R. 1999. Vertebrate Sprouty genes are induced by FGF signaling and can cause chondrodysplasia when overexpressed. *Development,* 126**,** 4465-75.

Minshew, N. J. & Williams, D. L. 2007. The new neurobiology of autism: cortex, connectivity, and neuronal organization. *Arch Neurol,* 64**,** 945-50.

Mission, J. P., Takahashi, T. & Caviness, V. S., Jr. 1991. Ontogeny of radial and other astroglial cells in murine cerebral cortex. *Glia,* 4**,** 138-48.

Miyata, T., Kawaguchi, A., Saito, K., Kawano, M., Muto, T. & Ogawa, M. 2004. Asymmetric production of surface-dividing and non-surface-dividing cortical progenitor cells. *Development,* 131**,** 3133-45.

Moldrich, R. X., Gobius, I., Pollak, T., Zhang, J., Ren, T., Brown, L., Mori, S., De Juan Romero, C., Britanova, O., Tarabykin, V. & Richards, L. J. 2010. Molecular regulation of the developing commissural plate. *J Comp Neurol,* 518**,** 3645-61.

Molnar, Z., Adams, R. & Blakemore, C. 1998. Mechanisms underlying the early establishment of thalamocortical connections in the rat. *J Neurosci,* 18**,** 5723-45.

Molnar, Z. & Blakemore, C. 1995a. Guidance of thalamocortical innervation. *Ciba Found Symp,* 193**,** 127-49; discussion 192-9.

Molnar, Z. & Blakemore, C. 1995b. How do thalamic axons find their way to the cortex? *Trends Neurosci,* 18**,** 389-97.

Molnar, Z. & Cordery, P. 1999. Connections between cells of the internal capsule, thalamus, and cerebral cortex in embryonic rat. *J Comp Neurol,* 413**,** 1-25.

Molyneaux, B. J., Arlotta, P., Menezes, J. R. & Macklis, J. D. 2007. Neuronal subtype specification in the cerebral cortex. *Nat Rev Neurosci,* 8**,** 427-37.

Mombaerts, P. 2006. Axonal wiring in the mouse olfactory system. *Annual review of cell and developmental biology,* 22**,** 713-737.

Monuki, E. S., Porter, F. D. & Walsh, C. A. 2001. Patterning of the dorsal telencephalon and cerebral cortex by a roof plate-Lhx2 pathway. *Neuron,* 32**,** 591-604.

Monuki, E. S. & Walsh, C. A. 2001. Mechanisms of cerebral cortical patterning in mice and humans. *Nat Neurosci,* 4 Suppl**,** 1199-206.

Muenke, M. & Beachy, P. A. 2000. Genetics of ventral forebrain development and holoprosencephaly. *Curr Opin Genet Dev,* 10**,** 262-9.

Murone, M., Rosenthal, A. & De Sauvage, F. J. 1999. Hedgehog signal transduction: From flies to vertebrates. *Experimental Cell Research,* 253**,** 25-33.

Muzio, L. & Mallamaci, A. 2005. Foxg1 confines Cajal-Retzius neuronogenesis and hippocampal morphogenesis to the dorsomedial pallium. *J Neurosci,* 25**,** 4435-41.

Naruse, I., Kato, K., Asano, T., Suzuki, F. & Kameyama, Y. 1990. Developmental brain abnormalities accompanied with the retarded production of S-100 beta protein in genetic polydactyly mice. *Brain Res Dev Brain Res,* 51**,** 253-8.

Naruse, I. & Keino, H. 1995. Apoptosis in the developing CNS. *Prog Neurobiol,* 47**,** 135-55.

Nery, S., Wichterle, H. & Fishell, G. 2001. Sonic hedgehog contributes to oligodendrocyte specification in the mammalian forebrain. *Development,* 128**,** 527-40.

Nguyen-Ba-Charvet, K. T., Plump, A. S., Tessier-Lavigne, M. & Chedotal, A. 2002. Slit1 and slit2 proteins control the development of the lateral olfactory tract. *The Journal of neuroscience : the official journal of the Society for Neuroscience,* 22**,** 5473-5480.

Nielsen, T., Montplaisir, J. & Lassonde, M. 1992. Sleep architecture in agenesis of the corpus callosum: laboratory assessment of four cases. *J Sleep Res,* 1**,** 197-200.

Nieto, M., Monuki, E. S., Tang, H., Imitola, J., Haubst, N., Khoury, S. J., Cunningham, J., Gotz, M. & Walsh, C. A. 2004. Expression of Cux-1 and Cux-2 in the subventricular zone and upper layers II-IV of the cerebral cortex. *J Comp Neurol,* 479**,** 168-80.

Niquille, M., Garel, S., Mann, F., Hornung, J. P., Otsmane, B., Chevalley, S., Parras, C., Guillemot, F., Gaspar, P., Yanagawa, Y. & Lebrand, C. 2009. Transient neuronal populations are required to guide callosal axons: a role for semaphorin 3C. *PLoS Biol,* 7**,** e1000230.

Niquille, M., Minocha, S., Hornung, J. P., Rufer, N., Valloton, D., Kessaris, N., Alfonsi, F., Vitalis, T., Yanagawa, Y., Devenoges, C., Dayer, A. & Lebrand, C. 2013. Two specific populations of GABAergic neurons originating from the medial and the caudal ganglionic eminences aid in proper navigation of callosal axons. *Dev Neurobiol*.

Nobrega-Pereira, S., Kessaris, N., Du, T. G., Kimura, S., Anderson, S. A. & Marin, O. 2008. Postmitotic Nkx2-1 controls the migration of telencephalic interneurons by direct repression of guidance receptors. *Neuron,* 59**,** 733-745.

Noctor, S. C., Martinez-Cerdeno, V., Ivic, L. & Kriegstein, A. R. 2004. Cortical neurons arise in symmetric and asymmetric division zones and migrate through specific phases. *Nat Neurosci,* 7**,** 136-44.

Nomura, T., Holmberg, J., Frisen, J. & Osumi, N. 2006. Pax6-dependent boundary defines alignment of migrating olfactory cortex neurons via the repulsive activity of ephrin A5. *Development,* 133**,** 1335-1345.

O'leary, D. D. & Sahara, S. 2008. Genetic regulation of arealization of the neocortex. *Curr Opin Neurobiol,* 18**,** 90-100.

Oeschger, F. M., Wang, W. Z., Lee, S., Garcia-Moreno, F., Goffinet, A. M., Arbones, M. L., Rakic, S. & Molnar, Z. 2012. Gene expression analysis of the embryonic subplate. *Cereb Cortex,* 22**,** 1343-59.

Oliver, G., Mailhos, A., Wehr, R., Copeland, N. G., Jenkins, N. A. & Gruss, P. 1995. Six3, a murine homologue of the sine oculis gene, demarcates the most anterior border of the developing neural plate and is expressed during eye development. *Development,* 121**,** 4045-55.

Orenic, T. V., Slusarski, D. C., Kroll, K. L. & Holmgren, R. A. 1990. Cloning and characterization of the segment polarity gene cubitus interruptus Dominant of Drosophila. *Genes Dev,* 4**,** 1053-67.

Ornitz, D. M. & Itoh, N. 2001. Fibroblast growth factors. *Genome Biol,* 2**,** REVIEWS3005.

Paek, H., Gutin, G. & Hã©Bert, J. M. 2009. FGF signaling is strictly required to maintain early telencephalic precursor cell survival. *Development (Cambridge, England),* 136**,** 2457-2465.

Parr, B. A., Shea, M. J., Vassileva, G. & Mcmahon, A. P. 1993. Mouse Wnt genes exhibit discrete domains of expression in the early embryonic CNS and limb buds. *Development,* 119**,** 247-61.

Parraga, H. C., Parraga, M. I. & Jensen, A. R. 2003. Cognitive, behavioral, and psychiatric symptoms in two children with agenesis of the corpus callosum: case report. *Int J Psychiatry Med,* 33**,** 107-13.

Paul, L. K., Brown, W. S., Adolphs, R., Tyszka, J. M., Richards, L. J., Mukherjee, P. & Sherr, E. H. 2007. Agenesis of the corpus callosum: genetic, developmental and functional aspects of connectivity. *Nat Rev Neurosci,* 8**,** 287-99.

Paul, L. K., Van Lancker-Sidtis, D., Schieffer, B., Dietrich, R. & Brown, W. S. 2003. Communicative deficits in agenesis of the corpus callosum: nonliteral language and affective prosody. *Brain Lang,* 85**,** 313-24.

Pedraza, M. & De Carlos, J. A. 2012. A further analysis of olfactory cortex development. *Front Neuroanat,* 6**,** 35.

Persohn, E. & Schachner, M. 1990. Immunohistological localization of the neural adhesion molecules L1 and N-CAM in the developing hippocampus of the mouse. *J Neurocytol,* 19**,** 807-19.

Piper, M., Plachez, C., Zalucki, O., Fothergill, T., Goudreau, G., Erzurumlu, R., Gu, C. & Richards, L. J. 2009. Neuropilin 1-Sema signaling regulates crossing of cingulate pioneering axons during development of the corpus callosum. *Cereb Cortex,* 19 Suppl 1**,** i11-21.

Pixley, S. K. & De Vellis, J. 1984. Transition between immature radial glia and mature astrocytes studied with a monoclonal antibody to vimentin. *Brain Res,* 317**,** 201-9.

Polleux, F., Giger, R. J., Ginty, D. D., Kolodkin, A. L. & Ghosh, A. 1998. Patterning of cortical efferent projections by semaphorin-neuropilin interactions. *Science,* 282**,** 1904-6.

Polleux, F., Morrow, T. & Ghosh, A. 2000. Semaphorin 3A is a chemoattractant for cortical apical dendrites. *Nature,* 404**,** 567-73.

Pratt, T., Vitalis, T., Warren, N., Edgar, J. M., Mason, J. O. & Price, D. J. 2000. A role for Pax6 in the normal development of dorsal thalamus and its cortical connections. *Development,* 127**,** 5167-78.

Puelles, L., Kuwana, E., Puelles, E., Bulfone, A., Shimamura, K., Keleher, J., Smiga, S. & Rubenstein, J. L. 2000. Pallial and subpallial derivatives in the

embryonic chick and mouse telencephalon, traced by the expression of the genes Dlx-2, Emx-1, Nkx-2.1, Pax-6, and Tbr-1. *J Comp Neurol,* 424**,** 409-38.

Purves, D., Augustine, G., Fitzpatrick, D., Hall, W., Lamantia, A. & White, L. 2007. *Neuroscience*, Sinauer.

Qiu, M., Anderson, S., Chen, S., Meneses, J. J., Hevner, R., Kuwana, E., Pedersen, R. A. & Rubenstein, J. L. 1996. Mutation of the Emx-1 homeobox gene disrupts the corpus callosum. *Dev Biol,* 178**,** 174-8.

Quinn, J. C., Molinek, M., Mason, J. O. & Price, D. J. 2009. Gli3 is required autonomously for dorsal telencephalic cells to adopt appropriate fates during embryonic forebrain development. *Dev Biol,* 327**,** 204-15.

Radhakrishna, U., Blouin, J. L., Mehenni, H., Patel, U. C., Patel, M. N., Solanki, J. V. & Antonarakis, S. E. 1997. Mapping one form of autosomal dominant postaxial polydactyly type A to chromosome 7p15-q11.23 by linkage analysis. *Am J Hum Genet,* 60**,** 597-604.

Radhakrishna, U., Bornholdt, D., Scott, H. S., Patel, U. C., Rossier, C., Engel, H., Bottani, A., Chandal, D., Blouin, J. L., Solanki, J. V., Grzeschik, K. H. & Antonarakis, S. E. 1999. The phenotypic spectrum of GLI3 morphopathies includes autosomal dominant preaxial polydactyly type-IV and postaxial polydactyly type-A/B; No phenotype prediction from the position of GLI3 mutations. *Am J Hum Genet,* 65**,** 645-55.

Ragsdale, C. W. & Grove, E. A. 2001. Patterning the mammalian cerebral cortex. *Curr Opin Neurobiol,* 11**,** 50-8.

Rakic, P. 1972. Mode of cell migration to the superficial layers of fetal monkey neocortex. *J Comp Neurol,* 145**,** 61-83.

Rakic, P. 1988. Specification of cerebral cortical areas. *Science,* 241**,** 170-6.

Rakic, P. 1995. A small step for the cell, a giant leap for mankind: a hypothesis of neocortical expansion during evolution. *Trends Neurosci,* 18**,** 383-8.

Rakic, P. 2003. Developmental and evolutionary adaptations of cortical radial glia. *Cereb Cortex,* 13**,** 541-9.

Rakic, P. & Caviness, V. S., Jr. 1995. Cortical development: view from neurological mutants two decades later. *Neuron,* 14**,** 1101-4.

Rallu, M., Corbin, J. G. & Fishell, G. 2002a. Parsing the prosencephalon. *Nat Rev Neurosci,* 3**,** 943-51.

Rallu, M., Machold, R., Gaiano, N., Corbin, J. G., Mcmahon, A. P. & Fishell, G. 2002b. Dorsoventral patterning is established in the telencephalon of mutants lacking both Gli3 and Hedgehog signaling. *Development,* 129**,** 4963-74.

Rash, B. G. & Grove, E. A. 2007. Patterning the dorsal telencephalon: a role for sonic hedgehog? *J Neurosci,* 27**,** 11595-603.

Rash, B. G. & Richards, L. J. 2001. A role for cingulate pioneering axons in the development of the corpus callosum. *J Comp Neurol,* 434**,** 147-57.

Richards, L. J., Plachez, C. & Ren, T. 2004. Mechanisms regulating the development of the corpus callosum and its agenesis in mouse and human. *Clin Genet,* 66**,** 276-89.

Rubin, A. N., Alfonsi, F., Humphreys, M. P., Choi, C. K., Rocha, S. F. & Kessaris, N. 2010. The germinal zones of the basal ganglia but not the septum generate GABAergic interneurons for the cortex. *J Neurosci,* 30**,** 12050-62.

Ruediger, T., Zimmer, G., Barchmann, S., Castellani, V., Bagnard, D. & Bolz, J. 2013. Integration of opposing semaphorin guidance cues in cortical axons. *Cereb Cortex,* 23**,** 604-14.

Ruiz I Altaba, A. 1998. Combinatorial Gli gene function in floor plate and neuronal inductions by Sonic hedgehog. *Development,* 125**,** 2203-12.

Ruiz I Altaba, A. 1999. Gli proteins and Hedgehog signaling: development and cancer. *Trends Genet,* 15**,** 418-25.

Runker, A. E., O'tuathaigh, C., Dunleavy, M., Morris, D. W., Little, G. E., Corvin, A. P., Gill, M., Henshall, D. C., Waddington, J. L. & Mitchell, K. J. 2011. Mutation of Semaphorin-6A disrupts limbic and cortical connectivity and models neurodevelopmental psychopathology. *PLoS One,* 6**,** e26488.

Ruppert, J. M., Kinzler, K. W., Wong, A. J., Bigner, S. H., Kao, F. T., Law, M. L., Seuanez, H. N., O'brien, S. J. & Vogelstein, B. 1988. The GLI-Kruppel family of human genes. *Mol Cell Biol,* 8**,** 3104-13.

Ruppert, J. M., Vogelstein, B., Arheden, K. & Kinzler, K. W. 1990. GLI3 encodes a 190-kilodalton protein with multiple regions of GLI similarity. *Mol Cell Biol,* 10**,** 5408-15.

Saha, B., Hari, P., Huilgol, D. & Tole, S. 2007. Dual role for LIM-homeodomain gene Lhx2 in the formation of the lateral olfactory tract. *The Journal of neuroscience : the official journal of the Society for Neuroscience,* 27**,** 2290-2297.

Sahara, S., Kawakami, Y., Izpisua Belmonte, J. C. & O'leary, D. D. 2007. Sp8 exhibits reciprocal induction with Fgf8 but has an opposing effect on anterior-posterior cortical area patterning. *Neural Dev,* 2**,** 10.

Sahara, S. & O'leary, D. D. 2009. Fgf10 regulates transition period of cortical stem cell differentiation to radial glia controlling generation of neurons and basal progenitors. *Neuron,* 63**,** 48-62.

Saisana, M. 2010. *The role of Gli3 in the formation of the pallial subpallial boundary.* MSc, University of Edinburgh.

Sanchez-Camacho, C., Ortega, J. A., Ocana, I., Alcantara, S. & Bovolenta, P. 2011. Appropriate Bmp7 levels are required for the differentiation of midline guidepost cells involved in corpus callosum formation. *Dev Neurobiol,* 71**,** 337-50.

Sarma, A. A., Richard, M. B. & Greer, C. A. 2011. Developmental dynamics of piriform cortex. *Cerebral cortex (New York, N.Y. : 1991),* 21**,** 1231-1245.

Sasaki, H., Nishizaki, Y., Hui, C., Nakafuku, M. & Kondoh, H. 1999. Regulation of Gli2 and Gli3 activities by an amino-terminal repression domain: implication of Gli2 and Gli3 as primary mediators of Shh signaling. *Development,* 126**,** 3915-24.

Sato, Y., Hirata, T., Ogawa, M. & Fujisawa, H. 1998. Requirement for early-generated neurons recognized by monoclonal antibody lot1 in the formation of lateral olfactory tract. *The Journal of neuroscience : the official journal of the Society for Neuroscience,* 18**,** 7800-7810.

Saulnier, A., Keruzore, M., De Clercq, S., Bar, I., Moers, V., Magnani, D., Walcher, T., Filippis, C., Kricha, S., Parlier, D., Viviani, L., Matson, C. K., Nakagawa, Y., Theil, T., Gã¶Tz, M., Mallamaci, A., Marine, J. C., Zarkower, D. & Bellefroid, E. J. 2012. The Doublesex Homolog Dmrt5 is Required for the

Development of the Caudomedial Cerebral Cortex in Mammals. *Cerebral cortex (New York, N.Y. : 1991)*.

Schimmang, T., Lemaistre, M., Vortkamp, A. & Ruther, U. 1992. Expression of the zinc finger gene Gli3 is affected in the morphogenetic mouse mutant extra-toes (Xt). *Development,* 116**,** 799-804.

Schinzel, A. 1979. Postaxial polydactyly, hallux duplication, absence of the corpus callosum, macrencephaly and severe mental retardation: a new syndrome? *Helv Paediatr Acta,* 34**,** 141-6.

Schinzel, A. & Kaufmann, U. 1986. The acrocallosal syndrome in sisters. *Clin Genet,* 30**,** 399-405.

Schmahl, W., Knoedlseder, M., Favor, J. & Davidson, D. 1993. Defects of neuronal migration and the pathogenesis of cortical malformations are associated with Small eye (Sey) in the mouse, a point mutation at the Pax-6-locus. *Acta Neuropathol,* 86**,** 126-35.

Schwob, J. E. & Price, J. L. 1984a. The development of axonal connections in the central olfactory system of rats. *The Journal of comparative neurology,* 223**,** 177-202.

Schwob, J. E. & Price, J. L. 1984b. The development of lamination of afferent fibers to the olfactory cortex in rats, with additional observations in the adult. *J Comp Neurol,* 223**,** 203-22.

Sheperd, G. 2003. *Synaptic organisation of the brain*.

Sherman, S. M. & Guillery, R. W. 2002. The role of the thalamus in the flow of information to the cortex. *Philosophical Transactions of the Royal Society B-Biological Sciences,* 357**,** 1695-1708.

Shimamura, K., Hartigan, D. J., Martinez, S., Puelles, L. & Rubenstein, J. L. 1995. Longitudinal organization of the anterior neural plate and neural tube. *Development,* 121**,** 3923-33.

Shimamura, K. & Rubenstein, J. L. 1997. Inductive interactions direct early regionalization of the mouse forebrain. *Development,* 124**,** 2709-18.

Shimogori, T., Banuchi, V., Ng, H. Y., Strauss, J. B. & Grove, E. A. 2004. Embryonic signaling centers expressing BMP, WNT and FGF proteins interact to pattern the cerebral cortex. *Development,* 131**,** 5639-47.

Shipley, M. T. & Ennis, M. 1996. Functional organization of olfactory system. *J Neurobiol,* 30**,** 123-76.

Shu T, B. K., Plachez C, Gronostajski Rm, Richards Lj 2003. Abnormal development of forebrain mindline glia nad commissural projections in Nfia knock-out mice. *The journal of Neuroscience,* 23**,** 203-212.

Shu, T., Puche, A. C. & Richards, L. J. 2003. Development of midline glial populations at the corticoseptal boundary. *Journal of Neurobiology,* 57**,** 81-94.

Shu, T. & Richards, L. J. 2001. Cortical axon guidance by the glial wedge during the development of the corpus callosum. *The Journal of neuroscience : the official journal of the Society for Neuroscience,* 21**,** 2749-2758.

Silver, J., Lorenz, S. E., Wahlsten, D. & Coughlin, J. 1982. Axonal Guidance during Development of the Great Cerebral Commissures - Descriptive and Experimental Studies, Invivo, on the Role of Preformed Glial Pathways. *Journal of Comparative Neurology,* 210**,** 10-29.

Simeone, A., Gulisano, M., Acampora, D., Stornaiuolo, A., Rambaldi, M. & Boncinelli, E. 1992. Two vertebrate homeobox genes related to the Drosophila empty spiracles gene are expressed in the embryonic cerebral cortex. *EMBO J,* 11**,** 2541-50.

Simoes, E. L., Bramati, I., Rodrigues, E., Franzoi, A., Moll, J., Lent, R. & Tovar-Moll, F. 2012. Functional expansion of sensorimotor representation and structural reorganization of callosal connections in lower limb amputees. *J Neurosci,* 32**,** 3211-20.

Simpson, T. I., Pratt, T., Mason, J. O. & Price, D. J. 2009. Normal ventral telencephalic expression of Pax6 is required for normal development of thalamocortical axons in embryonic mice. *Neural Dev,* 4**,** 19.

Skaliora, I., Singer, W., Betz, H. & Puschel, A. W. 1998. Differential patterns of semaphorin expression in the developing rat brain. *European Journal of Neuroscience,* 10**,** 1215-29.

Smith, K. M., Ohkubo, Y., Maragnoli, M. E., Rasin, M. R., Schwartz, M. L., Sestan, N. & Vaccarino, F. M. 2006. Midline radial glia translocation and corpus callosum formation require FGF signaling. *Nat Neurosci,* 9**,** 787-97.

Sousa, V. H., Miyoshi, G., Hjerling-Leffler, J., Karayannis, T. & Fishell, G. 2009. Characterization of Nkx6-2-derived neocortical interneuron lineages. *Cereb Cortex,* 19 Suppl 1**,** i1-10.

Soussi-Yanicostas, N., De Castro, F., Julliard, A. K., Perfettini, I., Chedotal, A. & Petit, C. 2002. Anosmin-1, defective in the X-linked form of Kallmann syndrome, promotes axonal branch formation from olfactory bulb output neurons. *Cell,* 109**,** 217-28.

Speksnijder, L., Cohen-Overbeek, T. E., Knapen, M. F., Lunshof, S. M., Hoogeboom, A. J., Van Den Ouwenland, A. M., De Coo, I. F., Lequin, M. H., Bolz, H. J., Bergmann, C., Biesecker, L. G., Willems, P. J. & Wessels, M. W. 2013. A De Novo GLI3 Mutation in a Patient With Acrocallosal Syndrome. *Am J Med Genet A*.

Squire, L. R., Bloom, F. E., Spitzer, N. C., Du Lac, S., Ghosh, A. & Berg, B. 2008. *Fundamental neuroscience*, Elsevier.

St John, J. A., Clarris, H. J., Mckeown, S., Royal, S. & Key, B. 2003. Sorting and convergence of primary olfactory axons are independent of the olfactory bulb. *J Comp Neurol,* 464**,** 131-40.

Stenman, J., Toresson, H. & Campbell, K. 2003. Identification of two distinct progenitor populations in the lateral ganglionic eminence: implications for striatal and olfactory bulb neurogenesis. *J Neurosci,* 23**,** 167-74.

Stettler, D. D. & Axel, R. 2009. Representations of odor in the piriform cortex. *Neuron,* 63**,** 854-864.

Stevenson, R. J. 2010. An initial evaluation of the functions of human olfaction. *Chem Senses,* 35**,** 3-20.

Stoykova, A., Fritsch, R., Walther, C. & Gruss, P. 1996. Forebrain patterning defects in Small eye mutant mice. *Development (Cambridge, England),* 122**,** 3453-3465.

Stoykova, A. & Gruss, P. 1994. Roles of Pax-genes in developing and adult brain as suggested by expression patterns. *J Neurosci,* 14**,** 1395-412.

Stoykova, A., Treichel, D., Hallonet, M. & Gruss, P. 2000. Pax6 modulates the dorsoventral patterning of the mammalian telencephalon. *J Neurosci,* 20**,** 8042-50.

Subramanian, L., Remedios, R., Shetty, A. & Tole, S. 2009. Signals from the edges: the cortical hem and antihem in telencephalic development. *Seminars in cell & developmental biology,* 20**,** 712-718.

Sugisaki, N., Hirata, T., Naruse, I., Kawakami, A., Kitsukawa, T. & Fujisawa, H. 1996. Positional cues that are strictly localized in the telencephalon induce preferential growth of mitral cell axons. *J Neurobiol,* 29**,** 127-37.

Sundaresan, V., Mambetisaeva, E., Andrews, W., Annan, A., Knoll, B., Tear, G. & Bannister, L. 2004. Dynamic expression patterns of Robo (Robo1 and Robo2) in the developing murine central nervous system. *J Comp Neurol,* 468**,** 467-81.

Sussel, L., Marin, O., Kimura, S. & Rubenstein, J. L. 1999. Loss of Nkx2.1 homeobox gene function results in a ventral to dorsal molecular respecification within the basal telencephalon: evidence for a transformation of the pallidum into the striatum. *Development,* 126**,** 3359-70.

Suzuki, N. & Bekkers, J. M. 2007. Inhibitory interneurons in the piriform cortex. *Clinical and experimental pharmacology & physiology,* 34**,** 1064-1069.

Tempe, D., Casas, M., Karaz, S., Blanchet-Tournier, M. F. & Concordet, J. P. 2006. Multisite protein kinase A and glycogen synthase kinase 3beta phosphorylation leads to Gli3 ubiquitination by SCFbetaTrCP. *Mol Cell Biol,* 26**,** 4316-26.

Theil, T. 2005. Gli3 is required for the specification and differentiation of preplate neurons. *Dev Biol,* 286**,** 559-71.

Theil, T., Alvarez-Bolado, G., Walter, A. & Ruther, U. 1999. Gli3 is required for Emx gene expression during dorsal telencephalon development. *Development,* 126**,** 3561-3571.

Theil, T., Aydin, S., Koch, S., Grotewold, L. & Rüther, U. 2002. Wnt and Bmp signalling cooperatively regulate graded Emx2 expression in the dorsal telencephalon. *Development,* 129**,** 3045-54.

Thien, H. & Ruther, U. 1999. The mouse mutation Pdn (Polydactyly Nagoya) is caused by the integration of a retrotransposon into the Gli3 gene. *Mammalian genome : official journal of the International Mammalian Genome Society,* 10**,** 205-209.

Tole, S., Christian, C. & Grove, E. A. 1997. Early specification and autonomous development of cortical fields in the mouse hippocampus. *Development,* 124**,** 4959-70.

Tole, S., Gutin, G., Bhatnagar, L., Remedios, R. & Hebert, J. M. 2006. Development of midline cell types and commissural axon tracts requires Fgfr1 in the cerebrum. *Dev Biol,* 289**,** 141-51.

Tole, S., Ragsdale, C. W. & Grove, E. A. 2000. Dorsoventral patterning of the telencephalon is disrupted in the mouse mutant extra-toes(J). *Dev Biol,* 217**,** 254-65.

Tomioka, N., Osumi, N., Sato, Y., Inoue, T., Nakamura, S., Fujisawa, H. & Hirata, T. 2000. Neocortical origin and tangential migration of guidepost neurons in

the lateral olfactory tract. *The Journal of neuroscience : the official journal of the Society for Neuroscience,* 20**,** 5802-5812.

Toyoda, R., Assimacopoulos, S., Wilcoxon, J., Taylor, A., Feldman, P., Suzuki-Hirano, A., Shimogori, T. & Grove, E. A. 2010. FGF8 acts as a classic diffusible morphogen to pattern the neocortex. *Development (Cambridge, England),* 137**,** 3439-3448.

Trommsdorff, M., Gotthardt, M., Hiesberger, T., Shelton, J., Stockinger, W., Nimpf, J., Hammer, R. E., Richardson, J. A. & Herz, J. 1999. Reeler/Disabled-like disruption of neuronal migration in knockout mice lacking the VLDL receptor and ApoE receptor 2. *Cell,* 97**,** 689-701.

Ueta, E., Nanba, E. & Naruse, I. 2002. Integration of a transposon into the Gli3 gene in the Pdn mouse. *Congenit Anom (Kyoto),* 42**,** 318-22.

Unni, D. K., Piper, M., Moldrich, R. X., Gobius, I., Liu, S., Fothergill, T., Donahoo, A. L., Baisden, J. M., Cooper, H. M. & Richards, L. J. 2012. Multiple Slits regulate the development of midline glial populations and the corpus callosum. *Developmental biology,* 365**,** 36-49.

Vortkamp, A., Gessler, M. & Grzeschik, K. H. 1991. GLI3 zinc-finger gene interrupted by translocations in Greig syndrome families. *Nature,* 352**,** 539-40.

Vyas, A., Saha, B., Lai, E. & Tole, S. 2003. Paleocortex is specified in mice in which dorsal telencephalic patterning is severely disrupted. *J Comp Neurol,* 466**,** 545-53.

Wallingford, J. B., Niswander, L. A., Shaw, G. M. & Finnell, R. H. 2013. The continuing challenge of understanding, preventing, and treating neural tube defects. *Science,* 339**,** 1222002.

Walther, C. & Gruss, P. 1991. Pax-6, a murine paired box gene, is expressed in the developing CNS. *Development,* 113**,** 1435-49.

Wang, B., Fallon, J. F. & Beachy, P. A. 2000. Hedgehog-regulated processing of Gli3 produces an anterior/posterior repressor gradient in the developing vertebrate limb. *Cell,* 100**,** 423-34.

Wang, H., Ge, G., Uchida, Y., Luu, B. & Ahn, S. 2011. Gli3 is required for maintenance and fate specification of cortical progenitors. *J Neurosci,* 31**,** 6440-8.

Weis-Garcia, F. & Massague, J. 1996. Complementation between kinase-defective and activation-defective TGF-beta receptors reveals a novel form of receptor cooperativity essential for signaling. *EMBO J,* 15**,** 276-89.

Wilson, S. W. & Rubenstein, J. L. 2000. Induction and dorsoventral patterning of the telencephalon. *Neuron,* 28**,** 641-51.

Winter, R. M. & Huson, S. M. 1988. Greig cephalopolysyndactyly syndrome: a possible mouse homologue (Xt-extra toes). *Am J Med Genet,* 31**,** 793-8.

Wizenmann, A., Brunet, I., Lam, J. S. Y., Sonnier, L., Beurdeley, M., Zarbalis, K., Weisenhorn-Vogt, D., Weinl, C., Dwivedy, A., Joliot, A., Wurst, W., Holt, C. & Prochiantz, A. 2009. Extracellular Engrailed Participates in the Topographic Guidance of Retinal Axons In Vivo. *Neuron,* 64**,** 355-366.

Xu, C. & Fan, C. M. 2008. Expression of Robo/Slit and Semaphorin/Plexin/Neuropilin family members in the developing

hypothalamic paraventricular and supraoptic nuclei. *Gene Expr Patterns,* 8**,** 502-7.

Xuan, S., Baptista, C. A., Balas, G., Tao, W., Soares, V. C. & Lai, E. 1995. Winged helix transcription factor BF-1 is essential for the development of the cerebral hemispheres. *Neuron,* 14**,** 1141-52.

Yates, P. A., Roskies, A. L., Mclaughlin, T. & O'leary, D. D. 2001. Topographic-specific axon branching controlled by ephrin-As is the critical event in retinotectal map development. *J Neurosci,* 21**,** 8548-63.

Yuan, W., Zhou, L., Chen, J. H., Wu, J. Y., Rao, Y. & Ornitz, D. M. 1999. The mouse SLIT family: secreted ligands for ROBO expressed in patterns that suggest a role in morphogenesis and axon guidance. *Developmental Biology,* 212**,** 290-306.

Yun, K., Potter, S. & Rubenstein, J. L. 2001. Gsh2 and Pax6 play complementary roles in dorsoventral patterning of the mammalian telencephalon. *Development,* 128**,** 193-205.

Zimmer, C., Lee, J., Griveau, A., Arber, S., Pierani, A., Garel, S. & Guillemot, F. 2010. Role of Fgf8 signalling in the specification of rostral Cajal-Retzius cells. *Development,* 137**,** 293-302.

Zou, Z., Horowitz, L. F., Montmayeur, J. P., Snapper, S. & Buck, L. B. 2001. Genetic tracing reveals a stereotyped sensory map in the olfactory cortex. *Nature,* 414**,** 173-9.